



**NATIONAL AND KAPODISTRIAN UNIVERSITY OF ATHENS**

**SCHOOL OF SCIENCES**

**DEPARTMENT OF CHEMISTRY**

**DOCTORAL THESIS**

**Identification of transformation products of emerging  
contaminants during tertiary treatment processes and their  
disposal in the environment by mass spectrometric techniques**

**NIKA MARIA-CHRISTINA**

**MSc CHEMIST**

**ATHENS 2017**









**ΕΘΝΙΚΟ ΚΑΙ ΚΑΠΟΔΙΣΤΡΙΑΚΟ ΠΑΝΕΠΙΣΤΗΜΙΟ ΑΘΗΝΩΝ**

**ΣΧΟΛΗ ΘΕΤΙΚΩΝ ΕΠΙΣΤΗΜΩΝ**

**ΤΜΗΜΑ ΧΗΜΕΙΑΣ**

**ΔΙΔΑΚΤΟΡΙΚΗ ΔΙΑΤΡΙΒΗ**

**Ταυτοποίηση προϊόντων μετασχηματισμού αναδυόμενων ρύπων  
κατά την τριτοβάθμια επεξεργασία λυμάτων και τη διάθεσή τους  
στο περιβάλλον με τεχνικές φασματομετρίας μάζας**

**ΝΙΚΑ ΜΑΡΙΑ-ΧΡΙΣΤΙΝΑ**

**MSc ΧΗΜΙΚΟΣ**

**ΑΘΗΝΑ 2017**



**DOCTORAL THESIS**

**Identification of transformation products of emerging  
contaminants during tertiary treatment processes and their  
disposal in the environment by mass spectrometric techniques**

**NIKA MARIA-CHRISTINA**

**Registration Number: 001306**

**Supervising Professor:**

Dr. Nikolaos S Thomaidis, Associate Professor

**Three – member consultative committee:**

Dr. Antony C. Calokerinos, Professor

Dr. Emmanuel Dasenakis, Professor

Dr. Nikolaos S. Thomaidis, Associate Professor

**Seven-member examination committee:**

Dr. Evangelos Bakeas, Associate Professor

Dr. Antony C. Calokerinos, Professor

Dr. Emmanuel Dasenakis, Professor

Dr. Anastasios Economou, Professor

Dr. Euaggelos Gikas, Assistant Professor at National and Kapodistrian  
University of Athens, Department of Pharmaceutical Chemistry

Dr. Constantinos Noutsopoulos, Assistant Professor at National Technical  
University of Athens, School of Civil Engineering

Dr. Nikolaos S Thomaidis, Associate Professor

**Defending Date: 24/11/2017**





## **ΔΙΔΑΚΤΟΡΙΚΗ ΔΙΑΤΡΙΒΗ**

# **Ταυτοποίηση προϊόντων μετασχηματισμού αναδυόμενων ρύπων κατά την τριτοβάθμια επεξεργασία λυμάτων και τη διάθεσή τους στο περιβάλλον με τεχνικές φασματομετρίας μάζας**

**ΝΙΚΑ ΜΑΡΙΑ-ΧΡΙΣΤΙΝΑ**

**Αριθμός μητρώου: 001306**

### **Επιβλέπων καθηγητής:**

Δρ. Νικόλαος Θωμαΐδης, Αναπληρωτής Καθηγητής

### **Τριμελής συμβουλευτική επιτροπή:**

Δρ. Εμμανουήλ Δασενάκης, Καθηγητής

Δρ. Νικόλαος Θωμαΐδης, Αναπληρωτής Καθηγητής

Δρ. Αντώνιος Καλοκαιρινός, Καθηγητής

### **Επταμελής εξεταστική επιτροπή:**

Δρ. Ευάγγελος Γκίκας, Επίκουρος Καθηγητής του Πανεπιστημίου Αθηνών,  
Τμήμα Φαρμακευτικής

Δρ. Εμμανουήλ Δασενάκης, Καθηγητής

Δρ. Νικόλαος Θωμαΐδης, Αναπληρωτής Καθηγητής

Δρ. Αντώνιος Καλοκαιρινός, Καθηγητής

Δρ. Ευάγγελος Μπακέας, Αναπληρωτής Καθηγητής

Δρ. Κωνσταντίνος Νουτσόπουλος, Επίκουρος Καθηγητής του Εθνικού Μετσόβιου  
Πολυτεχνείου, Σχολή Πολιτικών Μηχανικών

Δρ. Αναστάσιος Οικονόμου, Καθηγητής

**Ημερομηνία εξέτασης: 24/11/2017**



## **ABSTRACT**

The incomplete removal of emerging pollutants during the biological treatment applied in WWTPs is highly indicated by the existing literature. Although the primary purpose of tertiary treatment processes is the elimination of micropollutants, the provided oxidant agent reacts with emerging pollutants, leading to the formation of unknown transformation products. The main objectives of this thesis were the investigation of the removal of emerging pollutants and the identification of their transformation products which are produced during the disinfection methods that are applied as tertiary treatment in WWTPs.

Initially, an introduction on emerging pollutants and their probable transformation during the processes that are applied in WWTPs, and especially during chlorination and ozonation, is presented. Specific workflows and techniques for the identification of emerging contaminants and their transformation products, based on high-resolution mass spectrometric analysis, are then presented. The experimental section of this thesis is constituted of the following three parts: (i) Chlorination of benzothiazoles and benzotriazoles and transformation products identification by LC-HR-MS/MS (Chapter 3), (ii) Ozonation of ranitidine: effect of experimental parameters and identification of transformation products (Chapter 4) and (iii) Removal and transformation of citalopram and four of its biotransformation products during ozonation experiments (Chapter 5).

It is our strong belief that these studies will constitute a step forward in environmental analysis, by arousing the regulatory authorities concern, regarding that harmful transformation products produced during tertiary treatment processes in WWTPs, should also be incorporated in routine monitoring.

**SUBJECT AREA:** Analytical Chemistry

**KEYWORDS:** Emerging pollutants, Chlorination, Ozonation, LC-QTOF-MS, Transformation products, Non-target screening



## ΠΕΡΙΛΗΨΗ

Η διαθέσιμη βιβλιογραφία έχει καταδείξει την ατελή απομάκρυνση των αναδυόμενων ρύπων κατά τη βιολογική επεξεργασία που λαμβάνει χώρα στα Κέντρα Επεξεργασίας Λυμάτων (ΚΕΛ). Παρόλο που ο πρωταρχικός ρόλος της τριτοβάθμιας επεξεργασίας είναι η εξάλειψη των μικρορύπων, το παρεχόμενο οξειδωτικό μέσο αντιδρά με τους αναδυόμενους ρύπους, καταλήγοντας στο σχηματισμό άγνωστων προϊόντων μετασχηματισμού. Ο κύριος στόχος της παρούσας διπλωματικής εργασίας ήταν η διερεύνηση της απομάκρυνσης αναδυόμενων ρύπων καθώς και η ταυτοποίηση των προϊόντων μετασχηματισμού τους, τα οποία παράγονται κατά τις μεθόδους απολύμανσης που εφαρμόζονται σαν τριτοβάθμια επεξεργασία στα ΚΕΛ.

Αρχικά παρουσιάζεται μια εισαγωγή για τους αναδυόμενους ρύπους και τον πιθανό μετασχηματισμό τους κατά τη διάρκεια των διεργασιών που εφαρμόζονται στα ΚΕΛ, και ιδιαίτερος κατά τη διάρκεια της χλωρίωσης και οζόνωσης. Στη συνέχεια παρουσιάζονται συγκεκριμένες πορείες εργασίας και τεχνικές σχετικές με την ταυτοποίηση αναδυόμενων ρύπων και των προϊόντων μετασχηματισμού τους, οι οποίες βασίζονται σε αναλύσεις φασματομετρίας μάζας υψηλής διακριτικής ικανότητας. Το πειραματικό μέρος της παρούσας διπλωματικής εργασίας αποτελείται από τα ακόλουθα τρία μέρη: (α) Χλωρίωση βενζοτριαζολών και βενζοθειαζολών και ταυτοποίηση των προϊόντων μετασχηματισμού τους με υδροχρωματογραφία συζευγμένη με φασματομετρία μάζας υψηλής διακριτικής ικανότητας (Κεφάλαιο 3), (β) Οζόνωση ρανιτιδίνης: επίδραση των πειραματικών συνθηκών και ταυτοποίηση προϊόντων μετασχηματισμού (Κεφάλαιο 4) και (γ) Απομάκρυνση και μετασχηματισμός της σιταλοπράμης και τεσσάρων προϊόντων βιομετατροπής της κατά τη διάρκεια πειραμάτων οζόνωσης (Κεφάλαιο 5).

Είναι πεποίθησή μας πως οι μελέτες αυτές θα συνεισφέρουν στην περαιτέρω ανάπτυξη της περιβαλλοντικής ανάλυσης, διεγείροντας το ενδιαφέρον των κανονιστικών αρχών, σχετικά με την ενσωμάτωση επιβλαβών προϊόντων μετασχηματισμού, τα οποία παράγονται κατά την τριτοβάθμια επεξεργασία των ΚΕΛ, σε ελέγχους ρουτίνας

**ΘΕΜΑΤΙΚΗ ΠΕΡΙΟΧΗ:** Αναλυτική Χημεία

**ΛΕΞΕΙΣ ΚΛΕΙΔΙΑ:** Αναδύομενοι Ρύποι, Χλωρίωση, Οζόνωση, LR-MS, LC-QTOF-MS, Προϊόντα μετασχηματισμού, μη στοχευμένη σάρωση

## ACKNOWLEDGEMENTS

I owe my deepest gratitude to my supervisor Dr. Nikolaos Thomaidis for his guidance, support and encouragement throughout my PhD studies and for giving me the opportunity to carry out my research project as a member of TrAMS group. I would also like to deeply thank him for believing in me and for providing all the valuable professional and personal advice.

Special thanks are attributed to the three-member consultative committee and seven-member examination committee for their cooperation throughout this thesis and their valuable comments.

I would like to thank Reza Aalizadeh and Christophoros Christophoridis for their help and contribution in the experimental part of this thesis.

I am extremely grateful to my friends Anna Bletsou and Marilena Dasenaki, who have both played a key-role in my post-graduate studies. They inspired me to continue my studies at a PhD level and since 2012, they keep sharing with me their expertise and experiences.

I am thankful to each and every “TrAMSer” I met in the lab during all those years and that contributed to create a friendly and creative environment. Special thanks to my friends Vasiliki Beretsou, Violeta Borova, Dimitris Damalas, Christina Michali, George Koulis, and Katerina Psoma.

I would also like to thank the master students Lena Mila, Olga Dritsa and Ilias Tsilikidis for our collaboration during their studies.

Finally, these acknowledgments would not be complete without thanking my grandparents Maria and Christos, my parents Katerina and Kostas, my brother Minos, my friends and of course Christos for their enormous support and care through all these three years of my PhD and my life in general.





# CONTENTS

	<b>Pages</b>
<b>Abstract</b>	9
<b>Περίληψη</b>	11
<b>Acknowledgements</b>	13
<b>Contents</b>	15
<b>List of Figures</b>	19
<b>List of Tables</b>	21
<b>Preface</b>	23
<b>Chapter 1. Emerging Pollutants: Fate during Wastewater Treatment Plants processes and Instrumental analysis</b>	25
1.1. Introduction	25
1.2. Emerging Pollutants (EPs) and their transformation products (TPs)	26
1.2.1 Emerging Pollutants (EPs)	26
1.2.2 Transformation Products	27
1.3. Conventional wastewater treatment	28
1.3.1 Primary and Secondary treatment	29
1.3.2 Disinfection processes	30
<u>Chlorination</u>	30
<u>UV Disinfection</u>	33
<u>Ozonation</u>	33
<u>Advanced oxidation processes</u>	36
1.4. Identification approaches - Analytical techniques	37
1.4.1 Target analysis	39
1.4.2 Suspect screening of EPs - prediction of TPs	41
1.4.3 Non-target screening	43
1.4.4 Structure elucidation and identification confidence levels in HR-MS	45
1.5. Instrumental analysis	47
1.5.1 Gas Chromatography (GC) - Mass Spectrometry	47
1.5.2 Liquid Chromatography - High Resolution Mass Spectrometry (LC-HRMS)	48
<u>Chromatographic separation</u>	48
<u>High Resolution Mass Spectrometry</u>	49
<u>Time of Flight (TOF) MS</u>	50
<b>Chapter 2. Scope and Objectives</b>	53
2.1. The analytical problem	53

## CONTENTS

	Pages
2.2. Research objectives and Scope	55
<b>Chapter 3.</b> Chlorination of benzothiazoles and benzotriazoles and transformation products identification by LC-HR-MS/MS	57
3.1. Introduction	57
3.2. Scope of the study	59
3.3. Experimental part	59
3.3.1 Chemicals	59
3.3.2 Chlorination removal experiments	60
<u>Influence of operational parameters</u>	60
<u>Kinetics parameters determination</u>	61
3.3.3 Identification of transformation products	62
<u>Identification of TPs experiments</u>	62
<u>Identification workflows</u>	63
3.3.4 Instrumental analysis	64
3.4. Results and discussion	66
3.4.1 Removal of the tested contaminants	66
<u>Influence of operational parameters</u>	66
<u>Determination of the kinetic parameters</u>	68
3.4.2 Identification of transformation products	69
<u>Application of identification workflows</u>	69
<u>Retention time prediction</u>	78
<u>Environmental relevance – Toxicity assessment</u>	79
3.5. Conclusions	82
<b>Chapter 4.</b> Ozonation of ranitidine: effect of experimental parameters and identification of transformation products	83
4.1. Introduction	83
4.2. Scope of the study	85
4.3. Experimental part	85
4.3.1 Standards and reagents	85
4.3.2 Experimental setup	86
4.3.3 Instrumental analysis	88
<u>Monitoring of RAN removal</u>	88
<u>UHPLC MS analysis for TPs identification</u>	89
4.3.4 Applied workflows for TPs identification	90
<u>Screening workflows</u>	90
<u>Retention time prediction</u>	92
4.4. Results and discussion	93

## CONTENTS

	<b>Pages</b>
4.4.1. Effect of experimental conditions on RAN removal	93
<u>Effect of the initial ozone concentration</u>	93
<u>Effect of pH</u>	94
<u>Effect of matrix content</u>	95
<u>Mineralization of RAN</u>	96
4.4.2 Identification of ozonation transformation products	97
<u>Retention time prediction results</u>	112
<u>Identification Highlights</u>	113
4.5. Conclusions	116
<b>Chapter 5. Removal and transformation of citalopram and four of its biotransformation products during ozonation experiments</b>	<b>117</b>
5.1. Introduction	117
5.2. Scope of the study	121
5.3. Experimental Part	121
5.3.1 Standards and reagents	121
5.3.2 Ozonation experiments	122
5.3.3 Instrumental analysis	123
5.4 Data treatment	126
5.4.1 Automated Detection of TPs	126
5.4.2 Identification of ozonation TPs	129
5.4.3 Toxicity assessment	133
5.5. Results and Discussion	133
5.5.1 Removal of CIT and Identification of its ozonation TPs	136
5.5.2 Removal of DESCIT and Identification of its ozonation TPs	140
5.5.3 Removal of CTRAM and Identification of its ozonation TPs	144
5.5.4 Removal of CTRAC and Identification of its ozonation TPs	147
5.5.5 Removal of CTROXO and Identification of its ozonation TPs	149
5.5.6 Retention time prediction	152
5.5.7 Toxicity assessment	153
5.5.8 Common transformation pathways and produced TPs	155
5.6. Conclusions	158
<b>Chapter 6. Conclusions</b>	<b>159</b>

## CONTENTS

	<b>Pages</b>
<b>Abbreviations and Acronyms</b>	161
<b>References</b>	163
<b>Publications and Conferences</b>	187

## LIST OF FIGURES

	Pages
<b>Fig. 1.0</b> Graphical abstract of Chapter 1.	25
<b>Fig. 1.1.</b> Scheme of a Wastewater Treatment Plant.	29
<b>Fig. 1.2.</b> Flow chart of screening procedure of transformation products (TPs).	38
<b>Fig. 1.3.</b> Proposed identification confidence levels in HR-MS analysis.	47
<b>Fig. 1.4.</b> Schematic presentation of a Q-TOF instrument (Maxis Impact, Bruker).	52
<b>Fig. 2.0</b> Graphical abstract of Chapter 2.	53
<b>Fig. 3.0</b> Graphical Abstract of Chapter 3.	57
<b>Fig. 3.1.</b> Removal plots of all contaminants in the four molar ratios tested for chlorination time up to 30 minutes.	67
<b>Fig. 3.2.</b> Data dependent MS/MS (auto MS/MS) spectra of the detected produced TPs of (a) 2-amino-BTH and (b) XTRi.	73
<b>Fig. 3.3.</b> Data dependent MS/MS (auto MS/MS) spectra of (a) XTRi and (b) 2-amino-BTH.	74
<b>Fig. 3.4.</b> (a) EICs of $m/z$ 184.9935 from the standard solutions of 2-amino-4-chloro-BTH and 2-amino-6-chloro-BTH and (b) MS/MS spectra of $m/z$ 184.9935 from 2-amino-6-chloro-BTH standard solution.	76
<b>Fig. 3.5.</b> Confirmation of production of 1-H-BTRi as a chlorination transformation product of 1-OH-BTRi based on (a) retention time, (b) MS spectra and (c) fragmentation pattern.	79
<b>Fig. 3.6.</b> EICs of the detected TPs in chlorinated treated wastewater samples of (a) 1-OH-BTRi, (b) XTRi and (c) 2-amino-BTH.	81
<b>Fig. 4.0</b> Graphical Abstract of Chapter 4.	83
<b>Fig. 4.1.</b> Ranitidine removal under various initial ozone concentrations ( $C_o$ RAN: 5 mg L <sup>-1</sup> , matrix: ultrapure water).	94
<b>Fig. 4.2.</b> Ranitidine removal at different pH ( $C_o$ RAN: 5mg L <sup>-1</sup> , $C_o$ O <sub>3</sub> : 1 mg L <sup>-1</sup> , matrix: ultrapure water adjusted to pH 4.0, 7.0, 9.0 and 10.0).	95
<b>Fig. 4.3.</b> RAN removal in the presence of dissolved organic matter ( $C_o$ O <sub>3</sub> : 1 mg L <sup>-1</sup> ).	96
<b>Fig. 4.4.</b> Data dependent MS/MS (autoMS) spectra and their interpretation to support the identification of ozonation TPs of Ranitidine.	104

## LIST OF FIGURES

	<b>Pages</b>
<b>Fig. 4.5.</b> Ozonation transformation products of Ranitidine (Co Ranitidine: 5 mg L <sup>-1</sup> , Co O <sub>3</sub> : 1 mg L <sup>-1</sup> , matrix: ultrapure water, reaction time: 1 min).	115
<b>Fig. 5.0</b> Graphical abstract of Chapter 5.	117
<b>Fig. 5.1.</b> Gaussian curves for detection of TPs and parent compounds.	129
<b>Fig. 5.2.</b> MS/MS spectra similarity score extraction.	131
<b>Fig. 5.3.</b> Flowchart of data treatment and non-target screening with associated level of confidence in identification of TPs.	132
<b>Fig. 5.4.</b> Trend Analysis results for CIT and its ozonation TPs detected in pH 7.	140
<b>Fig. 5.5.</b> EICs of DESCIT and its ozonation TPs.	143
<b>Fig. 5.6 a)</b> Ozone dose profiling of CTRAM and its TPs. <b>Fig. 5.6 b)</b> Mass Balance of CTRAM and its TPs.	146
<b>Fig. 5.7</b> CTROXO TPs formation tree.	151
<b>Fig. 5.8.</b> Identified TPs of CIT and 4 of its biotransformation products. Common compounds are circled with the same color.	157
<b>Fig. 6.0</b> Graphical abstract of Chapter 6.	159

## LIST OF TABLES

	<b>Page</b>
<b>Table 1.1.</b> Advanced oxidation processes.	37
<b>Table 3.1.</b> Chlorination kinetic parameters of all tested contaminants in ultrapure water (95% confidence interval).	69
<b>Table 3.2.</b> Transformation products from the chlorination of XTRi, 2-amino-BTH and their identification parameters.	70
<b>Table 3.3.</b> ECOSAR results for (a) 2-amino-BTH, (b) XTRi and their identified transformation products.	81
<b>Table 4.1.</b> Extracted Ion Chromatograms of the identified transformation products of ranitidine (RAN) using RPLC and HILIC.	97
<b>Table 4.2.</b> Predicted and experimental retention time of identified compounds in RPLC and HILIC and the corresponding errors ( $\Delta t_R$ ).	113
<b>Table 5.1.</b> Ozonation experiments samples for every tested compound.	123
<b>Table 5.2.</b> The gradient elution program of LC-HRMS analysis.	124
<b>Table 5.3.</b> MS identification data for the identified TPs (including only the TPs that a specific formula is proposed).	134
<b>Table 5.4.</b> % Contribution of each CTRAM TP to the total TPs area.	146
<b>Table 5.5.</b> Toxicity prediction for CIT, DESCIT, CTRAM, CTRAC, CTROXO and their identified TPs.	154
<b>Table 5.6.</b> Common transformation pathways occurring during the ozonation of the parent compounds and the relative TPs that are formed.	155





## PREFACE

All the experimental parts of his work were conceived and performed at the Laboratory of Analytical Chemistry, Department of Chemistry of the National and Kapodistrian University of Athens, Greece, under the supervision of Dr. Nikolaos Thomaidis.

An extended Electronic Supplementary Material of **135** pages, consisting of **17** Sections (including **92** Figures and **14** Tables) is also available along with this thesis.

The first two experimental parts of this doctoral thesis (Chapters 3 and 4) have been co-financed by the European Union and Greek national funds through the Operational Program "Education and Lifelong Learning" of the National Strategic Reference Framework (NSRF) – ARISTEIA 624 (TREMEPOL project).

(<http://tremepol.chem.uoa.gr/>)

I would also like to express my sincere gratitude to A. G. Leventis Foundation for supporting me throughout my PhD studies, by awarding me a scholarship for three consecutive academic years (2014-2015 and approved renewal scholarships for 2015-2016 and 2016-2017). The awards were a great honor, and I hope my academic achievements fulfilled A. G. Leventis Foundation expectations.

(<http://www.leventisfoundation.org/el/>)





# CHAPTER 1.

## Emerging Pollutants: Fate during Wastewater Treatment Plants processes and Instrumental analysis

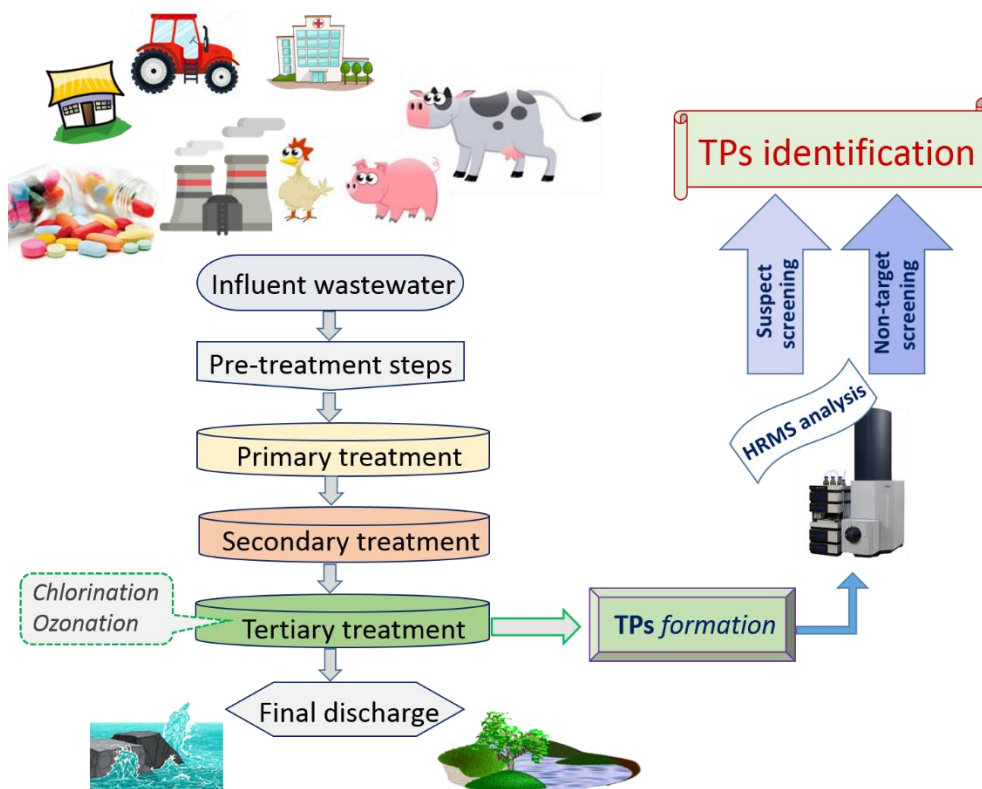


Fig. 1.0 Graphical abstract of Chapter 1.

### 1.1. Introduction

Overwhelming evidence has shown that organic micropollutants have been released from urban, industrial and agricultural activities, over the last decade and nowadays are ubiquitous in the aquatic environment. These substances, referred as “emerging pollutants” (EPs), include a wide array of different compounds, as well as metabolites and transformation products (TPs), can be detected with highly sensitive analytical methodologies in levels of parts per trillion (ppt), even in the most complex environmental matrices. Although environmental monitoring is making great progress, many pollutants still remain undetected and thus out of water controls. Because of the vast number of possible compounds, many studies have being carried out for different classes of emerging pollutants, according to priority lists established, taking into account consumption, predicted environmental concentrations, as well as

ecotoxicological, pharmacological and physicochemical data. However, their environmental impact (ecotoxicological and possible health risks for human) that is associated with their occurrence is still unknown. Although the reported concentrations are generally low, questions have been raised over the potential impacts of emerging pollutants in the environment on human and animal health after long-term exposure. Another fact that should be taken into consideration, is that TPs may be formed in the environment and may be detected in higher concentrations than the parent compounds, or even human metabolites could be excreted from the human body [1, 2]. There is very limited knowledge on the occurrence and environmental fate of human metabolites. Additionally, the extent in which the current water and wastewater treatment infrastructures can effectively remove these compounds is also, in great extent, an unknown parameter [3]. The inefficient removal poses a serious environmental problem. Thus, it is a topic of growing interest from both research and regulatory perspectives.

## **1.2. Emerging Pollutants (EPs) and their transformation products (TPs)**

### **1.2.1 Emerging Pollutants (EPs)**

The term “emerging pollutants” (or “emerging contaminants”, ECs) refers to compounds and their metabolites that are not currently covered by existing water-quality regulations, have not been often studied, overlooked, and/or are thought to be potential threats to environmental ecosystems and human health and safety. According to NORMAN network (Network of reference laboratories, research centers and related organisations for monitoring of emerging environmental substances), they are compounds that are not included in routine environmental monitoring programs and may be candidates for future legislation due to their adverse effects and/or persistency (<http://www.norman-network.net/>, last accessed September 2017). Most regulating and implementation bodies, responsible for water and wastewater treatment, are working on the assumption that the so-called priority pollutants are responsible for the most significant share of environmental, human health and economic risk, even though they are representing a minor fraction of the universe of both known and yet-to be identified chemicals [4].

The EPs encompass a diverse group of compounds, including pharmaceuticals and personal care products (PPCPs), illicit drugs and drug of abuse, hormones and steroids, benzothiazoles, benzotriazoles, polychlorinated naphthalenes (PCNs), perfluorochemicals (PFCs), polychlorinated alkanes (PCAs), polydimethylsiloxanes (PDMSs), synthetic musks, quaternary ammonium compounds (QACs), bisphenol A (BPA), triclosan (TCS), triclocarban (TCC), as well as polar pesticides, veterinary products, industrial compounds/ by-products, food additives, engineered nano-materials and the transformation products of all the aforementioned classes of compounds [5, 6].

### **1.2.2 Transformation Products**

Once released into the environment, EPs are subject to both biotic and abiotic transformation processes that are responsible for their transformation and/or elimination, according to their persistence, transport, and ultimate destination. Various transformations can take place, producing compounds that, to some extent, differ in their environmental behavior and ecotoxicological profile from the parent compound. Formation of TPs occurs mainly through oxidation, hydroxylation, hydrolysis, conjugation, cleavage, dealkylation, methylation and demethylation. The EPs and their TPs can move vertically through the soil profile to groundwater and away from the source site with mobile groundwater. They also have the potential to reach surface water, when they travel laterally either as surface runoff or through subsoil tile drains, entering streams, major rivers, reservoirs, and ultimately estuaries and oceans [7].

Since there is a gap on the information on the occurrence and toxicity of TPs in the environment, we are unable to evaluate their significance in risk assessment [8, 9]. Standardized toxicity tests can provide quantitative information on the toxicity of the TP, compared to its parent compound, but these studies are limited [10-12]. In general, transformation products are less toxic and more polar than the parent compounds. However, in some cases, they may be more persistent or exhibit higher toxicity or be present at much higher concentrations [13].

Although there is legislation regulating chemicals like pesticides, veterinary drugs, persistent organic pollutants (POPs) and others, few is mentioned for

their TPs. Concerns over the TPs of pesticides in plants have been expressed since 1991 (European Directive 91/414/EEC), while the term “metabolite” appears in Regulation (EC) 1107/2009 concerning the plant protection products and in Directives 2001/82/EC and 98/8/EC, concerning the veterinary medical and biocidal products, respectively. European Medicines Agency (EMA, 2006) referred also to the need for assessment of potential environmental risks of human medicinal products. However, in all these documents, there is no clarification on the determination, limits and toxicological effects of metabolites or TPs. In Organisation for Economic Co-operation and Development (OECD) guidelines, concerning the Aerobic and Anaerobic Transformation in Aquatic Sediment Systems, adopted in 2002, it is claimed that TPs detected at  $\geq 10\%$  of the applied radioactivity should be identified. Meanwhile, the EU Regulation 1907/2006 (REACH) requires the identification of major transformation and degradation products for the registration of the substance. In the Regulation (EC) 850/2004 on persistent organic pollutants, a reference to their transformation processes also exists.

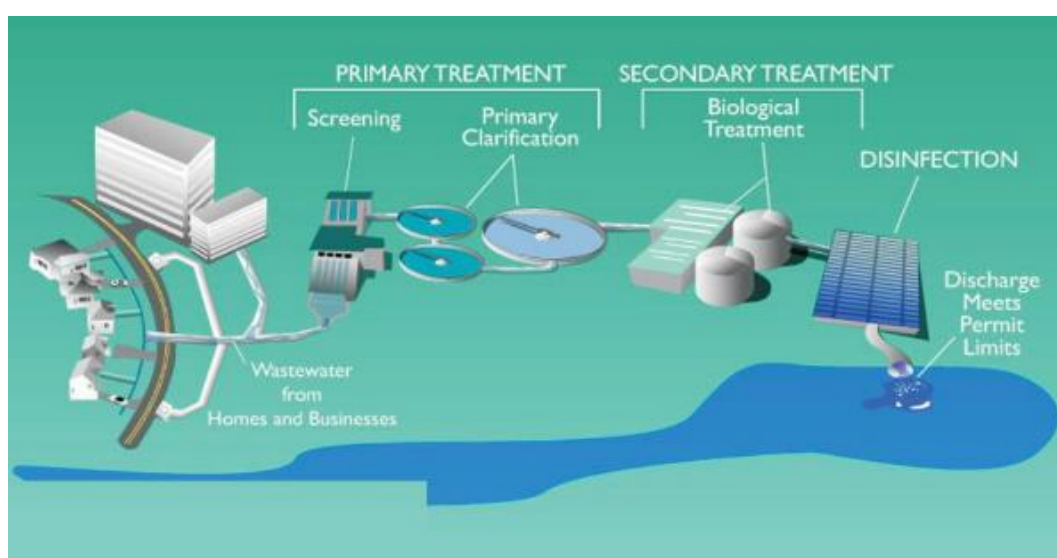
Transformation products occurring in the environment can be classified into two main categories: TPs formed by biotic or abiotic processes. The biotransformation products include human, animal and microbial metabolites in engineered and natural systems. The abiotic TPs are the outcome of hydrolysis, photolytic and photocatalytic degradation in the natural environment as well as water treatment processes, like chlorination, ozonation and advanced oxidation processes.

### **1.3. Conventional wastewater treatment**

Wastewater Treatment Plants (WWTPs) are designed to remove organic carbon, nutrients, suspended solids and pathogens [14, 15]. However, several types of micropollutants have been detected in secondary effluents of WWTPs which cannot be fully degraded by current treatment systems and they are discharged to receiving waters [16]. This is the reason why the fate of micropollutants during the treatment processes of WWTPs is extensively studied and especially their fate during the process of disinfection. A typical WWTP consists of a pre-treatment unit, a primary treatment unit, an activated sludge unit and a disinfection unit.

### 1.3.1 Primary and Secondary treatment

Primary treatment removes a large amount of settleable matter and suspended solids and a part of the organic carbon through sedimentation. A sufficient operated primary treatment system typically removes up to 90% of the settleable solids, 40% to 60% of the suspended solids and 20% to 40% of incoming organic carbon. Through primary settling tanks the floating scum, is also removed. In addition, primary sludge is produced for disposal or for further management [17].



Source: <http://watertreatmentprocess.net/waste-water-treatment-process/classification-sewage-water-treatment-process/>

**Fig. 1.1.** Scheme of a Wastewater Treatment Plant.

The main target of secondary treatment, referred as biological treatment, is to achieve a high percentage of removal of organic carbon along with nutrients (if required) than the one accomplished in the primary treatment. The most adopted approach is the activated sludge process, while the trickling filter (or its variations) approach and the rotating biological contractor (RBC) approach are also used. All of the aforementioned processes use the ability of microorganisms to convert dissolved, colloidal and suspended organic wastes to more stable, low-energy compounds which are further removed in secondary settling tanks. As defined by the Clean Water Act (CWA), secondary treatment produces an effluent with no more than 30 mg/L BOD<sub>5</sub> and 30 mg/L total suspended solids [18]. Based on Directive 91/271/EEC concerning urban waste-

water treatment, the requirements of urban WWTPs effluents were set to 25 mg/L BOD<sub>5</sub>, 35 mg/L total suspended solids, 10-15 mg/L total nitrogen and 1-2 mg/L total phosphorus.

### **1.3.2 Disinfection processes**

The important treatment process which focuses to the destruction or deactivation of pathogenic microorganisms and the removal of organic matter in WWTPs is called disinfection [19]. It includes the use of chemical agents such as compounds of chlorine, and/or nonchemical agents such as ultraviolet (UV) light. In order to choose the most suitable disinfectant process, the desired effectiveness to destroy microorganisms and the absence or minimal level of its attendant by-products which are often toxic, mutagenic and carcinogenic, should be taken into account [20].

Oxidation processes such as chlorination, chloramination, ozonation, UV treatment and advanced oxidation by UV/H<sub>2</sub>O<sub>2</sub> treatment are the major processes used in advanced wastewater treatment for disinfection and removal of emerging contaminants [13]. The oxidative reaction mechanisms rely often on the formation of reactive and short-lived oxygen containing intermediates such as hydroxyl radicals ( $\bullet$ OH) [21]. Generally, the TPs formed are correlated to the conditions of the process, like the physicochemical properties of the matrix, and the specific conditions of the treatment (time, medium, etc.).

#### **Chlorination**

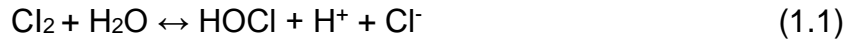
Chlorination is the most common disinfection method used in WWTPs due to its high effectiveness, increased availability in the market and its low cost [22]. Chlorine is delivered into the treatment system in liquid or gaseous form and the applied technology is targeted toward efficiency and effectiveness of the disinfectant, taking into consideration its distribution in it. The disinfection of wastewater is realized through the addition of chlorine as:

- Chlorine gas (Cl<sub>2</sub>)
- Chlorine dioxide (ClO<sub>2</sub>)
- Sodium hypochlorite (NaOCl)
- Calcium hypochlorite (Ca(OCl)<sub>2</sub>) and as
- Sodium chlorite (NaClO<sub>2</sub>)



Chlorine reacts with inorganic and organic compounds through oxidative reactions, losing its disinfectant role. The remaining (not reacted) quantity of chlorine, is available for disinfection and is called as free available chlorine.

When chlorine enters an aquatic media, hydrolysis and ionization reactions (Equations 1.1 and 1.2, respectively) take place.



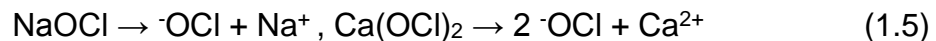
The corresponding rate constants (at 25 °C) of Eq. 1.1 and 1.2 are provided below as Eq. 1.3 and 1.4, respectively.

$$K_H = \frac{[\text{HOCl}][\text{H}^+][\text{Cl}^-]}{[\text{Cl}_2]} = 4.5 \cdot 10^{-4} \left(\frac{\text{mol}}{\text{L}}\right)^2 \quad (1.3)$$

$$K_i = \frac{[\text{H}^+][\text{OCl}^-]}{[\text{HOCl}]} = 3 \cdot 10^{-8} \left(\frac{\text{mol}}{\text{L}}\right)^2 \quad (1.4)$$

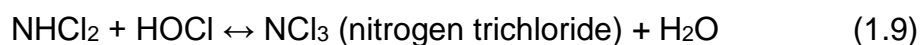
Hypochlorous acid and hypochlorite ions are called as “free available chlorine”. Their %molar ratio and distribution is highly affected by the pH value of the aqueous solution, a crucial chlorination operational parameter, since hypochlorous acid has 40 to 80 times more efficient germicidal effect compared to hypochlorite ion. Thus, an increase of pH value of the solution under chlorination treatment, will result in a decrease of disinfection effectiveness.

Whether chlorine is provided as hypochlorite salts, NaOCl and Ca(OCl)<sub>2</sub>, hypochlorous acid is formed by their hydrolysis (Eq. 1.5-1.6).



Wastewater contain nitrogen, in the form of ammonia and ammonium salt. Due to its high reactivity, hypochlorous acid rapidly reacts with ammonia for the formation of chloramines. The consecutive formation reactions of chloramines (monochloramine, dichloramine and nitrogen trichloride) are presented as Eq. 17-1.9.





Chlorine in the form of chloramines, is known as “bound chlorine”. The reactions of chloramines formations are affected by operational parameters like pH value, temperature, contact time, chlorine dose and the molar ration of chlorine and ammonia. For instance, the formation of monochloramine is favored by high pH values in combination with low chlorine to ammonia ratio. In general, monochloramine and dichloramine are the most predominant forms of chloramines, while nitrogen trichloride contribution is more or less negligible. Although chloramines can also be used as a disinfectant agent, their action rate is significantly lower [23].

Chlorine dose in WWTPs usually varies from 5 to 20 mg L<sup>-1</sup> depending on chlorine demand, wastewater characteristics and discharge requirement of a particular WWTP [24]. Although, the main purpose of chlorination is to eliminate pathogens, investigations have shown that chlorine reacts with micropollutants and natural organic matter in water and forms halogenated by-products which are toxic and can cause long-term health effects [22, 25].

In most cases, chlorination is not applied when oxidation of organic micropollutants is the goal, because it can produce biologically active TPs [26]. Especially when the inorganic content in the water matrix is very high, some reactive species like chloride or sulfate radicals are produced, which directly influence the formation of TPs. Chlorine radicals (Cl•) may lead to the formation of chlorinated organic compounds, which are known to be very harmful, and in some cases, able to generate persistent substances [27]. In this disinfection process, hypochlorous acid (HClO) is the main responsible reagent for pathogen destruction, but both HClO and ClO<sup>-</sup> react with organic compounds giving addition, substitution, or oxidation products. One of the major concerns regarding the disinfection by-products from chlorination is that NaClO is known to produce genotoxic TPs and can thus increase the acute toxicity [28]. It is recommended that the process of chlorination must be followed by dechlorination in order to remove the free and combined chlorine residuals.

Thus, it is crucial to decrease the toxicity of effluents before they end up in receiving waters [25].

### **UV Disinfection**

UV light is a growing technology for wastewater treatment disinfection. UV disinfection generally involves the use of electromagnetic energy generated from low pressure or medium pressure high intensity mercury arc lamps to inactivate efficiently several pathogens such as bacteria and viruses. The effectiveness of this method is determined by the quality of wastewater, the intensity of UV irradiation and the exposure time of microorganisms [20]. The required dose of UV irradiation which is used for disinfection purposes is 400 J/m<sup>2</sup> [29]. In addition, it has been noticed that the above mentioned dose of UV light may be sufficient to cause an important transformation of organic chemical components in water, both natural organic matter (NOM) and micropollutants [30]. Photochemistry represents an important degradation process, either in the environment, or as a light-related technical treatment process for advanced treatment of water. Many studies have been carried out regarding the direct and indirect photolytic or photocatalytic degradation of emerging pollutants. For pesticides, one review paper states the mineralization of a variety of pesticides by photocatalytic degradation [31], while a more recent work presents the by-products and intermediates of organophosphate pesticides by photocatalytic degradation [32]. Pharmaceuticals compounds [33-35], endocrine-disrupting compounds [34], UV filters [36], and phenol [37] have also been thoroughly surveyed for their fate, as well as for their TPs during photolysis. Disinfection of wastewater by UV irradiation is incubated as a promising alternative to chemical disinfection due to the absence of undesirable transformation products after treatment [38, 39].

### **Ozonation**

Ozone is a very strong oxidant and virucide. It is produced when oxygen molecules are separated by an energy source into oxygen atoms and instantly collide with an oxygen molecule to form an unstable gas. Due to its instability, ozone is decomposed to elemental oxygen within very short time and thus it is generated at the point of application [40]. In WWTPs, ozonation can be suitable

as a disinfection method after the secondary treatment, in order to remove the resistant substances remaining in the effluents [41]. Although it is considered as a more effective disinfectant than chlorine or UV, its application in urban WWTPs is limited due to the high cost of the method.

Ozonation is a technique of chemical oxidation which leads to complete or partial degradation of organic pollutants. Ozone is a very powerful oxidizing agent that can react with most species containing multiple bonds, such as C=C, C=N, N=N [42], but not with species containing single bonds like C-C, C-O, O-H, at high rates. This fact occurs because there is no easy chemical pathway for the oxidation to take place.

Moreover, ozone reacts with simple oxidizable ions such as  $S^{-2}$ . It is important to mention that the action of ozone usually depends on how it reacts with the pollutants. This means that the kinetic factors are determinant to know if ozone will oxidize a pollutant in a favorable time frame [43].

It has to be mentioned that, according to the literature, some operational parameters concerning the ozonation process can be optimized in order to achieve the maximum extend of pollutants' degradation in an energy efficient way [43]. Some of these important parameters are:

- *pH of the reaction solution*
- *Ozone partial pressure*
- *Contact time with the pollutant and interfacial area*
- *Presence of radical scavengers*
- *Operating temperature*
- *Combination with other oxidation processes (ex.  $O_3/UV$  ,  $O_3/US$  (Ultrasonic irradiation))*

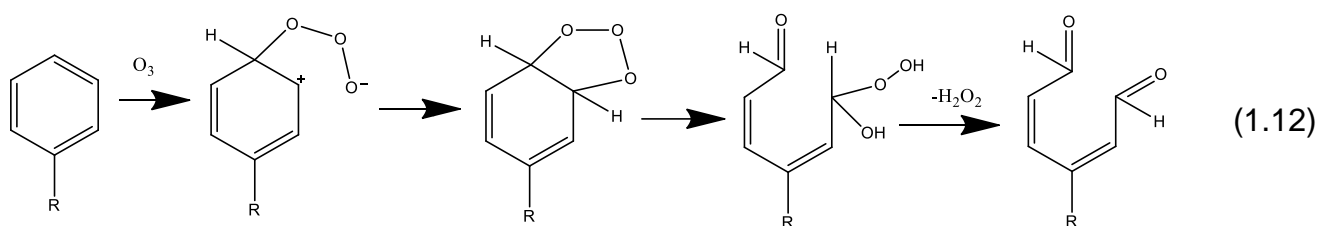
In addition, the reactions of ozone are characterized by high selectivity. However, ozone can be decomposed before the reactions with the pollutants-substrates take place. Beyond a critical parameter, the pH-value, decomposition products of ozone, usually the hydroxyl radicals ( $OH^*$ ), become the main oxidants. These reactions are unselective [44].

The reaction of ozone in aquatic solutions can be described with the following decomposition reactions:

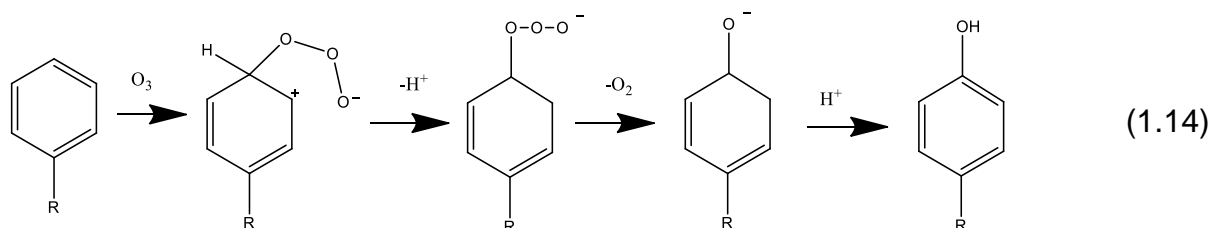
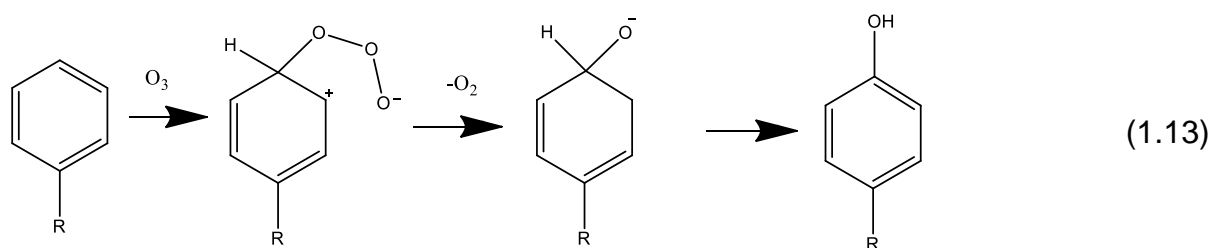


In order to control exclusively the process of oxidation with ozone, it is necessary to use scavengers. Scavengers are usually carbonate ions and less bicarbonate. They offer a protective effect due to electron transfer from  $CO_3^{2-}$  to  $OH^-$  and they act as inhibitors for the  $OH^\cdot$ -radical reactions with the substrate. Other substances, such as tertiary butanol (t-BuOH) and acetate, are used as  $OH^\cdot$  scavengers and prolong the lifetime of ozone [45].

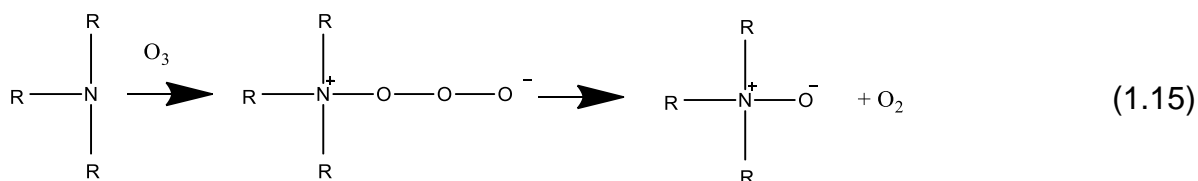
Some common reactions of ozone with aromatic compounds are presented below. First of all, the most predominant reaction between  $O_3$  and aromatic compounds is the formation of an ozonide, its breakdown and the formation of aldehyde groups:



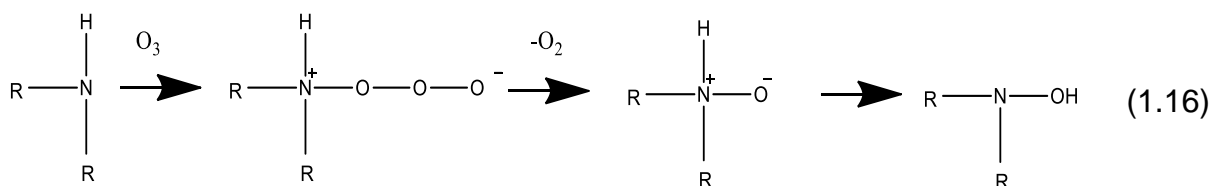
Another process that usually takes place is the hydroxylation of the starting material by two different pathways:



Furthermore, ozone reacts with tertiary amines in the following way, leading to the formation of N-oxides:



For secondary amines, the corresponding N-oxide is only a short-lived intermediate which rearranges into isomeric hydroxylamine:



Ozone has recently been implemented as a fourth full-scale treatment step in wastewater treatment [46-48]. This application of ozonation is under question because of the undetermined toxicity of the mostly unknown transformation products [49, 50]. Next to ozonation TPs, by-products formed by oxidation of matrix components such as carcinogenic N-nitrosodimethylamine (NDMA) and bromate have to be taken into a cost-benefit analysis of such technology [46, 47]. The degree of pesticide degradation, reaction kinetics, identity and characteristics of degradation by-products and intermediates, and possible degradation pathways through ozonation are covered and discussed in two review papers [51, 52]. An additional review on ozonation of pharmaceuticals has also showed satisfactory degradation efficiencies of a wide range of compounds in aqueous solution [53].

Nowadays, the researchers make an effort to identify ozonation TPs and specify if they are non-toxic or at least less toxic than the parent compound [15].

### **Advanced oxidation processes**

Advanced oxidation processes (AOPs) gain popularity as disinfection methods in WWTPs. Despite the fact that they all use different reacting systems, they

are having a common chemical feature which is the production of OH radicals. Some of the AOPs systems are presented in **Table 1.1**.

OH radicals are chemical species which react with organic compounds with a range of constant rates from  $10^{-6}$  to  $10^{-9}$   $M^{-1}s^{-1}$  [54]. OH radicals are characterized by low selectivity of attack which enables them to be strong oxidants in order to solve pollution problems in WWTPs. Moreover, the adaptability of AOPs in WWTPs is enhanced by offering various possible ways for OH radicals production, thus allowing a better compliance with the specific treatment requirements [55].

**Table 1.1.** Advanced oxidation processes [55].

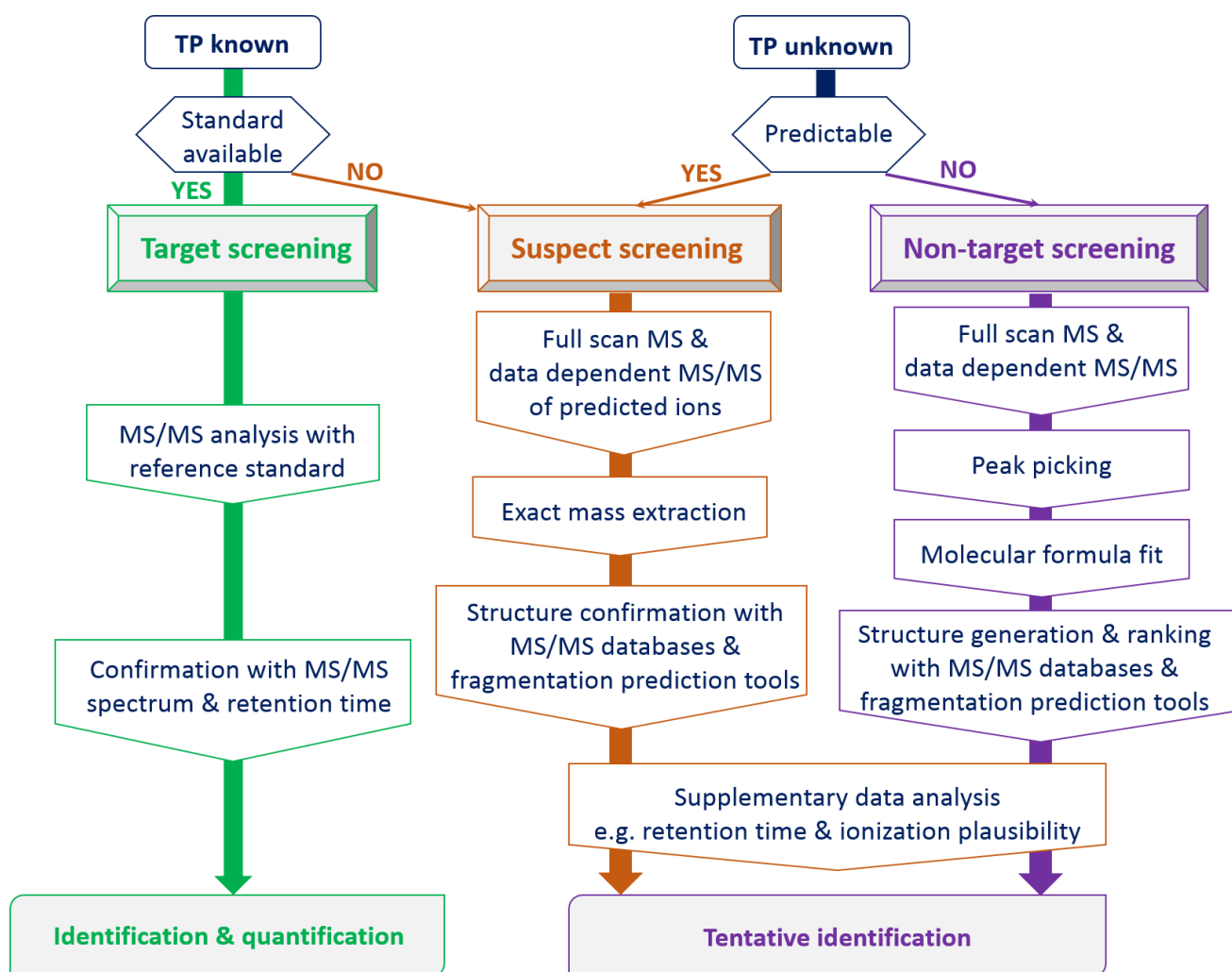
Oxidant	Type of process
$H_2O_2/Fe^{2+}$	Fenton
$H_2O_2/Fe^{3+}$	Fenton-like
$H_2O_2/Fe^{2+}$ ( $Fe^{3+}$ )/ UV	Photo assisted Fenton
$H_2O_2/Fe^{3+}$ - Oxalate	
$Mn^{2+}$ /Oxalic acid/ $O_3$	
$TiO_2$ / $h\nu$ / $O_2$	Photocatalysis
$O_3$ / $H_2O_2$	
$O_3$ / UV	
$H_2O_2$ /UV	

#### 1.4. Identification approaches - Analytical techniques

There are various workflows in the literature for the identification of TPs, dependent indispensably on the instrumentation and the available software. The main skeleton though is summarized below and is presented in **Fig. 1.2**:

- (a) The target analysis, which is based on the determination of already known TPs; the identification is carried out with standard solutions.
- (b) The suspect screening; a list of possible TPs is assembled from the literature or from prediction models and the samples are screened for those candidates.
- (c) The non-target screening; the identification of novel TPs is carried out with sophisticated post-acquisition data tools and supplementary analytical techniques.

Nowadays, liquid chromatography (LC) hyphenated to mass spectrometry (MS) using a variety of mass analyzers is the technique of choice for the investigation of EPs and TPs in environmental samples. LC is a suitable chromatographic technique for polar, thermo-labile compounds, thus for the identification of transformation products, which are generally more polar than their parent molecules. Mass analyzers commonly employed are the triple quadrupole (QqQ), time-of-flight (TOF), ion-trap (IT), Orbitrap and hybrid mass spectrometers, like quadrupole time-of-flight (Q-TOF), quadrupole-linear ion trap (Q-LIT), linear ion trap-Orbitrap or quadrupole-Orbitrap.



*'Known' TPs have been confirmed or confidently identified before, other TPs are considered as 'Unknown'*

**Fig. 1.2.** Flow chart of screening procedure of transformation products (TPs).

The development and use of powerful high resolution mass spectrometers (HR-MS) is the driving force to the development of novel analytical methodologies for the identification of TPs. Owing to their sensitivity in full-scan



acquisition mode and high mass accuracy, HR-MS are suitable for both target and non-target analysis, pre- and post- acquisition processing, retrospective analysis and discovery of TPs.

As a complement to LC-MS methods, gas-chromatography-MS (GC-MS) allows to investigate GC-amenable contaminants with low polarity and/or high volatility, such as siloxanes, musks, polychlorinatedbiphenyls (PCBs), polycyclic aromatic hydrocarbons (PAHs), poly-brominated diphenyl ethers (PBDEs), and certain pesticides, among others. Although single nominal analyzers like single quadrupole, ion trap or triple quadrupole can be used to this aim, HRMS is a superior technique for screening purposes. GC–HRMS has seldom been explored in environmental pollution monitoring until recently. Electron ionization (EI) source is the preferred ionization technique and the most widely applied due to its robustness, reproducibility and the existence of standardized commercial spectra libraries, which facilitates the identification of compounds. Databases are available with information for over 200,000 individual compounds, some of them already connected to software for non-target screening [56].

#### **1.4.1 Target analysis**

In target analysis, as shown in **Fig.1.2**, EPs and TPs are already known and standards are available, so that they can be included within a defined MS method and be monitored in routine analysis. LC hyphenated to triple quadrupole (LC-QqQ-MS/MS) is the workhorse nowadays in target analysis. The QqQ analyzer permits the application of various MS/MS modes, like product ion scan, precursor ion scan, neutral loss scan and selected reaction monitoring (SRM), which is the most predominant. SRM mode provides several advantages and interesting characteristics for target analysis such as increased selectivity, reduced interferences and high sensitivity, which allows a robust quantification. Another important point is the possibility of diminishing the analysis time, including extraction and instrumental determination.

With the use of LC-QqQ-MS/MS, adequate results have been obtained concerning the analysis of emerging contaminants and the identification and

quantification of their TPs, especially in the field of pesticides and pharmaceutical compounds, where standards are available.

In the past decades, multi-residue LC-MS methods were developed for the analysis of organic contaminants in environmental waters, such as drinking water, groundwater, surface waters, including seawater and fresh water and wastewaters [57]. The majority of these methods were aiming at the detection of pharmaceuticals [58], pesticides [59] and licit and illicit drugs [60]. Various review papers list multi-residue methods for the analysis of emerging pollutants [57, 61].

A list of various TPs of pesticides such as aldicarb, diuron, fipronil and malathion has been recorded by Martínez-Vidal et al. [59]. In 2006, Hernández et al. have developed a LC-QqQ-MS/MS method for the determination of 52 pesticides and known TPs in a multiple reaction monitoring mode [62].

Pharmacokinetic studies and identification of human metabolites have been carried out for the majority of pharmaceutical compounds and drugs. TPs of anthelmintics, NSAIDs, psychoactive and illicit drugs and drugs of abuse have been determined in literature by low resolution (LR)-MS [63-66]. Another study also presents a critical review of available literature on pharmaceutical metabolites since 2009, primarily focusing on their analysis with LR-MS and toxicological significance [67].

High resolution mass spectrometry (HR-MS) on target analysis offers promising solutions to the limitations of SRM analysis which allows only monitoring of specific TPs. Virtually all compounds present in a sample can be determined simultaneously with HR-MS instruments operating in full-scan mode, making no pre-selection of compounds and associated SRM transitions necessary. Target compounds included in a database are screened in the sample based on mass accuracy, isotopic pattern, retention time and MS/MS fragments. Alternatively, hybrid instruments offer the possibility of data-dependent MS/MS acquisition, where a MS/MS analysis is triggered if a compound from a target ion list is detected in the full scan. Moreover, HR-MS instruments have the ability to differentiate isobaric compounds with the same nominal mass but different molecular formula due to their higher resolving power [8, 68-71].

HR-MS outperforms LR-MS, regarding the level of identification of an unknown compound, since within decision 2002/657/EC, it gains more identification points and can provide mass accuracy, even in full scan mode. An ion in HR-MS gains 2 identification points, instead of 1 in LR-MS, whereas HR-MS<sup>n</sup> transition products gain 2.5 instead of 1.5. It is clear that in HR-MS full scan mode, more than one ions are present in the mass spectra and evaluated.

#### **1.4.2 Suspect screening of EPs - prediction of TPs**

Suspect screening is the technique of choice for the identification of compounds, when the confirmation of the analytes with a reference standard is not possible, but molecular formula and structure of suspected molecules can be predicted (**Fig. 1.2**) [69, 70, 72-74].

A suspect list can be compiled from theoretical assessment based on consumption data, registered organic synthetic insecticides, fungicides, biocides and acaricides, including all major metabolites of the most commonly used insecticides and fungicides, as well as important pharmaceuticals used in the country of the study, which were not yet included in the target list [75]. Over 2000 suspect compounds were chosen in another study based on literature reports and author's knowledge on the occurrence of these compounds in water or the expectation that a compound could be of importance for the water cycle, due to its use and its physicochemical properties [76].

In suspect screening, an important step of the identification workflow is the prediction of possible TPs using computational (*in silico*) prediction tools. Commercially available or freely accessible programs have been applied in the prediction step on environmental analysis, including the University of Minnesota Pathway Prediction System (UM-PPS) [10, 77], CATABOL [78], PathPred [79] and Meteor [80]

The prediction system should be properly selected by considering the organism/system where TPs are formed. Meteor was built based on mammalian biotransformation reactions of common functional groups and allows prediction of the most probable transformation products, providing in parallel relevant literature references. PathPred is a multi-step reaction prediction server for biodegradation pathways of xenobiotic compounds and

biosynthesis pathways of secondary metabolites. It is linked to KEGG metabolic pathway maps and it has the potential to link the prediction result to genomic information. CATABOL and UM-PPS predict microbial metabolic reactions based on biotransformation rules.

As UM-PPS is freely accessible and all applied rules are clearly assigned, it is the most common prediction tool in suspect screening and many researchers have tried to evaluate and improve its prediction power [10, 73, 74, 81]. The prediction rules behind UM-PPS are coming from the University of Minnesota Biocatalysis/Biodegradation Database (UM-BBD) and literature [82]. Since UM-BBD has integrated data generated from pure microbial cultures, the predicted pathways may not be completely appropriate for environmental systems [10]. The relatively high false positive rates of all prediction systems are of concern, since the inclusion of additional pathways increases the number of possible degradation products [83]. In UM-PPS combinatorial explosion can be limited by prioritizing the different rules using relative reasoning [84].

Suspect screening is performed by the HR-MS analysis; the exact mass for each of the predicted TPs is extracted from the chromatogram and checked by comparing with control samples. An intensity threshold value is applied to cutoff unclear spectra. The chromatographic retention time ( $t_R$ ) plausibility, isotopic pattern, and ionization efficiency are used as further filters to narrow down the number of candidate peaks. Furthermore, using the MS/MS or MS<sup>n</sup> operating mode, structures of suspected TPs are suggested based on the observed fragmentation pattern.

Depending on the above criteria, there are different identification confidence levels in HR-MS analysis of TPs. When all the above criteria are fulfilled, a probable structure is proposed based on library spectrum match or diagnostic evidence. Otherwise, tentative candidates or just unequivocal molecular formulas are the outcome of the suspect screening [85].

One approach for processing the data would be the identification of key TPs in terms of persistence over the time of the experiment. It is carried out by a data processing method which is established based on peak detection, time-trend filtration and structure assignment. Open-source software is used for peak

peaking (e.g. MZmine) and processing of the chromatograms (e.g. enviMass), by noise removal and blank subtraction. Then, a meaningful time-trend is inquired and the remaining-candidate peaks are compared with a list from UM-PPS or from literature for tentative identification [86].

Another approach for suspect screening is based on the use of characteristic fragmentation undergone by emerging pollutants during MS/MS fragmentation events [73, 87]. It is based on the assumption that many TPs maintain a similar structure than the parent compound and therefore have common fragment ions. Thus, searching for specific fragment ions in MS/MS spectra throughout the chromatographic run could lead to new TPs. This is evident when applying product ion and neutral loss scans, and other techniques, such as mass defect filtering [88].

### **1.4.3 Non-target screening**

Non-target screening implies the identification of compounds for which there is no previous knowledge available and is usually carried out after target and suspect screening. Non-target screening becomes a challenging task, but in case of TPs further information of the parent compound, like the molecular formula, the MS/MS spectrum, the retention time and other physico-chemical data may contribute for further ranking of possible structures and facilitate the identification process [89]. For non-target screening, high resolution mass spectrometry is strongly required in order to have mass accuracy for confirmation of molecular formula and a reliable interpretation of the MS/MS spectra [70, 90, 91].

The challenge associated with HR instrumentation is the generation of massive quantities of data and subsequently their evaluation and the export of results. Moreover, their ability of operating in full scan and MS/MS mode simultaneously, provide even more data in a single run. For this reason, post-acquisition data-processing tools are necessary; computer-aided techniques provide rapid, accurate and efficient data mining. There is a number of open-source and commercial software for non-target screening, including MZmine [92], XCMS (<https://xcmsonline.scripps.edu>), EnviMass, Nontarget, ACD MS/Workbook Suite and vendors software like Bruker Metabolite Tools and

ProfileAnalysis, Waters MassLynx and MetaboLynx, Thermo Networks and Sieve, Applied Biosystems Data Explorer (MDS-Sciex Analyst QS) and Agilent MassHunter.

The general procedure, as shown in **Fig. 1.2**, has several steps until it reaches the final result, which does not follow the same order in every software. The first step is always the peak picking. In this step, comparison of the sample with control or blank samples is important to exclude irrelevant peaks. The removal of noise peaks, mass recalibration and componentization of isotopes and adducts is usually carried out automatically as the next step. The assignment of the molecular formula to the accurate mass of the peak is performed using heuristic filters such as the seven golden rules of Kind and Fiehn [93]. Exploration of databases such as ChemSpider, PubChem, DAIOS database, NIST or structure generation may lead to candidate structures [94-96]. Thereby information on the parent compound (e.g. molecular formula, substructures) can help to restrict the databases search and possible structures are likely to be proposed for the compound. However, databases contain mostly only EPs but many TPs are not included yet.

Even after filtering and strict criteria and thresholds in the above parameters, the number of peaks, which correspond to non-targets can exceed the number of 1,000. It is clear that elucidation of all those peaks would demand a great amount of time and effort; prioritization of the most intense peaks is a common strategy [80].

Similar to suspect screening, the observation of the presence/absence of common characteristic ions in the fragmentation pattern of both the parent compound and the TPs, evidencing the stability/reactivity of certain parts of the molecule can be helpful [8]. For the ranking of the candidate structures, the information of MS/MS spectra has to be explored by comparing the fragmentation pattern with *in silico* mass spectral fragmentation or with spectra in libraries. There are a few databases with mass spectra, like MassBank [97] and MetLin (<http://metlin.scripps.edu/index.php>), however, most software usually do not take into account the fragmentation pattern. MOLGEN-MS, ACD/MS Fragmenter ([www.acdlabs.com/products/adh/ms/ms\\_frag](http://www.acdlabs.com/products/adh/ms/ms_frag)) and MassFrontier ([www.highchem.com/index.php/massfrontier](http://www.highchem.com/index.php/massfrontier)) both use

fragmentation rules, whereas MetFrag offers a purely combinatorial approach based just on bond energies. Although the overall candidate ranking with MetFrag is not quite as good as that obtained with Mass Frontier and MOLGEN-MS, the scoring function used in MetFrag can improve the ranking significantly [98]. MetFusion, the newest development, combines MetFrag with spectral database searching [98]. The use of fragmentation trees as performed in SIRIUS is another approach for the structure elucidation [99]. In any case, criteria must be established for the success of the identification of the unknowns by the accuracy of the molecular ion, the isotopic fitting and the characteristic fragment ions in MS/MS mode [8].

Müller et al. proposed another approach for non-target screening, focusing on relevant compounds (features). The sample is not regarded as an isolated specimen, but rather it is evaluated in relation to a set of other samples based on considerations of e.g., their temporal, spatial, or process-related connections. This covers also the comparison of assays and controls as carried out in evaluation of many transformation experiments. The features of the sample are considered as mathematical sets and treated with statistical tools [94].

#### **1.4.4 Structure elucidation and identification confidence levels in HR-MS**

High mass accuracy coupled with high isotopic abundance accuracy is fundamental to elicit a reliable molecular formula generated by the software incorporated in the HR-MS instruments. The acceptable deviation of the experimental  $m/z$  from its corresponding theoretical of parent ions is usually defined at 5 ppm. This limit guarantees the correct prediction of their molecular formula. Higher errors, generally below 10 ppm, are acceptable in the workflow regarding their characteristic fragment ions. In spite of the fact that the accurate extrapolation of the elemental composition of a TP is essential, it is not sufficient to lead in a correct structure proposal.

A process which is very helpful in structure investigation is the observation of the presence or absence of similar characteristic ions in the fragmentation pattern between the parent compounds and its TPs. In addition, information from experimental MS/MS spectra can be compared with *in silico* mass spectral

fragmentation tools (e.g. MetFrag, MetFusion, Mass Frontier, MOLGEN-MS and ACD/MS Fragmenter) or with mass spectra in libraries (e.g. MassBank and MetLin) [100]. On the other hand, the use of mass spectral libraries is restricted for LC/MS-MS data because they do not have a great amount of available data and mass spectra of different instruments are not so comparable [101].

Consequently, the HR-MS based identifications of TPs differ among studies and compounds because it is not always possible to synthesize each compound and confirm it. In order to make easier the communication of identification confidence of TPs, Schymanski et al. (2014) proposed a level system which is described below (**Fig. 1.3**) [85].

- **Level 1:** Confirmed structure is the perfect situation where the candidate structure is confirmed by the measurement of a reference standard with MS, MS/MS and retention time matching.
- **Level 2:** Probable structure refers to a proposal for an exact structure based on different evidence.
  - **Level 2a:** Library which includes indisputable matching between literature or library spectrum data and experimental.
  - **Level 2b:** Diagnostic which refers in the case of no other structure fits in experimental data, but no standard or literature information is available.
- **Level 3:** Tentative candidate(s) is the situation where there is evidence for possible structure(s) but the experimental information is insufficient to the exact proposal.
- **Level 4:** Unequivocal molecular formula describes the case of an unambiguous formula which is assigned by the spectral information but there is no sufficient evidence to propose possible structures.
- **Level 5:** Exact mass (m/z) is detected in the sample but no experimental information exists in order to propose even a formula.



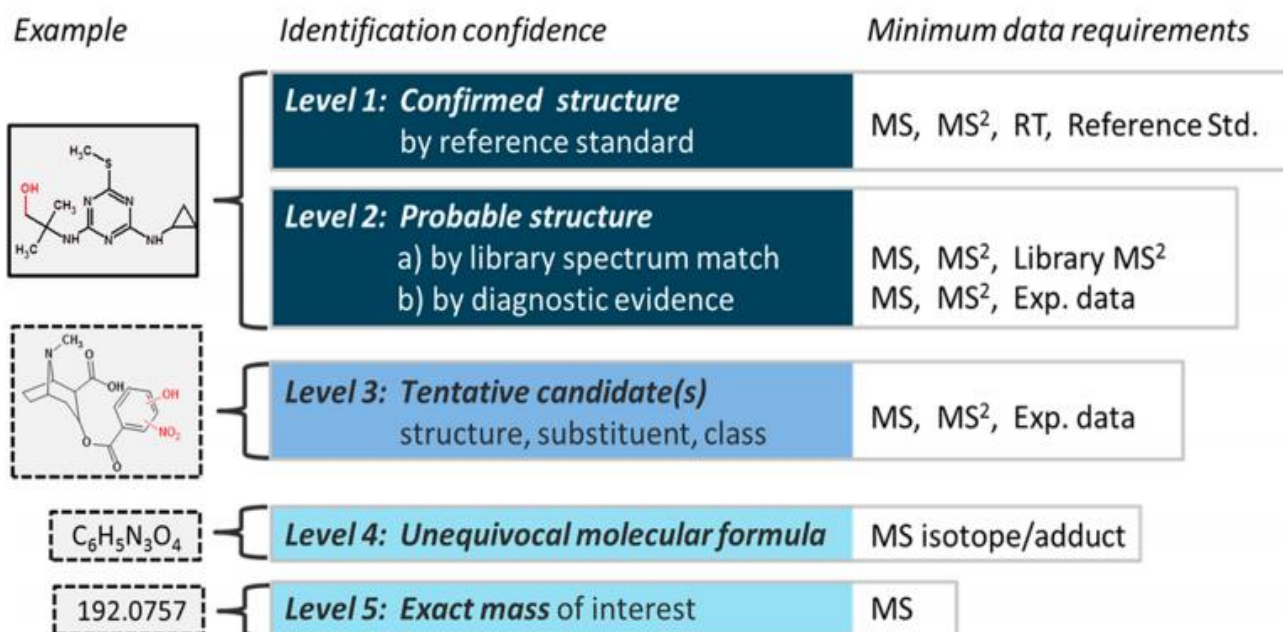


**Fig. 1.3.** Proposed identification confidence levels in HR-MS analysis [85].

## 1.5. Instrumental analysis

Both LC and GC are used for the determination of emerging pollutants, depending on the polarity, volatility and thermal stability of the concerning compounds. Due to the polarity of most pharmaceuticals, either LC-MS, or GC-MS combined with derivatization processes, is normally used for their determination [6, 102-105].

### 1.5.1 Gas Chromatography (GC) - Mass Spectrometry

Gas chromatography coupled to mass spectrometry (GC-MS) is the technique most commonly employed today for the analysis of volatile organic pollutants in environmental samples. The very high number of applications is the result of the efficiency of gas chromatography separation and the good qualitative information and high sensitivity provided by mass spectrometry.

The MS fragmentation pattern can often provide unambiguous component identification by comparison with library spectra. Huge electron ionization mass spectral libraries are commercially available, such as NIST Library, which contains 250,000 spectra and the Wiley Library with 720,000 spectra with the new combined version including approximately 950,000 spectra (<http://www.sisweb.com/software/ms/wiley.htm>). The identification process is

based on search algorithms that compare the obtained spectra with those of a library, which are generally implemented in the GC-MS instrument.

Several ionization techniques are used in GC-MS. Among them, electron ionization (EI) is the most popular because it often produces both molecular and fragment ions. In EI, gas analyte molecules are bombarded by energetic electrons (typically 70 eV), which leads to the generation of a molecular radical ion ( $M^+$ ) that can subsequently generate ionized fragments. This technique generally allows for the determination of both relative molecular mass and the structure of the molecule. One important feature of electron ionization spectra is that they are highly reproducible, which means that mass spectral libraries can be used for identification of unknowns. However, in some cases, EI does not provide the sensitivity required for the analysis of very small amounts of compounds in environmental samples. This is mainly due to extensive fragmentation [106].

Mixtures to be analyzed are injected into an inert gas stream and swept into a tube packed with a solid support coated with a resolving liquid phase. The compounds most commonly analyzed by GC-MS include alkanes, polycyclic aromatic hydrocarbons (PAHs), pesticides, polychlorinated biphenyls (PCBs), as well as endocrine disrupting chemicals [106]. For the determination siloxanes and synthetic musks in wastewater and soil samples, the method of choice is gas chromatography-mass spectrometry [107, 108].

### **1.5.2 Liquid Chromatography - High Resolution Mass Spectrometry (LC-HRMS)**

#### **Chromatographic separation**

A prerequisite for proper identification of TPs is the adequate separation of sample components. The parent compound and the TPs normally have part of the molecule in common, and the mass spectra have ions in common; therefore, the separation is important [109]. Because of the *a priori* unknown nature of the TPs generated, it is not possible to optimize the chromatographic separation conditions. Liquid chromatography is commonly performed in reversed-phase (RP) mode using C18 columns. A linear mobile phase gradient covering a large variety of polarities is the preferred choice for TPs separation.

An interesting approach that can be useful in the identification of more polar TPs is Hydrophilic Interaction Chromatography (HILIC). HILIC is a relatively recently introduced mode of liquid-phase separations that allows the separation of highly polar compounds by using a gradient of increasing aqueous content to elute analytes from a hydrophilic stationary phase. HILIC is becoming an attractive alternative or complementary approach to RP chromatography, due to the ability to separate hydrophilic compounds, which are poorly retained on RP columns [110]. On the other hand, HILIC coupled with electrospray ionization (ESI) potentially enables a higher sensitivity because the higher percentage of organic solvent in the HILIC mode contributes to more efficient desolvation during ESI [111].

### **High Resolution Mass Spectrometry**

LC-MS techniques provide a universal approach applicable to the widest number of emerging pollutants and this is the reason why they have today become the technique of choice in the field of environmental analysis. Among the different mass analyzers usually applied for target analysis, triple quadrupole (QqQ) is the most widely used for measuring and quantifying residues of EPs. However, a recent trend towards the high-resolution mass spectrometry (HR-MS; i.e. time-of-flight, TOF; Orbitrap; Fourier Transform-Ion Cyclotron Resonance, FT-ICR) is undoubtedly observed. HRMS gives the user access to a number of diagnostic tools which were not available earlier.

High resolution mass analyzers and hybrid mass analyzers, such as Q-TOF, LIT-Orbitrap, have opened a new era in environmental analysis. Due to their high resolving power resulting in accurate mass measurements, together with the isotopic fitting information and the fragmentation pattern elucidation can provide identification with high level of confidence for target analytes. Additionally, tentative identification of suspect and unknown compounds is feasible.

The use of LC-HRMS in target analysis has some advantages derived from the full-scan operation mode of this system. Full-scan data can be reprocessed without any *a priori* knowledge about the presence of certain compounds; that is, no analyte-specific information is required before injecting a sample and the

presence of newly identified compounds can be confirmed in previously analyzed samples simply by reprocessing the data. This retrospective analysis is the greater advantage of HR-MS target screening.

The application range of MS/MS is today extremely wide, providing different acquisition modes. It can facilitate sensitive and specific quantitative target measurements when operating in MRM mode. But also it can provide powerful untargeted approaches based on advanced scanning techniques like data-dependent or data-independent acquisitions.

### **Time of Flight (TOF) MS**

The basic principle of a Q-TOF instrument is outlined in **Fig. 1.4**.

TOF resolution is directly related to the length of the flight path. As a consequence modern high resolution instruments share the characteristics of flight paths with a combined length of several meters. The introduction of a reflectron doubles the flight path and regulates the kinetic energy, resulting in higher resolution. Since resolution is related to the length of flight time, TOF provides the highest resolution for relatively high  $m/z$  ion masses. Technical specifications often define resolution at such optimal  $m/z$  values. Resolving power is defined at full width at half maximum (FWHM) as  $m/\Delta m$ , where  $m$  is the  $m/z$  and  $\Delta m$  the width of the mass peak at half peak height. Orbitrap instruments produce the highest resolution for low  $m/z$  ions, which is opposite to the typical TOF performance. Of course, the price to be paid for high resolution is the number of acquired data points per time unit. Mass-resolving power in TOFMS is limited and increasing the mass-resolving power in Orbitrap-MS requires a reduced acquisition speed. Moreover in TOF instruments, the ratio of mass-to-peak width (at FWHM) is relatively constant over the entire mass range in contrast with Orbitrap analyzers.

The importance of sufficient mass resolution is that accurate and precise mass ( $m/z$ ) measurements become possible. Mass-measurement uncertainty in terms of mass accuracy (i.e. average mass error) and mass precision (i.e. standard deviation on the mass error) is based on calculating the relative (ppm) or absolute (mDa) difference between the measured accurate mass and the calculated exact mass of an analyte. Both mass accuracy and precision are

essential for proper measurements of accurate mass, and pinpointing different causes of mass-measurement uncertainty can lead to improvement [57].

Hybrid tandem mass instruments, such as the Q-TOF, provide relevant structural information by obtaining product ion full spectra at accurate mass. QTOF MS/MS experiments are an excellent way of confirming potential positives, and are highly useful for elucidating the structures of unknown compounds. There are 2 main MS/MS, also reported in the literature, depending on the nature of the analysis. For target analysis, data-independent acquisition (IDA) is the most preferred one. This approach, termed MS<sup>E</sup> (Waters) or bbCID (broad band Collision Induced Dissociation) (Brukers), involves simultaneous acquisition of accurate mass data at low and high collision energy. By applying low energy (LE) in the collision cell, no fragmentation is taking place and the information obtained is actually is full scan MS spectrum. At high collision energy (HE), fragmentation of the ions takes place and MS/MS spectra are acquired. With IDA, both molecular and fragment ion are obtained in a single acquisition without the need of pre-selection of the analytes.

On the other hand, for suspect and non-target analysis, data-dependent acquisition (DDA) is more favorable, since information over specific ions can be collected. In this case, two possibilities are available. Either, 2 injections are made, one as a survey and the next with pre-selected ions, or the determination of the candidates of interest for MS/MS information is based on predefined selection criteria. So, there is a first scan, which is processed “on-the-fly” to determine the ions that will be fragmented in a second (data-dependent) scan. The major advantage of this approach is the collection of structural information in just one injection [112].

One of the drawbacks of TOF analyzers is the possibility of the detector saturation which usually implies loss of mass accuracy. Temperature changes are responsible for small thermal expansion or contraction of the flight tube length. This is why it is very important to perform mass calibration. There are three levels of mass calibration, external, internal and lock mass calibration. External and internal calibration must include at least the mass range of interest and can be performed with the same calibrant mixture. Lock mass calibration

provides an automated way of applying the linear correction calibration to each spectrum in the analysis and it requires the presence of a continuous signal.

## Schematic Hardware Overview

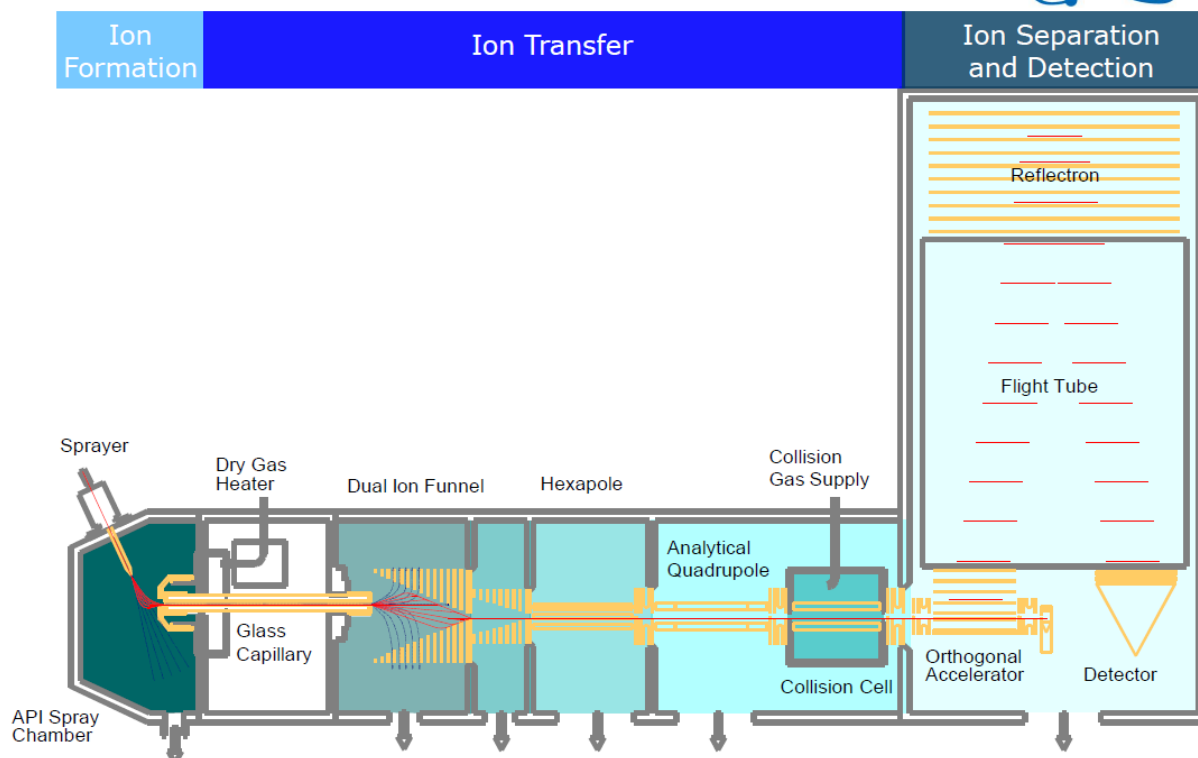


**Fig. 1.4.** Schematic presentation of a Q-TOF instrument (Maxis Impact, Bruker).

Full scan HRMS data contains a wealth of information. Unfortunately, more often than not, only a fraction of the information is extracted and utilized. Existing limitations are related to hard- and software. Most post-acquisition data processing strategies are based on the high information content provided by the measured accurate masses.

HRMS is particularly suited for multiresidue methods where a theoretically unlimited number of compounds can be monitored. Unfortunately, the currently available software is responsible for a number of existing bottlenecks. Current limitations are the speed of data processing and the availability of tools for the confirmation of suspected findings. Insufficient as well is the current tool box regarding software capable in utilizing the rich information present in HRMS data (data mining).

## CHAPTER 2.

### Scope and Objectives

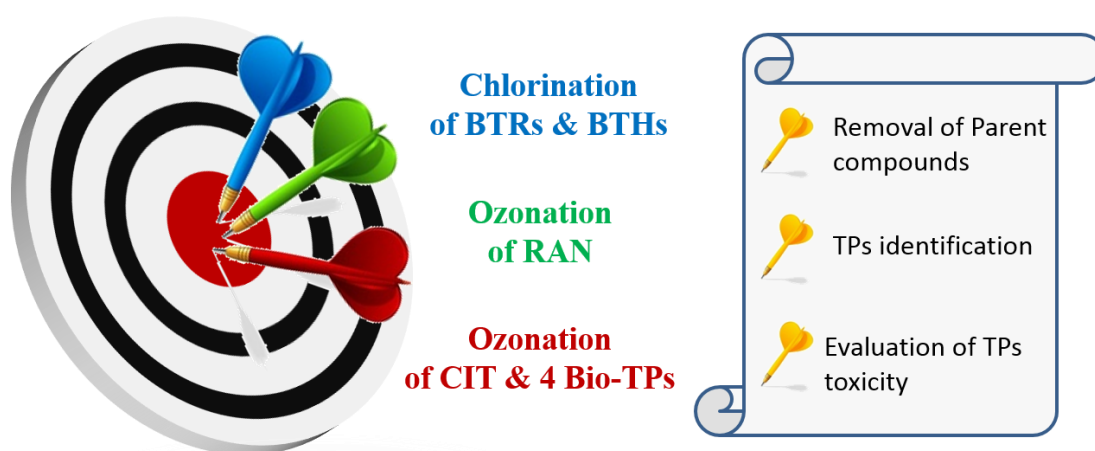


**Fig. 2.0** Graphical abstract of Chapter 2.

#### 2.1. The analytical problem

A large number of emerging pollutants, including pharmaceuticals and industrial chemicals are present in domestic, agricultural and industrial wastewaters, which end up to WWTPs. Many of these micropollutants are not entirely removed with the conventional processes that are applied in WWTPs, and thus are detected at various concentrations in environmental samples, like surface waters. The application of a disinfection step prior to the final discharge of the effluents into the environment, may significantly contribute to EPs elimination. Chlorination, ozonation, exposure to UV radiation, or advanced oxidation processes are basically used as tertiary treatment processes worldwide. The operational parameters of these processes, like the pH value of the reaction solution, applied dose, temperature, contact time etc., highly affect the removal of EPs, while the optimum values can be extracted through experimental investigation. Although the primary purpose of disinfection processes is the effluents disinfection and the elimination of micropollutants via oxidation, several investigations have shown that the applied oxidant (chlorine, ozone, hydroxyl radicals) reacts with micropollutants leading in the production of undesired by-products and the formation of their transformation products. Concern has been raised over the last five years on the identification of TPs,

whose structure, physicochemical properties and potential toxicity are unknown. Those compounds may be formed in high concentration levels and may also be more persistent and toxic than their precursors.

Recent advances and improvements in analytical techniques, and especially in high resolution mass spectrometry, have opened up new windows of opportunity in the field of detection and identification of unknown compounds, even in complex matrices, like wastewater. Moreover, the development and application of suspect and non-target screening methods enabled the tentative identification of TPs, while toxicity prediction models can be used for the risk assessment of their occurrence.

Due to all the aforementioned reasons, the investigation of EPs removal during tertiary treatment processes, the identification of their TPs and finally their toxicity evaluation, has become a significant trend in Environmental Chemistry studies. However, the TPs identification approaches can be enhanced through the use of HILIC as a complementary chromatographic method to RPLC, due to its capacity to strongly retain polar TPs (with higher sensitivity) and separating isomeric TPs that may co-elute in RP (since additional retention mechanisms take place in HILIC). The use of HILIC for the identification of polar TPs has not been extensively reported in the existing literature. Furthermore, the use of retention time prediction model in order to support the proposed tentatively identified TPs structures has recently been incorporated into non-target workflows. Although sophisticated software is used for the application of non-target screening methods, this procedure still requires the implementation of several steps in order to reach identification and remains the most time-consuming workflow. For this purpose, advanced chemometrics tools need to be developed to proceed non-target screening as a fully automated task.

Last but not least, so far, studies concerning the transformation of emerging contaminants during a disinfection method (ozonation, chlorination, UV treatment), have been focused on the probable transformation of known contaminants and less frequently on their known human metabolites. Disinfection processes follow biodegradation processes (secondary treatment) in real WWTPs conditions. Since recent literature has revealed the formation of biotransformation products of emerging contaminants during secondary



biological treatment, their probable transformation during tertiary treatment should not be overlooked, since they may also pose a significant environmental risk to the aquatic system.

From now on throughout this thesis, any reference to the “tertiary treatment processes”, would imply the use of disinfection methods.

## **2.2. Research objectives and Scope**

The experimental part of this doctoral thesis is consisted of three individual studies.

In the first study (**Chapter 3**), chlorination batch experiments were performed. The fate of four benzotriazoles [1-H-benzotriazole (1-H-BTRi), tolyltriazole (TTRi), xylyltriazole (XTRi) and 1-hydroxy-benzotriazole (1-OH-BTRi)] and three benzothiazoles [benzothiazole (BTH), 2-hydroxy-benzothiazole (2-OH-BTH) and 2-amino-benzothiazole (2-amino-BTH)], during chlorination was investigated. In the first step, their degradation under different experimental conditions (applied molar ratio of NaOCl and the target contaminant (m.r.), reaction’s contact time, pH value of the reaction’s solution and the influence of total suspended solids (TSS) presence) was evaluated and their removal kinetics parameters ( $k_{obs}$  and  $t_{1/2}$ ) were determined. In the second step, LC-QTOF-MS/MS was used for the detection and identification of their TPs formed during chlorination, through the application of suspect and non-target screening approaches, while their retention time was also evaluated in order to support the proposed structures, by using an in-house retention time prediction model. Moreover, secondary treated wastewater samples from Psyttaleia WWTP (Athens, Greece) were spiked with the tested compounds and then subjected to batch chlorination experiments in order to prove that the identified TPs can also be formed in real conditions. The environmental relevance of their occurrence in real samples was also assessed through toxicity Ecological Structure Activity Relationships (ECOSAR) software calculations.

The second study (**Chapter 4**) focused on the effect of experimental parameters on the removal of ranitidine (RAN) during ozonation batch experiments and the identification of the formed TPs. The influence of pH value, the initial ozone concentration, the inorganic and the organic matter on RAN’s

removal were evaluated. The analysis of the ozonated samples was realized through the complementary use of both Reversed Phase (RP) and Hydrophilic Interaction Liquid Chromatography (HILIC) QTOF-MS/MS. This approach was followed in this study for a holistic detection of polar TPs that have not been eluted in the RPLC chromatographic system or for isomeric compounds that may have been co-eluted in RPLC. Suspect and non-target screening workflows were followed for the identification of RAN ozonation TPs, while an in-house retention time prediction model was used as a supporting tool for the proposed TPs structures.

Finally, the third study (**Chapter 5**), evaluates the fate of citalopram (CIT) and four of its biotransformation products [N-desmethyl CIT (DESCIT), CIT amide (CTRAM), CIT carboxylic acid (CTRAC) and 3-oxo-CIT (CTROXO)] during ozonation batch experiments. To our knowledge, this is the first study where the transformation of biotransformation products during tertiary treatment processes is tested. Their removal and transformation in reaction with six different ozone concentrations ranging from 0.06 to 12 mg/L were investigated. A Gaussian curve based trend analysis, using an in-house developed program, was performed for the first time for the automated detection of ozonation TPs. The structure elucidation of the detected TPs was realized based on their high resolution MS/MS spectra interpretation, where their spectra similarity score with the corresponding parent compound was also taken into consideration. The hypothesis that structurally-alike parent compounds follow common transformation pathways in reaction with ozone and that common TPs can be formed through the ozonation of different structurally-alike compounds, was also investigated. Moreover, the toxicity of the identified TPs, against three aquatic species, was predicted with an in-house risk assessment program to emphasize the environmental relevance of their detection.

## CHAPTER 3.

### Chlorination of benzothiazoles and benzotriazoles and transformation products identification by LC-HR-MS/MS

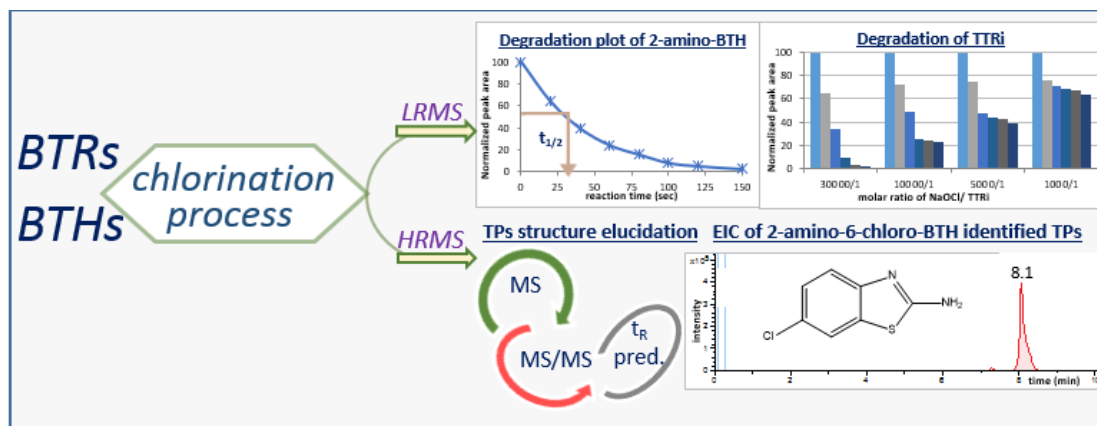


Fig. 3.0 Graphical Abstract of Chapter 3.

### 3.1. Introduction

In recent years, the occurrence and toxicity of contaminants in the aquatic environment, is a burning issue due to their possible adverse effects on the ecosystem and public health [102]. Emerging contaminants are compounds that are currently not included in routine monitoring programs but may be candidates for future regulation, depending on research evidence on their ecotoxicity, potential health effects, public awareness, and monitoring data revealing their occurrence in various environmental compartments [113]. 1,2,3-benzotriazoles (BTRs) and 1,3-benzothiazoles (BTHs) are classified as high production volume emerging environmental pollutants due to their broad industrial and domestic applications [21]. BTRs are used as corrosion inhibitors, de-icing fluids for aircraft, industrial cooling systems and silver protection in household dishwashing agents [114], while BTHs are used as vulcanization accelerators in rubber production, biocides in paper and leather industry, chemotherapeutic agents and corrosion inhibitors [115-118]. BTRs and BTHs seem to be only partially removed by the conventional primary and secondary treatment processes applied in wastewater treatment plants (WWTPs), since they have been detected in treated wastewater of various WWTPs in Europe [48, 114, 117, 119-124] and receiving water bodies [48, 114, 120, 125]. A review on their occurrence in different environmental samples worldwide is

provided in **Table S3.1** (Section S3.1.). In a recent study in Greece, the average concentrations of BTRs and BTHs in treated wastewater ranged between 11 ng/L and 3.0 µg/L [124]. Studies focused on their toxicity, have reported that benzothiazole (BTH) may pose a health risk at sufficiently high exposure [126]. Moreover, there is evidence supporting the toxicity of 1-H-benzotriazole (1-H-BTRi) and 5-methyl-1-H-benzotriazole (5-Me-BTRi) to terrestrial mammals and plants [127].

According to U.S. Environmental Protection Agency [25], an adequate process of disinfection, prior to the discharge of the effluents, is required. Nowadays, chlorination is the most prevalent disinfection method applied. Chlorine can be supplied as sodium hypochlorite (NaOCl) which reacts in water to produce the disinfectants hypochlorous acid (HOCl) and hypochlorite ion (OCl<sup>-</sup>), otherwise known as free chlorine [128]. Although the primary purpose of chlorination is the elimination of pathogens, several investigations have shown that chlorine reacts with micropollutants leading to the production of undesired transformation products [100, 129, 130]. Chlorine is a reactive chemical oxidant, capable of destructing micropollutants. But, since aqueous chlorine is not such a strong oxidant to completely mineralize micropollutants, numerous transformation products (TPs), generated through oxidation or substitution reactions, may be formed.

Recently, the identification and evaluation of chlorination TPs has been a topic of growing interest, since they may pose an environmental or human health risk, even higher than their parent compounds do. As an example, the reaction of the common pain reliever acetaminophen with hypochlorite leads in the formation of two toxicants 1,4-benzoquinone and N-acetyl-p-benzoquinone imine [74].

The last five years, researchers have been focused on the degradation and TPs' formation of some BTRs and BTHs derivatives *via* biotransformation [73, 131, 132], as well as using ozonation [118, 133, 134] and ultraviolet radiation [10]. Regarding chlorination, so far there are only two studies, performed by the same research team, investigating only the degradation of 1-H-BTRi in water and wastewater matrices [135, 136]. To our knowledge, no other studies have been published on the kinetics and TPs' identification of various BTRs and BTHs commonly found in treated wastewater.

### 3.2. Scope of the study

The aim of this study was to assess the fate of four BTRs [1-H-BTRi, Tolyltriazole (TTRi); the mixture of isomers 4-methyl-1-H-benzotriazole (4-Me- BTRi) and 5-Me-BTRi, 5,6-dimethyl-1-H-benzotriazole (known also as xylyltriazole, XTRi) and 1-hydroxy-benzotriazole (1-OH-BTRi)] and three BTHs [BTH, 2-hydroxy-benzothiazole (2-OH-BTH) and 2-amino-benzothiazole (2-amino-BTH)], during chlorination. Initially, lab-scale experiments were conducted in ultrapure water and secondary treated wastewater samples from Psyttaleia WWTP (Athens, Greece) in order to investigate the degradation of the aforementioned contaminants under different chlorination conditions (applied molar ratio of NaOCl and the target contaminant (m.r.), reaction's contact time, pH value of the reaction's solution, presence of total suspended solids (TSS)) and to determine their kinetics parameters by ultrahigh-performance liquid chromatography (UHPLC) coupled with tandem mass spectrometry (MS/MS). Thereafter, UHPLC high resolution (HR) MS technique was used in order to investigate the formation of possible TPs in the ultrapure water chlorinated samples and then verify their occurrence in spiked wastewater samples treated with chlorine. Retention time prediction was performed in order to support TPs identification, in addition to mass accuracy, isotopic and fragmentation pattern. Finally, toxicity assessment was carried out for the environmental relevance of the detected TPs.

### 3.3. Experimental part

#### 3.3.1 Chemicals

Standards of 1-H-BTRi (99%), BTH (97%) and 2-OH-BTH (98%) were purchased from Alfa Aesar GmbH & Co KG (Karlsruhe, Germany). Standards of 5-Me-BTRi (98%), 5,6-di-Me-BTRi hydrate (99%) and 2-amino-BTH (97%) were purchased from Acros Organics (Morris Plains, NJ). Standards of 1-OH-BTRi hydrate ( $\geq 98\%$ ), 4-Me-1-H-BTRi ( $\geq 90\%$ ) and sodium sulfite ( $\text{Na}_2\text{SO}_3 \geq 98\%$ ) were obtained from Sigma-Aldrich (Steinheim, Germany). Standard stock solutions (1000  $\mu\text{g}/\text{mL}$ ) of all target analytes were prepared in MeOH and were stored at  $-20\text{ }^\circ\text{C}$  for up to 3 months.

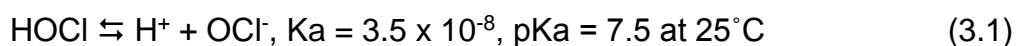
The probable TPs, 2-amino-4-chloro-1,3-benzothiazole (97%) and 2-amino-6-chloro-1,3-benzothiazole (99%), were purchased from Sigma-Aldrich (Steinheim, Germany). Ammonium acetate (cryst., 96%) and ammonia solution (25%) were purchased from Merck (Darmstadt, Germany), while glacial acetic acid (99.7%) was from Panreac Quimica SA (Barcelona, Spain). Methanol (MeOH) and acetonitrile (ACN) of LC-MS grade were obtained from Merck (Darmstadt, Germany). Ammonium acetate for mass spectrometry, formic acid [eluent additives for LC-MS] and ammonium formate LC-MS Ultra [eluent additive for UHPLC-MS] were from Fluka Analytical/Sigma-Aldrich (Steinheim, Germany). Chlorine was introduced as NaOCl from a commercial solution (4.8 g/100 g) (KLINEX, Greece). Solutions at the desired level were prepared daily, just before being used, by dilution in Milli-Q water, 18.2 MΩ/cm, (Millipore, Bedford, MA) and their concentration was standardized by the N,N-diethyl-p-phenylenediamine (DPD) method [137].

### **3.3.2 Chlorination removal experiments**

#### **Influence of operational parameters**

Chlorination experiments for the ultrapure water samples were carried out in closed amber vials that were maintained at room temperature ( $25 \pm 2^\circ\text{C}$ ). Synthetic raw water was prepared by spiking the tested contaminants in 10 mL of ultrapure water, adjusted to  $\text{pH } 7.0 \pm 0.2$  with 1 mM of ammonium acetate buffer solution ( $\text{CH}_3\text{COONH}_4$ ). Zero-time samples were removed, before NaOCl was added to the remaining solution. Aliquots of the reaction mixture were withdrawn at different time intervals and they were added to vials containing an excess of  $\text{Na}_2\text{SO}_3$  for the immediate quenching of the reaction. Four different concentrations (30, 100, 200 and 1000  $\mu\text{g/L}$ ) of all examined contaminants, corresponding to average m.r. 30000, 10000, 5000 and 1000/1, respectively, were tested and the experiments were conducted in triplicate.

The aqueous chemistry of chlorine is significantly pH dependent, thus various species of this oxidant with different reactivities with micropollutants, may be present in solutions [138]. Hypochlorous acid (HOCl), the active chlorine form in disinfection reactions, is a weak acid that further dissociates into two components, the hydrogen ion ( $\text{H}^+$ ) and the hypochlorite ion ( $\text{OCl}^-$ ), as follows:



From the Equation 3.1, it can be concluded that HOCl and OCl<sup>-</sup> species are equally distributed at pH 7.5, while HOCl and OCl<sup>-</sup> form predominates at lower and higher pH values, respectively. So, additional chlorination experiments were performed at pH 5.0, 7.0 and 9.0 (±0.2) for contact time up to 10 days and a m.r. equal to 200, for the evaluation of the influence of pH value and contact time on the contaminants' removal. The pH of the buffer solution was adjusted to the preferred value by dropwise addition of CH<sub>3</sub>COOH or NH<sub>3</sub> solution.

Afterwards, chlorination batch experiments were performed in secondary treated wastewater samples, for the evaluation of the matrix effect on the degradation of the tested contaminants. In these experiments, 20 ng/L of the tested compounds were spiked and NaOCl was added after the removal of the zero-time sample. Aliquots were taken at different reaction times and Na<sub>2</sub>SO<sub>3</sub> was added to stop the reaction. Samples were cleaned-up and the tested contaminants were fifty fold pre-concentrated by solid phase extraction (SPE) through Strata™-X cartridges, as previously described elsewhere [119]. Suspended solids contain organic substances that may compete with the target compounds for chlorine. To investigate the role of TSS on removal of the target compounds during chlorination, two concentration levels of TSS were tested (20 and 50 mg/L, representing a typical and a high suspended solids concentration in the effluent of secondary treated wastewater). The influence of the pH value (5.0, 7.0 and 9.0) on the effluent matrix was also tested.

### **Kinetics parameters determination**

All chlorination experiments were performed in a large excess of chlorine (m.r. of 1000-30000/1, **Table 3.1**) where the concentration of chlorine remains practically stable during the reaction ([chlorine] = [chlorine]<sub>0</sub>). In these experimental conditions, a pseudo-first-order dependence on the tested analytes' concentrations was displayed. Therefore, the chlorination kinetics equations can be written:

$$-\frac{d[\text{analyte}]}{dt} = k \times [\text{chlorine}] \times [\text{analyte}] \quad (3.2)$$

$$-\frac{d[\text{analyte}]}{dt} = k_{\text{obs}} \times [\text{analyte}] \quad (3.3)$$

$$\text{Ln} \frac{[\text{analyte}]_t}{[\text{analyte}]_0} = -k_{\text{obs}} \times t \quad (3.4)$$

where  $k$  is the second-order rate constant and  $k_{\text{obs}}$  is the observed pseudo-first-order rate constant.

From the linear time-course plots of  $\text{Ln}([\text{analyte}]_t/[\text{analyte}]_0)$ ,  $k_{\text{obs}}$  and  $t_{1/2}$  were determined based on the following equations:

$$k_{\text{obs}} = \left| \frac{\text{Ln} \frac{[\text{analyte}]_t}{[\text{analyte}]_0}}{t} \right| \quad (3.5)$$

$$t_{1/2} = \left| \frac{\text{Ln} \frac{1}{2}}{k_{\text{obs}}} \right| \quad (3.6)$$

### 3.3.3 Identification of transformation products

#### Identification of TPs experiments

The chlorinated samples (in ultrapure water) of all the tested contaminants, even those whose degradation was negligible, were analyzed by LC-QTOF-MS/MS for the investigation of the formation of probable TPs. The initial concentrations of the contaminants for these experiments were: 1000 µg/L for XTRi, 2-OH-BTH and 2-amino-BTH (m.r. 1000/1), 200 µg/L for 1-OH-BTRi and TTRi (m.r. 5000/1) and 100 µg/L for 1-H-BTRi and BTH (m.r. 10000/1). The chlorination experiments were conducted separately for each tested contaminant, even for the isomers 4-Me-BTRi and 5-Me-BTRi.

Then, the chlorination experiments were repeated in secondary treated wastewater samples to verify their production in real effluent matrix. Each contaminant was spiked at the desired level in the wastewater matrix, which had been previously filtered through 47 mm Whatman glass microfiber filters (GE Healthcare, UK).

For the TPs investigation, a blank sample, consisting of the buffer solution (or wastewater matrix, respectively), the disinfectant and the reaction's quencher, was also prepared as a control sample.



## **Identification workflows**

For the identification of possible produced TPs of BTRs and BTHs, a two-step post-acquisition data processing approach was followed, previously described by Gago-Ferrero et al [139], adjusted to the objectives of this study. Firstly, a suspect database of plausible TPs was compiled, including known BTRs' and BTHs' TPs that have already been identified in relevant degradation studies in the literature and proposed TPs by *in silico* prediction tools. Two prediction tools were used. The Eawag-Biocatalysis/Biodegradation Database Pathway Prediction System, which can predict candidate TPs based on biotransformation rules set in the Eawag-BBD (<http://eawag-bbd.ethz.ch/predict/>, last accessed September 2017) and scientific literature, and Metabolite Predict software (Metabolite Tools 2.0, Bruker Daltonics, Bremen, Germany), which proposes products by using a rule-based system according to the reactions occurring in mammals' metabolism. Metabolite Predict software also provides the opportunity of creating a new reaction to be considered. For example, in this study, a chlorination rule (i.e. chlorine atom(s) addition to the parent structure) was added, since chlorinated TPs are expected to be the most predominant compounds produced during the conducted experiments. Furthermore, since chlorination is an oxidation process, TPs being generated either by the oxidation of the parent compound or through the breakdown of the parent compound's structure are expected to be formed. Since our knowledge on these suspect compounds is most of the times restricted, their molecular formula is adequate for the initial full-scan screening. After compiling this list, all samples were screened for the detection of these database-suspect TPs. Taking into consideration that TPs are produced during the reaction, they should be detected only in the treated samples; neither in the blank nor in the zero-time sample. If a candidate TP was detected, then MS and MS/MS data were combined to support the proposed structure and result in the tentative identification of the TP.

In a second step, the non-target screening approach was followed, where the subtraction of the background signal is imperative in order to reveal any unknown peaks of potential TPs that could be present in the chromatogram, but could not be detected because they were covered up by the chromatographic

noise. Thus, from every chromatogram of the chlorinated samples (consisting of the buffer solution, the parent contaminant, the chlorine, the chlorination reaction's quencher reagent and the produced TPs) the chromatogram of the zero-time sample (consisting of the buffer solution and the parent contaminant) was removed by using Metabolite Detect software. The result of this subtraction is the creation of a new chromatogram where only the peaks that are much more intense in the treated samples than in the zero-time sample are now obvious in the base peak chromatogram. These peaks imply the presence of possible TPs and can be further treated as "suspect peaks".

The degradation of the contaminants during chlorination was measured by LC-MS/MS by using a triple quadrupole (QqQ) mass analyzer, in Selected Reaction Monitoring (SRM) mode of acquisition. Moreover, a quadrupole - time of flight (Q-TOF) mass spectrometer was used for the TPs screening due to the high resolving power, mass accuracy, and sensitivity in full scan acquisition.

#### **3.3.4 Instrumental analysis**

Two LC-MS instruments were used. The first one comprised a Thermo Scientific (San Jose, CA, USA) liquid chromatographic system consisting of a degasser, a UHPLC Accella pump, incorporating a column thermostat and an autosampler, interfaced to a Thermo Scientific triple stage quadrupole (TSQ) Quantum Access mass analyzer. The low resolution mass analyzer was used for the degradation monitoring, where compounds were separated on a Waters Atlantis T3 (100 mm×2.1 mm, 3 μm) column connected to a Phenomenex C18 guard column (4.0 mm×2.0 mm, 5 μm). Chromatographic analysis was carried out using a gradient elution program with ACN and Milli-Q water (acidified with 0.1% v/v formic acid) as binary mobile phase mixture at a flow rate of 200 μL/min. The gradient elution started with 5% (v/v) ACN and increased linearly to 40% ACN in 6.5 min, and then to 100% ACN in 10.5 min which was held for 4.1 min (until 14.6 min), reverted to 5% ACN at 15 min and re-equilibrated for 6.0 min (from 15.0 to 21.0 min) at 5% ACN for a total run time of 21.0 min. The MS analysis was performed with electrospray ionization (ESI) interface in the positive ion mode with a capillary voltage of 4000 V. The sheath gas (N<sub>2</sub>) and the auxiliary gas (N<sub>2</sub>) flow rates were set at 23 and 20 arbitrary units, respectively. The ion transfer capillary temperature was 290°C. The SRM and

the optimal operating conditions for tandem mass spectrometric analysis of the examined contaminants, that have been determined and reported in a previous study [119], are presented in **Table S3.2.** (Section S3.2.). The second LC-MS system comprised of a Dionex UltiMate 3000 RSLC system (Thermo Fisher Scientific, Dreieich, Germany) interfaced to a Quadrupole-Time of Flight mass spectrometer (QTOF Maxis Impact, Bruker Daltonics, Bremen, Germany). The high-resolution mass analyzer was used for the TPs identification. The chromatographic separation was performed on a Thermo Scientific Acclaim TM RSLC 120 C18 (100 mm×2.1 mm, 2.2µm) column. The Q-TOFMS system was equipped with an ESI interface and the MS analysis for the TPs' identification was performed in both positive and negative ionization mode. Chromatographic analysis was carried out using a gradient elution and flow rate program of twenty minutes duration, as shown in **Table S3.3.** (Section S3.2.). Milli-Q water/MeOH (90/10) (A) and MeOH (B), both containing 5 mM of ammonium formate and acidified with 0.01% v/v formic acid, were used as binary mobile phase mixtures, for the investigation of TPs in positive ionization mode, while Milli-Q water/MeOH (90/10) (A) and MeOH (B), both containing 5 mM of ammonium acetate, were used in negative ionization mode, respectively. The injection volume was set up to 5 µL. The operating parameters of the ESI were: capillary voltage, 2500 V (positive mode) and 3500 V (negative mode); end plate offset, 500 V; nebulizer, 2 bar; drying gas, 8 L min<sup>-1</sup>; dry temperature, 200 °C. The scan range applied in the full-scan mode was *m/z* 50-1000 at a 2 Hz scan rate, while resolving power was always between 36,000 to 40,000 (39,274 at *m/z* 226.1593, 36,923 at *m/z* 430.9137 and 36,274 at *m/z* 702.8636). After interpretation of the full-scan data, auto MS/MS analysis, based on an inclusion *m/z* list (data dependent MS/MS), was carried out in order to acquire clear fragmentation spectra of the investigated TPs. A Q-TOFMS external calibration was daily performed with a sodium formate solution, and a segment (0.1–0.25 min) in every chromatogram was used for internal calibration, using a calibrant injection at the beginning of each run. The sodium formate calibration mixture consists of 10 mM sodium formate in a mixture of water/isopropanol (1:1). The theoretical exact masses of calibration ions with formulas Na(NaCOOH)<sub>1-14</sub> in the range of 50–1000 Da were used for mass calibration. Mass spectra acquisition and data treatment was processed with Data Analysis 4.1,

Metabolite Tools 2.0 and Target Analysis 1.3 Bruker Daltonics software packages (Bremen, Germany).

### **3.4. Results and discussion**

#### **3.4.1 Removal of the tested contaminants**

##### **Influence of operational parameters**

Due to the low degradability of BTRs and BTHs observed upon chlorination with low chlorine concentration (tested molar ratios (m.r.) equal to 10, 30 and 100/1) in preliminary tests, all chlorination experiments were conducted with an extreme excess of chlorine. Thus, four different concentrations 30, 100, 200 and 1000  $\mu\text{g/L}$  of all contaminants in reaction with 6.5 mmol/L NaOCl, corresponding to average m.r. 30000, 10000, 5000 and 1000/1, respectively, were examined.

**Fig.3.1** shows the results obtained from the chlorination experiments, conducted in triplicates, of all contaminants in ultrapure water with the four tested m.r. (contact time up to 30 minutes). The analysis signals (peak areas) of the analytes in the chlorinated samples were normalized according to the corresponding zero-time sample. The removal rate of the BTRs was enhanced when increasing the applied m.r., thus the maximum removal of all BTRs was observed when the m.r. was 30000/1. In particular, 1-H-BTRi and TTRi were removed up to 62 and 98%, respectively, while 1-OH-BTRi and XTRi were totally eliminated. Even when the m.r. was 10000 and 5000/1, all BTRs were reduced by more than half. 1-H-BTRi was the only exception with removal lower than 24%. This finding agrees with Acero's et al. conclusion that chlorination is not a suitable procedure for the abatement of 1-H-BTRi [135, 136]. Regarding BTHs, no specific trend was observed. Either they appeared to be adequately removed within the first minutes of the reaction or not reacting at all. The removal of 2-OH-BTH and 2-amino-BTH during chlorination was higher than 59% and 93%, in the first 10 and 5 minutes of the reaction, respectively, regardless of the applied m.r. On the contrary, BTH did not seem to significantly react in all tested m.r. The maximum removal observed in m.r. 10000/1 was 45% after 30 minutes of reaction.

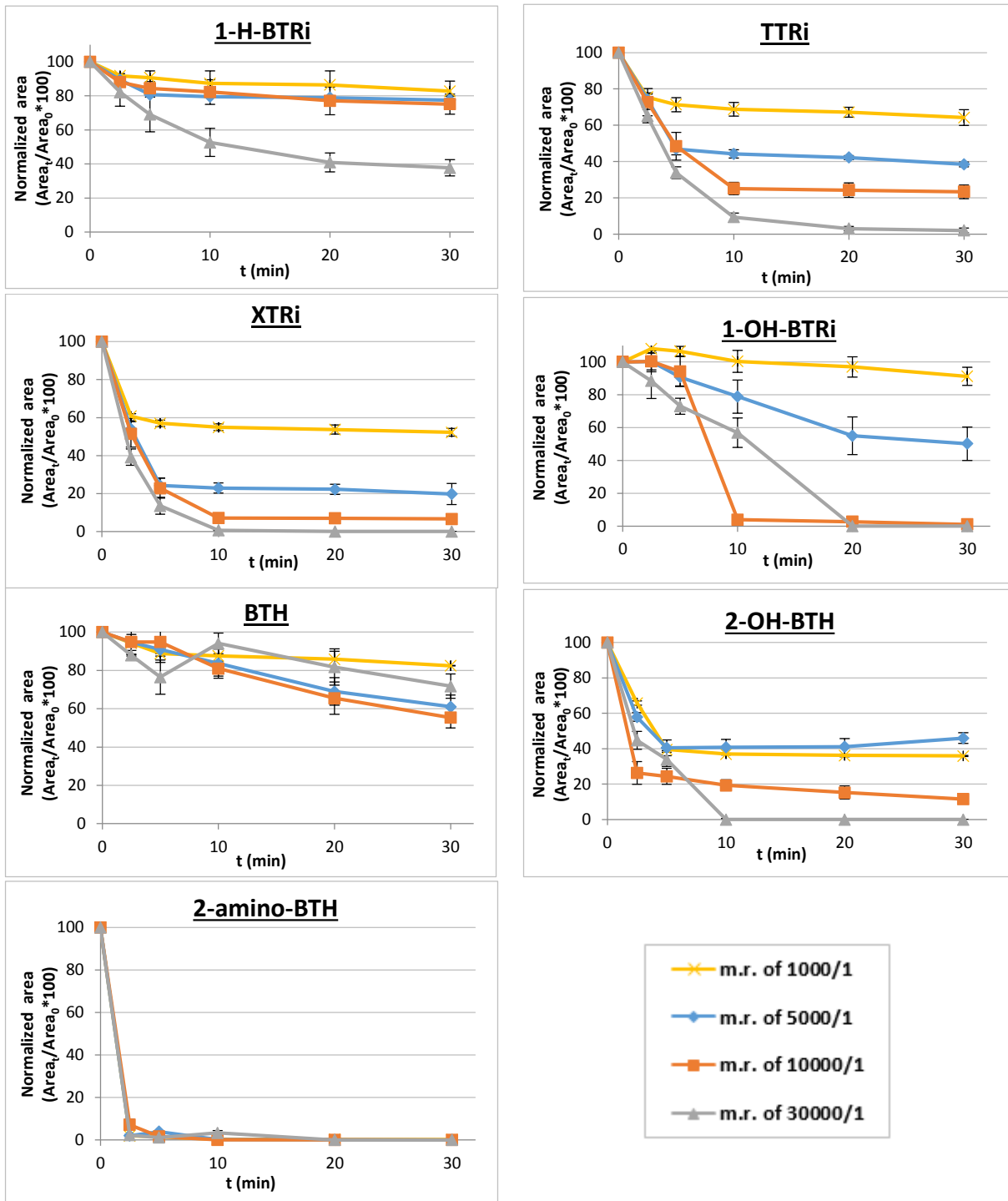


**Fig. 3.1.** Removal plots of all contaminants in the four molar ratios tested for chlorination time up to 30 minutes.

When a lower m.r. (200/1) was applied, 2-OH-BTH, 2-amino-BTH and 1-OH-BTRi reacted significantly within the first three days (**Fig. S3.1**, Section S3.3.). All the other contaminants were reduced to more than 50% after ten days of chlorination, except for BTH which was not reacted significantly.

Experiments with ultrapure water at different pH values showed that 2-amino-BTH and 1-OH-BTRi removal was accelerated at pH 5.0, while at pH 9.0 their elimination was poor (**Fig. S3.2**, Section S3.3.). These results are consistent with the literature as HOCl is more reactive and a much stronger disinfectant than OCl<sup>-</sup>, thus, chlorination's efficiency is promoted at lower water pH [140]. Quintana et al. observed a higher  $t_{1/2}$ , and thus a lower removal rate, of the tested pharmaceuticals as the pH increased [141]. Moreover, Acero et al. published higher rate constant concerning the removal of most of the tested compounds, including 1-H-BTRi, at lower pH [135, 138]. Similar results for the role of pH was also obtained in experiments with ultrapure water for TTRi, XTRi and 2-OH-BTH as well as when wastewater was used for 2-amino-BTH, 1-OH-BTRi, XTRi and 2-OH-BTH.

On the other hand, TTRi was not efficiently removed in the wastewater matrix. Regarding the effect of TSS on micropollutants' degradation, the presence of 20 and 50 mg/L of TSS in wastewater matrix did not affect contaminants' removal during chlorination primarily due to the high chlorine dose.

### **Determination of the kinetic parameters**

Taking into account the removal results obtained under the four different tested molar ratios, the kinetic parameters for each contaminant were determined in the concentration level in which at least 50% removal during chlorination was observed and the time-course plot of  $\ln ([\text{analyte}]_t / [\text{analyte}]_0)$  could be obtained with at least four data points, after the elimination of the outliers. The selected m.r. and the results are compiled in **Table 3.1**. It is obvious that 2-amino-BTH was removed faster than all tested contaminants during chlorination, bearing in mind that not only its kinetic parameters were determined when the lowest m.r. (1000/1) was applied, but also its removal during the chlorination experiment was higher than 90% just in a few seconds. 1-OH-BTRi was removed rapidly in both 30000 and 10000/1 m.r. Due to good linearity fitting, kinetic parameters were calculated at the 5000/1 m.r., resulting in a half-time of 30 min at this molar ratio. Finally, the contaminants, whose  $k_{\text{obs}}$  and  $t_{1/2}$  were determined with the same m.r., can be classified by increasing removal rate, according to the following order: 1-H-BTRi < TTRi and BTH < 2-OH-BTH < XTRi. Even if total elimination of micropollutants can be realized with

economically relevant chlorine doses, total mineralization is not achieved most of the times. As a consequence, TPs with unknown toxicological and ecotoxicological potentials may be formed.

**Table 3.1.** Chlorination kinetic parameters of all tested contaminants in ultrapure water (95% confidence interval).

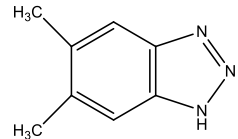
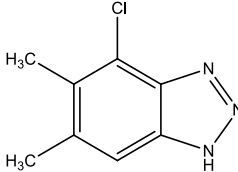
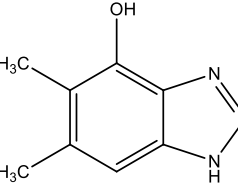
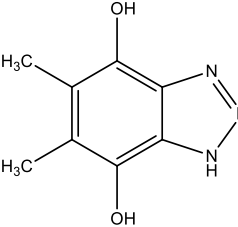
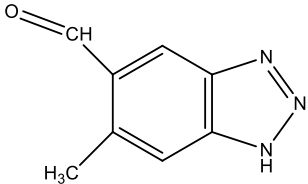
Contaminant	Molar ratio of NaOCl/contaminant	R <sup>2</sup>	k <sub>obs</sub>	t <sub>1/2</sub>
1-H-BTRi	30000/1	0.991	0.0635 (±0.0042) min <sup>-1</sup>	11.0 (±0.2) min
1-OH-BTRi	5000/1	0.992	0.0238 (±0.0012) min <sup>-1</sup>	30.1 (±0.4) min
TTRi	30000/1	0.994	0.241(±0.013) min <sup>-1</sup>	2.88 (±0.04) min
XTRi	10000/1	0.995	0.266 (±0.013) min <sup>-1</sup>	2.62 (±0.03) min
BTH	10000/1	0.990	0.0204 (±0.0010) min <sup>-1</sup>	34.7 (±0.4) min
2-OH-BTH	10000/1	0.998	0.058 (±0.035) min <sup>-1</sup>	8 (±1) min
2-amino-BTH	1000/1	0.733	0.0246 (±0.0004) sec <sup>-1</sup>	28.9 (±0.1) sec

### 3.4.2 Identification of transformation products

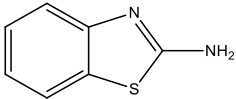
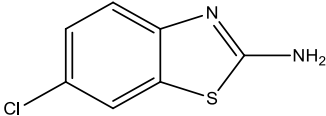
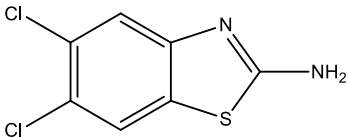
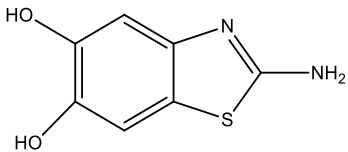
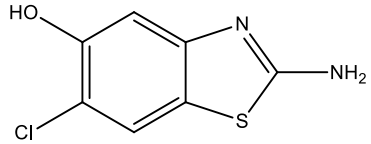
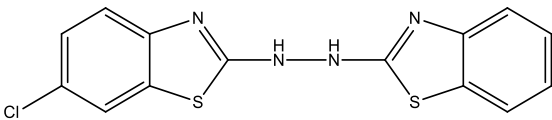
#### Application of identification workflows

Taking into account that TPs are produced in lower abundance than their parent compounds and that most of the tested contaminants were not completely removed during chlorination, high enough initial concentration of the contaminants is required to detect the probable formed TPs. However, the chlorination efficiency of most BTRs and BTHs decreased when higher initial concentration was used, as it was previously discussed, so an initial concentration compromise was necessary. Since 2-amino-BTH seemed to be rapidly and completely removed, an experiment with initial concentration of 10 mg/L (m.r. 100/1) was conducted in order to gain more abundant TPs' peaks. Through the application of the suspect screening approach, four TPs of XTRi and four of 2-amino-BTH, were detected in positive ionization mode. Their formation was verified based on their mass accuracy (m.a.), retention time (t<sub>R</sub>) and fragmentation and isotopic pattern. Their molecular formulas, structure, mass error, isotopic fitting and retention time are listed in **Table 3.2**, while their auto MS spectra are illustrated in **Fig. 3.2**.

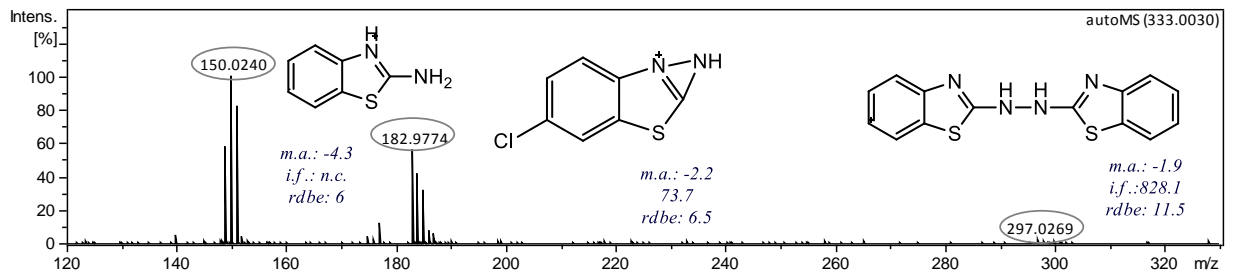
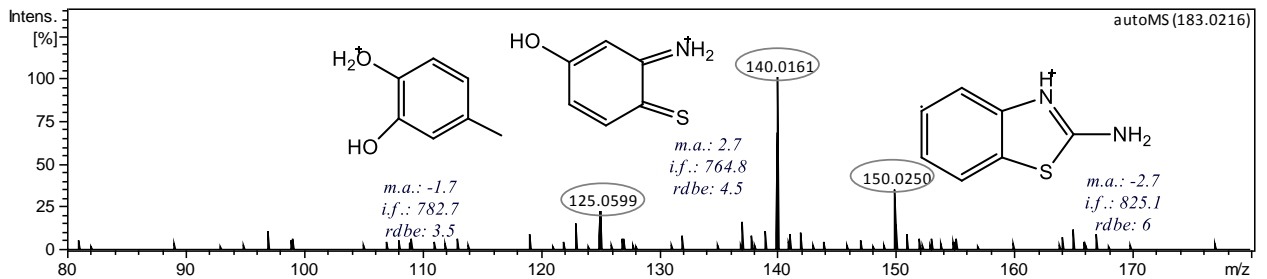
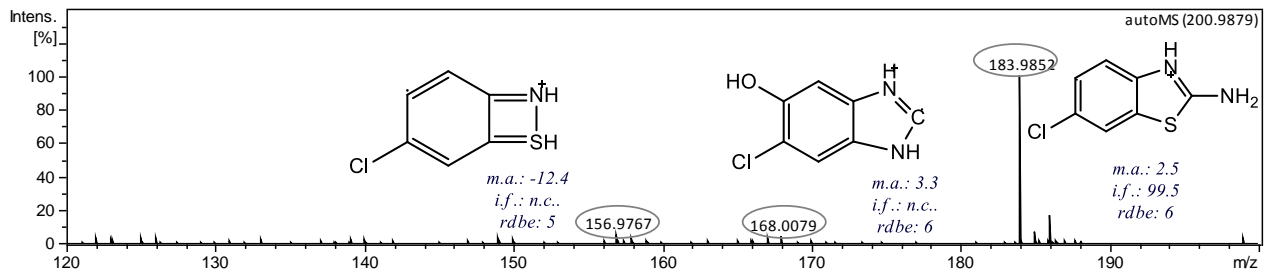
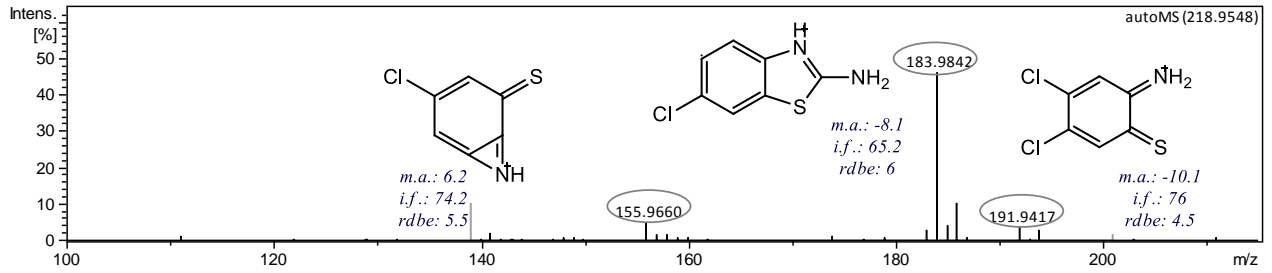
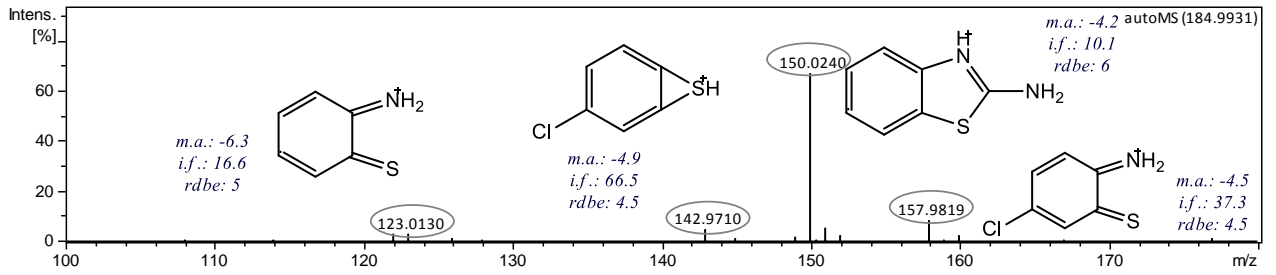
**Table 3.2.** Transformation products from the chlorination of XTRi, 2-amino-BTH and their identification parameters.

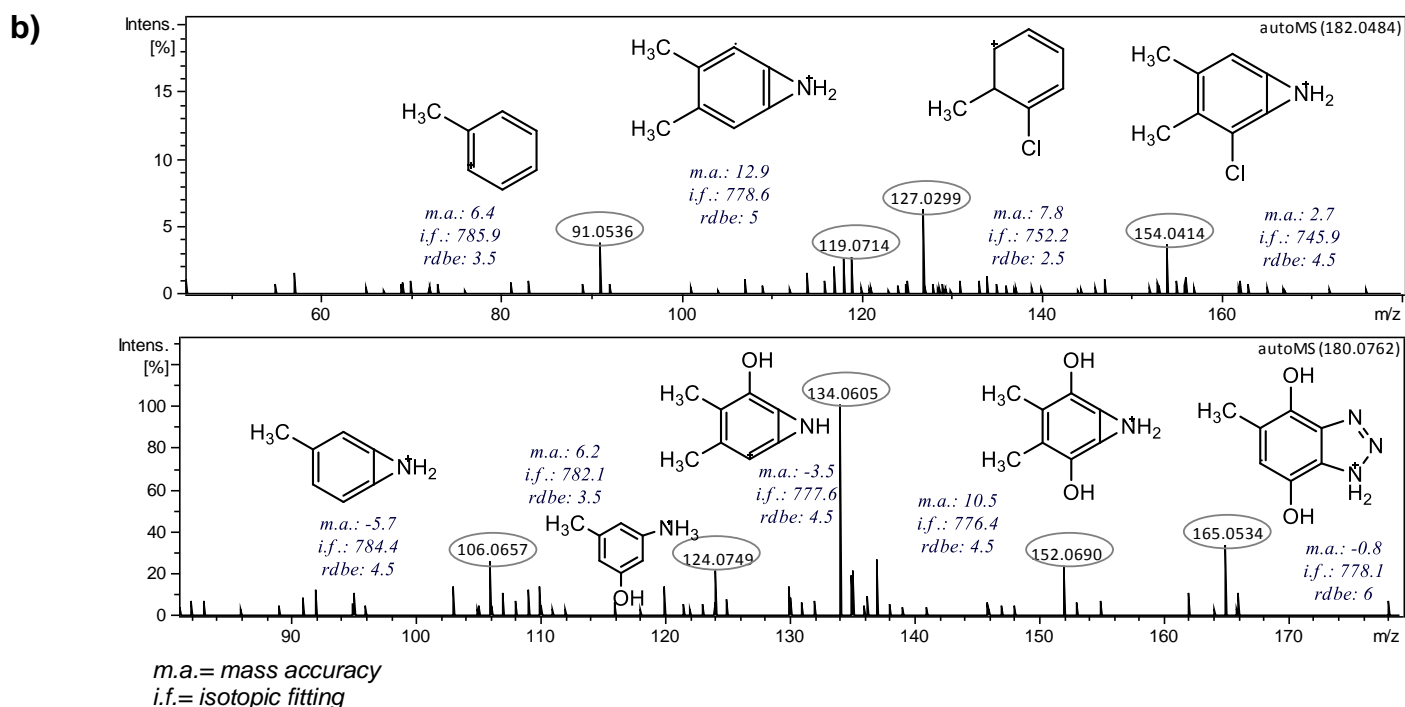
Name	Structure	Ion formula	Exp. $m/z$	Mass accuracy (ppm)	Mass error (mDa)	Isotopic fitting (mSigma)	rdbe	$t_R$ (min)
<i>XTRi</i>		$C_8H_{10}N_3$	148.0864	3.4	0.5	19.1	5.5	6.6
4-chloro- <i>XTRi</i>		$C_8H_9ClN_3$	182.0484	-2.2	0.4	58.4	5.5	8.0
4-hydroxy- <i>XTRi</i>		$C_8H_{10}N_3O$	164.0810	4.9	0.8	774.4 (low intensity)	5.5	4.4
4,7-di-hydro- <i>XTRi</i>		$C_8H_{10}N_3O_2$	180.0762	3.3	0.6	773.3 (low intensity)	5.5	3.6
5-methyl-BTR-6-carbaldehyde		$C_8H_8N_3O$	162.0654	4.9	0.8	774.5 (low intensity)	6.5	5.1



Name	Structure	Ion formula	Exp. $m/z$	Mass accuracy (ppm)	Mass error (mDa)	Isotopic fitting (mSigma)	rdbe	$t_R$ (min)
2-amino-BTH		$C_7H_7N_2S$	151.0323	0.7	0.1	20.5	5.5	5.9
2-amino-6-chloro-BTH		$C_7H_6ClN_2S$	184.9931	2.2	0.4	10.1	5.5	8.1
2-amino-5,6-di-chloro-BTH		$C_7H_5Cl_2N_2S$	218.9548	0.9	0.2	57.5	5.5	9.6
2-amino-5,6-di-hydroxy-BTH		$C_7H_7N_2O_2S$	183.0216	3.8	0.7	10.9	5.5	4.0
2-amino-6-chloro-5-hydroxy-BTH		$C_7H_6ClN_2OS$	200.9879	2.5	0.5	9.2	5.5	5.3
2-[2-(BTH-2-yl)hydrazin-1-yl]-6-chloro-BTH		$C_{14}H_{10}ClN_4S_2$	333.0030	-0.1	0	54.1	11.5	9.5

a)

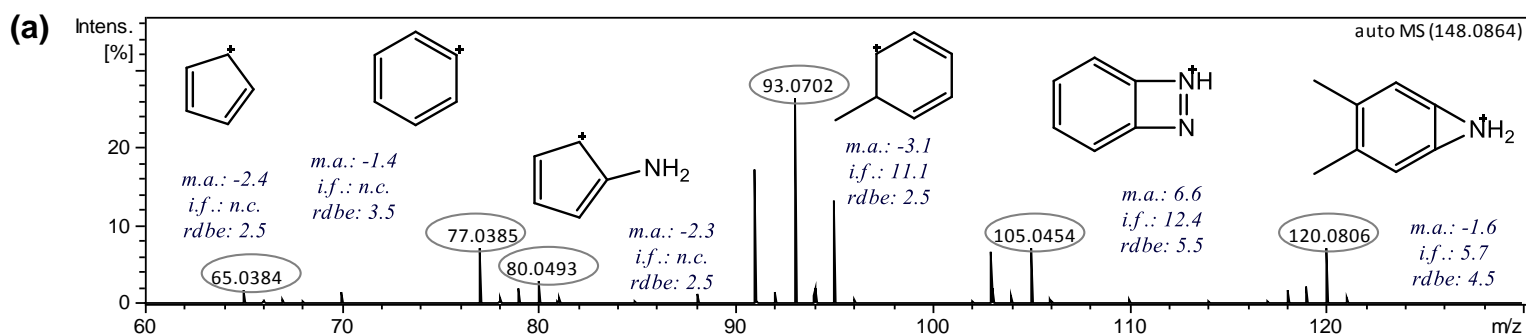




**Fig. 3.2.** Data dependent MS/MS (auto MS/MS) spectra of the detected produced TPs of (a) 2-amino-BTH and (b) XTRi.

Due to the low intensity of the produced TPs, the chlorinated samples were pre-concentrated through evaporation under a stream of nitrogen, in order to make the auto MS analysis feasible.

A mono-chlorinated XTRi derivative ( $C_8H_8ClN_3$ ) with  $m/z$  182.0484 was detected at  $t_R$  8.0 min. The two fragments with  $m/z$  154.0414 and 127.0299, indicate the addition of the chlorine atom to the benzene ring, so 4-chloro-XTRi can be proposed. Moreover, the fragment  $m/z$  154.0414 corresponds to  $m/z$  120.0806 of the parent compound (**Fig. 3.3**) after the addition of one chlorine atom.



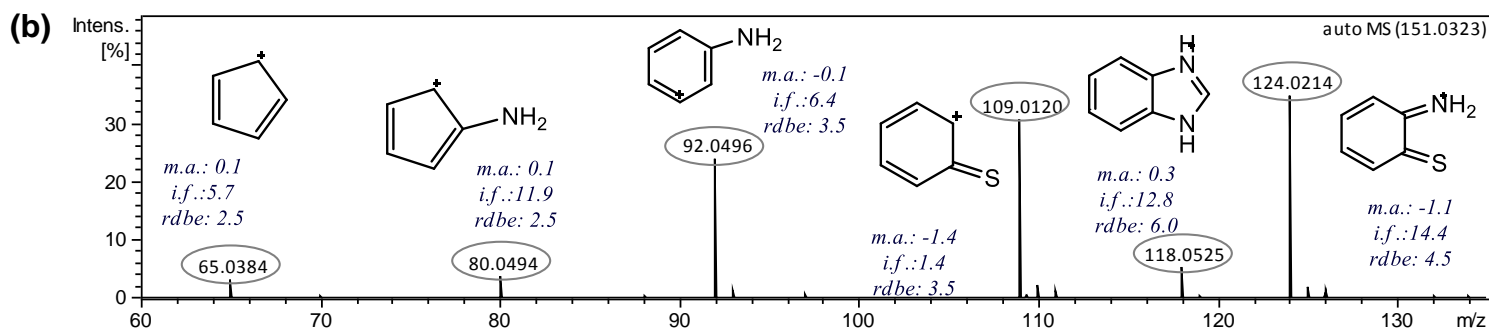


**Fig. 3.3.** Data dependent MS/MS (auto MS/MS) spectra of (a) XTRi and (b) 2-amino-BTH.

Three more TPs, were detected and signify that oxidative reactions took place during XTRi's chlorination. The compound eluted at  $t_R$  4.4 min, is detected as  $m/z$  164.0810. Its formula fits the mono-hydroxylated derivative of XTRi ( $C_8H_9N_3O$ ), with excellent mass accuracy of 4.9 ppm, which can be identified as 4-hydroxy-XTRi. Moreover, 4,7-di-hydro-XTRi ( $C_8H_9N_3O_2$ ) with  $m/z$  180.0762, eluted at  $t_R$  3.6 min, is probable generated by the further hydroxylation of the mono-hydroxylated derivative. Its fragmentation pattern depicts two fragments containing two hydroxyl groups ( $m/z$  165.0534 and 152.0693) and two more containing one group ( $m/z$  134.0605 and 124.0749). The hydroxylated fragments with  $m/z$  152.0693 and 134.0605 resemble to the fragment  $m/z$  120.0690 of the parent compound. Finally, a TP with  $m/z$  162.0654 was detected at  $t_R$  5.1 min. Since its abundance was not high enough to enable data dependent MS/MS acquisition, the proposed structure is based on the formula obtained from the MS spectra with a mass accuracy of 4.9 ppm. The addition of one oxygen to the TP's formula ( $C_8H_7N_3O$ ) compared to that of the parent compound ( $C_8H_9N_3$ ) and the increase of the ring double bond equivalent (rdbe) from 5.5 to 6.5 indicate the presence of a ketone. So, 5-methyl-BTR-6-carbaldehyde can be proposed for this structure.

2-amino-6-chloro-BTH, 2-amino-5,6-dichloro-BTH, 6-chloro-5-hydroxy-BTH and 2-amino-5,6-di-hydroxy-BTH were detected in the chlorinated samples of 2-amino-BTH and were tentatively identified.

At  $t_R$  8.1 min, a TP with  $m/z$  184.9931 was detected. Its distinct isotopic pattern and the mass accuracy of -2.2 ppm indicate the formation of a mono-chlorinated 2-amino-BTH derivative ( $C_7H_5ClN_2S$ ). The fragments with  $m/z$  157.9819 and 142.9710 demonstrate that the chlorine atom addition occurred in the benzene

moiety of the parent structure. Provided that this formula could be attributed to a number of isomers, two commercially available compounds, 2-amino-4-chloro-BTH and 2-amino-6-chloro-BTH were purchased. After analysis of the standard solutions, the produced TP was proved to be 2-amino-6-chloro-BTH. The  $t_R$  of the two isomers were significantly different (7.2 and 8.0 min, respectively), while the fragmentation pattern of the detected chlorinated TP matches to 2-amino-6-chloro-BTH MS/MS spectra. The extracted ion chromatograms (EICs) of  $m/z$  184.9935 derived from the standard solutions of the two isomers and the data dependent MS/MS spectra of 2-amino-6-chloro-BTH are presented in **Fig. 3.4**. Consequently, the structure of the produced TP was fully confirmed *via* analysis of the reference standard, reaching level 1 of identification confidence [85].

A di-chlorinated TP with  $m/z$  218.9537 ( $C_7H_4Cl_2N_2S$ ) was also detected at  $t_R$  9.6 min. The fragment 191.9417 clearly indicates the addition of the two chlorine atoms in the benzene moiety, while the fragment 183.9842 resembles the mono-chlorinated moiety. Furthermore, the chlorinated fragment  $m/z$  191.9417 corresponds to the fragment  $m/z$  124.0214 of 2-amino-BTH. Bearing in mind the confirmed structure of the mono-chlorinated TP, it can undoubtedly be proposed that the di-chlorinated TP is 2-amino-5,6-dichloro-BTH.

Moreover, two additional hydroxylated TPs were detected. Through the oxidation of the parent compound and the addition of two hydroxyl groups to the benzene moiety, 2-amino-5,6-di-hydroxy-BTH ( $C_7H_6N_2O_2S$ ) was formed and detected at 4.0 min as  $m/z$  183.0216. Two hydroxylated fragments,  $m/z$  140.0161 and 125.0599 are shown in its data dependent MS/MS spectra. The fragment  $m/z$  140.0161 suits to the hydroxylated derivative of the most abundant fragment ( $m/z$  124.0214) of the parent compound. The compound eluted at  $t_R$  5.3 min, 2-amino-6-chloro-5-hydroxy-BTH ( $C_7H_5ClN_2OS$ ), is generated by the hydroxylation of the mono-chlorinated TP and the fragments  $m/z$  183.9849 and  $m/z$  156.9738 clearly support this hypothesis.

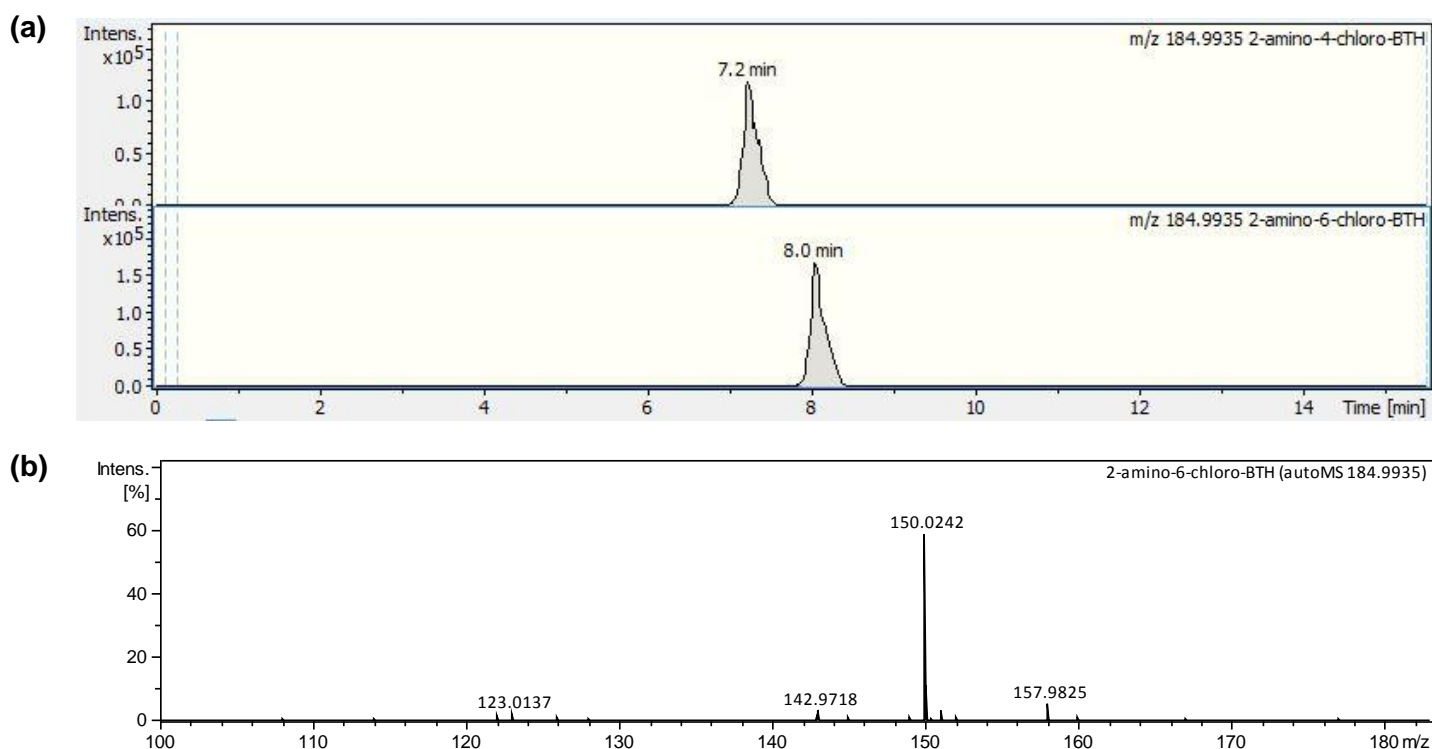


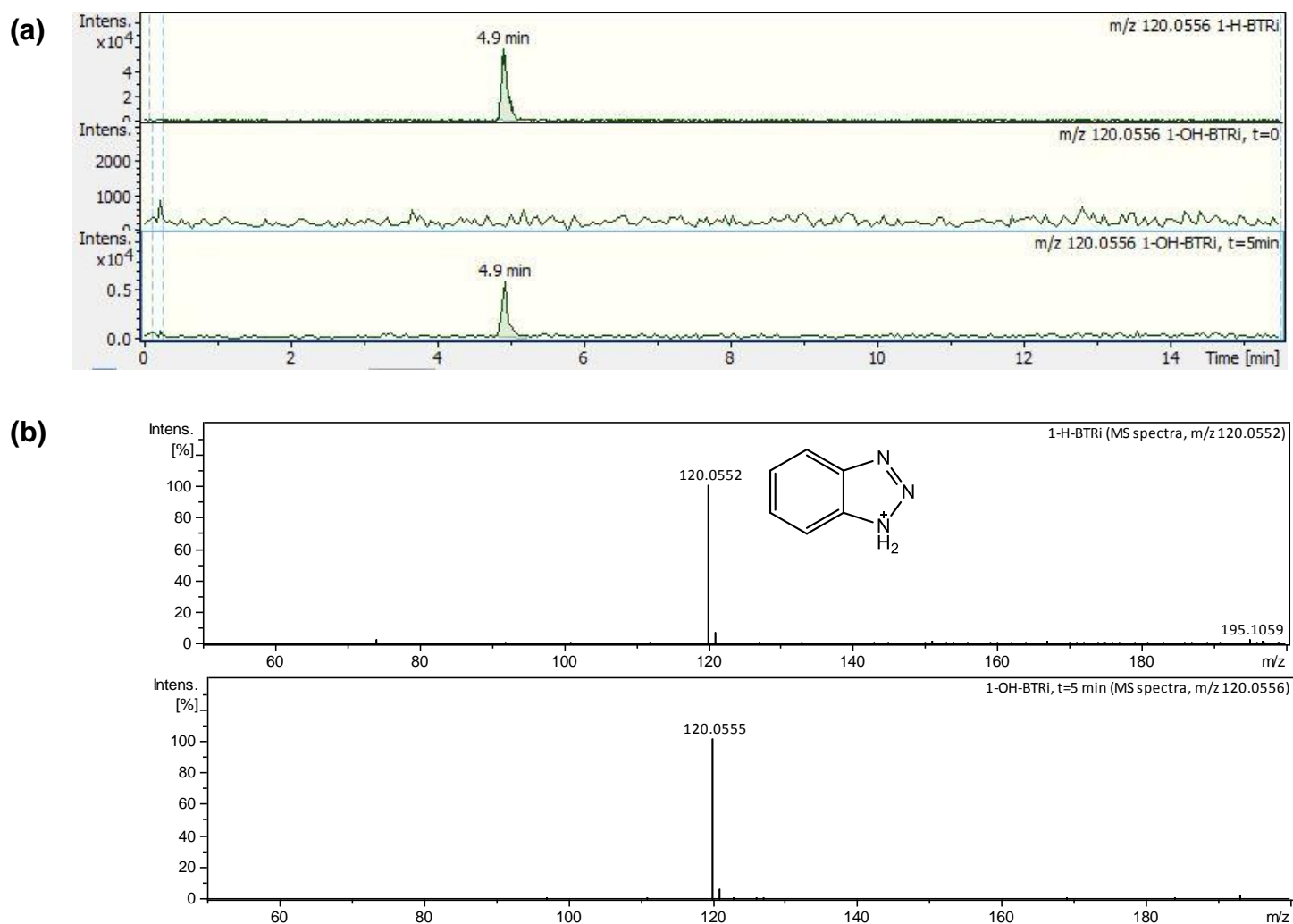
**Fig. 3.4.** (a) EICs of  $m/z$  184.9935 from the standard solutions of 2-amino-4-chloro-BTH and 2-amino-6-chloro-BTH and (b) MS/MS spectra of  $m/z$  184.9935 from 2-amino-6-chloro-BTH standard solution.

Moreover, through the non-target treatment of the MS data, an additional TP resulting from the dimerization of 2-amino-BTH, followed by the substitution of one benzoic hydrogen by one chlorine atom, 2-[2-(BTH-2-yl)hydrazin-1-yl]-6-chloro-BTH ( $C_{14}H_9ClN_4S_2$ ) was detected at 9.5 min. Its structure is further enhanced by the generation of the two fragments  $m/z$  150.0240 and 182.9774, which represent the two monomeric structures, 2-amino-BTH and 2-amino-6-chloro-BTH, respectively.

Although chlorinated transformation products of BTRs and BTHs are reported for the first time in this study, hydroxylated TPs of BTRs have already been identified in literature. Benitez et al. proposed the formation of one dihydroxylated and two mono-hydroxylated TPs of 1-H-BTRi during ozonation [8]. The authors stated that electrophilic substitutions occur preferentially at C4 and C7 positions [118]. This agrees with the hydroxylated TPs of XTRi proposed in our study (4-hydroxy-XTRi and 4,7-hydroxy-XTRi). Moreover, 4-hydroxy-BTRi and 5-hydroxy-BTRi were confirmed to be produced by the biodegradation of

1-H-BTRi, while two mono-hydroxylated derivatives, with molecular formula  $C_7H_7N_3O$ , were formed by 4-Me-BTRi [132].

Furthermore, an interesting observation is the formation of 1-H-BTRi as a degradation product of 1-OH-BTRi during chlorination. Its occurrence in the chlorinated samples of 1-OH-BTRi was confirmed with a reference standard by comparing the retention time, MS and MS/MS spectra as presented in **Fig. 3.5**. 1-H-BTRi is rapidly formed within the first minutes of the reaction of 1-OH-BTRi with the sodium hypochlorite.



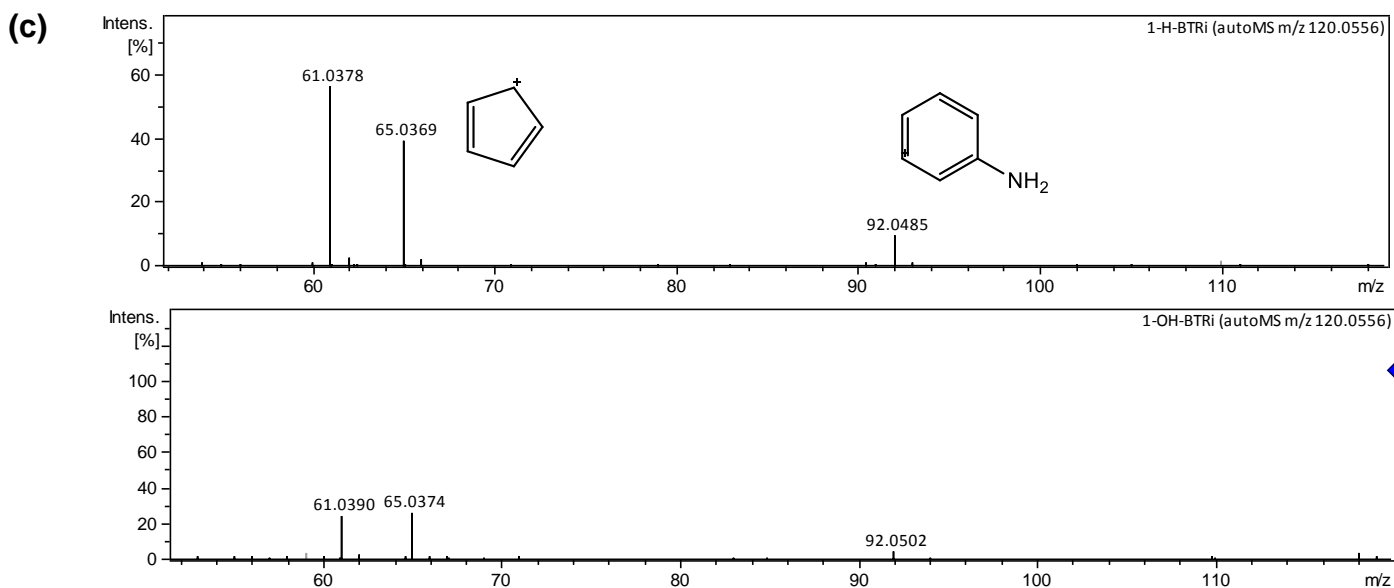


**Fig. 3.5.** Confirmation of production of 1-H-BTRi as a chlorination transformation product of 1-OH-BTRi based on (a) retention time, (b) MS spectra and (c) fragmentation pattern.

### Retention time prediction

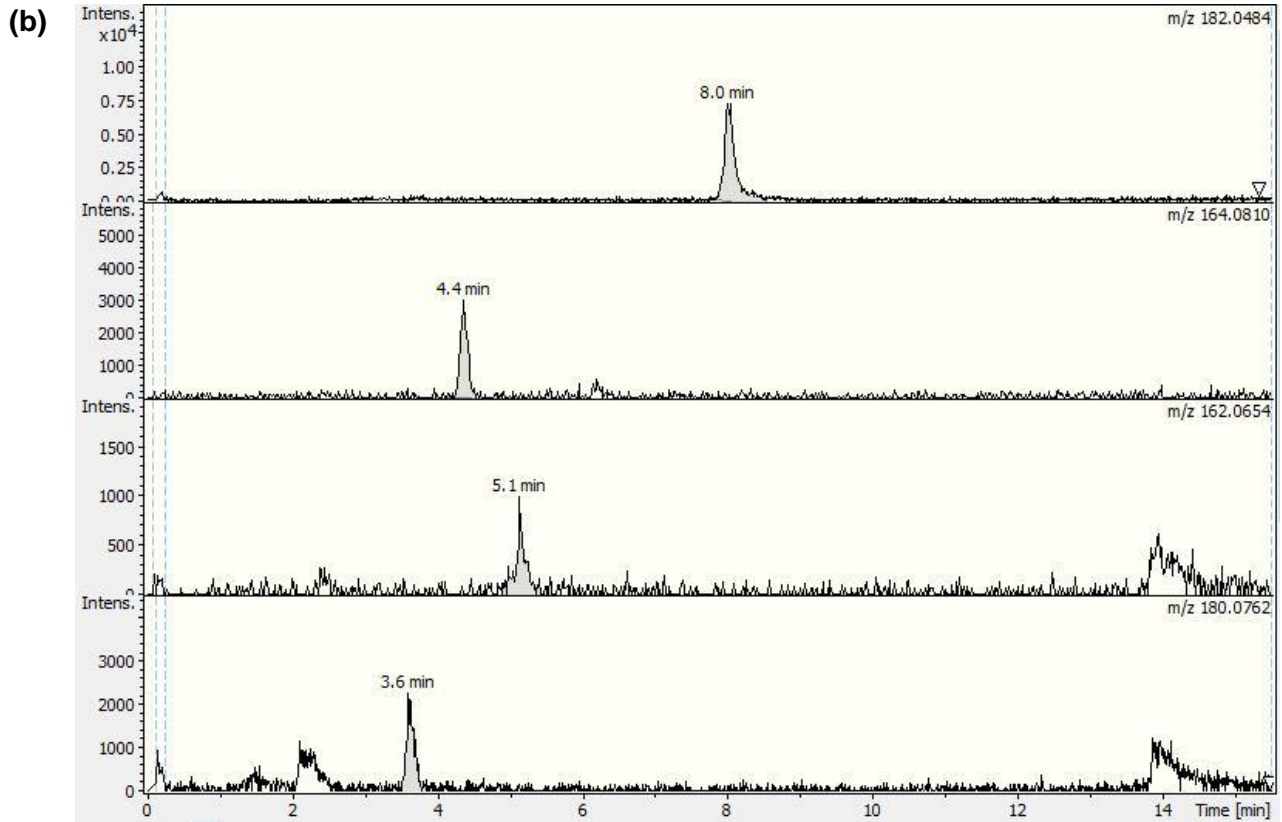
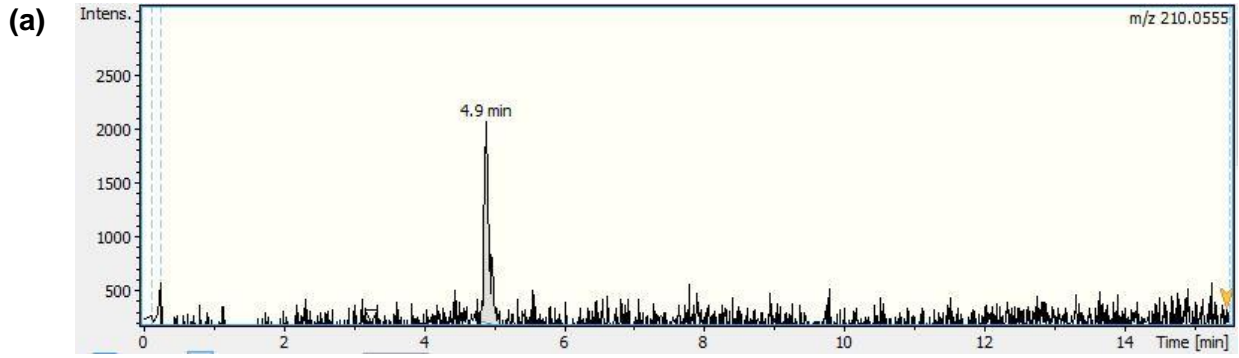
In order to support the proposed structures for the identified TPs, retention time prediction was performed. Chemometric tools were utilized for the prediction, taking into account the proposed structure, its physicochemical properties and the chromatographic system (analytical column, gradient elution program and pump) that was used. An extensive dataset of over 1800 compounds was provided for the in-house Quantitative Structure–Retention Relationship (QSRR) prediction model development, for the positive ESI [142]. If the structure of the tested compounds is within the applicability domain of the prediction model and the error between the experimental and the predicted retention time is below  $\pm 2$  min, then the proposed structure can be further supported. The results shown in **Table S3.4** (Section S3.4.) indicate that the experimental retention time of all the detected TPs shows a good fitting to the predicted one, enhancing the confidence of the proposed structures. Despite the error of 2.7 min in the prediction of 4,7-di-hydro-XTRi, the observed fragmentation pattern can strongly support the proposed structure. Moreover, although the prediction of 2-amino-5,6-di-chloro-BTH surpasses the set threshold, this result can be justified and overlooked, by taking into account that



the error for 2-amino-6-chloro-BTH, whose structure was confirmed through the analysis of the corresponding reference standard, was -2.6 min.

### **Environmental relevance – Toxicity assessment**

In order to assess the environmental impact of the findings of this study, secondary treated wastewater samples (pH 8.0) from Psytallia WWTP were spiked with 1-OH-BTRi, XTRi and 2-amino-BTH and afterwards the chlorination procedure was followed. After qualitatively pre-concentrating the samples, all the already identified TPs were detected and their EICs are shown in **Fig.3.6**, indicating that they can be produced in real chlorinated wastewater samples. Furthermore, toxicity calculations with ECOSAR software [143] were performed, so as to obtain an insight on the acute toxicity of the identified TPs for two classes of aquatic organisms; namely fish and algae. This program provides the probable toxicity of a compound according to its octanol/water partition coefficient ( $K_{ow}$ ) value and its structure similarity with other compounds whose toxicity in aquatic environment has been previously estimated. The calculated values are LC50 (median lethal concentration) for fish and EC50 (median effective concentration) for algae and are listed in **Table 3.3**. XTRi and its TPs were considered as benzotriazoles structure-alike chemicals, while 2-amino-BTH and its produced chlorination TPs were considered as unhindered anilines-structure alike chemicals. As it can be concluded from the results, the chlorinated derivatives of both XTRi and 2-amino-BTH seem to be more toxic than their parent compounds, while the hydroxylated derivatives are proved to be less hazardous. The toxicity effect of 2-[2-(BTH-2-yl)hydrazin-1-yl]-6-chloro-BTH is not presented because this chemical may not be soluble enough to show predicted values. Although these results are not derived from real toxicity experiments, they are indicative of the potential environmental risk of the detected TPs.



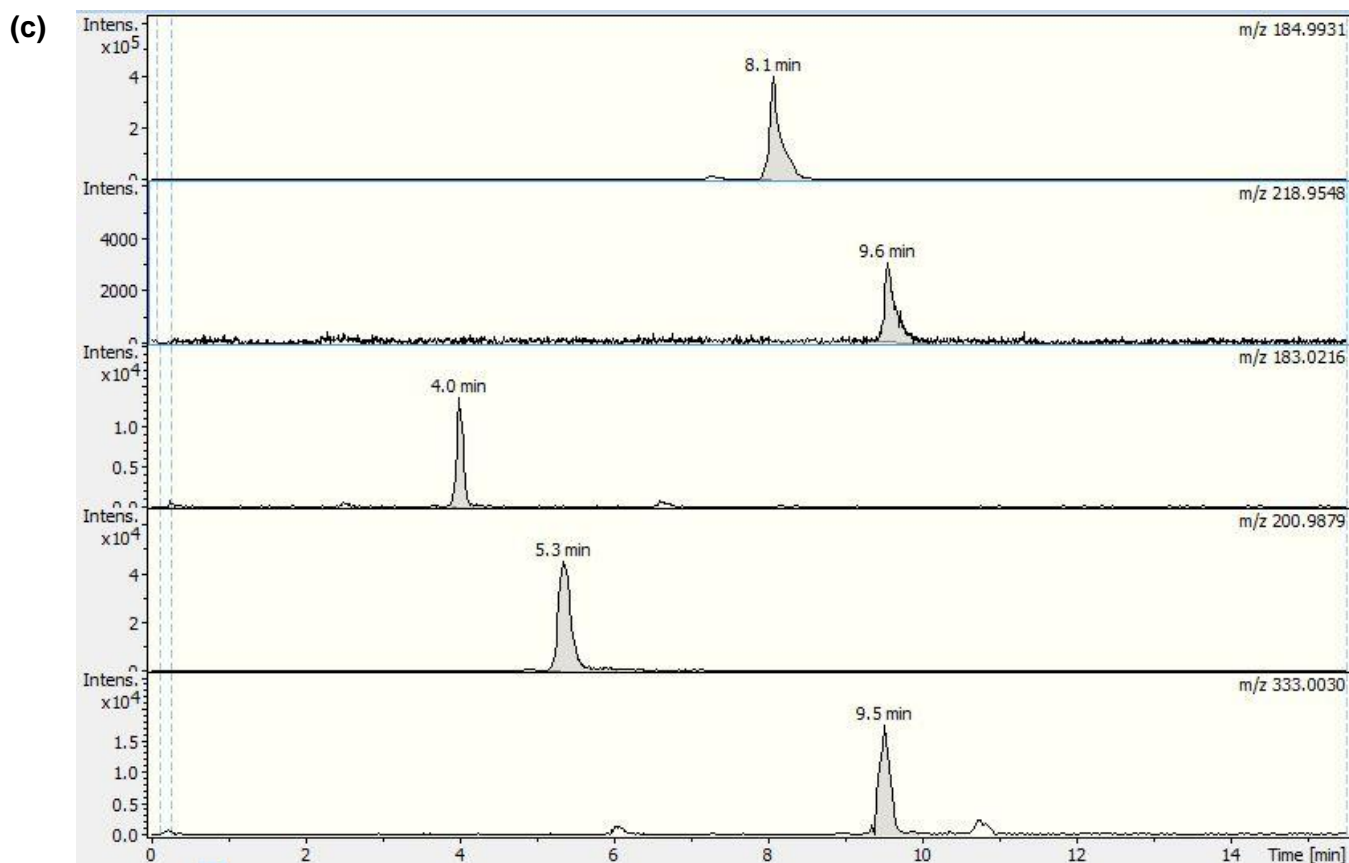


**Fig. 3.6.** EICs of the detected TPs in chlorinated treated wastewater samples of (a) 1-OH-BTRi, (b) XTRi and (c) 2-amino-BTH.

**Table 3.3.** ECOSAR results for (a) 2-amino-BTH, (b) XTRi and their identified transformation products.

(a) for XTRi

Organism (96 h)	Predicted mg/L (LC50 for fish and EC50 for algae)				
	XTRi	4-chloro-XTRi	4-hydroxy-XTRi	4,7-di-hydro-XTRi	5-methyl-BTR-6-carbaldehyde
Fish	9.4	5.2	19	36	28
Green Algae	2.5	1.6	4.4	7.8	6.1

**(b) for 2-amino-BTH**

Organism (96 h)	Predicted mg/L (LC50 for fish and EC50 for algae)				
	2-amino-BTH	2-amino-6-chloro-BTH	2-amino-5,6-di-chloro-BTH	2-amino-5,6-di-hydroxy-BTH	2-amino-6-chloro-5-hydroxy-BTH
Fish	21	9.3	3.9	121	22
Green Algae	1.7	1.5	1.2	3.5	2.1

### 3.5. Conclusions

In this study, the kinetics and the formation of TPs were investigated after the reaction of chlorine with four selected BTRs and three BTHs in laboratory batch experiments. The removal rate of BTRs seemed to increase with the applied molar ratio, while no relevant trend was observed for BTHs. The chlorination efficiency in removal was accelerated at low pH values but did not seem to be affected by the presence of TSS in the two examined concentrations. 2-amino-BTH was removed faster than all tested contaminants during chlorination, while the rest of them can be ranked by increasing removal rate, according to the order: 1-H-BTRi < TTRi and BTH < 2-OH-BTH < XTRi. Four TPs of both XTRi and 2-amino-BTH were identified through suspect screening approach, while one additional TP of 2-amino-BTH was detected through non-target screening. Moreover, 1-H-BTRi was produced during the chlorination of 1-OH-BTRi. Since the toxicity calculation with ECOSAR software indicated that the produced chlorinated TPs are more harmful than their parent compounds, their toxicity effects need to be further investigated.

## CHAPTER 4.

### Ozonation of ranitidine: effect of experimental parameters and identification of transformation products

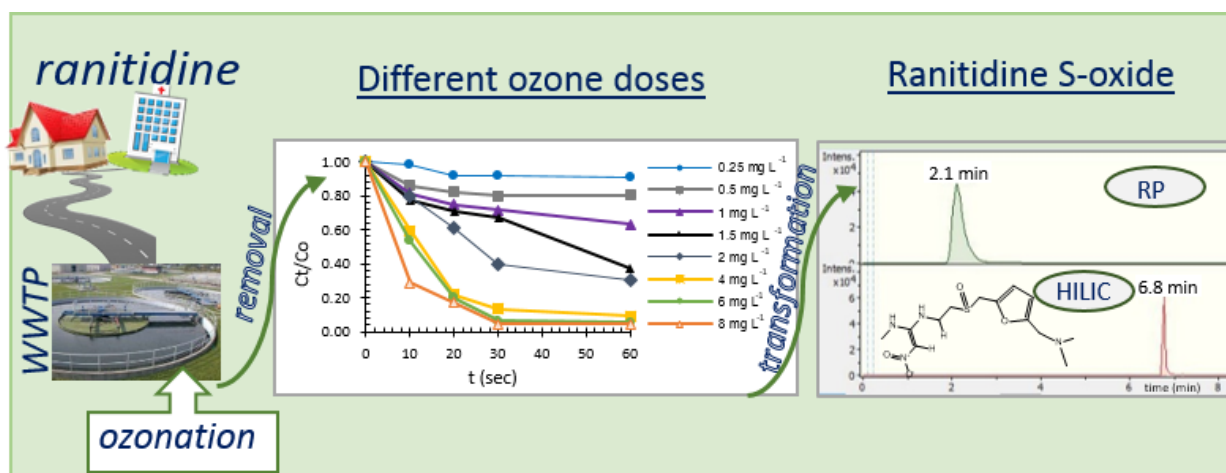


Fig. 4.0. Graphical Abstract of Chapter 4.

#### 4.1. Introduction

Recent studies have shown that numerous pharmaceuticals have been introduced into the environment, mainly through anthropogenic sources of pollution [144]. These compounds, after being discharged from WWTPs, are detected in the environment at various concentration levels (from ng to  $\mu\text{g}$  per liter) depending on their water solubility, physicochemical characteristics, local consumption rates and biodegradability [60, 145-147]. Many micropollutants are not entirely removed even through wastewater or drinking water treatment processes, thus they are consequently detected at various concentrations in drinking water supplies [148, 149].

Various oxidation processes have been proposed, studied and applied for the removal of emerging pollutants and they have shown increased ability to significantly degrade or transform selected micropollutants [53]. Ozonation has been proven to be an effective, robust and widely accepted oxidation technique [150, 151], where oxidative degradation occurs mainly through direct reaction with aqueous ozone or through indirect reaction with ozone decay products (mainly hydroxyl radicals). Ozonation has been also applied for the disinfection of drinking water [152], wastewater [153, 154] and hospital effluents [155].

Although the degradation or removal of many pollutants may be significant, often total mineralization is not achieved. As a consequence, TPs, which may be more toxic than their parent compounds, may be produced. So, over the last decade, the detection, identification and toxicity assessment of the produced TPs is a field of growing interest. The development of high resolution mass spectrometers and sophisticated computer tools, have enabled this achievement [156].

Molecular ozone selectively attacks organic compounds with high electron density functional groups, such as double bonds, activated aromatic rings, amines and thioethers. Hydroxyl radicals, produced during the decomposition of ozone in water, could lead to further oxidative non-selective reactions [157]. For an overall study of the degradation caused by ozonation processes, a kinetic study is useful, since it offers a time-dependent view of the pollutants' remediation.

Ranitidine (RAN), a commonly used drug in the treatment of ulcer, gastrointestinal hypersecretory conditions and gastroesophageal refluxes (common trade names: Zantac, Taladine, Nu-Ranit, Raniplex), presents pKa values 8.13 and 1.95 [158, 159] and log  $K_{ow}$  0.27 [160]. RAN acts as a histamine  $H_2$ -receptor antagonist due to the furan ring present in its structure [161, 162]. The occurrence of RAN in surface waters and wastewaters has already been reported in several studies [163-165]. RAN was found in the effluents of STPs in Greece at a median level of 1059 ng L<sup>-1</sup> [166] and in river waters of Spain at a median concentration of 396.5 ng L<sup>-1</sup> [167]. It is excreted partly as an untransformed (30-70%) compound in urine and partly as its main metabolites, RAN N-oxide, N-desmethyl RAN and RAN S-oxide [168, 169], in urine and feces.

The removal of RAN in ultrapure water and wastewater samples has already been studied through the application of electrochemical processes [170], ozonation competitive kinetics [158], photochemical oxidation [171], photolysis [172] and solar photocatalysis [173]. RAN structure encompasses multiple reactive sites that are labile to ozone oxidation (e.g. amine, conjugated diene, sulphide and electron-rich alkene group) [173]. However, the degradation and TP formation of RAN through an ozonation process has not been extensively

studied. Furthermore, the identification of TPs is crucial for the determination of the removal pathway.

## **4.2 Scope of the study**

The objective of this study was the systematic investigation of RAN removal in water, using a lab-scale ozonation apparatus. Focus was given on the effect of various operational parameters (pH value, initial concentration of oxidant and analyte, matrix effect as well as the presence of organic matter) on the removal of the compound. Furthermore, the main TPs were detected, identified and structurally elucidated, using liquid chromatography coupled with quadrupole-time-of-flight tandem mass spectrometry (LC-Q-ToF/MS). Two complementary chromatographic systems were used for the analysis, reversed phase liquid chromatography (RPLC) and hydrophilic interaction liquid chromatography (HILIC), in order to investigate their complementarity for the detection of additional compounds. The hierarching hypothesis behind the use of HILIC is that polar TPs are well-retained in HILIC with higher sensitivity, additional retention mechanisms may lead to the separation of isomeric TPs, thus increased selectivity is achieved (better and clearer MS/MS information and higher confidence in identification). In-house developed QSRR prediction models were also used to support identification.

## **4.3. Experimental part**

### **4.3.1 Standards and reagents**

Ranitidine hydrochloride (CAS 66357-59-3), ( $\geq 98\%$  HPLC) was purchased by Sigma-Aldrich, Germany. The reference standards of Ranitidine S-oxide and Ranitidine N-oxide solutions (1000 mg/L in methanol) were donated by the Swiss Federal Institute of Aquatic Science and Technology (Eawag, Department of Environmental Chemistry). Hydrochloric acid (37.0-38.0% wt., ACS grade) and sodium hydroxide ( $>99\%$ , ACS grade) were supplied by Merck, Germany.  $K_2SO_4$  ( $>99\%$ ),  $Na_2SO_4$  ( $>99\%$ ),  $NaHCO_3$  ( $>99\%$ ),  $CaCl_2 \cdot 2H_2O$  ( $>99\%$ ) and  $MgCl_2 \cdot 6H_2O$  ( $>99\%$ ) were supplied by Fluka, Germany. Formic acid (LC-MS Ultra) was provided by Fluka Analytical, Sigma-Aldrich, Germany. LC-MS ultrapure water was produced on site using a Milli-Q water purification system (18.2 M $\Omega$ /cm, Millipore Direct-Q UV, Bedford, MA, USA). MeOH for

HPLC (M/4056/17) was provided by Fisher Scientific, Germany. MeOH LC–MS grade was purchased from Merck (Darmstadt, Germany). ACN (LC-MS grade) for LC-Q-ToFMS analysis was provided by Merck. Ammonium formate and ammonium acetate were purchased from Fluka (Buchs, Switzerland). For the experiments including dissolved organic matter (DOM), humic acid (CAS 0001415936, (technical grade) was used, which was purchased by Sigma-Aldrich (Germany).

#### **4.3.2 Experimental setup**

The ozonation experiments were carried out as follows. Ozone was produced from industrial/biomedical grade oxygen (99.5%, Revival Bottled Gas, Athens, Greece) using AZCOZON VMUS-2 ozone generator, by AZCO Industries Ltd (Canada). The gas flow rate was kept constant at 40 L h<sup>-1</sup> and dosed through a sintered sparger at the bottom of a 1 L glass reactor, which was placed in a bucket filled with ice. A saturated ozone stock solution (20-25 mg L<sup>-1</sup>) was prepared daily. The concentration of dissolved ozone in stock solution was determined by direct absorption determination at 258 nm ( $\epsilon = 2700 \text{ cm}^{-1} \text{ mol}^{-1} \text{ L}$ ) [174].

Ozonation experiments were conducted in sealed bottles by mixing a predefined amount of the ozone saturated solution with an aqueous solution of RAN, in order to obtain the desirable aqueous ozone concentration. An aliquot was taken before the addition of ozone, representing the zero-time sample. During the course of experiments, samples were withdrawn at predefined time points and were added into vials containing KI for the immediate quenching of the reaction. Initial experiments, which lasted 30 min, showed that RAN ozonation reaction is very fast, therefore samples were withdrawn at predefined time points, up to 2 min.

For the investigation of the initial ozone concentration influence on RAN removal, experiments with 5 mg L<sup>-1</sup> of RAN in reaction with 0.25, 1, 1.5, 2, 4, 6 and 8 mg L<sup>-1</sup> of ozone were conducted.

The pH of the solution plays an important role in the overall removal and kinetics of RAN ozonation [158, 175]. Ozone aqueous solution is more stable under acidic conditions. Higher pH values (pH >8) contribute to faster ozone decay,



due to the formation of hydroxyl radicals deriving from hydroxyl anions, as shown below in Equations 4.1-4.6) [176]:



The presence of  $\cdot\text{OH}$  results in immediate reaction with ozone, even at neutral pH, where the concentration of hydroxyl anions is limited ( $10^{-7}$  M). At acidic solutions ozone decay is limited (reported values around  $3 \times 10^{-6} \text{ s}^{-1}$ ) [177]. The decomposition of ozone is accelerated at increased pH or with the addition of hydrogen peroxide, leading to the production of radicals, thus advanced oxidation processes with the participation of ozone and hydroxyl radicals can take place.

For the investigation of pH value influence, pH was adjusted to 4.0 by dropwise addition of HCl solution (0.1 M) and to 7.0, 9.0 and 10.0 with NaOH solution (0.1 M), respectively ( $C_0$  RAN:  $5 \text{ mg L}^{-1}$  and  $C_0$   $\text{O}_3$ :  $1 \text{ mg L}^{-1}$ ). The stability of RAN under various initial pH values (4.0 – 11.0) in the absence of oxidants and light, has been reported in the past [158, 171, 173]. Nevertheless, control hydrolysis experiments on the stability of RAN, under different initial pH (4.0, 7.0, 9.0 and 10.0) in the absence of ozone and light, were performed.

Moreover, the influence of the matrix effect was examined. Three different DOM concentrations ( $C_0$  RAN 1 and  $2 \text{ mg L}^{-1}$  and  $C_0$  DOM: 1, 2 and  $5 \text{ mg L}^{-1}$ ) and simulated drinking water of different hardness and ion content were tested ( $C_0$  RAN and  $\text{O}_3$ :  $1 \text{ mg L}^{-1}$ ). The stability of ozone in surface and wastewater is largely dependent on the presence of DOM, which varies in origin, concentration and nature. Part of the dissolved aqueous ozone is consumed through reaction with DOM. Ozone reaction with electron-rich aromatic components of DOM has been suggested to produce hydroxyl radicals

(reactions 4.7-4.10) and peroxy-radicals (reactions 4.11-4.12) which can subsequently react with ozone and promote its decay [176, 178].



also



Simulated soft drinking water was prepared consisting of (in mg per L of ultrapure water water):  $\text{K}^+$  (1.0),  $\text{Na}^+$  (10.0),  $\text{HCO}_3^-$  (50.0),  $\text{Ca}^{2+}$  (20.0),  $\text{Mg}^{2+}$  (10.0),  $\text{Cl}^-$  (20.0),  $\text{SO}_4^{2-}$  (20.0). Simulated hard drinking water consisted of  $\text{K}^+$  (5.0),  $\text{Na}^+$  (30.0),  $\text{HCO}_3^-$  (150.0),  $\text{Ca}^{2+}$  (50.0),  $\text{Mg}^{2+}$  (25.0),  $\text{Cl}^-$  (100.0),  $\text{SO}_4^{2-}$  (50.0).

For the investigation RAN mineralization, experiments with  $10 \text{ mg L}^{-1}$  of RAN in reaction with  $8 \text{ mg L}^{-1}$  of ozone were conducted at 3 different pH (3.0, 4.0, 5.8).

For the TPs identification, an ozonation experiment in ultrapure water was conducted. The initial RAN and ozone concentrations were  $5 \text{ mg L}^{-1}$  and  $1 \text{ mg L}^{-1}$  respectively. Samples were collected at selected time points during the ozonation process, while a blank sample, comprised of water, ozone and the reaction's quencher, was also prepared as a control sample.

An overview of the experimental setup (initial RAN and ozone concentrations, pH of the solution and matrix) is given in **Table S4.1 (Section S4.1)**.

### 4.3.3 Instrumental analysis

#### Monitoring of RAN removal

RAN removal was monitored by HPLC (Agilent technologies, series 1100 (USA)) equipped with a UV detector. The separation was performed on a reversed phase (RP) ZORBAX Eclipse XDB-C18 column (4.6 x 150 mm,  $5 \mu\text{m}$ ) (Agilent, USA). A gradient elution program was applied in the chromatographic

analysis with (A) ultra-pure water and (B) MeOH, as binary mobile phases. The gradient elution program started with 30% MeOH, remained stable for 3 min, then increased to 100% MeOH in 10 min, kept constant for 3 min and re-equilibrated for 2 more minutes. The flow rate was 1 mL min<sup>-1</sup>. The residual aqueous ozone was determined using the indigo method [174] based on the bleaching of indigo at 600 nm. For the spectroscopic measurements of remaining aqueous ozone, a Hitachi-U2000 photometer (Japan) was used. Mineralization was followed by measuring the Dissolved Organic Matter (DOM) using a Shimadzu V-csh TOC analyzer (Japan). The pH was measured with an IntelliCAL PHC101 pH-meter (Hach Co. Colorado, USA).

### **UHPLC MS analysis for TPs identification**

For the identification of the TPs formed during the ozonation process, the samples were analyzed by an UHPLC system (Dionex UltiMate 3000 RSLC, Thermo Fisher Scientific, Germany) coupled to a Q-ToF mass spectrometer (Maxis Impact, Bruker Daltonics, Bremen, Germany).

The use of hydrophilic interaction liquid chromatography (HILIC), complementary to RPLC, has recently been applied in various -omics approaches in order to detect and identify polar biomarkers or transformation products [179-181]. This approach was followed in this study for a holistic detection of polar transformation products that have not been eluted in the RPLC chromatographic system or for isomeric compounds that may have been co-eluted in RPLC. The samples were analyzed by RPLC and consequently by HILIC, within 2 days, in order to preserve the stability of the analytes.

In RPLC, the chromatographic separation was achieved using an Acclaim RSLC C18 column (2.1 x 100 mm, 2.2 µm) from Thermo Fisher Scientific (Dreieich, Germany) connected to a guard column of the same packaging material, kept at 30°C. A thorough description of the applied chromatographic method under positive and negative ionization mode is given in **Table S4.2** (Section S4.2).

In HILIC, separation was performed on an ACQUITY UPLC BEH Amide column (2.1 × 100 mm, 1.7 µm) obtained from Waters (Dublin, Ireland) preceded by a guard column of the same packaging material, kept at 40 °C. A description of

the chromatographic method is described in **Table S4.2** (Section S4.2). For HILIC analysis the samples were dried and reconstituted in ACN/water (95:5) prior to analysis.

An electrospray ionization interface (ESI), operating in positive and negative mode, was employed in Q-ToF-MS with the following operation parameters: end plate offset 500 V, capillary voltage 2500 V (PI) and 3500 (NI), nebulizer gas pressure 2 bar (N<sub>2</sub>), drying gas 8 L min<sup>-1</sup> (N<sub>2</sub>) and drying temperature 200 °C.

Full scan mass spectra were recorded over the range of 50–1000 *m/z*. MS/MS experiments were conducted using AutoMS data dependent acquisition mode based on the fragmentation of the five most abundant precursor ions per scan. If needed, due to the low intensity of the *m/z* of interest, a second analysis with AutoMS (data dependent acquisition) mode including a list of selected precursor ions was carried out. The collision energy applied was set to predefined values, according to the mass and the charge state of every ion.

A sodium formate calibration solution (10 mM sodium formate in a mixture of water/isopropanol) was used for external and internal calibration of Q-ToFMS. More information about the calibration procedure can be found in the Supporting material. Mass spectra acquisition and data analysis was processed with DataAnalysis 4.1, TargetAnalysis 1.3 (Bruker Daltonics, Bremen, Germany) and Metabolite Tools 2.0, SR4 Bruker's software (Germany).

#### **4.3.4 Applied workflows for TPs identification**

##### **Screening workflows**

The identification of RAN TPs was realized by acquiring and analyzing LC-Q-ToF-MS data. For each sample two chromatograms were acquired in a single run: a full MS chromatogram, recording mass spectra over the range of 50–1000 *m/z* and a MS/MS chromatogram using AutoMS acquisition mode (data dependent fragmentation for the 5 most abundant precursors per scan). Apart from the data obtained from RPLC-HRMS, the complementary use of HILIC-HRMS was also investigated in order to achieve efficient chromatographic separation of certain isomers of TPs and to identify products not detected using

RPLC. For the unambiguous identification of corresponding peaks observed using RPLC and HILIC, MS and MS/MS spectra were compared for each peak. For the identification of possible produced TPs of RAN, a two-step post-acquisition data processing approach was followed, previously described by Gago-Ferrero et al. [139], adjusted to the objectives of this study. First, a suspect database of plausible TPs was compiled, including RAN impurity products, known RAN TPs that have been identified in relevant degradation studies in the literature and proposed TPs by *in silico* prediction tools. Two prediction tools were used. The Eawag-Biocatalysis / Biodegradation Database Pathway Prediction System [182], which can predict candidate TPs based on biotransformation rules set in the Eawag-BBD, scientific literature and Metabolite Predict software (Metabolite Tools 2.0, Bruker Daltonics, Bremen, Germany), which proposes products by using a rule-based system according to the reactions occurring in mammals' metabolism. Since oxidative reactions are predominant in ozonation experiments, TPs resulting either from the oxidation of the parent compound or through the breakdown of the parent compound's structure are expected to be formed. After compiling this list, all samples were screened for the detection of these database-suspect TPs. If a candidate TP was detected, then MS and MS/MS data were interpreted and tentative identification was realized.

Following the suspect screening, non-target screening was performed. The first step is the background subtraction; the full scan MS chromatogram of the zero-time (or the blank) sample is subtracted by the full scan MS chromatogram of each treated sample. The result of this subtraction is the creation of a new chromatogram where only the peaks that are much more intense in the treated samples than in the zero-time (or blank) sample are now present in the base peak chromatogram. These peaks imply the presence of possible TPs and can be further treated as "suspect peaks". The detected TPs were tentatively identified according to mass accuracy and isotopic pattern of the precursor ion, their fragmentation pattern and the retention time of the extracted-ion chromatographic peak. Elemental compositions of the precursor and fragment ions were suggested and molecular formulas were proposed using Bruker's Data Analysis SmartFormula Software Tool. The algorithm for isotope matching

fit (SigmaFit) is included in Bruker Daltonics software. HRMS spectra in combination with MS/MS spectra (autoMS) were assessed in order to determine the elemental formula and structure of the proposed TPs.

The suspect peak lists were obtained using the function Find Compounds–Chromatogram (TargetAnalysis software), which creates the base peak chromatograms for the masses that accomplish thresholds of intensity and accuracy previously selected (excluding their isotopic peaks). These thresholds are: (a) a mass accuracy threshold of 2 mDa or 5 ppm on the monoisotopic peaks, (b) maximum of 50 mSigma in the isotopic pattern fit (mSigma-Value is a measure for the goodness of fit between measured and theoretical isotopic pattern (mass and ion ratios): the smaller the isotopic matching, the better; nevertheless, in less abundant peaks, the mSigma values are increased and (c) intensity threshold of 500 counts. Thus, the thresholds for some of the fragments' identification are more lenient due to their lower intensity ((a) mass accuracy threshold of 10 ppm and (b) the mSigma value sometimes could not even be calculated by the software).

The system presented by Schymanski et al. (2014) to communicate the level of confidence achieved in the identification of the detected compounds was also used [85]. Level 1 corresponds to confirmed structures where a reference standard is available, level 2 to probable structures (2a-Evidence by spectrum matching from literature or library; 2b-Diagnostic evidence where no other structure fits the experimental MS/MS information), level 3 for tentative candidate(s), level 4 to unequivocal molecular formulas and level 5 to exact mass(es) of interest. The detected compounds were labeled based on this classification.

### **Retention time prediction**

Additionally to the use of HILIC, retention time ( $t_R$ ) prediction was used as a complementary tool for the identification of TPs, since reference standard solutions were not commercially available for most of the identified compounds. An extensive dataset of over 1800 compounds in RP [142] and about 900 in HILIC [183] was used for the in-house QSRR prediction model development (for positive ionization analyses). The prediction was carried out using

advanced chemometric tools, where the proposed structure, its physicochemical properties and the chromatographic system (analytical column, gradient elution program and pump) that was used for the analysis, were taken into account. The predicted retention time was considered to match if it was within  $\pm 3\delta$  (standardized residual) of the measured value, as this covers 99.7% of normally distributed data. For most retention times, this is approximately equivalent to  $\pm 2$  min. More information about the development and optimization of the Support Vector Machine (SVM) model can be found in the Electronic Supplementary Material (Section S4.6).

#### **4.4. Results and discussion**

##### **4.4.1. Effect of experimental conditions on RAN removal**

The decay of aqueous ozone in ultrapure water was tested, and results indicate that during the course of the ozonation experiments, ozone concentration remains practically stable (**Fig. S4.1** - Section S4.3).

##### **Effect of the initial ozone concentration**

The assessment of RAN reactivity towards aqueous ozone was tested using increasing ozone concentrations, in order to determine the ozone concentration necessary for the total removal of RAN. The reaction of ozone with RAN is fast especially at increased ozone concentrations. Past literature has shown that RAN is extremely reactive with ozone, especially at increased levels of ozone, where competitive kinetics should be applied for the extraction of direct constants [158]. As shown in **Fig. 4.1**, the overall removal is significantly influenced by the initial ozone concentration. RAN is removed fast with ozone in ultrapure water solutions, within the first minutes of the reaction. An initial concentration of  $4 \text{ mg L}^{-1}$  of ozone is adequate to remove more than 85% of the compound in half a minute. More than 50% of maximum RAN removal was observed in less than 2 minutes when the initial applied ozone concentration was  $2 \text{ mg L}^{-1}$ . Results demonstrate that RAN is highly reactive to ozone, since RAN was effectively removed ( $>40\%$  removal) in the first minute of the reaction, even when low initial ozone concentration ( $1 \text{ mg L}^{-1}$ ) was applied.

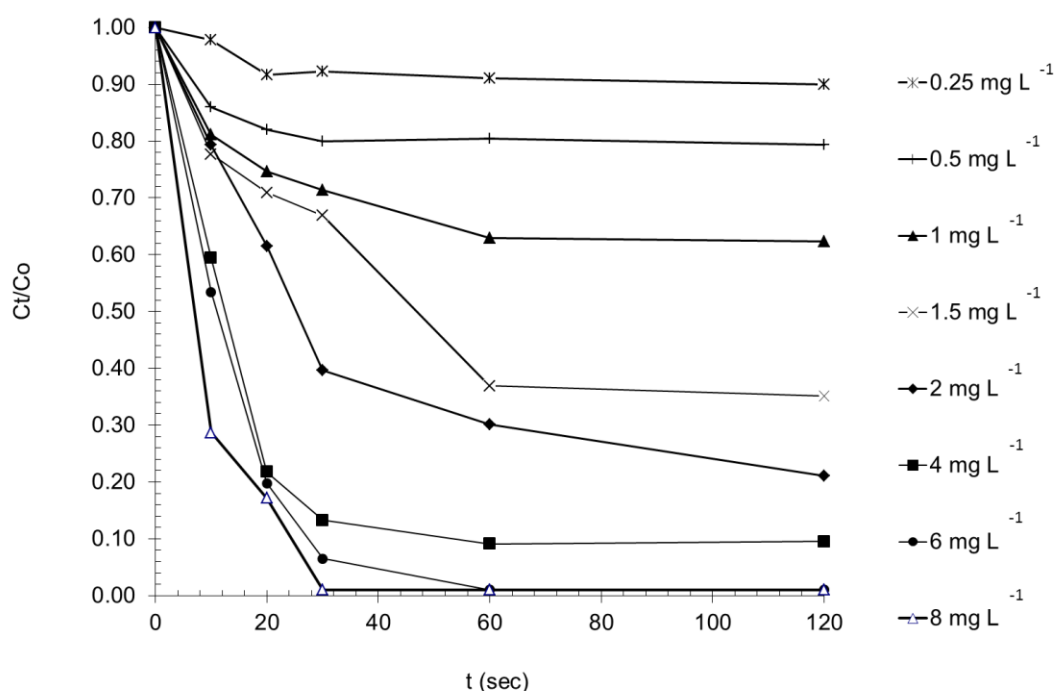


**Fig. 4.1.** Ranitidine removal under various initial ozone concentrations ( $C_o$  RAN:  $5 \text{ mg L}^{-1}$ , matrix: ultrapure water).

### Effect of pH

Ozone aqueous solution is more stable under acidic conditions. On the other hand, pH values  $>8$  contribute to faster ozone decay, due to the formation of hydroxyl radicals, as mentioned in detail in paragraph 4.3.2. Moreover, the value of pH also affects the charged state and ionic form of organic compounds. Amines and alkyl-substituted amines readily react with ozone, mainly in their non-protonated form [157, 184]. As shown in **Fig. 4.2**, RAN degradation is slower and overall removal is getting restricted as the pH value of the reaction solution decreases. RAN's structure incorporates one tertiary and two secondary amine groups. Under pH 8.1 ( $pK_a$  8.13), the tertiary amine functional group is gradually protonated [159], reacting slowly and less efficiently with ozone. At pH values above 8.1, the non-protonated form of the tertiary amine is more abundant and the degradation of RAN can be faster and more efficient. At pH 10.0, a removal of 95% was achieved within the first 30 seconds of the reaction. Control hydrolysis experiments clearly showed that under all tested initial pH values, RAN concentration remains stable during at least the first 2



days of the experiment, a time period far longer than the ozonation time (**Fig. S4.2** –Section S4.4).

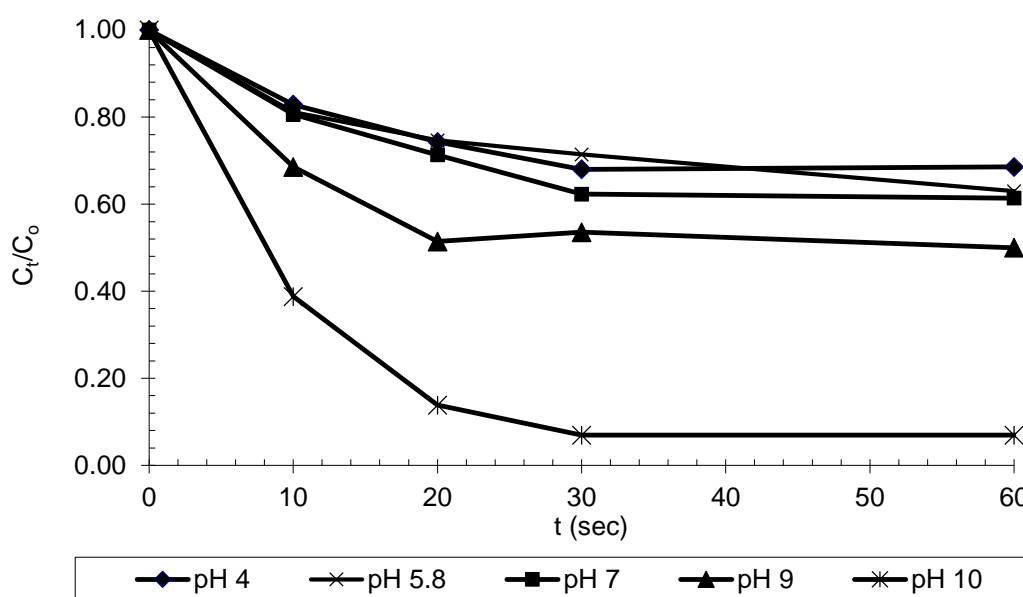


**Fig. 4.2.** Ranitidine removal at different pH ( $C_0$  RAN:  $5\text{ mg L}^{-1}$ ,  $C_0$   $\text{O}_3$ :  $1\text{ mg L}^{-1}$ , matrix: ultrapure water adjusted to pH 4.0, 7.0, 9.0 and 10.0).

### Effect of matrix content

The effect of various matrix constituents was studied, in order to assess their ability to enhance or inhibit the reaction kinetics of RAN with aqueous ozone. Soft and hard simulated drinking water was used as well as various DOM concentrations in ultrapure water.

**Fig. 4.3** demonstrates the effect of DOM on the ozonation of RAN. Three different levels of DOM concentrations usually found in real water systems were tested. Results indicated that at low initial concentration of RAN ( $C_0$   $1\text{ mg L}^{-1}$ ), the application of  $1\text{ mg L}^{-1}$   $\text{O}_3$  is enough to almost totally eliminate RAN (90% removal), regardless of the applied DOM concentration. In surface and wastewater systems, RAN is often found in much lower concentration (levels of  $\mu\text{g L}^{-1}$ ), than the ones applied in this study. Therefore, the application of ozone even at low concentrations of  $1\text{ mg L}^{-1}$  should be enough to completely remove RAN even in the presence of DOM. Nevertheless, at higher RAN concentration ( $2\text{ mg L}^{-1}$ ), DOM starts to play a considerable role to RAN degradation. Low

DOM concentration ( $1 \text{ mg L}^{-1}$ ) does not seem to significantly affect RAN removal, but at 2 and  $5 \text{ mg L}^{-1}$  the degradation efficiency is reduced, since RAN removal is reduced to 50% and 42%, respectively. These results can be attributed to the potential simultaneous consumption of ozone by DOM.

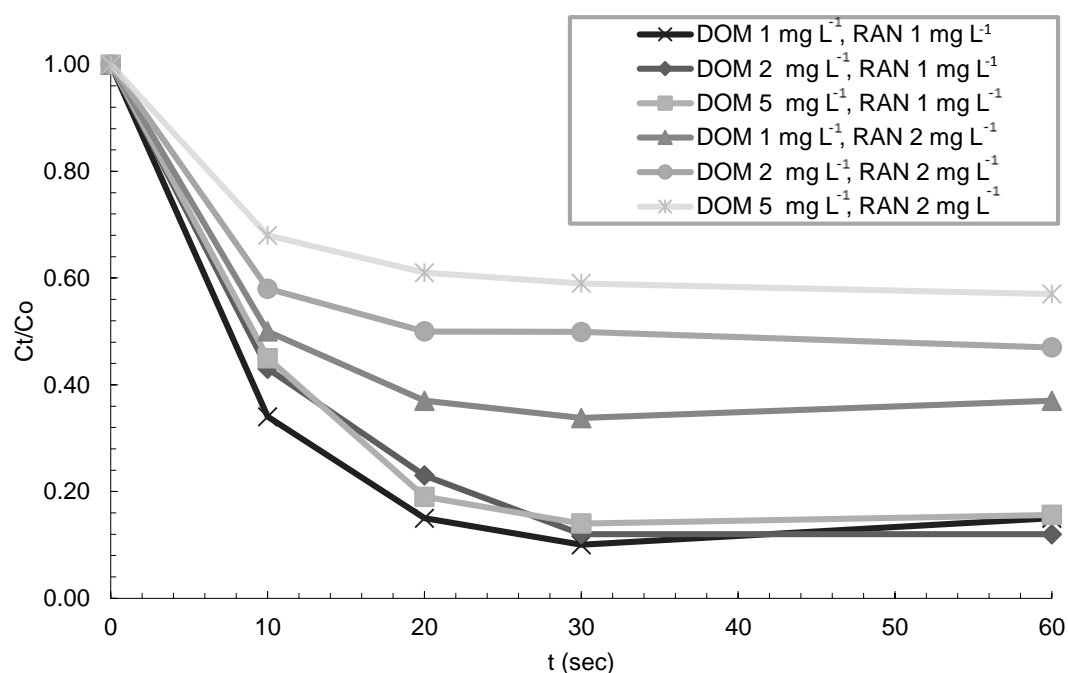


**Fig. 4.3.** RAN removal in the presence of dissolved organic matter ( $C_0 \text{ O}_3$ :  $1 \text{ mg L}^{-1}$ ).

Ozonation of RAN in different inorganic matrix (soft and hard drinking water) did not exhibit significant changes in the % removal (35-40%) of RAN. Also, the different water hardness and anion content did not indicate significant differences in RAN ozonation.

### **Mineralization of RAN**

Mineralization of RAN at the selected conditions is low. For initial RAN concentration of  $10 \text{ mg L}^{-1}$ , applied ozone concentration  $8 \text{ mg L}^{-1}$  and 3 different pH (3.0, 4.0, 5.8), mineralization did not exceed 22% for 1 min of total reaction time, although at the same conditions RAN is completely removed. Mineralization of RAN at pH 10 reached 43 %, which was attributed to the formation of OH radicals which promote RAN's mineralization. Thus, it can be

deducted that RAN is transformed into various TPs which require the application of increased ozone concentration or a continuous application of ozone dose in order to achieve higher mineralization.

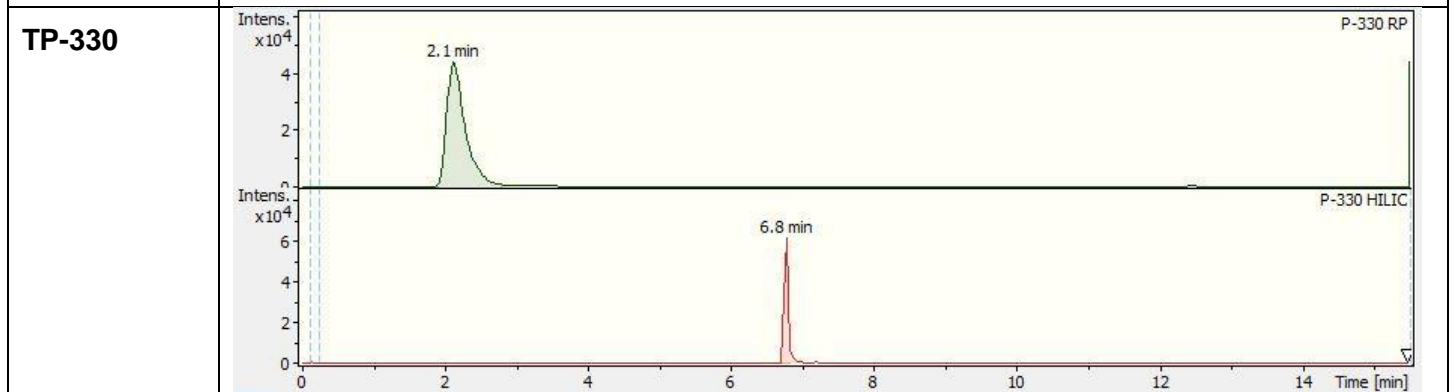
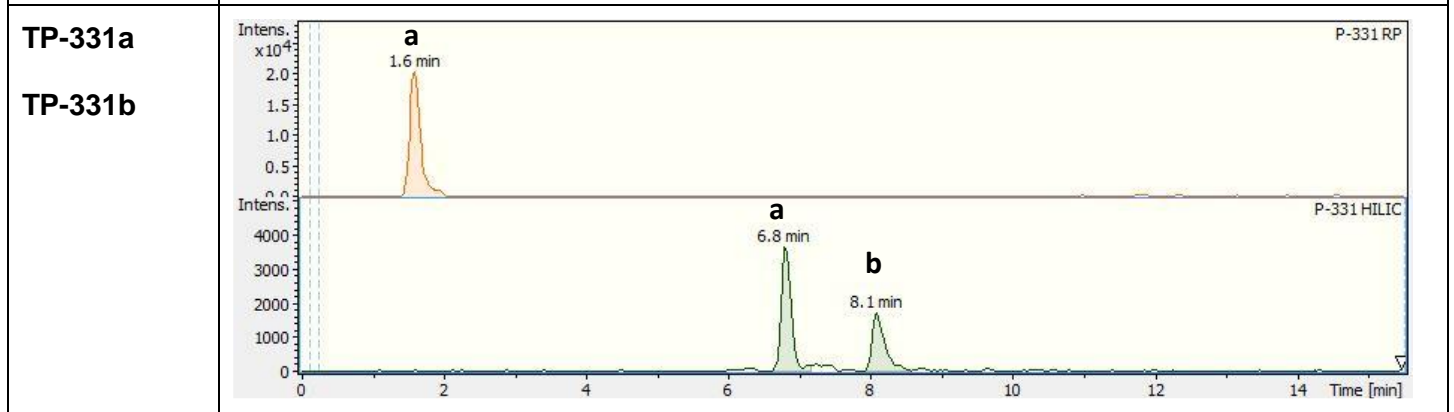
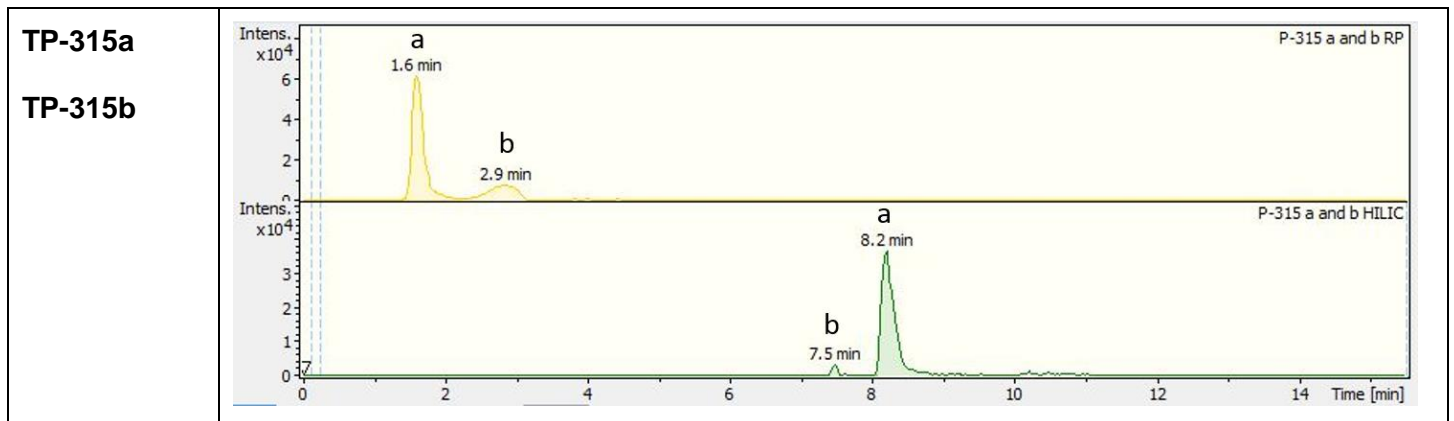
#### 4.4.2 Identification of ozonation transformation products

Through the application of the two screening approaches, “suspect” peaks were detected only in positive ionization mode (PI). No positive results were obtained in negative ionization (NI), maybe due to insufficient ionization of the produced TPs in this mode.

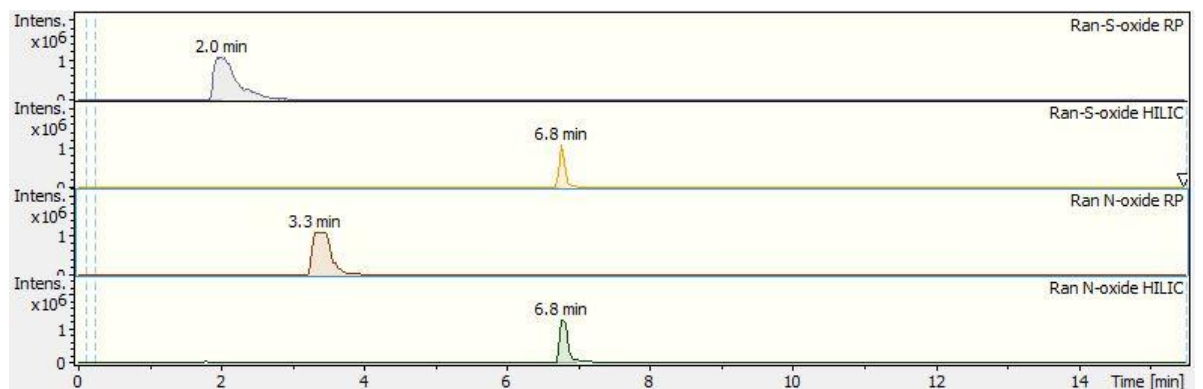
Overall, eleven (11) TPs of RAN were detected and structurally elucidated. **Table 4.1** depicts the corresponding RPLC and HILIC Extracted Ion Chromatograms in PI for RAN and its TPs produced during the first minute of the ozonation experiment.

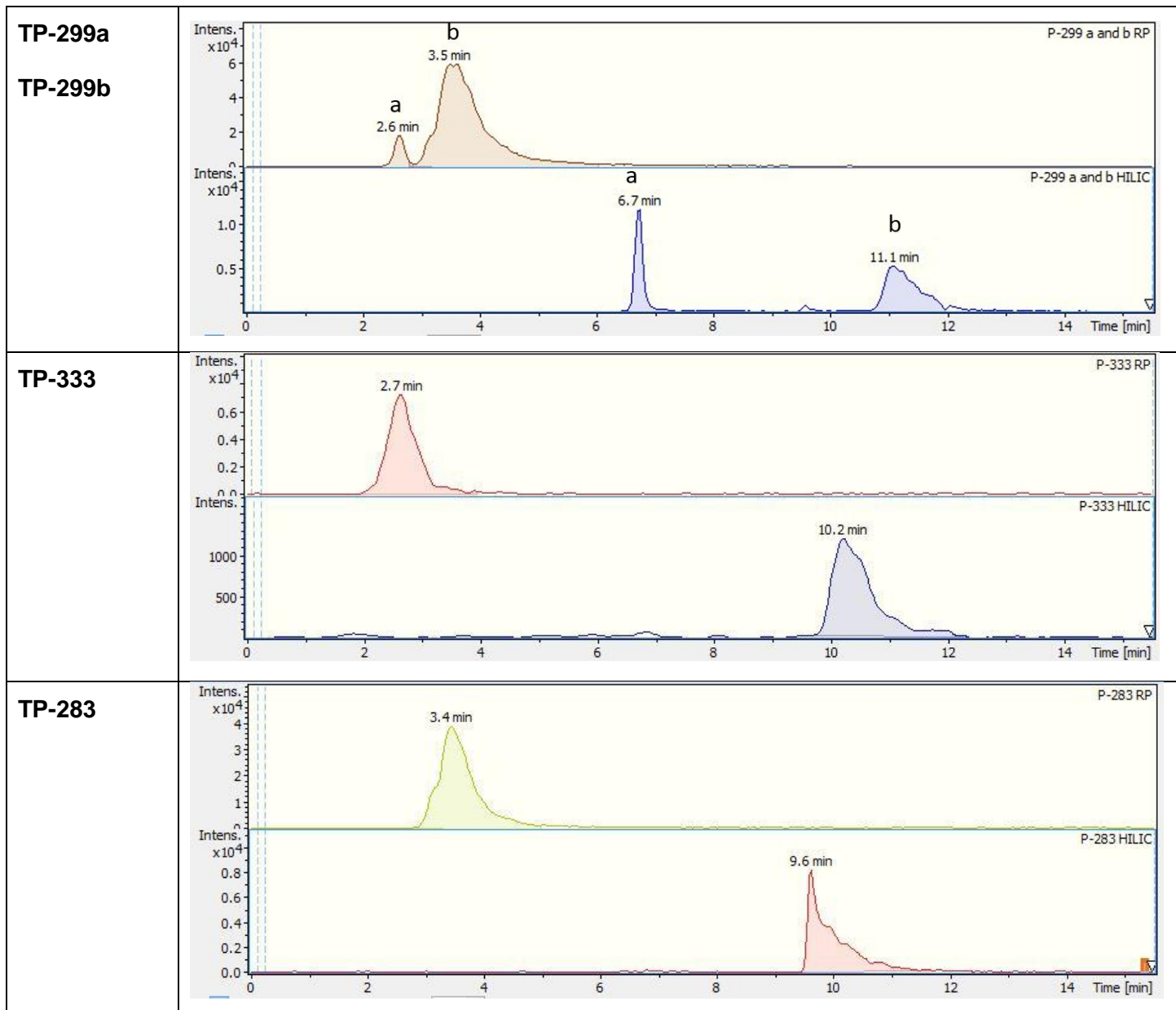
**Table 4.1.** Extracted Ion Chromatograms of the identified transformation products of ranitidine (RAN) using RPLC and HILIC.

Compound	Chromatogram
RANITIDINE	
TP-304	



### Ran S- and N-oxide reference standards





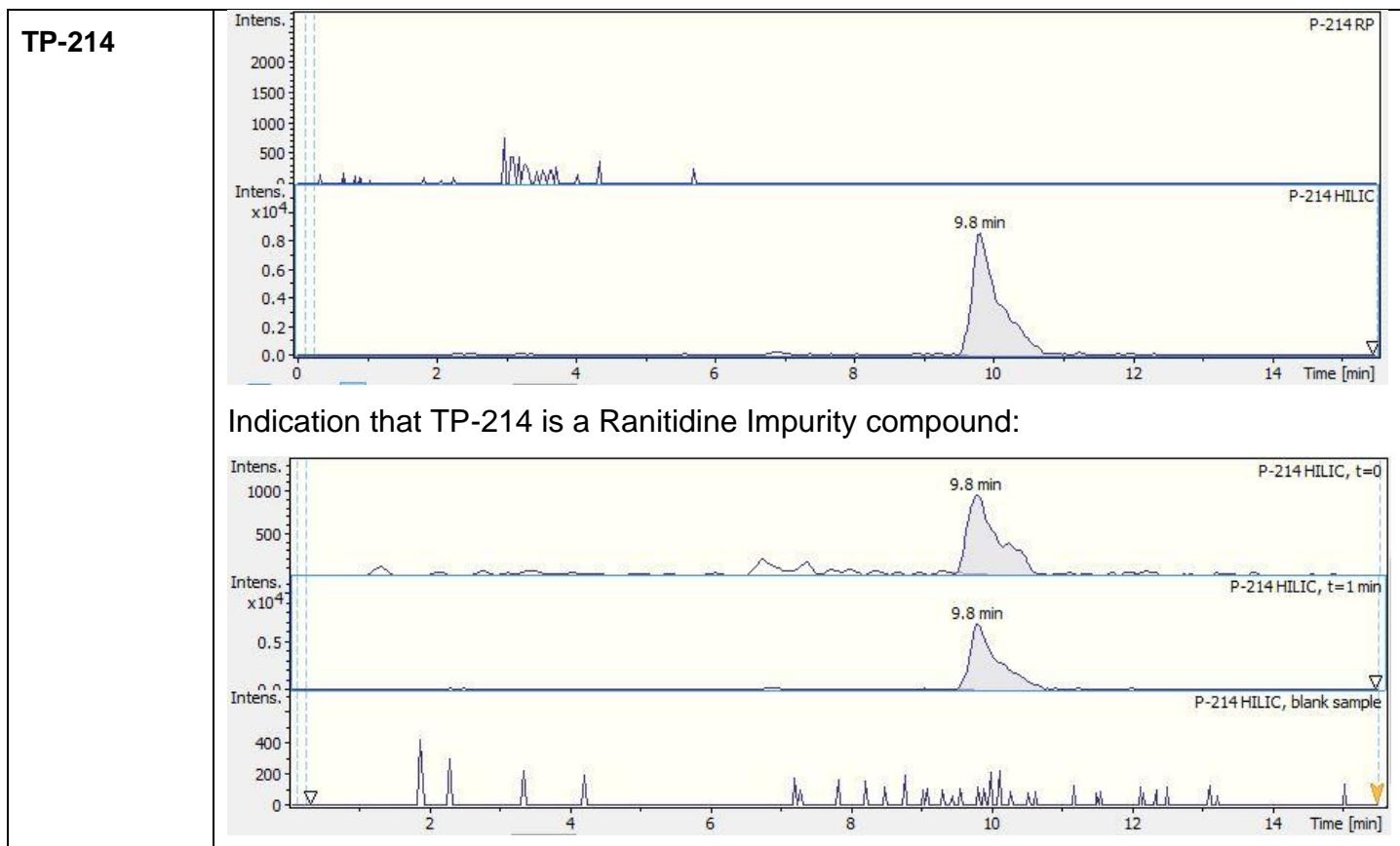
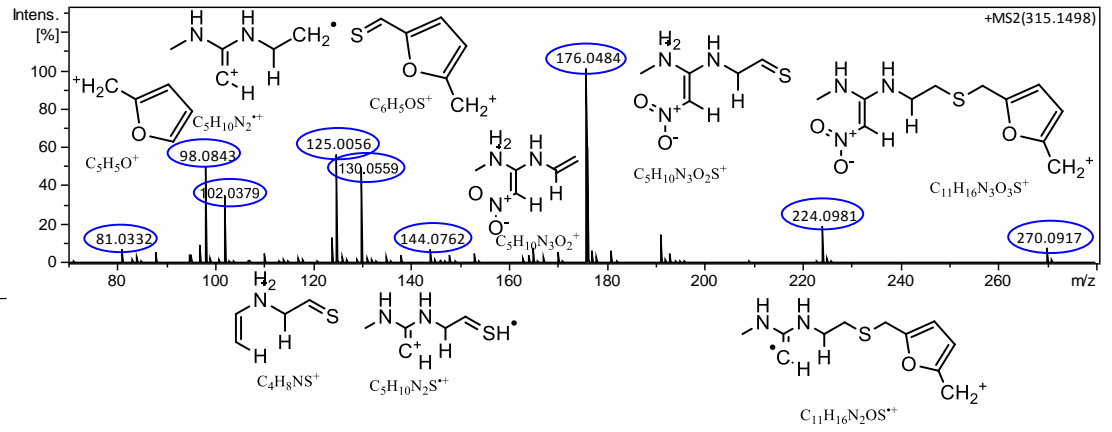
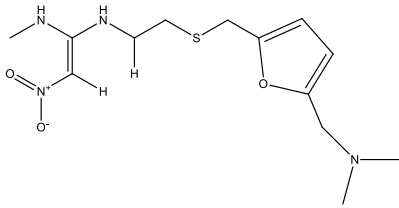
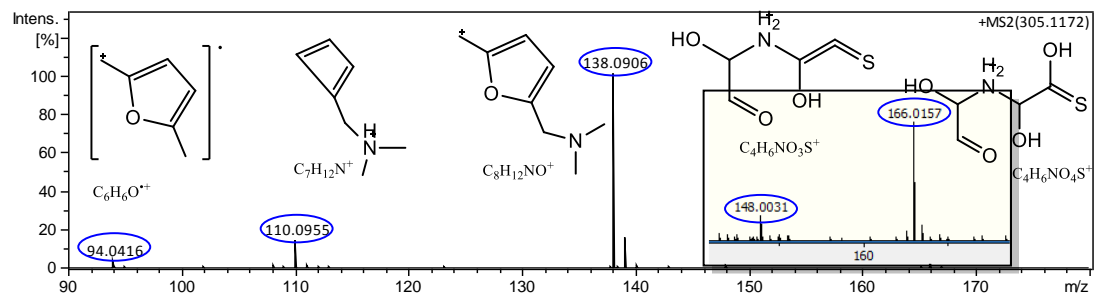
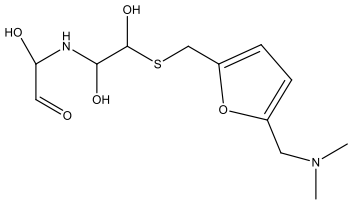


**Table S4.3** (Section S4.5) includes information on the retention time, elemental formula, proposed structure, experimental accurate mass, theoretical mass, mass error (ppm) and isotopic fit (mSigma) for the precursor and fragment ions of the identified TPs. It also provides the level of confidence for the identification for each proposed TP. **Fig. 4.4** provides the MS/MS (AutoMS) spectra and the corresponding proposed structures of the most abundant fragments attributed to the identified ozonation TPs, as well as selected MS spectra where in source fragmentation was observed.

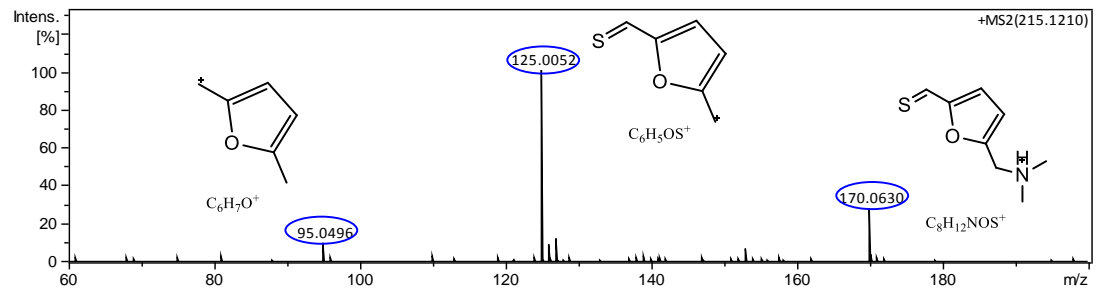
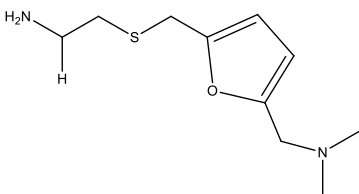
### RAN



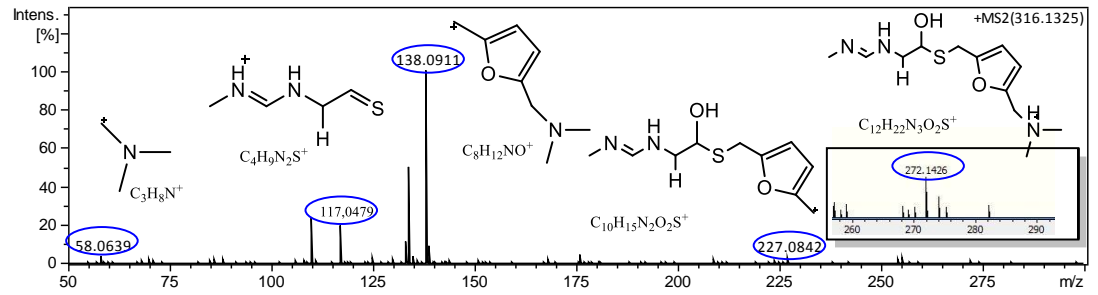
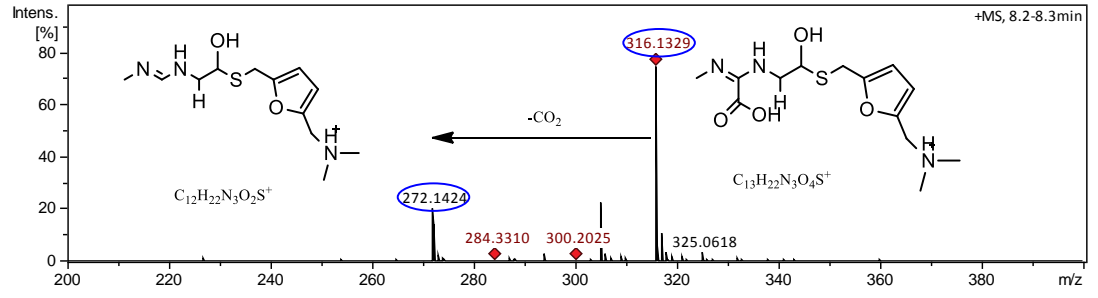
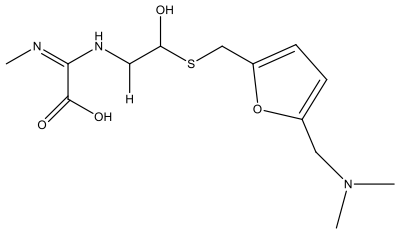
### TP-304



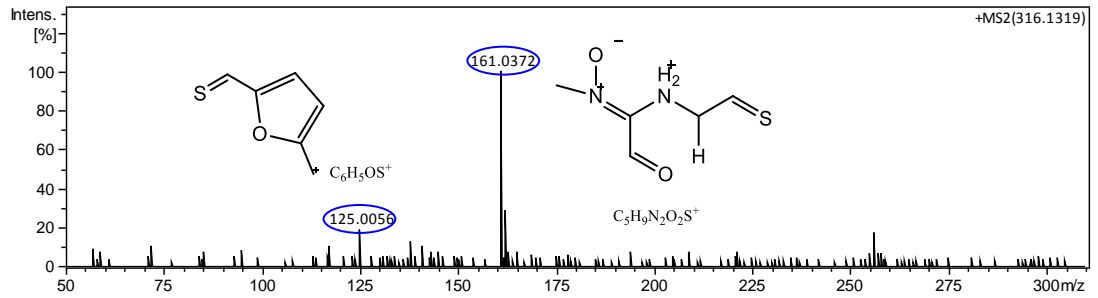
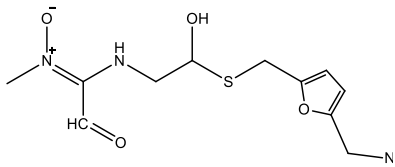
### TP-214



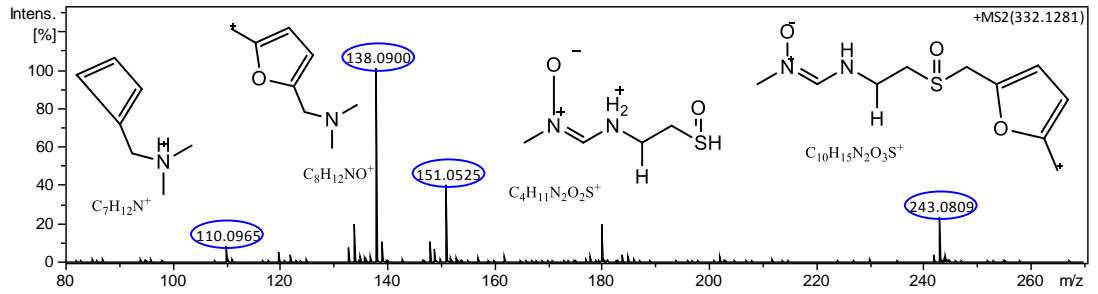
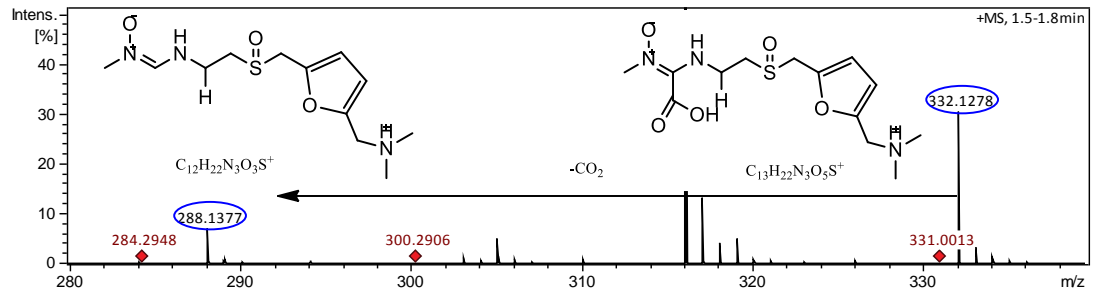
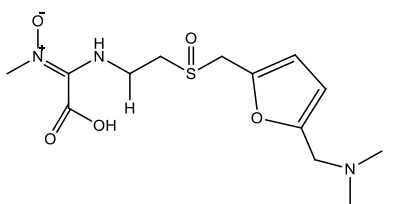
**TP-315a**



**TP-315b**

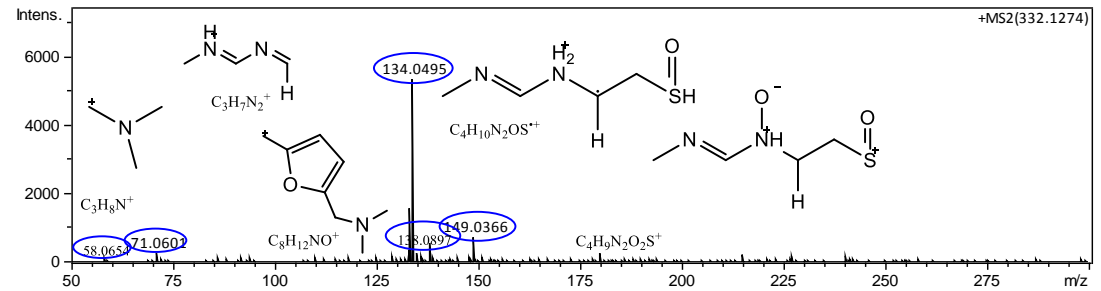
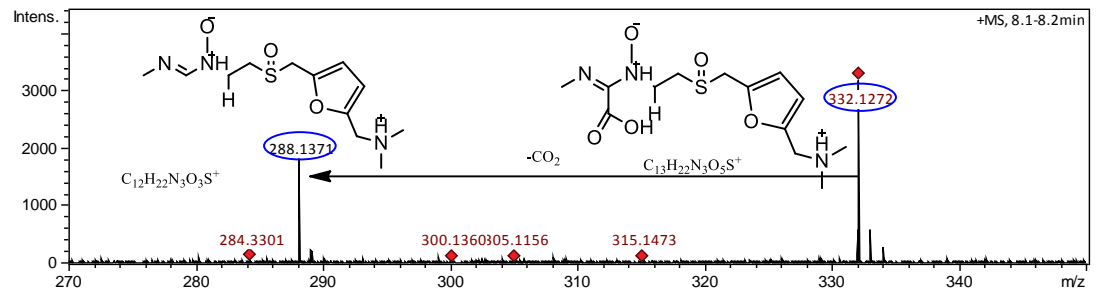
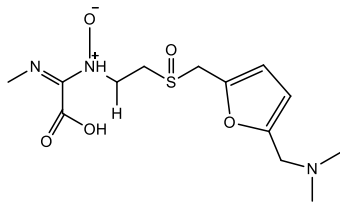


**TP-331a**

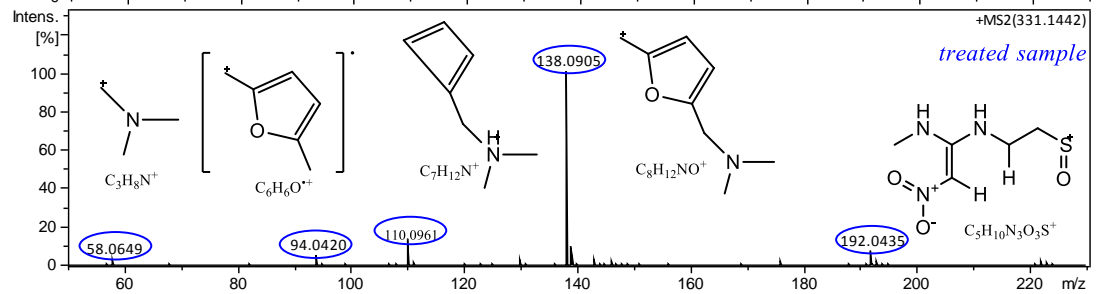
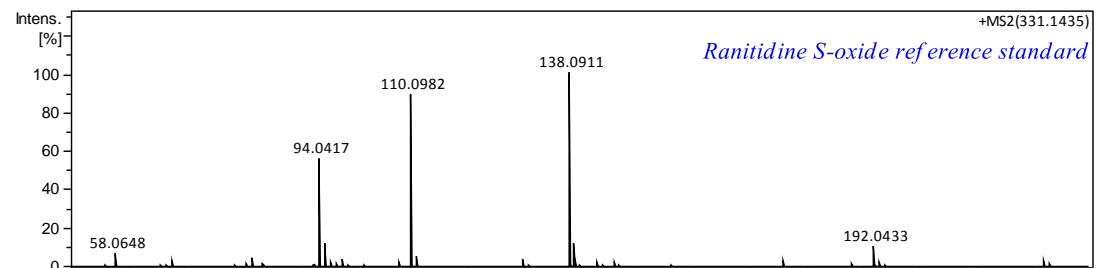
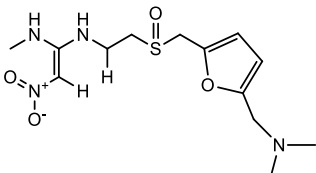




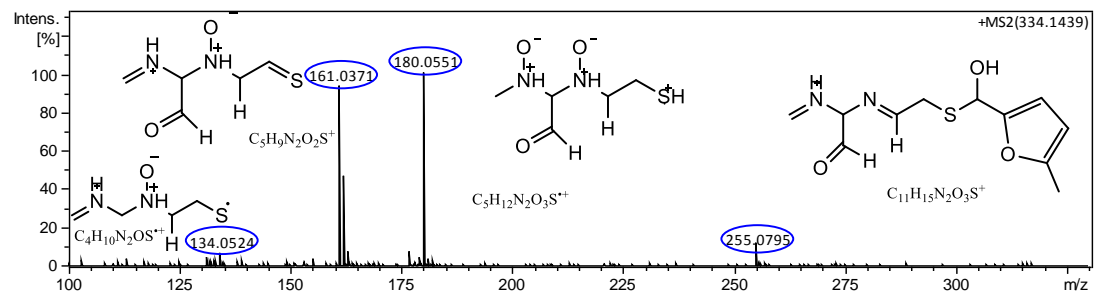
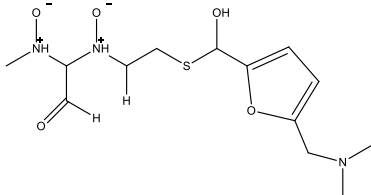
### TP-331b



### TP-330



### TP-333



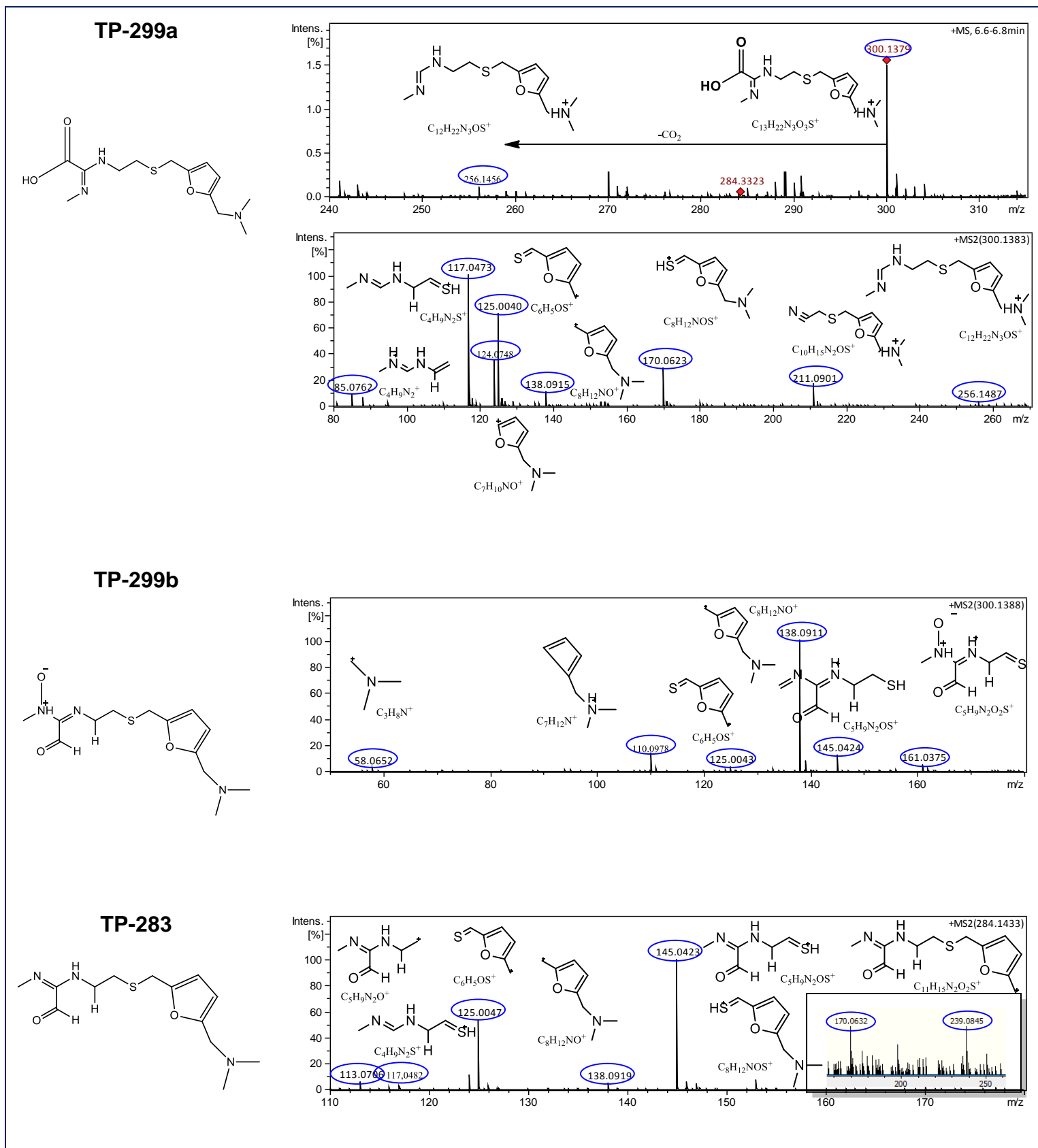


**Fig. 4.4.** Data dependent MS/MS (autoMS) spectra and their interpretation to support the identification of ozonation TPs of Ranitidine.

RAN elutes at  $t_R=3.3$  min in the RPLC column and at 6.7 min in the HILIC column (**Table 4.1**). The MS spectrum shows the molecular ion of  $[M+H]^+$   $C_{13}H_{23}N_4O_3S^+$  at  $m/z$  315.1498. AutoMS spectrum (**Fig. 4.4**) showed a fragment ion at  $m/z$  270.0907, corresponding to a molecular formula of  $C_{11}H_{16}N_3O_3S^+$  and a fragment loss of  $m/z$  45.0578, representing a typical loss of N,N-dimethyl-amino moiety. Fragment ion 224.0981 is attributed to the loss of the nitro group and the formation of a charged radical. The fragment with  $m/z$  176.0491 is attributed to the structure proposed in **Table S4.3**, which is formed through a C-S bond rupture and the removal of the part containing the furan ring. Further loss of a sulfide group from the fragment with  $m/z$  176.0491 produces the fragment with  $m/z$  144.0762, while the abstraction of a nitro group leads to the formation of  $m/z$  130.0559. Consequent loss of sulfide group from  $m/z$  130.0559 forms  $m/z$  98.0843. The fragment at  $m/z$  81.0332 corresponds to the 2-methyl-furane ring structure.

At  $t_R$  1.5 min (RPLC) and 8.1 min (HILIC), TP-304 is detected, with the molecular ion at  $m/z$  305.1172 (**Table 4.1**). The proposed structure corresponds to the abstraction of the  $NO_2$  group and the addition of a hydroxyl group and the formation of an aldehyde. Furthermore, hydroxylation of the two carbon atoms next to sulfur occurs. This structure is supported by the AutoMS mass spectra obtained from this precursor ion (**Fig. 4.4**). AutoMS spectrum includes fragment ion at  $m/z$  138.0906 ( $C_8H_{12}NO^+$ ), which corresponds to the furan-containing part of the molecule which remains unchanged (**Table S4.3**), as well as fragments  $m/z$  110.0955 ( $C_7H_{12}N^+$ ) and  $m/z$  94.0416 ( $C_6H_6O^+$ ), originating from this part of the molecule and indicating that ozonation did not affect this part. The fragment at  $m/z$  166.0157 ( $C_4H_8NO_4S^+$ ) indicates that it originates from the alkyl part of the molecule, including a hydroxyl group next to the sulfur atom. The loss of a water molecule leads to the formation of  $m/z$  148.0031. The full MS or MS/MS spectra do not contain fragments corresponding to a loss of  $CO_2$  group thus indicating that the oxidized part of the molecule does not contain a carboxyl group. Moreover, the double bond equivalent (DBE) of  $m/z$  305.1172, equal to 3.5 indicates that 3 oxygen atoms are added as hydroxyl groups and one as aldehyde or ketone.

TP-315a and TP-315b are eluted at  $t_R=1.6$  min and 2.9 min in RPLC and  $t_R=8.2$  min and 7.5 min in HILIC, respectively (**Table 4.1**). The allocation of the peaks was based on the comparison of the full MS and AutoMS spectra. The experimental  $m/z$  of these two products is equal to 316.1329 and 316.1319, respectively which both adequately fit to the proposed chemical formula  $C_{13}H_{22}N_3O_4S^+$  in both cases. TP-315a and TP-315b, both include the same carbon atoms as RAN, one less N and one more oxygen atom ( $C_{13}H_{22}N_3O_4S^+$ ). In the case of TP-315a, the precursor mass fits the formula  $C_{13}H_{22}N_3O_4S^+$  (mass error equal to 2 ppm) and the proposed structure (**Table S4.3**) indicates the abstraction of the  $NO_2$  moiety, the addition of a carboxyl group and the formation of a C=N double bond (imine). The presence of a carboxyl group in the molecule of TP-315a is supported by the MS spectrum, which includes an in-source fragment at  $m/z$  272.1426 ( $C_{12}H_{22}N_3O_2S^+$  with mass error 0.4ppm) corresponding to a loss of  $CO_2$  ( $m/z$  43.9893). A further loss of the N,N-dimethyl-amino moiety is indicated by fragment  $m/z$  227.0821. Furthermore, the presence of  $m/z$  138.0911 indicates that ozonation did not affect the part of the molecule including the furan ring. At  $m/z$  117.0479, a fragment containing the imine part of the molecule and sulfur was generated by the precursor ion, due to the rupture of C-S bond. The formation of a C=S bond in the fragment  $m/z$  117.0479 indicates the loss of a water molecule. Therefore, the hydroxyl group in the structure of TP-315a is located next to the sulfur atom.

TP-315b, with the molecular ion  $m/z$  316.1319 corresponds to a structure similar to 315a with the difference that it includes an aldehyde group in the place of the carboxyl group and a N-oxide group (**Fig. 4.4**). This structure is supported by the fact that neither MS (due to potential in source fragmentation) nor AutoMS data indicate towards a loss of  $CO_2$ . The fragment at  $m/z$  161.0372 ( $C_5H_9N_2O_2S^+$ ) corresponds to the hydroxylated alkyl part of the molecule (**Table S4.3**), which includes a nitron ( $RCH=N^+-O^-$ ) group attached to the imine moiety, originating from ozone attack to the imine nitrogen [157, 176, 185]. Also the fragment at  $m/z$  125.0056 ( $C_6H_5OS^+$ ) is part of the intact furan-containing part of the molecule.

TP-331a is eluted at  $t_R=1.6$  min in the RPLC column (**Table 4.1**), corresponding to  $m/z$  332.1281. The proposed formula ( $C_{13}H_{22}N_3O_5S^+$ ) is in good fit with the

experimental mass (mass error 1.9 ppm) and it indicates a loss of nitrogen and an addition of oxygen in the initial RAN molecule. MS spectrum of the obtained peak, shows that there is a loss of CO<sub>2</sub> at the ionization source ( $m/z$  288.1378), pointing towards the existence of a carboxyl group in the TP-331a structure. AutoMS spectrum (**Fig. 4.4**) provides 4 fragments generated from TP-331a, which support the suggested structure. Fragmentation of TP-331a (DBE of 4.5) leads to the loss of CO<sub>2</sub> (carboxyl group) generating a fragment with  $m/z$  288.1376 (C<sub>12</sub>H<sub>22</sub>N<sub>3</sub>O<sub>3</sub>S<sup>+</sup>, mass error 0.5 ppm), and a DBE of 3.5, also proving that the abstracted group included one double bond (carboxyl group). A further abstraction of the N,N-methyl-amino group leads to the formation of fragment at  $m/z$  243.0809 (C<sub>10</sub>H<sub>15</sub>N<sub>2</sub>O<sub>3</sub>S<sup>+</sup>), which matches the structure containing a N-oxide and a S-oxide group (**Table S4.3**). The furan-containing part of the molecule is further fragmented into  $m/z$  138.0900 and  $m/z$  110.0965, with well-fitted formulas (low mass error) that do not include additional oxygen atoms, showing that the oxidation did not occur in this part of the molecule. Finally, the fragment at  $m/z$  151.0525 is formed from the rupture of the C-S bond and the abstraction of the furan-containing part, representing a part of the molecule which contains the N-oxide and a S-oxide groups (DBE 0.5). Data indicate that TP-331a is produced by RAN with the abstraction of the NO<sub>2</sub> moiety, the formation of a carboxyl group and the oxidation of the sulfur and nitrogen atoms. The use of HILIC provided two chromatographic peaks for  $m/z$  332.1281. The first one, eluting at  $t_R$  6.8 min in HILIC, corresponds to the TP-331a which eluted at  $t_R$ =1.6 min using RPLC. The MS and AutoMS spectra obtained for both peaks present an adequate match. The second peak at  $t_R$  8.1 min represents TP-331b, which provided similar MS but different AutoMS spectra to those of TP-331a. MS spectrum shows a loss of CO<sub>2</sub> ( $m/z$  288.1373) denoting the presence of a carboxyl group in the molecule. Further fragmentation leads to the formation of  $m/z$  138.0897, corresponding to the furan-part of the molecule, after the rupture of C-S bond, and to the formation of  $m/z$  149.0366 and  $m/z$  134.0495, representing the alkyl-part of TP-331b. Further fragmentation leads to the formation of  $m/z$  71.0601 corresponding to C<sub>3</sub>H<sub>7</sub>N<sub>2</sub><sup>+</sup> with the formation of a double C=N bond on the second amine group, indicating the presence of a hydroxyl group next to the second amine group. Abstraction of H<sub>2</sub>O through fragmentation leads to the formation of C=N double bond.

Mass spectrum data indicate that TP-331b is produced by RAN during ozonation, probably through the cyclic addition of ozone on the double bond next to the nitro-group of RAN. Group rearrangement, leads to the cleavage of NO<sub>2</sub> and the formation of a carboxyl group and a double C=N bond.

At  $t_R=2.1$  min (RPLC) and 6.8 min (HILIC) TP-330 is eluted (**Table 4.1**), which corresponds to  $m/z$  331.1442 and fits the proposed formula C<sub>13</sub>H<sub>22</sub>N<sub>3</sub>O<sub>3</sub>S<sup>+</sup> with low mass error (2.3 ppm). This formula suggests that there is just one additional oxygen present in the TP-330 compared to RAN. The fragment at  $m/z$  192.0435 (C<sub>5</sub>H<sub>10</sub>N<sub>3</sub>O<sub>3</sub>S<sup>+</sup>) corresponds to TP-330 after the rupture of C-S bond and the loss of the furan part (**Table S4.3**). The rest of the obtained AutoMS peaks ( $m/z$  138.0905,  $m/z$  110.0961 and  $m/z$  94.0420) correspond to fragments of the furan-containing part of the molecule, suggesting that the additional oxygen is located on the alkyl-part of the molecule. In order to determine whether TP-330 corresponds to RAN S-oxide or RAN N-oxide, reference standard solutions of these compounds were analyzed under the same chromatographic and mass spectrometry conditions. **Table 4.1** shows that the retention time of RAN S-oxide and TP-330 are matching both in RPLC and HILIC. Moreover, the  $m/z$  peaks obtained by MS and MS/MS spectra (**Fig. 4.4 and Table S4.3**) of the two compounds also match, reaching identification confidence of level 1.

TP-299a and TP-299b are eluted at  $t_R=2.6$  min and 3.5 min for RPLC and  $t_R=6.7$  min and 11.1 min, for HILIC, respectively (**Table 4.1**). The allocation of the peaks was realized by comparing MS and AutoMS spectra.

TP-299a corresponds to the molecular ion  $m/z$  300.1383 which fits to the proposed chemical formula C<sub>13</sub>H<sub>22</sub>N<sub>3</sub>O<sub>3</sub>S<sup>+</sup> (mass error -2.4 ppm). This formula indicates that TP-299a in comparison to RAN, retains all the carbon atoms but loses one nitrogen-containing group, which implies that the N,N-dimethylamine terminal group remains intact. Moreover, there is no addition of oxygen atoms and sulfur atoms are still present in the structure. DBE remains the same as in the case of RAN (4.5). The data suggest that there is a structure change at the part of the molecule containing the NO<sub>2</sub> moiety. MS spectrum includes a peak at  $m/z$  256.1476, which perfectly fits the formula C<sub>12</sub>H<sub>22</sub>N<sub>3</sub>OS<sup>+</sup> (mass error 0.8 ppm and adequate isotopic fitting 31 mSigma) and is attributed to the loss of CO<sub>2</sub> ( $m/z$  43.9905), indicating the presence of a carboxyl group in the molecular

structure of TP-299a. This is supported by the reduction of DBE from 4.5 to 3.5, due to the loss of the double bond C=O. AutoMS spectrum provides seven (7) more fragments giving information on the molecular structure of TP-299a. Fragments at  $m/z$  170.0693,  $m/z$  138.0915,  $m/z$  125.0040 and  $m/z$  124.0748 are all generated by the cleavage and further fragmentation of the furan-containing part, which is not affected by oxidation and remains intact during ozonation (**Table S4.3**). Therefore, oxidative transformations must have occurred in the alkyl-part of the molecule. Further fragmentation of  $m/z$  256.1476 leads to the abstraction of  $C_2H_7N$  - loss of the terminal C=N-CH<sub>3</sub> group (imine) - and the formation of  $m/z$  211.0901, perfectly fitting formula  $C_{11}H_{15}N_2O_3S^+$  (mass error -1.0 ppm). The fragment at  $m/z$  117.0473 corresponds to  $C_4H_9N_2S^+$  which fits the alkyl-part of the molecule after the loss of carboxyl group. Further abstraction of sulfide moiety generates  $m/z$  85.0762. The mass spectrum data lead to the conclusion that for the formation of TP-299a, ozonation probably occurs in one of the two secondary amine centers or the double bond next to the nitro-group. Since there is no carbon loss in the suggested formula compared to RAN, it can be deduced that, after the reaction of ozone on the double bond next to nitro-group or the attack of O<sub>3</sub> to the secondary amine with the methyl group, an intramolecular rearrangement occurs, eventually leading to the formation of C=O and finally -COOH. All the AutoMS fragment data, demonstrated low mass error and good isotopic fitting, compared to the suggested formulas.

TP-299b corresponds to  $m/z$  300.1375, accurately fitting the formula  $C_{13}H_{22}N_3O_3S^+$ , with a mass error equal to 0.5 ppm and an excellent isotopic fitting (18.1 mSigma) (**Table S4.3**). This formula compared to RAN includes one less nitrogen atom, but no reduction in the carbon atoms present in the molecule, pointing towards the loss of the NO<sub>2</sub> moiety and an addition of oxygen. The AutoMS spectrum of TP-299b presents differences compared to that of TP-299a (**Fig. 4.4**). There is no evident loss of CO<sub>2</sub>, indicating the absence of a carboxyl moiety, although DBE value is 4.5 equal to TP-299a, therefore the addition of the oxygen was carried out through the formation of a C=O bond. Fragments at  $m/z$  138.0911, 125.0043, 110.0978 and 58.0652 represent the gradual fragmentation of the furan-containing part, which does

not seem to have been affected by ozonation. Fragment at  $m/z$  161.0375 adequately fits to the formula  $C_5H_9N_2O_2S^+$ , with an  $rdbe$  of 2.5, indicating the presence of 3 double bonds. The formula corresponds to the part of the molecule after the rupture of C-S bond and the abstraction of the furan-containing part, which includes an aldehyde moiety and an N-oxide group. Further fragmentation generates  $m/z$  145.0424 indicating a loss of  $H_2O$  from the N-oxide and the adjacent carbon atom, with the formation of a double bond. As in the case of TP-299a, there is no carbon loss compared to the structure of RAN, indicating that during ozonation either the double bond or the adjacent secondary amine of RAN is attacked and a subsequent intramolecular rearrangement occurs.

Since molecular ozone selectively attacks organic compounds with high electron density functional groups, such as double bonds, or amines (especially secondary or tertiary without a positive charge), the addition of ozone to the secondary amines of the alkyl-chain in the RAN molecule presents a plausible oxidative reaction [157]. TP-333, eluting at  $t_R = 2.7$  min (RP) and 10.2 min (HILIC), at  $m/z$  334.1439 (**Table 4.1**), represents the formula  $C_{13}H_{24}N_3O_5S^+$ , with low mass error (-2.3 ppm) and good isotopic fitting (20 mSigma), which points towards a structure with no carbon losses, a reduction of nitrogen atoms by one and the addition of oxygen. The MS and MS/MS spectra, as well as the reduced DBE value of 3.5, indicate a structure containing multiple hydroxylated positions. MS and MS/MS spectra do not contain fragments generated by the loss of  $CO_2$ , proving the absence of a carboxyl group, but the presence of an aldehyde group, similar to other TPs previously mentioned. The fragment at  $m/z$  255.0795, which perfectly fits formula the  $C_{11}H_{15}N_2O_3S^+$ , is generated by the loss of the N,N dimethyl amino group and the abstraction of two  $H_2O$  molecules from the N-oxide moieties and their adjacent carbons, thus forming two double bonds. The fragment at  $m/z$  180.0551 adequately fits the formula  $C_5H_{12}N_2O_3S^{++}$  which corresponds to the alkyl - part of TP-333 after the cleavage of the C-S bond (**Table S4.3**). This fragment includes 3 oxygen atoms, leading to the conclusion that one hydroxyl group is attached to the furan part of the molecule and more specifically to the carbon atom between sulfur and furan ring. This is supported by the total absence of fragments at approximately  $m/z$



138.08 and  $m/z$  110.09, indicating that the furan-containing part of TP-333 did not remain intact through ozonation, as in most of the previously mentioned TPs.

TP-283 elutes at  $t_R=3.4$  min in RPLC and 9.6 min in HILIC (**Table 4.1**). It is closely eluted to TP-299b and the chromatographic peaks show similar shape, therefore the HILIC elution profile of the two TPs was compared, showing that they present different elution times ( $t_R$  11.1 min and 9.6 min for TP-299b and TP-283 respectively). At  $m/z$  284.1433 the proposed formula is  $C_{13}H_{22}N_3O_2S^+$ , with excellent fit (mass error of 2.0 ppm) and good isotopic fitting (18.1 mSigma). Similar to the other proposed TPs, the  $NO_2$  moiety seems to have been replaced by a carbonyl bond and the formation of an adjacent C=N bond. MS/MS spectrum includes 7 fragments (**Fig. 4.4**). Due to the loss of N,N-dimethylamine group,  $m/z$  239.0845, with the proposed formula  $C_{11}H_{15}N_2O_2S^+$ , is generated. Further fragmentation generates  $m/z$  145.0423, which can be described by the formula  $C_5H_9N_2OS^+$ , which includes the imine moiety and the aldehyde group. Further fragmentation generates  $m/z$  117.0482, and  $m/z$  113.0706, which represent the structures obtained after the loss of CO and sulfide, respectively. The smaller fragments of  $m/z$  170.0632, 138.0919, 125.0047 correspond to the gradual fragmentation of the furan-containing part (**Table S4.3**), which has not been oxidized through the ozonation process.

HILIC was proven to be a successful tool for the identification of polar compounds and its complementarity to RPLC was highly indicated by the fact that some TPs were detected only in HILIC.

TP-214 was not detected in RPLC, while in HILIC it was eluted at  $t_R$  9.8 min with high sensitivity (**Table 4.1**). TP-214 ( $m/z$  215.1210) perfectly matches the proposed formula  $C_{10}H_{19}N_2OS^+$ , with a mass error of -0.3 ppm, an excellent isotopic fitting of 18.6 mSigma and the DBE value equal to 2.5 (**Table S4.3**). This TP is generated by a C-N bond rupture in the parent compound's structure. The fragments  $m/z$  170.0630, 125.0052 and 95.0496 indicate that the furan-containing part of the molecule has remained intact during the reaction. TP-214 seems to be a RAN impurity product [Ranitidine impurity B (Ph.Eur.)], so  $m/z$  215.1210 was also detected in the sample obtained at zero-time of the experiment. But, the fact that its intensity increased during the ozonation

reaction, leads to the conclusion that TP-214 can also be characterized as a RAN ozonation TP (**Table 4.1**).

Moreover, TP-331 was eluted as one chromatographic peak in RP, while the application of HILIC revealed the presence of two isomers (**Table 4.1**). Using HILIC also resulted in the efficient separation of the two isomers TP-299a and TP-299b.

### **Retention time prediction results**

Apart from the use of HILIC, retention time prediction was also applied as a complementary technique for the identified TPs using two in-house developed QSRR prediction models. The results shown in **Table 4.2** indicate that most of the predicted retention times are in accordance with the experimental ones, since only the prediction error for TPs 315a and 333 (in RPLC and HILIC, respectively) just reaches the set threshold. Considering the absolute window of  $\pm 2$  min for a compound that has different chemical structure from the training set may lead to wrong conclusion. For this reason, in order to evaluate the prediction results, an in-house developed tool was used [142]. This tool examines the origin of residuals between predicted and experimental retention time.

The exported results (shown as bubble plots, **Figures S4.3** and **S4.4**, Section S4.6) show if the observed residual is due to the wrong chemical structure (leading to wrong prediction of retention time) or because the tested structure is outside the applicability domain of the model. More information concerning the evaluation of the applicability domain is provided in the Electronic Supplementary Material (Section S4.6).

As it can be seen from **Figures S4.3** and **S4.4**, most of the predicted retention times are inside boxes 1 and 2, suggesting that the prediction results are accepted. However, there are two compounds (TPs 299a and 333), located in box 3 in HILIC analysis. The bubble sizes for these two compounds are quite large, indicating that the source of the observed residual can be the large chemical structure diversity. Thus, these two compounds are outside the applicability domain of the prediction model, so, retention time prediction cannot be used as supporting information for their identification.

**Table 4.2.** Predicted and experimental retention time of identified compounds in RPLC and HILIC and the corresponding errors ( $\Delta t_R$ ).

Compound	RP			HILIC		
	$t_R$ pred. (min)	$t_R$ exp. (min)	$\Delta t_R$ (min)	$t_R$ pred. (min)	$t_R$ exp. (min)	$\Delta t_R$ (min)
RAN	3.3	3.3	0	6.6	6.7	-0.1
TP-214	-	n.d.	-	9.8	9.8	0
TP-283	2.9	3.4	-0.5	8.5	9.6	-1.1
TP-299 a	2.6	3.5	-0.9	9.4	11.1	-1.7
TP-299 b	3.5	2.6	0.9	7.4	6.7	0.7
TP-304	2.1	1.5	0.6	9.2	8.1	1.1
TP-315 a	3.6	1.6	2.0	7.1	8.2	-1.1
TP-315 b	2.2	2.9	-0.7	8.1	7.5	0.6
TP-330	1.7	2.1	-0.4	6.7	6.8	-0.1
TP-331 a	2.5	1.6	0.9	6.9	6.8	0.1
TP-331 b	-	n.d.	-	8.0	8.1	-0.1
TP-333	2.3	2.7	-0.4	8.2	10.2	-2.0

\*n.d. not detected

### **Identification Highlights**

TP-330 has been identified as the RAN S-oxide, at level 1 of identification confidence [85], since the structure has been confirmed by the analysis of the RAN S-oxide reference standard (MS, MS/MS and  $t_R$  matching). It is produced by direct oxidation of RAN at the sulfide group of the structure (**Table 4.1**).

TP-214, is a RAN impurity product, which was detected in the initial RAN sample at low intensities, but was also produced during ozonation, through the C-N bond rupture adjacent to the  $\text{NO}_2$  moiety and the subsequent methyl abstraction from the terminal secondary amine.

Overall, 11 ozonation TPs were identified and were structurally elucidated. **Fig. 4.5** presents the proposed structures of the identified TPs. In all cases, except for TP-330, the oxidation occurs in the alkyl-part of the RAN molecule, more specifically at the double bond or the adjacent secondary amine, followed by an intramolecular rearrangement.

The suggested reaction pathways for the production of TP-283 are presented in **Fig. S4.5** (Section S4.7) [157, 176, 185]. Pathway (1) describes the cyclic

addition of ozone on the double bond next to nitro-group. Group rearrangement, leads to the cleavage of  $\text{NO}_2$  and the formation of  $\text{C}=\text{O}$ . Reaction pathway (2) suggests the attack of  $\text{O}_3$  to the secondary amine with the methyl group. Rearrangement eventually leads to the formation of  $\text{C}=\text{O}$  and TP-283. Similar reaction pathways and further oxidation could lead to the formation of TPs containing a carboxyl group, hydroxylated carbons or N-oxide moieties.

Apart from RAN-S-oxide which was confirmed by the analysis of the corresponding reference standard, all the proposed structures were based on the MS and MS/MS data (characteristic fragments), the retention time prediction and the oxidation reactions that could occur during the ozonation of RAN (oxidation of a known structure). With all this evidence, an identification level of 2b was assigned to the tentative TPs.

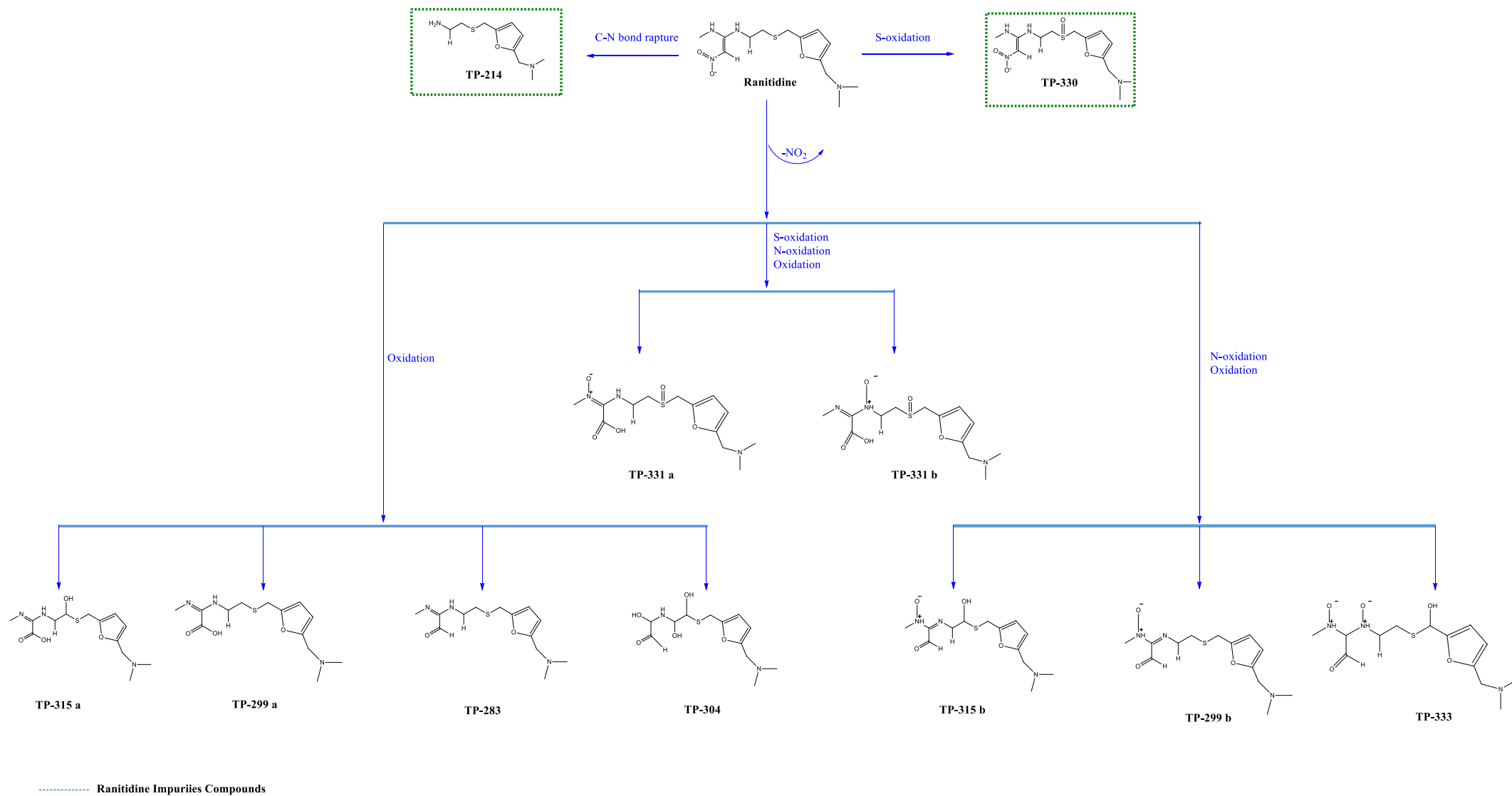


**Fig. 4.5.** Ozonation transformation products of Ranitidine (Co Ranitidine: 5 mg L<sup>-1</sup>, Co O<sub>3</sub>: 1 mg L<sup>-1</sup>, matrix: ultrapure water, reaction time: 1 min).

#### 4.5. Conclusions

Ranitidine is highly reactive with molecular aqueous ozone. Ozone concentration and pH significantly affected the % removal of RAN during ozonation. Higher % removal was observed at increased pH and high ozone concentrations. At neutral and acidic pH, mineralization reached 22%. DOM reacts with ozone and reduces RAN's overall removal especially at higher RAN concentrations. The presence of inorganic ions in the aqueous matrix did not seem to affect RAN ozonation.

Eleven (11) TPs have been identified and structurally elucidated. For most of the TPs (TP-304, TP-315b, TP-299b, TP-333, TP-283) the oxidation occurs in the alkyl-part of the RAN molecule, more specifically at the double bond or the adjacent secondary amine, with the abstraction of NO<sub>2</sub> moiety, generating TPs with an aldehyde moiety and an imine C=N bond. Further oxidation leads to the formation of oxidized derivatives of RAN, including a carboxylic group in their structure. RAN S-oxide has also been identified as an ozonation product (TP-330) and its structure has been confirmed through the analysis of a reference standard. Finally TP-214, was also produced during ozonation, through the C-N bond rupture.

HILIC was successfully used for the identification of polar compounds as a complementary tool to RP, since some TPs were only detected in HILIC and was proven to be extremely useful for the separation and identification of TPs with isomeric structures.

Retention time prediction was also used as a supporting tool for the identification of TPs. The predicted t<sub>R</sub> of most compounds in both RPLC and HILIC were comparable to the experimental ones, supporting the proposed structures.

## CHAPTER 5.

### Removal and transformation of citalopram and four of its biotransformation products during ozonation experiments

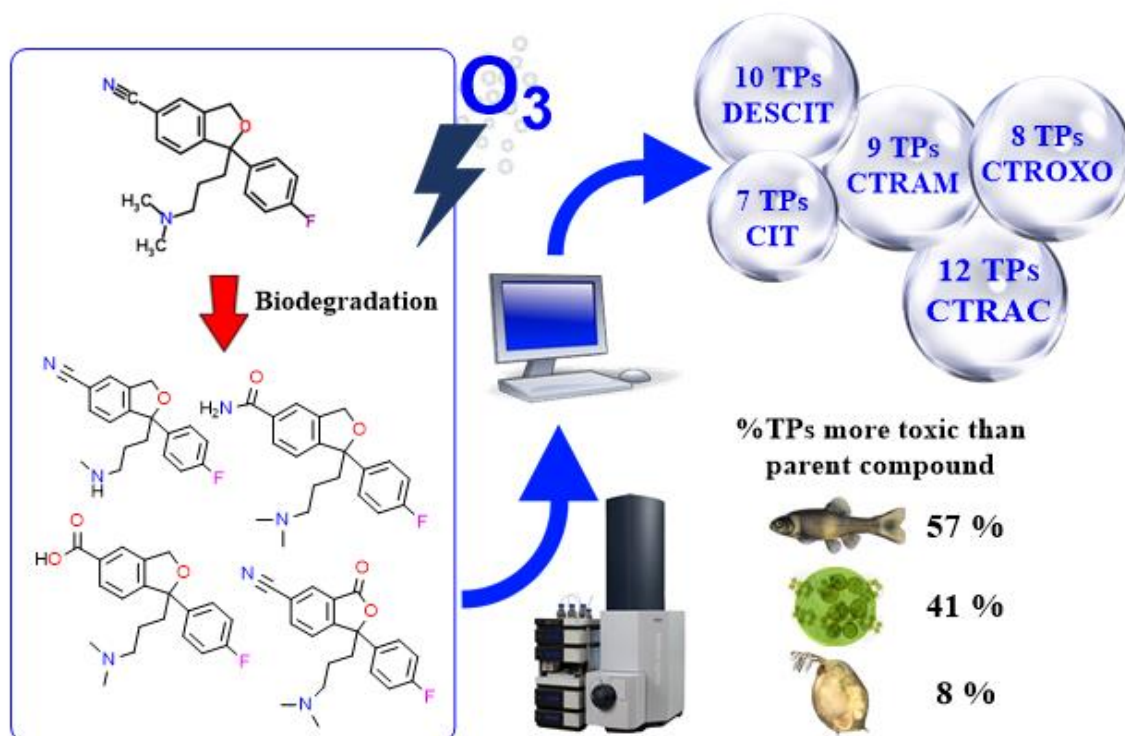


Fig. 5.0 Graphical abstract of Chapter 5.

### 5.1. Introduction

The continuous discharge of pharmaceuticals in effluents from production facilities, hospitals, and private households, improper disposal of unused drugs, and the direct discharge of veterinary medicines, all lead to environmental waters contamination [186]. WWTPs process various emerging pollutants, their metabolites and their known TPs [187]. The applied treatment sequence includes the following steps: a primary gravity settling, a secondary biological treatment and finally a tertiary step which includes advanced oxidation processes for disinfection and removal of micropollutants [13]. Treatment with ozone appears to be one of the most promising disinfection technologies for the removal of these compounds. Although the removal of many pollutants may be significant, often total mineralization is not achieved. Since the reactivity of ozone towards organic compounds is high, TPs with unknown physicochemical properties and toxicity, could be produced. Therefore, emerging pollutants

incompletely removed in WWTPs and their TPs produced through secondary or tertiary treatment can be released into the aquatic environment, forming a major source of contamination. Thus, their fate during the processes applied in WWTPs is of great environmental importance [80, 188]. On the context of target, suspect and non-target screening workflow [139], target screening methods can only cover a relatively small proportion of these organic contaminants and their known TPs. Thus, one of the hottest trends in the environmental analysis based on liquid chromatography (LC) coupled to high resolution mass spectrometry (HRMS) is to develop non-targeted based methods to unveil the unknown chemicals and their TPs [22, 103, 112, 189].

Most non-target screening approaches result in an identification of new substances out of hundreds of thousand chemical fingerprints for a sample analyzed by HRMS. Although, non-targeted methods provide full details about the chemical profile of a sample, and each  $m/z$  could be a potential mass of interest according to identification confidence [85], the data analysis could be extremely time-consuming due to the searching space of these exact masses of interest. Some pre-treatment steps could however decrease the false positives, procedural blank chemical features (contaminations caused while performing the analytical procedure) or ion source contamination [190].

Ion Fusion [191] and Mass Spectral Feature List Optimizer (MS-FLO) [190] are two known tools to assist removal of isotopes and the fusion of ion adducts as well as identifying duplicate or contaminate peaks. Duplicate peak removal involves scanning the LC-HRMS peaks-list to identify  $m/z$  that have been incorrectly aligned as separate peaks by data processing methods such as CAMERA R package [192]. From analytical point of view, the isotopes and adducts are important for deconvolution of mass spectra of precursor ions and their identification [139]. However, these  $m/z$  are not important in prioritization task while performing non-target screening over a mass of interest. Therefore, chemometrics methods used extensively to perform non-target screening only over those  $m/z$  that have highest explained variance or Variable Importance in Projection (VIP) between a set of samples according to their labels/classes [193-195]. The simple yet challenging approach that has been applied recently in case of LC-HRMS study for the detection and identification of TPs, is trend



analysis of the intensity of a  $m/z$  during several time points [196]. Trend analysis can decrease dramatically the searching space for LC-HRMS peaks-list and promote the identification of unknown TPs efficiently.

A simple trend analysis can be done based on the spearman correlation coefficient (SCC) of intensities of a mass of interest analyzed in several time points [196]. In case of ozonation study of an interesting compound (like pharmaceuticals), present in environmental samples at high concentration, SCC can be obtained based on projection of intensity of a mass of interest versus various ozonation doses added. Although, using SCC is prone to error in identification of TPs that have been formed in a certain ozone concentration and subsequently removed when higher concentration is added, it could provide useful information about TPs with increasing trend in their intensities alongside ozonation doses. Having a flexible statistical means to detect one point generation and removal of TPs is therefore of imperative need in case of non-targeted screening. In addition to SCC, an automatic approach based on the quality of Gaussian curve fitting between intensities of possible TPs and added ozone concentration could reveal the TPs having an increasing trend or one-point generation-removal at certain ozonation doses.

When emerging substances like pharmaceuticals are degraded in the environment, they may form persistent and toxic TPs, which can pose an increasing threats to aquatic life, environment, as well as human being [13]. This is of growing concern since higher toxicity values for TPs than their parent compounds have been already reported in the literature [197-199]. Therefore, any wastewater or surface water treatment process should be accounted for the risk assessment of the known and unknown TPs detected in the environmental samples. TPs have become under focus not only due to their formation in the environment, but also during advanced water treatment processes, where various commonly used water tertiary treatment methods can result in rapid formation of TPs. Prioritization of TPs based on their environmental risk could arise the alarm to take measures against removal of any persistent and toxic TP. Environmental risk assessment (developed to predict the toxicity in environmental/aquatic life form (i.e. water flea daphnia magna, algae or fish)) as well as environmental fate models can promote the

quantitative estimation of toxicity of newly identified TPs and thus trigger the establishment of precautionary measurements against their occurrence, if this is indicated. At the same time, innovative and accurate with defined applicability domain (AD) approaches like Quantitative Structure-Toxicity Relationship (QSTR) could be useful to estimate the toxicity of TPs in aquatic multispecies [200]. Therefore, a QSTR model could be suitable to predict the toxicity and to prioritize TPs on the basis of their environmental risk.

Citalopram (CIT), a selective serotonin re-uptake inhibitor, is a compound of interest due to its worldwide high consumption for the treatment of depression. Several studies reported the occurrence of CIT in different environmental matrices worldwide, including influent and effluent wastewaters, sewage sludge and surface waters [201-203]. Despite its high environmental occurrence rate, the studies evaluating its fate and transformation are limited. The identification of TPs formed after exposure to simulated sunlight [204] and oxidation technologies (including ozone and ClO<sub>2</sub>) [205] was performed by low resolution MS analysis. High resolution analytical instruments, like quadrupole time-of-flight (QTOF) mass spectrometry, are extensively used for real time detection and identification of oxidation products, due to their high confirmatory capabilities, derived from the high resolving power and the mass accuracy in MS and MS/MS modes, along with the developed sophisticated software. Moreover, using LC-Q-ToF analysis, Beretsou et al. (2016) detected 14 biotransformation products of CIT, among which 9 were tentatively identified and 4 were confirmed through the analysis of authentic reference standard [206].

So far, studies concerning the transformation of emerging contaminants during a disinfection method (ozonation, chlorination, UV treatment), have been focused on the probable transformation of known contaminants and less frequently on their known human metabolites [207-211]. Since recent literature has revealed the formation of biotransformation products of emerging contaminants during secondary biological treatment, their probable transformation during tertiary treatment should not be overlooked.

## **5.2. Scope of the study**

The aim of this study was to investigate the removal and transformation of CIT and four of its biotransformation products during ozonation. N-desmethyl CIT (DESCIT), CIT amide (CTRAM), CIT carboxylic acid (CTRAC) and 3-oxo-CIT (CTROXO), were identified as CIT biotransformation products in a previous study conducted in our laboratory [206], by means of high resolution mass spectrometric techniques and their structure was confirmed through the analysis of the corresponding reference standard. These compounds were also detected through retrospective analysis in real secondary treated wastewater samples, underlying the need for further investigation of their fate during tertiary treatment processes. Thus, the fate of CIT, DESCIT, CTRAM, CTRAC and CTROXO during ozonation was investigated in this study. Advanced chemometric techniques were developed for the first time for the automated detection of their TPs and the extraction of their formation profile versus ozone concentration. The detected TPs were then structurally elucidated based on their MS/MS spectra interpretation considering also its similarity with that of the respective parent compound. In order to assess the potential threat for aquatic organisms, an environmental risk assessment study was performed, using an in-house toxicity prediction program. Finally, an overview of the identified TPs of all tested compounds was provided to demonstrate the correlation in the transformation of commonly structured parent compounds and the formation of the same TPs from different precursors.

## **5.3. Experimental Part**

### **5.3.1 Standards and reagents**

The purity of all reference standards was higher than 95%. CIT (CAS No: 59729-33-8) was purchased from LGC Promochem (Molsheim, France), CTROXO (CIT Related Compound C, CAS No: 372941-54-3) was provided by US Pharmacopoeia (Twinbrook Parkway, Rockville, MD, USA), and the rest three parent compounds, DESCIT, CTRAM and CTRAC (CAS Nos: 144010-85-5, 64372-56-1 and 440121-09-5, respectively) were obtained by Jubilant Life Sciences Ltd (Shanghai, China).

For LC-HRMS analysis, ultrapure water was produced using a Milli-Q water purification system (18.2  $\mu\Omega/\text{cm}$ , Millipore Direct-Q UV, Bedford, MA, USA). Methanol (MeOH) LC-MS grade was purchased from Merck (Darmstadt, Germany), and 2-propanol and ethyl acetate of LC-MS grade were from Fisher Scientific (Geel, Belgium). Sodium hydroxide monohydrate for trace analysis  $\geq 99.9995\%$ , ammonium formate  $\geq 99.0\%$  LC-MS Ultra (eluent additive for UHPLC-MS) and formic acid 99% (eluent additive for LC-MS) were purchased from Fluka (Buchs, Switzerland). For buffer solutions preparation, ammonium acetate (cryst., 96%) and ammonia solution (25%) were purchased from Merck (Darmstadt, Germany), while glacial acetic acid (99.7%) was from Panreac Quimica SA (Barcelona, Spain).

### 5.3.2 Ozonation experiments

Batch ozonation experiments were carried out using a concentrated ozone stock solution (25-30 mg/L), which was prepared daily, in a 1 L glass bottle filled with ultrapure water and placed in a bucket filled with ice. Ozone was produced from industrial/biomedical grade oxygen (99.5%, Revival Bottled Gas, Athens, Greece) using AZCOZON VMUS-2 ozone generator, by AZCO Industries Ltd (Canada). The gas flow rate was kept constant at 40 L/h and dosed through a sintered sparger, at the bottom of the glass bottle. The dissolved ozone concentration was determined spectrophotometrically by measuring the absorbance of the solution at 258 nm and using a molar absorptivity value of  $2950 \text{ M}^{-1} \text{ cm}^{-1}$  [174].

The ozonation experiments were performed in sealed bottles. Separate reaction bottles were used for evaluating the removal and transformation of each parent compound (CIT, DESCIT, CTRAM, CTRAC and CTROXO) in every tested experimental condition. The initial concentration of the tested compounds was kept always at 2 mg/L. Although this concentration is 4-5 orders of magnitude higher than those detected in environmental samples, it was selected for facilitating the detection of as many TPs as possible and to acquire abundant and clear MS/MS spectra that would lead to TPs structure elucidation. Probable reactions due to hydroxyl radicals formation, were suppressed by the addition of a scavenger-compound [50 mM of tert-butanol (t-BuOH)] in every reaction solution. Once the appropriate volume of ozone

stock solution was added to each reaction bottle, they were wrapped in aluminum foil to avoid exposure to light, and mixed for 1 h to ensure that the reaction was completed until full depletion of ozone.

Two series of batch experiments were conducted; in the first batch the influence of ozone concentration on the removal of the parent compound and the formation of TPs was investigated, while in the second one, the influence of the pH value of the reaction mixture was tested, using ammonium acetate buffers of 1mM. Six different initial ozone concentrations of 0.06, 0.3, 1.5, 3, 6 and 12 mg/L were examined at pH 7.0 ( $\pm 0.2$ ), reflecting the pH of wastewater. Furthermore, experiments at pH 4 and 10 ( $\pm 0.2$ ), in reaction with 3 mg/L of ozone were also conducted. Thus, a great range of pH was investigated taking into consideration both the ozone stability and reactivity and the dissociation forms of the tested compounds, which highly influence the ozonation reaction [212, 213]. An overview of the samples taken from the ozonation experiments in different experimental conditions for every tested compound, is presented in **Table 5.1**.

**Table 5.1.** Ozonation experiments samples for every tested compound.

Samples $C_{t=0}^*$ , parent compound: 2 mg/L, $C_{t=0}$ , t-BuOH: 50 mM)	pH of the solution		
	7.0	4.0	10.0
Zero-time sample (t=0)	✓	✓	✓
$C_{t=0}$ , ozone: 0.06 mg/L	✓		
$C_{t=0}$ , ozone: 0.3 mg/L	✓		
$C_{t=0}$ , ozone: 1.5 mg/L	✓		
$C_{t=0}$ , ozone: 3 mg/L	✓	✓	✓
$C_{t=0}$ , ozone: 6 mg/L	✓		
$C_{t=0}$ , ozone: 12 mg/L	✓		

\* $C_{t=0}$ : Initial concentration

### 5.3.3 Instrumental analysis

The analysis was carried out using a UHPLC-QTOF-MS system, equipped with a UHPLC apparatus (Dionex UltiMate 3000 RSLC, Thermo Fisher Scientific, Dreieich, Germany), consisting of a solvent rack degasser, an auto-sampler, a

binary pump with solvent selection valve and a column oven coupled to the QTOF-MS mass analyzer (Maxis Impact, Bruker Daltonics, Bremen, Germany). The chromatographic separation was performed on a Thermo Scientific Acclaim<sup>TM</sup> RSLC 120 C18 (100 mm×2.1 mm, 2.2µm) column), preceded by an ACQUITY UPLC BEH C18 1.7 µm, VanGuard Pre-Column from Waters (Dublin, Ireland), and thermostated at 30 °C. The Q-TOFMS system was equipped with an electrospray ionization (ESI) interface. Chromatographic analysis was carried out using a gradient elution and flow rate program of twenty minutes duration, as shown in **Table 5.2**. Milli-Q water/MeOH (90/10) (A) and MeOH (B), both containing 5 mM of ammonium formate and acidified with 0.01% v/v formic acid, were used as binary mobile phase mixtures. The ESI parameters used in positive mode were the following: capillary voltage, 2500 V; end plate offset, 500 V; nebulizer pressure, 2 bar (N<sub>2</sub>); drying gas, 8 L/min (N<sub>2</sub>); and drying temperature, 200 °C.

**Table 5.2.** The gradient elution program of LC-HRMS analysis.

<b>Aqueous solvent:</b> ( <i>H<sub>2</sub>O/MeOH 90/10, 5 mM HCOONH<sub>4</sub>, 0.01% FA</i> )			
<b>Organic Solvent:</b> ( <i>MeOH, 5 mM HCOONH<sub>4</sub>, 0.01% FA</i> )			
<b>Time (min)</b>	<b>Flow rate (mL min<sup>-1</sup>)</b>	<b>Aqueous solvent %</b>	<b>Organic Solvent %</b>
0	0.2	99	1
1	0.2	99	1
3	0.2	61	39
14	0.4	0.1	99.9
16	0.48	0.1	99.9
16.1	0.48	99	1
19.1	0.2	99	1
20.0	0.2	99	1

The samples were analyzed by two MS modes, using three different MS methods; a data-independent fragmentation method and two different data-dependent methods. In the first run, the QTOF-MS system was operating in broadband collision-induced dissociation (bbCID, data-independent) acquisition mode and recorded spectra over the range m/z 50–1000 with a scan rate of 2 Hz. This mode provides MS and MS/MS spectra at the same time, working at two different collision energies; at low collision energy (4 eV), MS spectra were acquired. At high collision energy (25 eV), no isolation is taking

place at the quadrupole, and the ions from the preselected mass range are fragmented at the collision cell. This main advantage of this mode is that it provides high sensitivity in MS mode and the chromatograms include the total profile (“fingerprint”) of the sample, including precursors and fragments. Thus, the chromatograms obtained by bbCID analysis were used for TPs detection. It has to be ensured that the instrument permits the comparison over  $k$  injections without discriminating against single ones. Issues such as column bleed, carryover, major system fluctuations or loss of sensitivity over time would considerably affect the intensity of each  $m/z$  recorded [214]. Therefore, each sample was injected 3 times within the sequence of analysis, to enable peak recognition and trace any major fluctuations in the intensity of detected TPs from one injection to another to monitor the true stability of the detected TPs (fluctuations in the intensities of TPs that are irrelevant to instrument repeatability).

The second MS analysis was performed in AutoMS (data-dependent) acquisition mode. This is a data-dependent mode, where the five most abundant ions per MS scan are selected and fragmented. The collision energy applied was set to predefined values, according to the mass and the charge state of every ion. This mode provides clear and compound-specific fragmentation spectra that is used for structure confirmation of known compounds as well as structure elucidation of unknown TPs. The drawback of this method is that if the  $m/z$  of interest is not within the five most abundant ions per MS scan, then no MS/MS spectrum is obtained. For this reason, a third analysis was performed for acquiring the MS/MS spectra of the low intensity detected TPs. The samples where the highest concentration of the TPs of interest were noticed, were pre-concentrated under a gentle stream of nitrogen and then AutoMS analysis was followed. The fragmentation in the last applied method is defined by an inclusion (preselected) mass list containing the precursor ions of interest (exact masses). The fragmentation of these  $m/z$  is triggered when their intensity in the MS spectra exceeds the set intensity threshold of 1,000 counts. The collision energy applied to the data-dependent methods was set to predefined values, according to the mass and the charge state of every ion.

A QTOF-MS external calibration was performed daily with a sodium formate solution (10 mM). For internal calibration, a segment in every chromatogram (0.1–0.25 min) was used, where the calibration solution was injected at the beginning of each run. The theoretical exact masses of calibration ions with formulas  $\text{Na}(\text{NaCOOH})_{1-14}$  in the range of 40–800 Da, were used for calibration. The instrument provided a typical resolving power of 36000–40000 during calibration.

Data treatment and evaluation were processed with DataAnalysis 4.1 and TargetAnalysis 1.3 (Bruker Daltonics, Bremen, Germany). All the recorded raw data were further processed with TrendTrAMS, a new automatic TPs detection software (in-house program written in MATLAB). Moreover, XCMS online [215] was used for pairwise comparison between experiments done at different pH values.

## 5.4 Data treatment

### 5.4.1 Automated Detection of TPs

All samples analyzed by LC-QTOF-MS/MS were firstly converted to mzML files using ProteoWizard and then transferred to R environment in order to perform peaks picking, using XCMS. The detailed optimization of peaks picking parameters is available in the Electronic Supplementary Material (**Section S5.1**). The pre-treated LC-HRMS peaks-list for each experimental batch was followed by a prioritization method based on their intensity trends towards the ozonation doses. Additionally, to compare experiments done in different pH values (4, 7 and 10), unpaired parametric t-test (p-value threshold for a mass to be highly significant was set to 0.05) was used in XCMS online [215]. The assumption was that different pH values could create different TPs and this would create two different independent groups (therefore, experiments done at different pH considered to be parametric (and also independent)). Any m/z found to be unique in two groups were identified through a cloud plot showing the fold changes (based on intensity variations) [216]. The parameters optimized by IPO for peaks picking were also used in XCMS online before performing the pairwise comparison between the samples of different experimental pH values. Moreover, the list of m/z (potential TPs) extracted for every parent compound was narrowed based on the theory that TPs retention



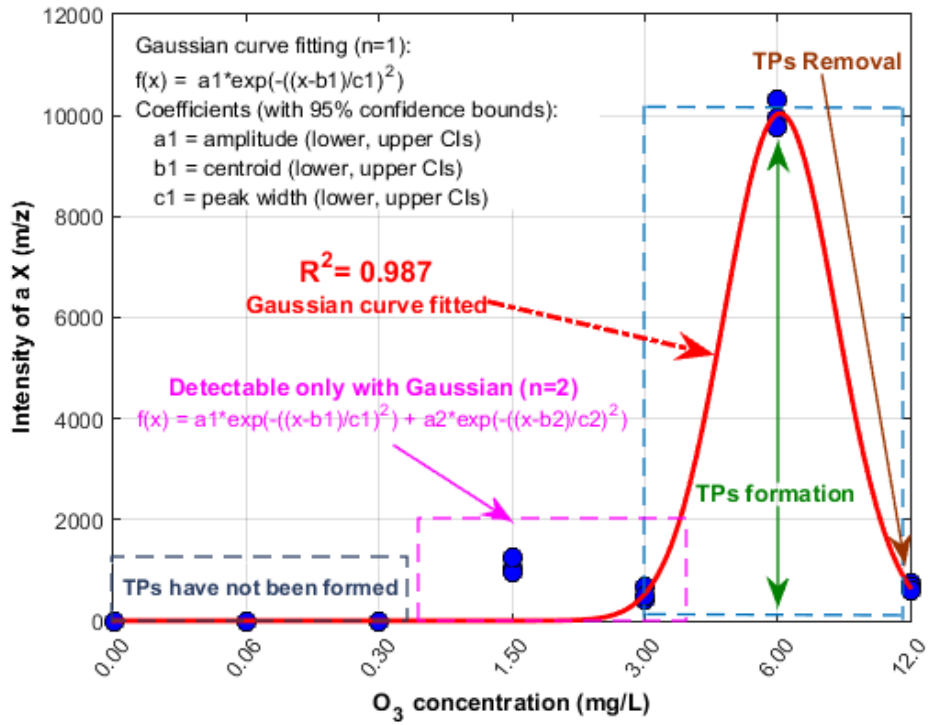
time and  $m/z$  can be linked to those of the parent compound, if the transformation reactions are known. Ozonation includes oxidative reactions that result mainly in the formation of more polar compounds or as polar as the parent compound. Ozonation TPs are produced through the breakdown of the parent structure or through the oxidation of the parent compound (mostly addition up to 5 oxygen atoms). For example, for this study, if the parent compound elutes at  $X$  min with  $m/z_P$ , then its TPs would elute from 0 to  $(X+2)$  min and would be detected as  $50 < m/z_{TP} < (m/z_P + 100)$ .

An automatic approach based on Gaussian curve fitting was developed to explore potential TPs among thousands of  $m/z$ , extracted from XCMS. The purpose of this method was to fit Gaussian curve to peaks list from XCMS according to the samples label (here was the ozonation dose) with a dynamic algorithm to evaluate the quality of the fitting based on the squared correlation coefficient for all the  $m/z$  in the peaks list. The Gaussian curve fits to peak shape and therefore, can be used to study those TPs that have been formed and then removed from one ozonation dose to another, due to further reaction with ozone. Furthermore, half Gaussian curve would also describe those TPs that have increasing trend in their intensities as ozonation dose increases. Generally, a Gaussian curve can be fitted to the set of data points as presented in Equation 5.1.:

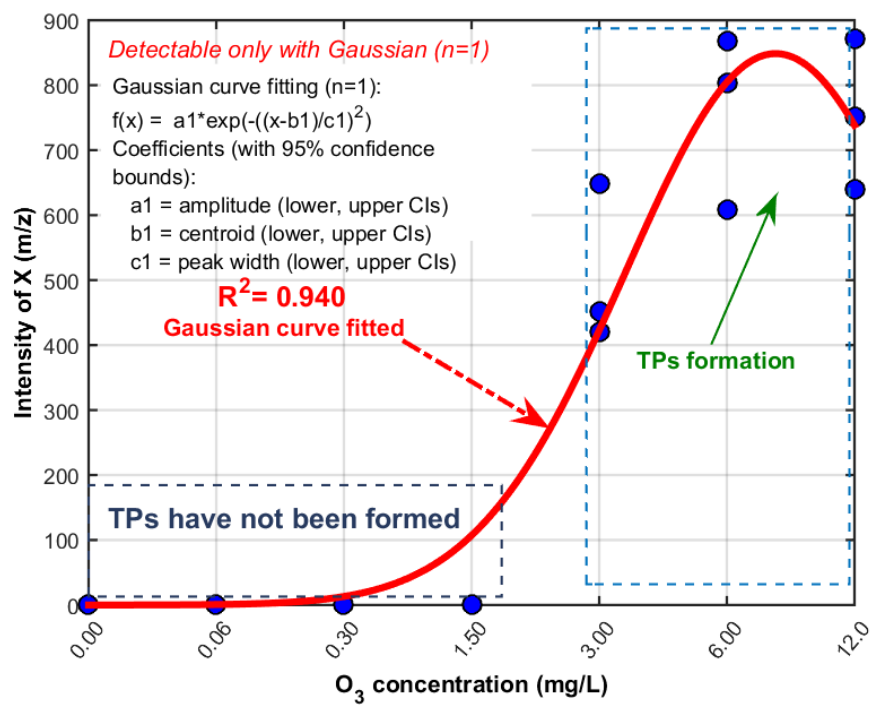
$$f(x) = a_i e^{\left[-\left(\frac{x-b_i}{c_i}\right)^2\right]} \quad (5.1)$$

where  $a$  is the amplitude,  $b$  is the centroid (location),  $c$  is related to the peak width and  $x$  is the samples label (level of ozonation dose (i.e. 0 (0 mg/L), 1 (0.06 mg/L), 2 (0.3 mg/L), 3 (1.50 mg/L), 4 (3.00 mg/L), 5 (6.00 mg/L), 6 (12.0 mg/L)). **Fig. 5.1** shows the various types of Gaussian curves which could relate to potential TPs and parent compounds. Afterwards, the non-target screening workflow was applied over the detected  $m/z$  showing squared correlation coefficient above 0.5 for the fitted Gaussian curve. The steps followed in trend analysis are provided in the Electronic Supplementary Material (**Section S5.2**).

a)



b)



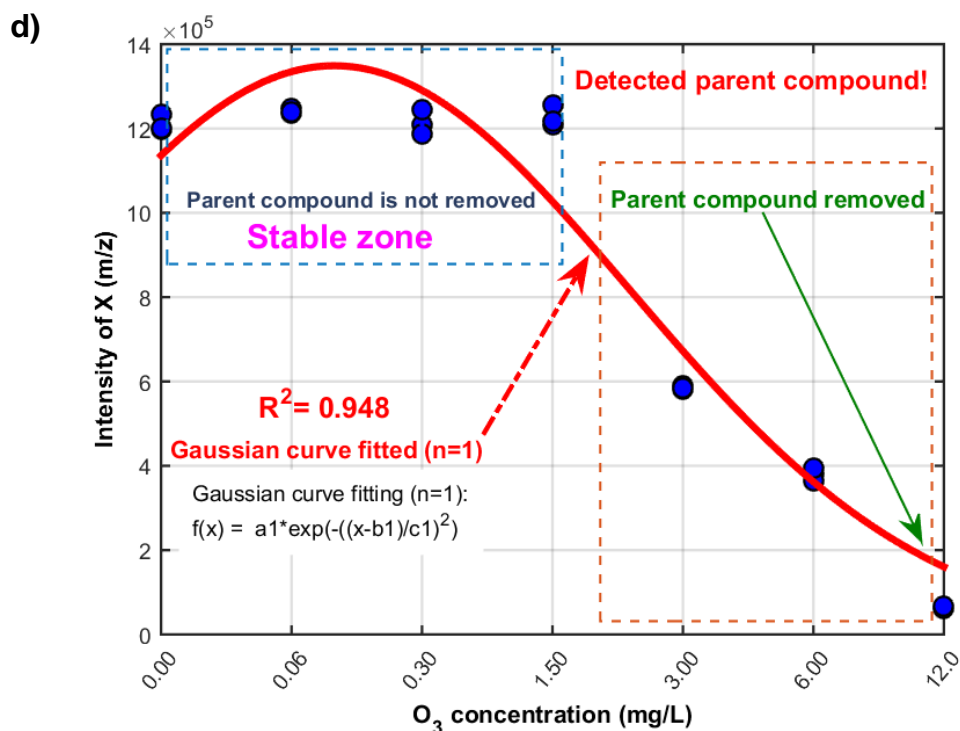
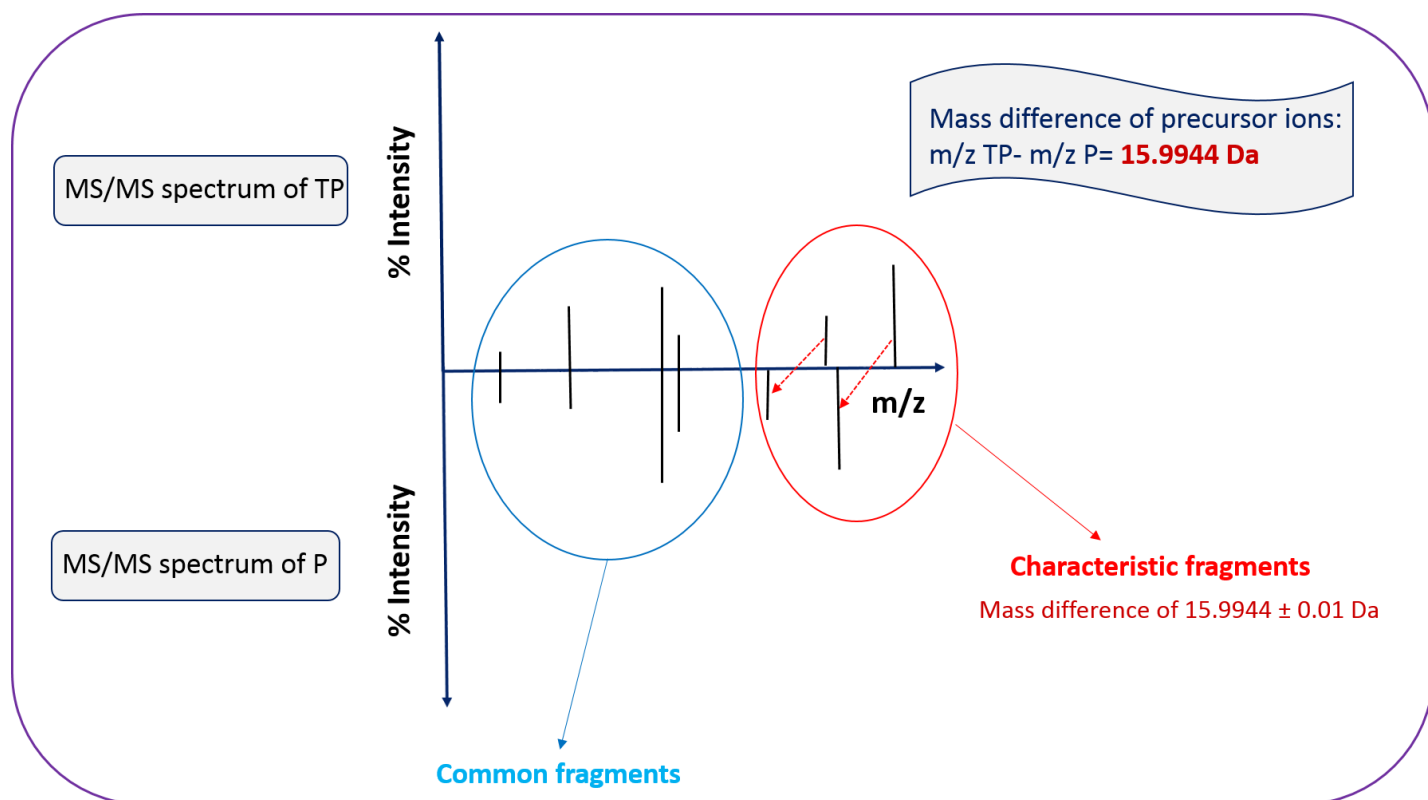


**Fig. 5.1.** Gaussian curves for detection of TPs and parent compounds.

#### 5.4.2 Identification of ozonation TPs

The extended non-target screening workflow proposed by Gago- Ferrero et al. [139], was used for the identification of the prioritized m/z based on their intensities trend. The applied identification workflow involved 1) flagging and removing of any selected m/z that exist in procedural blank or zero-time samples with the same fold changes (ratio of intensities average for the selected m/z in the samples and control samples), 2) evaluating the distinctive isotopic patterns for the selected m/z, 3) checking a mass accuracy threshold of 2 mDa and 5 ppm on the selected m/z, as well as evaluating the isotopic pattern of the precursor ion (less than 100 mSigma). mSigma represents the goodness of fit between the measured and theoretical isotopic pattern (mass and ion ratios): the smaller the better, 4) assigning and evaluating molecular formula based on the seven golden rules and characteristic adduct ions, 5) MS/MS spectral interpretation, 6) distinctive and similar MS/MS pattern should exist between selected m/z (possible TPs) and a parent compound. Spectral similarity calculated by OrgMassSpecR package in R (here a threshold of 0.5 was used) [217]. The MS/MS spectra similarity value shows whether the TP and the parent compound share common fragments. If the transformation

highly affects the fragmentation profile, then the MS/MS spectra similarity score between the TP and the parent compound would be low. However, in our study the presence of characteristic fragments was also taken into consideration, for the first time, for the calculation of MS/MS spectra similarity score, in order to significantly support the proposed TPs structures. Those characteristic fragments in the MS/MS spectrum of the tested TP, have the same mass error to the corresponding fragment ion of the parent compound, as their precursor ions do, since their structure includes the part of the molecule which has been transformed. The incorporation of characteristic fragments in the calculation of MS/MS spectra similarity score, enhances the extracted similarity value. A graphical illustration of how MS/MS spectra similarity is extracted, is presented in **Fig. 5.2**, 7) the chromatographic retention time plausibility, using an in-house Quantitative Structure–Retention Relationship (QSRR) retention time prediction model with relative acceptance window for prediction error according to chemical similarity (OTrAMS) and LC gradient elution time [142, 218], 8) confirming the tentatively identified TPs by MS/MS spectra match with existing literature, online databases or reference standard (if commercially available). The level of confidence (LoC) for the identification of the detected compounds was used according to Schymanski et al. [85], where Level 1 corresponds to confirmed structures (reference standard is available), level 2 to probable structures (2a-Evidence by spectrum matching from literature or library; 2b-Diagnostic evidence where no other structure fits the experimental MS/MS information), level 3 for tentative candidate(s), Level 4 to unequivocal molecular formulas, and level 5 to exact mass(es) of interest. **Fig. 5.3** shows the used workflow for TPs prioritization and structure elucidation.



**MS/MS spectra similarity score extraction: Detection of common & characteristic fragments**

Due to the fragments generated by the **structurally-alike moiety** between the tested TP and its parent compound

These fragments include in their structure the part of the molecule which was **transformed**

**Fig. 5.2.** MS/MS spectra similarity score extraction.

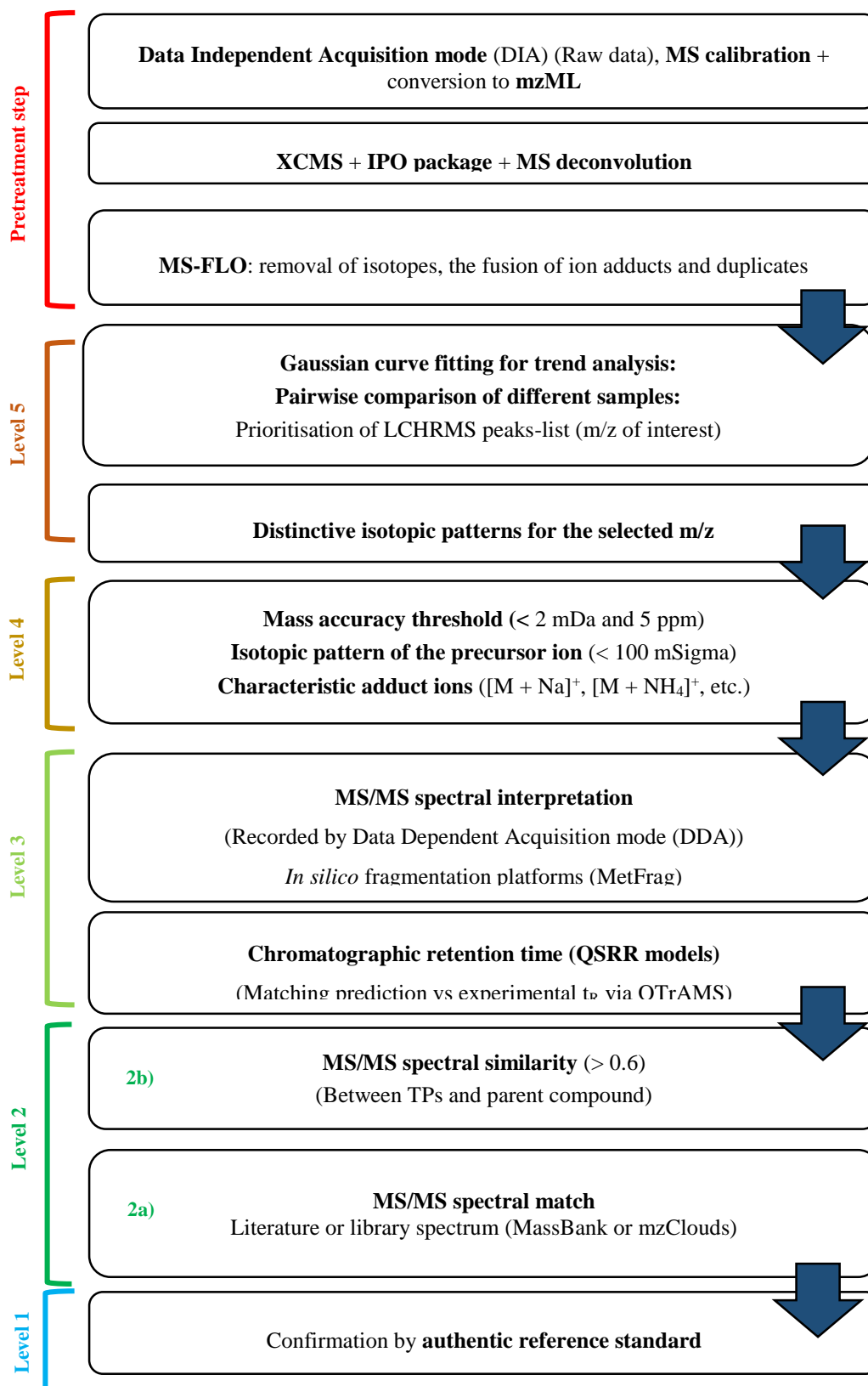


**Fig. 5.3.** Flowchart of data treatment and non-target screening with associated level of confidence in identification of TPs.

### 5.4.3 Toxicity assessment

The acute toxicity of all the identified TPs and parent compounds were predicted with ToxTrAMS, an in-house risk assessment program. Acute toxicity values were predicted towards three aquatic species; daphnia magna (planktonic crustacean, measurement was based on LC<sub>50</sub> (mg/L) after 48 h of exposure), *pseudokirchneriella subcapitata* (algae, measurement was based on EC<sub>50</sub> (mg/L) after 72 h of exposure) and Pimephales promelas (fish, measurement was based on LC<sub>50</sub> (mg/L) after 96 h of exposure). A wide scope model, which was built based on 1353 emerging contaminants with their experimental pLC<sub>50</sub> information, was used to estimate acute toxicity in daphnia magna. The molecular features behind the model were hydrophobicity, polarizability, summation of solute-hydrogen bond basicity and minimum atom-type E-state of –OH [200]. The models used to predict the toxicity in algae and fish were also built based on a large set of 537 and 4060 emerging contaminants, respectively [219]. In the case of algae model, molecular features were log*P*, number of nitrogen, number of rotatable bonds and excessive molar refraction [220]. For risk assessment in fish, the molecular features were hydrophobicity, sum of atom-type E-state of =CH- and –OH, modified information content index (neighborhood symmetry of 1-order), molecular distance edge between all tertiary carbons, number of 6-membered rings [221] and 3D topological distance based autocorrelation - lag 6 / weighted by covalent radius [222]. The applicability domains of the applied models over the identified TPs with unknown toxicity were carefully studied considering the effect of chemical structure similarity (or chemical space failure) to avoid using any incorrect prediction results [200].

### 5.5. Results and Discussion

In total 46 ozonation TPs were detected; 7 TPs of CIT, 10 of DESCIT, 9 of CTRAM, 12 of CTRAC and 8 of CTROXO. Their detection was based on the trend of their formation/removal and the respective figures derived from TrendTrAMS, along with the extracted Gaussian equation, are presented in **Fig. S5.2** (5.2.1: DESCIT, 5.2.2: CTRAM, 5.2.3: CTRAC and 5.2.4: CTROXO) and for CIT in **Fig. 5.4**. The identification data derived from their MS spectra (ion formula, adduct ions, mass accuracy and isotopic fitting) are listed in **Table 5.3**,

while the extracted ion chromatograms (EIC) of their precursor ions are shown in **Fig. S5.3** (5.3.1: CIT, 5.3.2: CTRAM, 5.3.3: CTRAC and 5.3.4: CTROXO) and in **Fig. 5.5** for DESCIT. The structure elucidation of the detected TPs was achieved through the interpretation of their MS/MS spectra, which are depicted in **Fig. S5.4** (5.4.1: CIT, 5.4.2: DESCIT, 5.4.3: CTRAM, 5.4.4: CTRAC and 5.4.5: CTROXO). The fragmentation of the tested parent compounds was studied, since it provides valuable information about characteristic fragments of the respective TPs that lead to structure elucidation. The MS/MS similarity figures for selected TPs are presented in **Fig S5.5** (5.5.1: CIT, 5.5.2: DESCIT, 5.5.3: CTRAM, 5.5.4: CTRAC and 5.5.5: CTROXO). **Fig. S5.6** includes the proposed structures of the identified TPs for CIT (5.6.1), DESCIT (5.6.2), CTRAM (5.6.3) and CTRAC (5.6.4), while **Fig. 5.7** for CTROXO.

**Fig. S5.7** [CIT (5.7.1), DESCIT (5.7.2), CTRAC (5.7.3) and CTROXO (5.7.4)] presents the ozone dose profiling (a) and mass balance graphs of the parent compounds and their TPs (b), while the corresponding figures for CTRAM are presented in **Fig. 5.6**. **Tables S5.1-5.4** include the %contribution of each TP to the total TPs content per treated sample is also placed under the graphs. The results of removal and identification of TPs for the 5 tested compounds are discussed in the following sections.

**Table 5.3.** MS identification data for the identified TPs (including only the TPs that a specific formula is proposed).

Compound	Ion formula	Ion type	m/z experimental	m/z theoretical	Mass error (ppm)	Isotopic fitting (mSigma)
CIT	$C_{20}H_{22}FN_2O$	$[M+H]^+$	325.1720	325.1711	2.9	13.3
	$C_{20}H_{21}FN_2NaO$	$[M+Na]^+$	347.1539	347.1530	2.5	36.7
CIT-341	$C_{20}H_{22}FN_2O_2$	$[M+H]^+$	341.1670	341.1660	-3.0	22.1
	$C_{20}H_{21}FN_2NaO_2$	$[M+Na]^+$	363.1473	363.1479	1.8	17.7
CIT-311	$C_{19}H_{20}FN_2O$	$[M+H]^+$	311.1563	311.1554	2.8	16.7
CIT-263	$C_{14}H_{19}N_2O_3$	$[M+H]^+$	263.1393	263.1390	1.0	7.8
	$C_{14}H_{17}N_2O_2$	$[M+H-H_2O]^+$	245.1282	245.1285	-1.0	27.7
CIT-355	$C_{20}H_{20}FN_2O_3$	$[M+H]^+$	355.1463	355.1452	-3.0	24.2
CIT-357	$C_{20}H_{22}FN_2O_3$	$[M+H]^+$	357.1619	357.1609	-2.9	25.7
CIT-339 a	$C_{20}H_{20}FN_2O_2$	$[M+H]^+$	339.1511	339.1503	-2.4	26.9
	$C_{20}H_{19}FN_2NaO_2$	$[M+Na]^+$	361.1333	361.1323	-3.0	16.7
CIT-339 b (pH 4)	$C_{20}H_{20}FN_2O_2$	$[M+H]^+$	339.1511	339.1503	-2.3	20.6



Compound	Ion formula	Ion type	m/z experimental	m/z theoretical	Mass error (ppm)	Isotopic fitting (mSigma)
<b>DESCIT</b>	$C_{19}H_{20}FN_2O$	$[M+H]^+$	311.1560	311.1554	-1.8	6.9
DESCIT-297	$C_{18}H_{18}FN_2O$	$[M+H]^+$	297.1407	297.1398	3.0	26.3
DESCIT-327	$C_{19}H_{20}FN_2O_2$	$[M+H]^+$	327.1504	327.1503	0.2	19.4
DESCIT-341	$C_{20}H_{22}FN_2O_2$	$[M+H]^+$	341.1663	341.1660	0.8	13.1
DESCIT-325 a	$C_{19}H_{18}FN_2O_2$	$[M+H]^+$	325.1353	325.1347	1.9	40.8
DESCIT-325 b	$C_{19}H_{18}FN_2O_2$	$[M+H]^+$	325.1350	325.1347	-1.0	22.0
	$C_{19}H_{17}FN_2NaO_2$	$[M+Na]^+$	347.1165	347.1166	-0.3	9.2
	$C_{19}H_{17}FKN_2O_2$	$[M+K]^+$	363.0901	363.0906	1.3	18.6
DESCIT-339	$C_{20}H_{20}FN_2O_2$	$[M+H]^+$	339.1510	339.1503	2.1	28.2
	$C_{20}H_{19}FN_2NaO_2$	$[M+Na]^+$	361.1330	361.1323	-2.1	5.9
DESCIT-280	$C_{18}H_{15}FN_0$	$[M+H]^+$	280.1129	280.1132	1.2	125.0
	$C_{18}H_{13}FN$	$[M+H-H_2O]^+$	262.1026	262.1027	-0.1	34.0
DESCIT-369	$C_{21}H_{22}FN_2O_3$	$[M+H]^+$	369.1627	369.1609	4.9	24.2
DESCIT-344 (pH 4)	$C_{20}H_{23}FNO_3$	$[M+H]^+$	344.1655	344.1656	-0.4	29.5
<b>CTRAM</b>	$C_{20}H_{24}FN_2O_2$	$[M+H]^+$	343.1829	343.1816	3.6	36.8
CTRAM-281	$C_{14}H_{21}N_2O_4$	$[M+H]^+$	281.1489	281.1496	2.4	38.8
	$C_{14}H_{19}N_2O_3$	$[M+H-H_2O]^+$	263.1388	263.139	0.7	15.3
CTRAM-375	$C_{20}H_{24}FN_2O_4$	$[M+H]^+$	375.1718	375.1715	-0.9	13.8
CTRAM-373	$C_{20}H_{22}FN_2O_4$	$[M+H]^+$	373.1564	373.1558	1.6	24.6
CTRAM-359	$C_{20}H_{24}FN_2O_3$	$[M+H]^+$	359.1770	359.1765	-1.3	37.8
CTRAM-360	$C_{20}H_{23}FNO_4$	$[M+H]^+$	360.1601	360.1606	1.3	15.4
CTRAM-325	$C_{20}H_{22}FN_2O$	$[M+H]^+$	325.1718	325.1711	-2.2	16.3
CTRAM-341	$C_{20}H_{22}FN_2O_2$	$[M+H]^+$	341.1660	341.1660	0	19.5
CTRAM-388	$C_{21}H_{23}FNO_5$	$[M+H]^+$	388.1558	388.1555	-0.7	21.3
CTRAM-329 (pH 4)	$C_{19}H_{22}FN_2O_2$	$[M+H]^+$	329.1666	329.166	-1.9	74.0
<b>CTRAC</b>	$C_{20}H_{23}FNO_3$	$[M+H]^+$	344.1664	344.1656	-2.2	36.4
CTRAC-376 a	$C_{20}H_{23}FNO_5$	$[M+H]^+$	376.1538	376.1555	4.3	18.9
CTRAC-376 b	$C_{20}H_{23}FNO_5$	$[M+H]^+$	376.1551	376.1555	-1.1	21.0
CTRAC-374	$C_{20}H_{21}FNO_5$	$[M+H]^+$	374.1408	374.1398	2.5	17.1
CTRAC-330	$C_{19}H_{21}FNO_3$	$[M+H]^+$	330.1505	330.1500	-1.5	9.3
CTRAC-360	$C_{20}H_{23}FNO_4$	$[M+H]^+$	360.1619	360.1606	3.7	36.3
CTRAC-311	$C_{19}H_{20}FN_2O$	$[M+H]^+$	311.1556	311.1554	0.5	98.2
CTRAC-282	$C_{14}H_{20}NO_5$	$[M+H]^+$	282.1325	282.1336	-3.9	21.4
	$C_{14}H_{18}NO_4$	$[M+H-H_2O]^+$	264.1230	264.1230	0	7.5
CTRAC-358	$C_{20}H_{21}FNO_4$	$[M+H]^+$	358.1458	358.1449	-2.5	30.1
CTRAC-374.17	$C_{21}H_{25}FNO_4$	$[M+H]^+$	374.1766	374.1762	0.9	22.9
CTRAC-388	$C_{21}H_{23}FNO_5$	$[M+H]^+$	388.1554	388.1555	-0.1	22.2

Compound	Ion formula	Ion type	m/z experimental	m/z theoretical	Mass error (ppm)	Isotopic fitting (mSigma)
CTROXO	$C_{20}H_{20}FN_2O_2$	$[M+H]^+$	339.1505	339.1503	0.6	8.4
	$C_{20}H_{19}FN_2NaO_2$	$[M+Na]^+$	361.1321	361.1323	-0.5	9.9
CTROXO-373 a	$C_{20}H_{22}FN_2O_4$	$[M+H]^+$	373.1561	373.1558	-0.7	15.2
CTROXO-373 b	$C_{20}H_{22}FN_2O_4$	$[M+H]^+$	373.1558	373.1558	0	13.8
CTROXO-343	$C_{20}H_{24}FN_2O_2$	$[M+H]^+$	343.1820	343.1816	-0.9	29.8
CTROXO-359	$C_{20}H_{24}FN_2O_3$	$[M+H]^+$	359.1764	359.1765	0.3	0.1
CTROXO-371	$C_{20}H_{20}FN_2O_4$	$[M+H]^+$	371.1404	371.1402	0.7	22.4
CTROXO-355	$C_{20}H_{20}FN_2O_3$	$[M+H]^+$	355.1462	355.1452	2.9	2.6
CTROXO-388	$C_{21}H_{23}FNO_5$	$[M+H]^+$	388.1557	388.1555	-0.7	9.5
CTROXO-391 (pH 10)	$C_{20}H_{24}FN_2O_5$	$[M+H]^+$	391.1666	391.1664	0.6	20.5

### 5.5.1 Removal of CIT and Identification of its ozonation TPs

CIT, detected as m/z 325.1720 ( $[M+H]^+$ ), along with its  $[M+Na]^+$  adduct with m/z 347.1539, was eluted at 6.7 min. 52% of the initial concentration reacted with 0.3 mg/L of  $O_3$ , while 1.5 mg/L  $O_3$  was adequate to completely remove CIT. CIT presented extensive fragmentation where 8 fragments were structurally elucidated.

In total 6 TPs of CIT were detected in pH 7, whereas 1 additional TP was formed only at the ozonation experiment performed at pH 4. Among them, 3 TPs (CIT-341, 311 and 339b (pH 4)) have already been reported as CIT ozonation TPs by Hörsing et al. [205], while Beretsou et al. have identified CIT-341, 311, 355 and 339b (pH 4) as biotransformation products of CIT, as well [206]. CIT-341 and 311 have also been formed as photodegradation TPs of CIT when exposed to sunlight [204].

The oxidation of the trimethylamine moiety of CIT resulted in the formation of CIT-341 (m/z: 341.1670,  $t_R$ : 7.1 min), the N-oxide of CIT. The acquired MS/MS spectra matches the one of CIT-N-oxide reference standard which has been previously reported by Hörsing et al. [205], reaching LoC 2a. CIT-341 presented the highest MS/MS similarity score with CIT, up to 0.966. CIT-341 reached its maximum abundance when 1.50 mg/L of  $O_3$  were applied, while in higher doses it further reacted with ozone (20% removal of CIT-341 was notice) to produce more N-oxide TPs. CIT-355, 357 and 263 were rapidly produced in parallel with CIT-341 removal. CIT-355 formula ( $C_{20}H_{19}FN_2O_3$ ) indicates the addition of one oxygen atom to the structure of CIT-341, while the 8 detected fragments, clearly

show that the oxidation took place in the furan ring moiety. Moreover, LoC 2a was attributed to this TP, since there is MS/MS spectrum match with CTR 355, reported by Beretsou et al. [206]. The ion formula  $C_{20}H_{22}FN_2O_3^+$ , fits to the  $m/z$  357.1619, which was eluted at 6.2 min. Although a TP sharing the same formula, CTR 357, was detected by Beretsou et al. [206], retention time (since the same chromatographic system was used in this study) and MS/MS fragmentation reveal that these two TPs have different structures. The characteristic fragment with  $m/z$  62.0586 clearly supports the formation of an N-oxide ozonation TP, instead of the oxidized derivative of the amide moiety produced during biodegradation. Moreover, the hydroxylation of benzonitrile moiety is supported by the detection of  $m/z$  156.0444 and 240.0819 fragments in the MS/MS spectrum of CIT-357. A more polar TP, CIT-263 ( $m/z$ : 263.1397,  $t_R$ : 3.4 min) was formed through the breakdown of CIT-357 structure, after fluorobenzene moiety removal. Its in-source fragment, after  $H_2O$  molecule neutral loss ( $m/z$  245.1289), was detected in higher abundance. This assumption is verified through the MS and MS/MS spectra of these two  $m/z$ ; a) they share the same  $t_R$ , b)  $m/z$  245 was detected in the MS/MS spectra of  $m/z$  263 and c) their fragmentation patterns are identical. The LoC attributed to CIT-357 and 263 is 2b.

Two TPs with  $m/z$  339.1511 were detected. CIT-339a was detected in ozonation experiment performed at all tested pH, whereas CIT-339b was detected only at pH 4. The extended fragmentation of CIT-339a revealed  $m/z$  72.0444 fragment, among 10 detected fragments. This fragment is characteristic for ketone formation in trimethylamine moiety. Such formamide derivative has already been reported as oxidation TP of tramadol (OP 278) which also contains a trimethylamine moiety in its structure [223], reaching LoC 2b for CIT-339a. CIT-339b (pH 4), eluted at 6.6 min was identified as CTROXO, considering  $t_R$  and MS/MS spectrum match with the corresponding reference standard (LoC 1). Beretsou et al. (2016) have also reported 2 biotransformation products with the same formula ( $C_{19}H_{20}FN_2O_2$ ), CTR 339A which was identified as CTROXO and CTR 339B to which no specific structure could be proposed [206]. The  $t_R$  (8.2 versus 6.6 min) and MS/MS spectra of CIT-339a and CTR

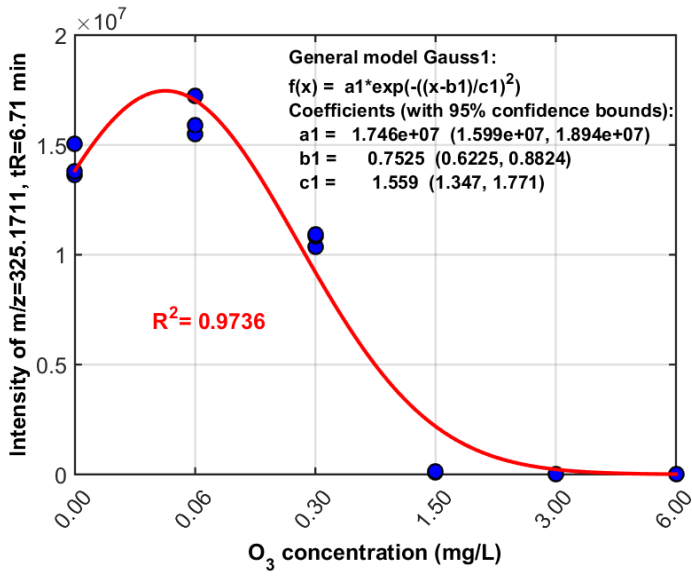
339B, do not match, showing that different TPs were formed during ozonation and biodegradation.

CIT-311 (m/z: 311.1563,  $t_R$ : 6.8 min) was formed when the ozone dose was up to 0.30 mg/L, but was proven to be an unstable TP, since when higher ozone doses were applied, it was completely removed. The molecular formula of this TP ( $C_{19}H_{19}FN_2O$ ) fits to DESCIT. The retention time, MS and MS/MS spectra match to those of DESCIT reference standard, so level 1 was achieved. CIT-355 and 311 are co-eluted compounds. However, the totally different formation profile indicates that they are attributed to different TPs.

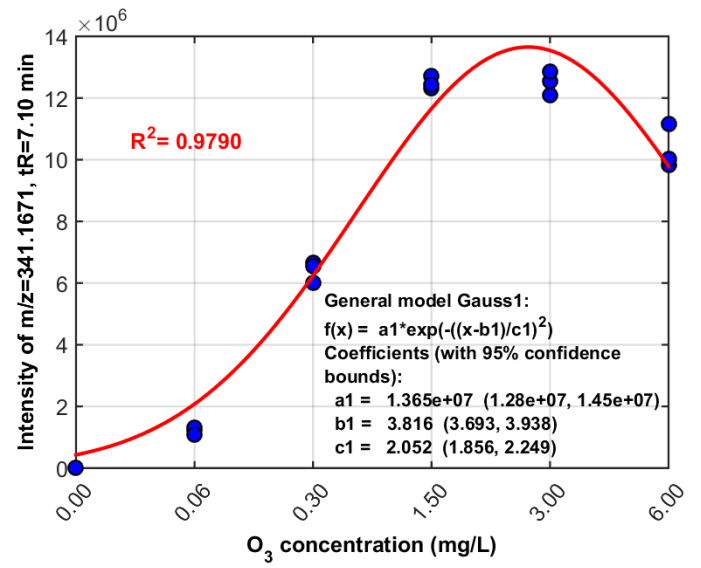
Comparison between the peak areas of CIT and the sum of peak areas of the detected TPs (based on the assumption that CIT and its TPs have the same response factor between peak area and concentration) revealed that 72% of the initial concentration has been transformed to TPs. However, to perform a complete mass balance, quantification of TPs with corresponding reference standards is required, which are currently unavailable for most of the TPs. The rest undetected 28% may be assigned to mineralization of the parent compound, formation of unstable TPs, or TPs that could not be detected with the applied method of determination. The most abundant TP was CIT-341, which was up to 98% of the total TPs content in all tested ozone doses.

Due to experimental error, the results of analysis for the sample where 12 mg/L of  $O_3$  were added, are not discussed for CIT.

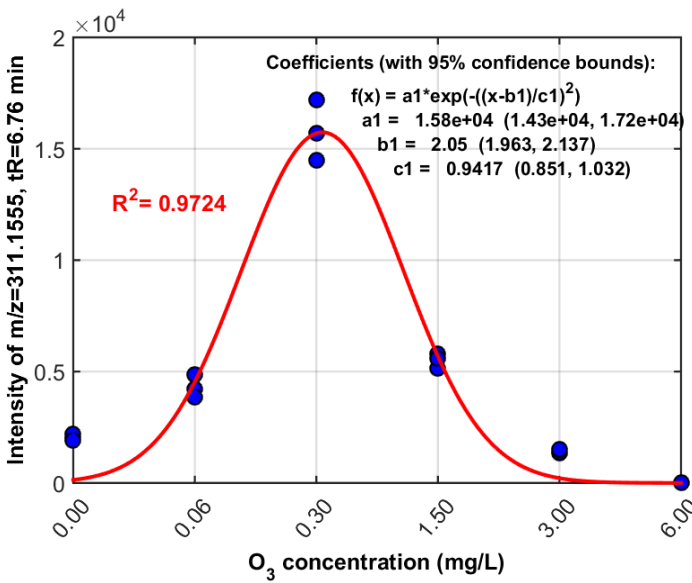
### CIT



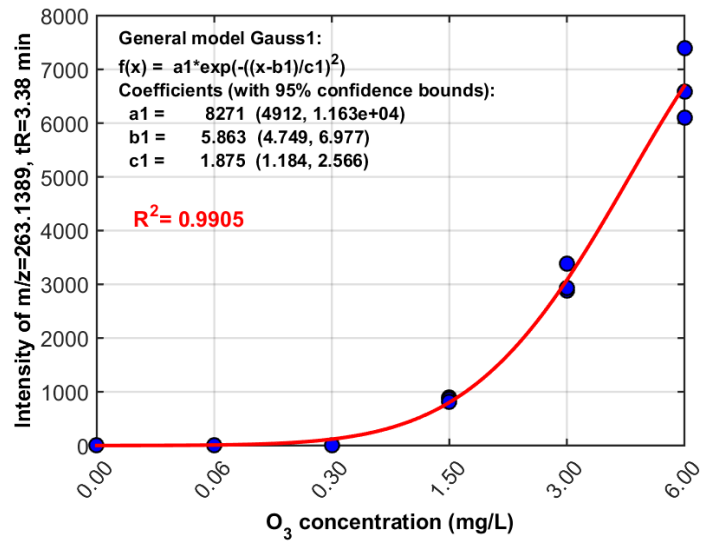
### CIT-341



### CIT-311



### CIT-263



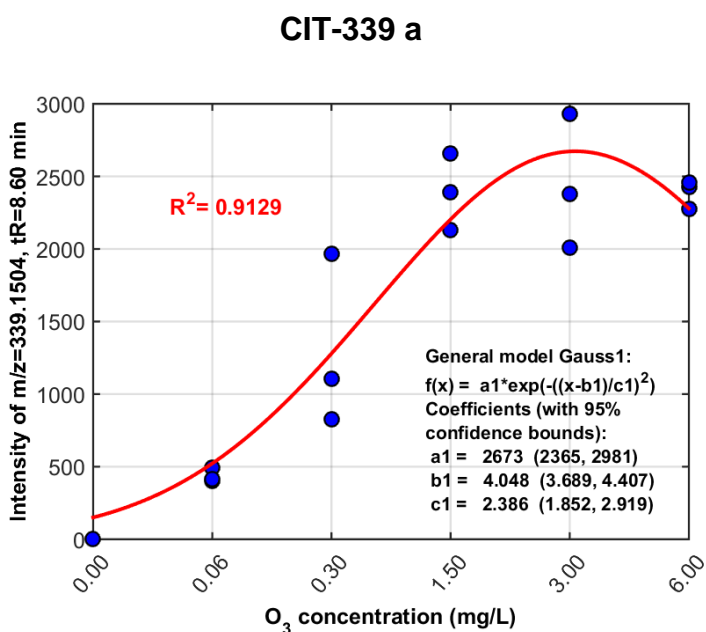
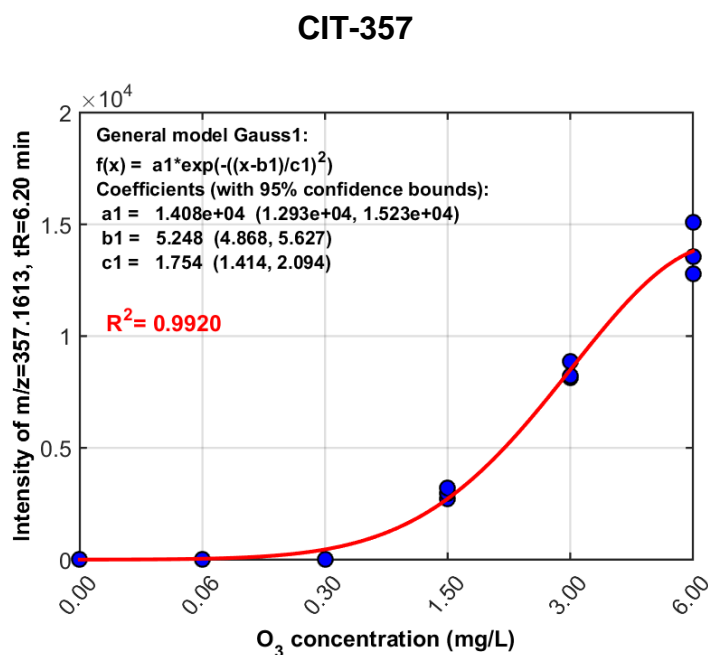
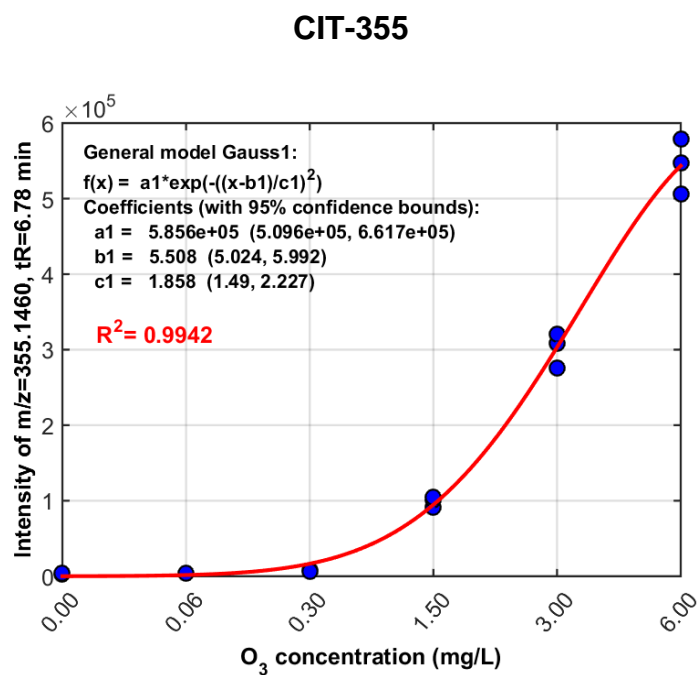


**Fig. 5.4.** Trend Analysis results for CIT and its ozonation TPs detected in pH 7.

### 5.5.2 Removal of DESCIT and Identification of its ozonation TPs

The removal of DESCIT was significant when ozone concentration exceeded 1.5 mg/L. In reaction with 3 mg/L of  $O_3$ , 70% of removal was obtained, whereas DESCIT was almost totally removed (97%) when 12 mg/L were added. Through the fragmentation of DESCIT, 7 fragments were structurally elucidated and were used as reference point for TPs MS/MS spectra interpretation. Nine TPs

were detected in pH 7, while DESCIT-344 was formed only at pH 4. Although DESCIT transformation is profound, the mass balance between DESCIT and its ozonation TPs displays a great fission, since only 3% of the initial DESCIT concentration seems to be transformed into LC-HRMS detectable TPs.

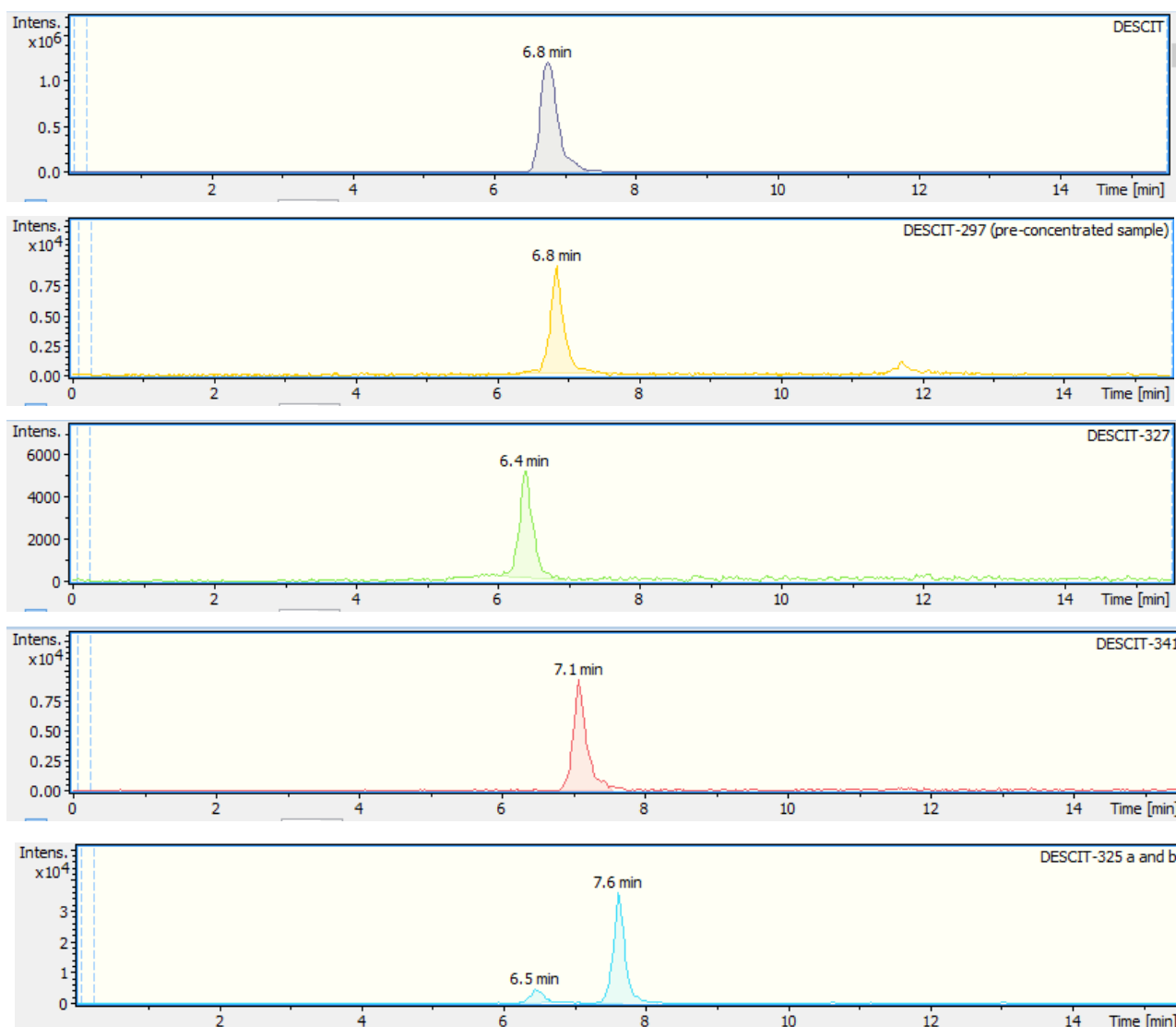
Taking into consideration that DESCIT was identified as CIT ozonation TP, then all DESCIT TPs are second generation TPs of CIT. However, their low intensities even in DESCIT ozonated samples, made their detection in CIT samples infeasible. In general, the transformation of DESCIT follows the same pattern of CIT.

DESCIT-297 ( $m/z$ : 297.1407,  $t_R$ : 6.8 min) is formed by N-demethylation of DESCIT. Its MS/MS spectra is identical to that of DESCIT, apart from the characteristic fragment with  $m/z$  279.1294 which is 14.0157 Da lower than the corresponding fragment of DESCIT. This is also the mass difference between their precursor ions (loss of  $-CH_3$ ). Thus, a high MS/MS similarity score of 0.773 was achieved. Moreover, there is a MS/MS spectrum match with didesmethylcitalopram reported by Hörsing et al. [205].

$M/z$  327.1504 eluted at 6.4 min fits to the ion formula of  $C_{19}H_{20}FN_2O_2^+$ , with excellent mass accuracy of 0.2 ppm. The N-oxidation of the dimethylamine moiety led to the formation of DESCIT-327, which reached its higher abundance when 0.3 mg/L of  $O_3$  reacted with DESCIT, while it was below the limit of quantitation in  $O_3$  concentrations  $\geq 3$  mg/L. Four  $m/z$  (including a pair of isomers) were linked to DESCIT fragments, providing a MS/MS similarity score of 0.338.

Two isomeric structures with theoretical  $m/z$  325.1347 were eluted at 6.5 and 7.6 min. The mass difference between these TPs and DESCIT, is as that observed between CIT and CIT-339 a & b. Their elemental composition ( $C_{19}H_{17}FN_2O_2$ ) has an additional oxygen atom in comparison to DESCIT. Considering characteristic fragments in both MS/MS spectra, DESCIT-325a was attributed to furan ring oxidation TP, whereas DESCIT-325b was identified as DESCIT formamide derivative. The later was the most abundant TP of DESCIT.

Although DESCIT formula includes 19 atoms of carbon ( $C_{19}H_{19}FN_2O$ ), three of its ozonation TPs were attributed to formulas with 20 carbon. DESCIT-341 and 339 fit to the  $t_R$  and fragmentation pattern of CIT-341 and 339a, respectively. This fact implies that although CIT was not detected in DESCIT ozonated samples, it was produced during the ozonation of DESCIT and further reacted with ozone to produce more TPs.





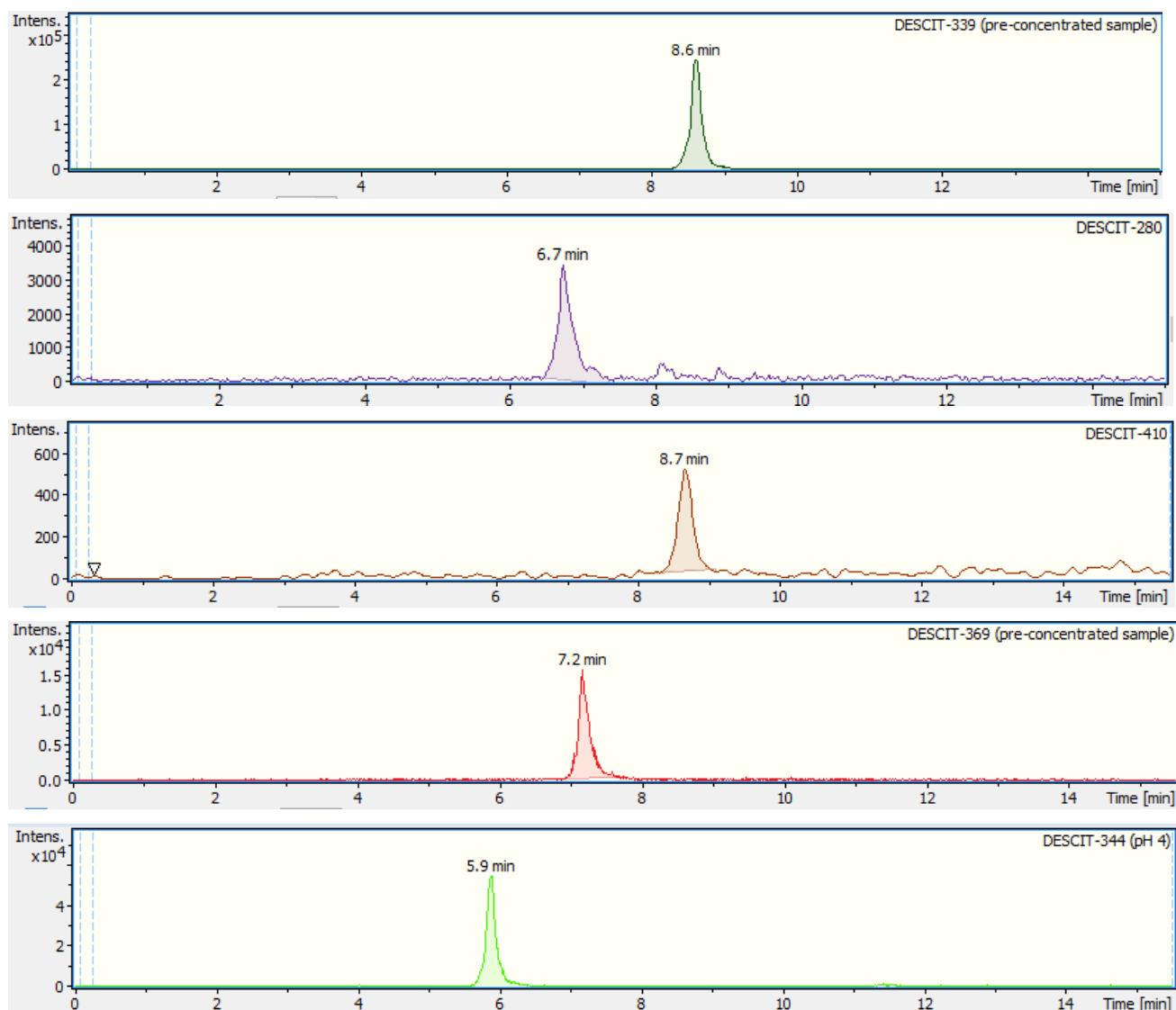


**Fig. 5.5.** EICs of DESCIT and its ozonation TPs.

DESCIT-344 with  $m/z$  344.1655 (ion formula:  $C_{20}H_{23}FNO_3$ ,  $t_R$ : 5.9 min) was identified as CTRAC, through the analysis of the corresponding reference standard.

DESCIT-280 ( $m/z$  280.1129,  $t_R$ : 6.7 min) was formed from the breakdown of the parent compound, after  $-NCH_3$  moiety removal. Its in-source fragment (neutral loss of water,  $m/z$  262.1026) was more abundant in the MS spectra. The fragmentation pattern of both  $m/z$  (precursor and in-source fragment) is DESCIT-MS/MS spectra-alike.

DESCIT-410 ( $m/z$  410.1485) was detected at 8.7 min. This TP was not abundant enough to let the acquisition of its MS/MS spectra and it was an

unstable compound, since it was below the limit of detection when a second analysis was performed in pre-concentrated samples. An unequivocal molecular formula corresponding to  $C_{21}H_{22}FN_2O_3$  was annotated to DESCIT-369 ( $m/z$  369.1630), eluted at 7.2 min. Although the MS/MS spectra was available, the detected fragments did not lead to any structure elucidation. Only  $m/z$  262.1021 was a common fragment of CIT-derivatives.

DESCIT-344 was identified at LoC 1, while DESCIT-297 and 341 were finally detected at 2a LoC. LoC 2b was assigned to DESCIT-327, 325a, 325b, 339 and 280, whereas LoC 4 and 5 were proposed for DESCIT-369 and 410, respectively.

All DESCIT TPs, apart from 410, were proven to be prone to removal using 12 mg/L of  $O_3$ .

### **5.5.3 Removal of CTRAM and Identification of its ozonation TPs**

The reaction of  $O_3$  towards CTRAM ( $m/z$  343.1829,  $t_R$ : 5.3 min) was very efficient, since 0.3 mg/L of ozone removed almost 40% of the initial CTRAM concentration, while application of  $\geq 1.5$  mg  $O_3$  /L led to CTRAM total removal. Eight TPs of CTRAC were detected and identified at experiments performed at pH 7, while CTRAM-388 was detected only at pH 10. The formation profiling of CTRAM TPs versus ozone clearly indicates the subsequence of transformation.

CTRAM-325 reached its higher abundance when 0.3 mg  $O_3$ /L were applied and then reacted further with ozone to produce CTRAM-341. CTRAM-325 and 341 were identified as CIT and CIT-N-oxide based on  $t_R$ , MS and MS/MS spectra similarity with LoC 1 and 2a, respectively.

The most abundant TP of CTRAM was CTRAM-359 ( $C_{20}H_{23}FN_2O_3$ ), reaching more than 90% of the total TP content in most of the tested ozone doses. This TP, eluted at 5.6 min and detected as  $m/z$  359.1770, corresponds to the same  $t_R$  and MS/MS spectra with CTRAM-N-oxide which was previously identified by Beretsou et al. [206], thus LoC 2a was assigned. Its MS/MS similarity with CTRAM was 0.831. CTRAM-359 further reacted with ozone, losing up to 25% of its abundance, to form further oxidized N-oxide TPs. A sharp formation trend was noticed for CTRAM-375, 281 and 373 alongside with CTRAM-359 removal. The MS/MS spectra of CTRAM-375 ( $m/z$  375.1718,  $t_R$ : 5.0 min), shows three

characteristic fragments that support the proposed structure (LoC: 2b). The fragment with  $m/z$  62.0601 indicated that CTRAM-375 is an N-oxide TP,  $m/z$  109.0230 includes the intact part of the molecule and  $m/z$  314.1187 corresponds to  $m/z$  298.1238 fragment of CTRAM-359 after hydroxylation of benzamide moiety. Further reaction of CTRAM-375 with ozone led to fluorobenzene moiety removal, resulting in the formation of CTRAM-281 ( $m/z$ : 281.1489, LoC: 2b). Its in-source fragment of  $m/z$  263.1388 was formed after  $H_2O$  neutral loss which was the most abundant in the acquired MS spectra of the chromatographic peak. This is the most polar TP of CTRAM, eluted at 2.4 min. CTRAM-359 reaction with ozone also resulted in the formation of an oxidized furan ring derivative, CTRAM-373 ( $m/z$  373.1564,  $t_R$ : 5.5 min, LoC: 2b). The presence of fragments  $m/z$  294.0933 and 312.1040 in its MS/MS spectra, compared to CTRAM-359 fragments  $m/z$  280.1133 and 298.1243, respectively, strongly contributed to CTRAM-373 structure elucidation.

Two TPs identified by Beretsou et al. [206], as CIT biotransformation products were detected in our study as CTRAM ozonation TPs (CTRAM-360 and 329), reaching to LoC 2a, since there is  $t_R$  and fragmentation pattern match. The formation of CTRAM-360 ( $m/z$  360.1601,  $t_R$ : 6.3 min), which is CTRAC-N-oxide TP, implies that CTRAC was formed and immediately reacted with ozone to produce CTRAM-360. CTRAM-329 ( $m/z$  329.1666,  $t_R$ : 5.3 min) was formed in higher intensity at the experiment performed at pH 4 (3 times higher intensity than in pH 7 or 10). In general, its MS/MS spectra is CTRAM-alike, apart from the trimethylamine moiety fragment ( $m/z$  58.0645) and the mass difference of fragments  $m/z$  311.1552 and 325.1715 which corresponds to  $(-CH_3+H)$ .

One additional TP, CTRAM-388, was formed only in basic experimental conditions (pH 10). The data acquired through MS and MS/MS analysis were not proven useful for CTRAM-388 structure elucidation. Thus, neither unequivocal molecular formula could be proposed for this TP (LoC 5).

The whole quantity of CTRAM was transformed to the aforementioned identified TPs based on mass balance results, ranging from 97 to 115% of transformation in reaction with  $\geq 1.5$  mg  $O_3/L$ .

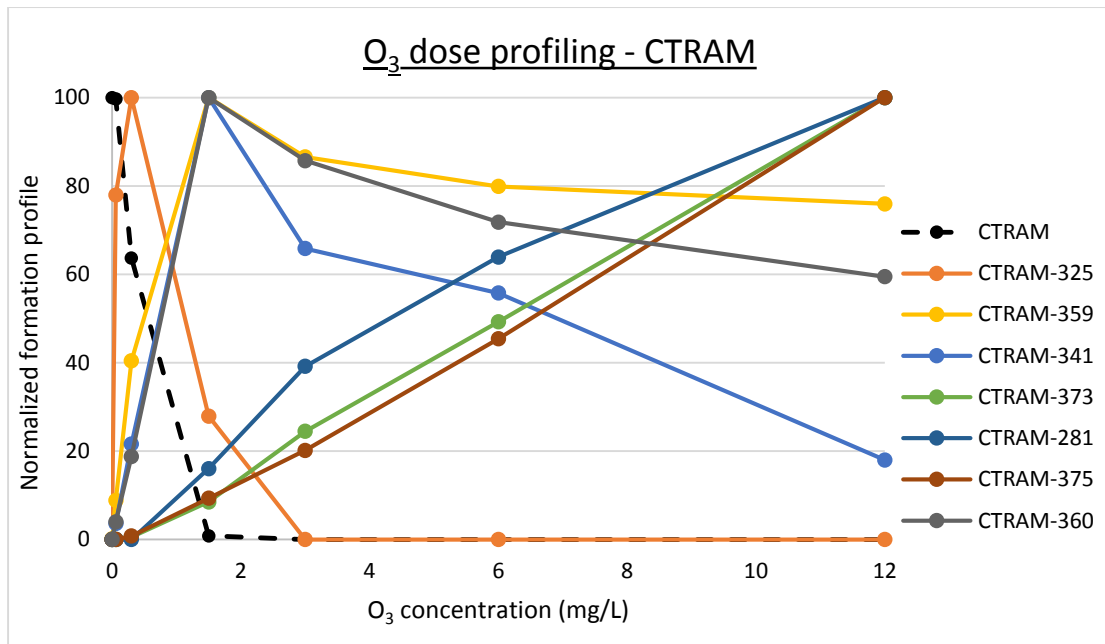


Fig. 5.6 a) Ozone dose profiling of CTRAM and its TPs.

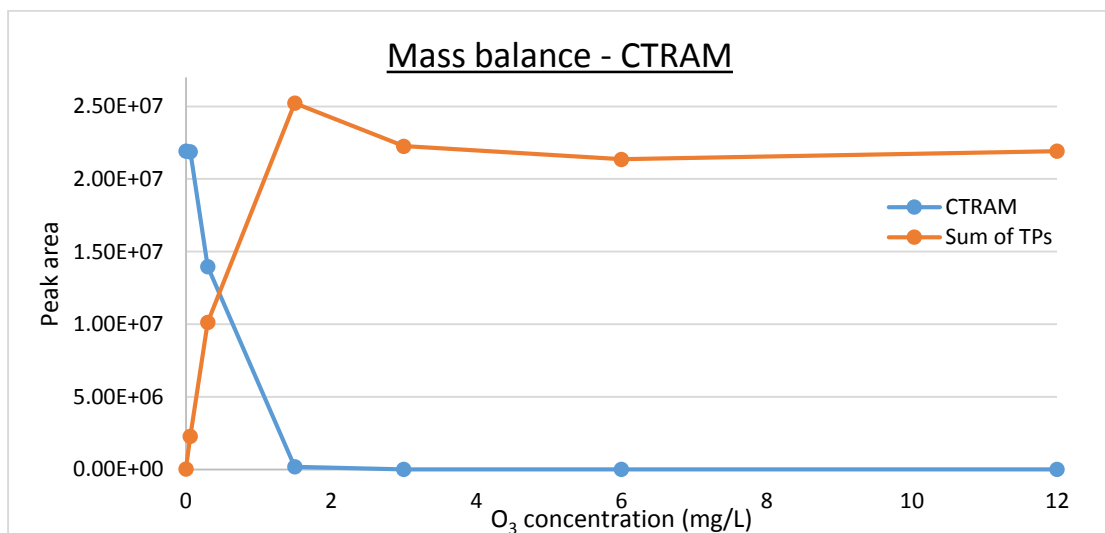


Fig. 5.6 b) Mass Balance of CTRAM and its TPs.

Table 5.4. % Contribution of each CTRAM TP to the total TPs area.

C <sub>O3</sub> (mg/L)	% Contribution of each TP							Area (Sum of TPs)/ Area (CTRAM, t=0)
	CTRAM-325	CTRAM-359	CTRAM-341	CTRAM-373	CTRAM-281	CTRAM-375	CTRAM-360	
0.06	4.6	94.7	0.2	-	-	-	0.52	10.5
0.3	1.3	97.6	0.3	0.11	-	0.09	0.55	46.2
1.5	0.15	97.0	0.6	0.67	-	0.41	1.2	115.0
3	-	95.1	0.4	2.2	0.11	1.0	1.1	101.5
6	-	91.5	0.4	4.6	0.18	2.3	1.0	97.4
12	-	84.8	0.12	9.0	0.27	5.0	0.81	99.9

#### 5.5.4 Removal of CTRAC and Identification of its ozonation TPs

CTRAC ( $m/z$  344.1664,  $t_R$ : 6.0 min) presented high reactivity towards  $O_3$ , since 30% of removal was noticed when 0.3 mg  $O_3/L$  were used. The application of  $O_3 \geq 1.5$  mg/L resulted in the complete removal of CTRAC. In total 12 TPs were detected; 10 in pH 7 and two additional in pH 4. Among them, CTRAC-330 and 360 have already been reported as CIT biotransformation products (LoC 2a). CTRAC-330 was formed reaching a maximum of intensity at 1.5 mg  $O_3/L$  and then totally removed in reaction with 6 mg  $O_3/L$ . There are only 2 fragments that differentiate the MS/MS spectra of CTRAC-330 ( $m/z$  330.1505,  $t_R$ : 6.1 min) and CTRAC, clearly demonstrating that N-demethylation took place; the absence of trimethylamine moiety ( $m/z$  58.0646) and the presence of  $m/z$  312.1392 instead of 326.1558. CTRAC-360 ( $m/z$  360.1619,  $t_R$ : 6.3 min), identified as CTRAC-N-oxide, was the most abundant TP, since its peak area represented up to 96% of the total TPs' peak area. Its MS/MS spectra similarity with its precursor compound was 0.876. This TP was also previously identified as CTRAM ozonation TP.

Two isobaric TPs, CTRAC-376a and b, fitting the molecular formula  $C_{20}H_{22}FNO_5$ , were detected at 4.5 and 5.5 min, respectively. Although MS/MS spectra was available for CTRAC-376a ( $m/z$  376.1538), the ring double bond equivalents value (rdbe) proposed by the formula annotation tool for the fragments, was too low to permit structure elucidation. Thus, it was not possible to go beyond the determination of the unequivocal molecular formula for this TP and as a result LoC 4 was reached. On the other hand, CTRAC-376b ( $m/z$  376.1551) presented extended fragmentation, where 11 fragments were structurally elucidated, revealing that CTRAC-360 was further oxidized to produce CTRAC-376b, its hydroxylated benzoic acid ring derivative (LoC 2b). The detected 7  $m/z$  (including 2 pairs of ions) in its MS/MS spectra, relevant to those of CTRAC, contributed to a similarity score of 0.495. The subsequent further reaction of CTRAC-376b with ozone, caused the formation of CTRAC-282 ( $t_R$ : 2.6 min, LoC: 2b), after the removal of the fluorobenzene part of the molecule. CTRAC-282 was detected as  $m/z$  282.1325 but its in-source fragment ( $-H_2O$ ) with  $m/z$  264.1230 presented higher intensity in the MS spectra. According to the transformation of CIT and CTRAM to CIT-355 and

CTRAM-373, respectively, CTRAC-374 (m/z 374.1408,  $t_R$ : 5.6 min, LoC: 2b) was formed by the furan ring oxidation of CTRAC-360.

The  $t_R$  (6.8 min) and MS/MS spectra of CTRAC TP with m/z 311.1556, which reached its maximum abundance when 0.3 mg/L of ozone were added, were identical to DESCIT. Thus, LoC 1 was attributed to CTRAC-311.

CTRAC-358 (m/z 358.1458,  $t_R$ : 5.3 min) was detected at pH 4 in 100 times higher intensity than pH 7. The 6 structurally elucidated fragments in its MS/MS spectra obviously display that the furan ring is oxidized. After comparison with the MS/MS spectra of CTRAC, 9 m/z (including two pairs of isotopic ions) were correlated (characteristic fragments), contributing to a MS/MS similarity score of 0.720. Thus a LoC 2b was attributed to CTRAC-358.

CTRAC-302 (m/z 302.1187,  $t_R$ : 4.7 min) was detected in all pH values, while CTRAC-127 (m/z 127.0972,  $t_R$ : 1.5 min) was detected only in pH 4. Although, both MS and MS/MS data were available, LoC 5 was assigned to these two TPs, since no unequivocal formula could be proposed. Three fragments in the MS/MS spectra of CTRAC-302 were related to fragments of CTRAC.

The acquired MS/MS data for the detected TPs CTRAC-388 (m/z 388.1554,  $t_R$ : 7.8 min) and CTRAC-374.17 (m/z 374.1766,  $t_R$ : 8.1 min) did not help their structure elucidation. The indisputable molecular formulas of  $C_{21}H_{22}FNO_5$  and  $C_{21}H_{24}FNO_4$  were attributed to CTRAC-388 and 374.17, respectively (LoC 4). Even though, a specific structure could not be proposed for CTRAC-388, its  $t_R$  and MS/MS similarity indicate that it is the same TP with CTRAM-388. Considering that this TP was detected as an ozonation TP of both CTRAM and CTRAC and that CTRAC was formed during the ozonation of CTRAM, then it can be assumed that CTRAC-388 is produced through the ozonation of CTRAC. Therefore, it is a second generation TP of CTRAM.

The formation of CTRAC-358, 282 and 374 was proportional to the applied ozone concentration, thus its maximum abundance was noticed in the samples where 12 mg/L of ozone were added. The transformation rate of CTRAC was remarkable, since up to 95.4% of CTRAC 2 mg/L were transformed to the previously discussed detected TPs.

### 5.5.5 Removal of CTROXO and Identification of its ozonation TPs

More than 44% of CTROXO ( $m/z$  339.1505,  $t_R$ : 6.5 min) has been efficiently removed in reaction with 0.3 mg/L of ozone, while when  $\geq 1.5$  mg  $O_3/L$  were applied, CTROXO reached total removal. Its MS/MS spectra revealed 6 diagnostic fragments, which will be helpful for TPs structure elucidation. Totally, 8 TPs of CTROXO were detected in this study. Since CTROXO was formed as a CIT ozonation TP, all CTROXO ozonation TPs can be considered as CIT second generation ozonation TPs.

In case of CTROXO-343 ( $m/z$  343.1820,  $t_R$ : 5.3 min) and CTROXO-359 ( $m/z$  359.1764,  $t_R$ : 5.6 min),  $t_R$  and MS/MS spectra similarity match to CTRAM and CTRAM-359 causing their identification to be at LoC 1 and 2a, respectively. CTROXO-343 was formed in low ozone doses and in higher ones was further oxidized to its N-oxide derivative. The detection of CTROXO-388 ( $m/z$  388.1557,  $t_R$ : 7.8 min, LoC 4), which was identified as CTRAM-388 and CTRAC-388 due to  $t_R$  and fragmentation similarity, in the ozonated samples of CTROXO, implies the formation and further transformation of CTRAC.

The N-oxide derivative of CTROXO (CTROXO-355) was detected and identified as  $m/z$  355.1462 at 6.8 min. Its MS/MS spectra presents 5 common fragments with CTROXO (0.407 similarity score), along with the characteristic fragment of N-oxide moiety ( $m/z$  62.0594). This TP has already been reported as CIT biotransformation products [206], so LoC 2a was assigned. CTROXO-355 contribution to the total CTROXO TPs content reached 98.5%, showing that it is by far the most abundant TP. Four more N-oxide derivatives were detected; CTROXO-371, 373a and b and 391. CTROXO-371 was formed by CTROXO-355 through further hydroxylation of benzonitrile ring moiety. It was eluted at 6.5 min and detected as  $m/z$  371.1404. The detection of diagnostic fragments with  $m/z$  196.0386, 250.0663, 292.0761 and 310.0909 led to LoC 2b. Two peaks eluted at the fifth min of the chromatogram correspond two isomeric TPs fitting the formula  $C_{20}H_{21}FN_2O_4$ . The MS/MS spectrum of CTROXO-373a ( $m/z$  373.1561,  $t_R$ : 5.0 min) depicted 3 characteristic fragments ( $m/z$  258.0703, 294.0918 and 355.1446) which support the proposed peroxide derivative structure (LoC 2b). CTROXO-373b was identified as CTRAM-373, due to  $t_R$  and fragmentation pattern similarity (LoC 2b). The last N-oxide TP, CTROXO-391

was formed only at highly basic experimental conditions (pH 10). The hydrolysis of nitrile resulted in the formation of this TP, which was detected at 3.9 min as  $m/z$  391.1666 (LoC 2b).

A maximum of 64.4 of the initial CTROXO concentration was transformed to these eight detected TPs.



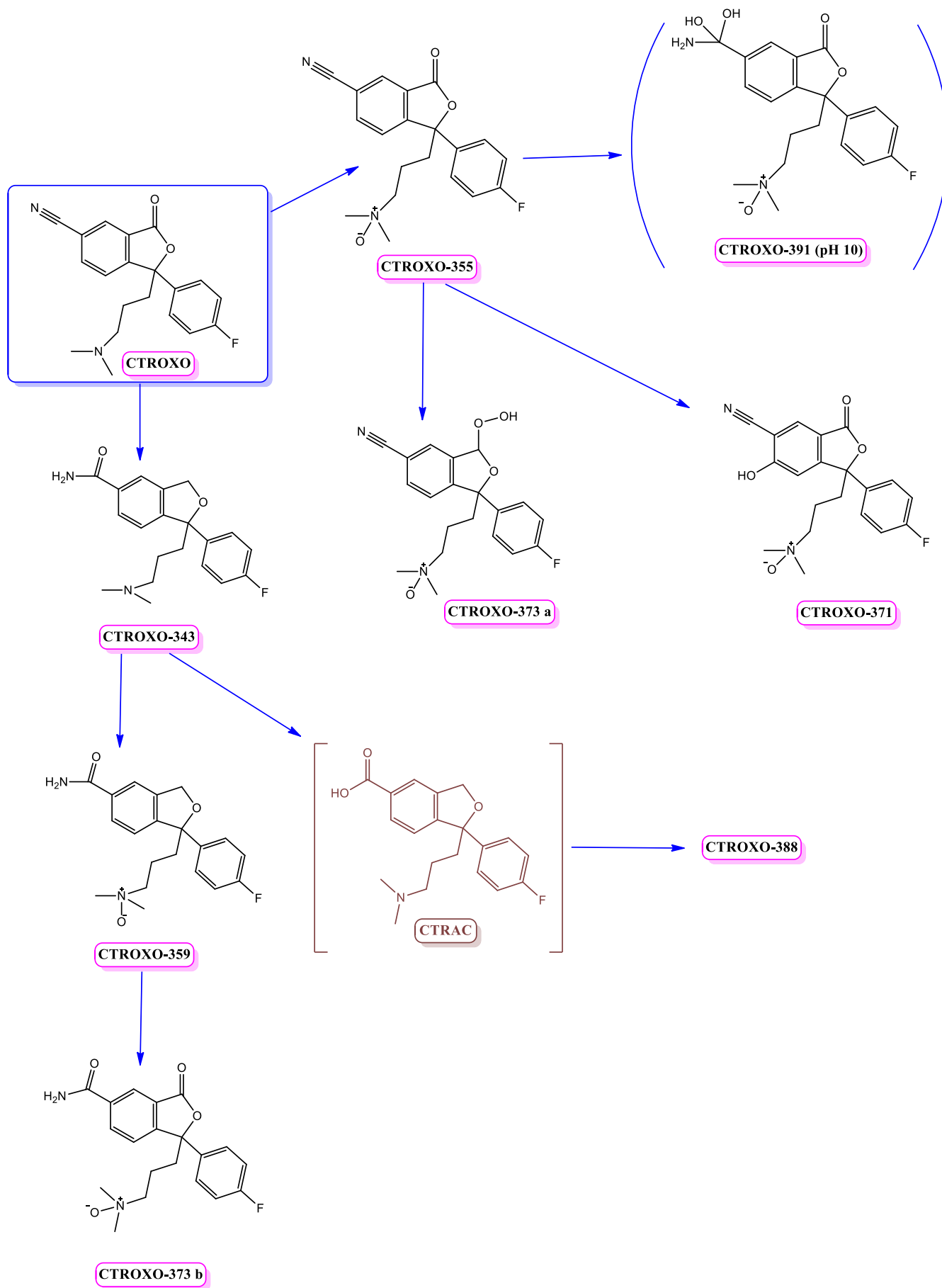


Fig. 5.7 CTROXO TPs formation tree.

### 5.5.6 Retention time prediction

Since reference standard solutions were not commercially available for most of the identified compounds, retention time prediction was performed as additional identification supporting tool.

An in-house QSRR prediction model, developed based on extensive dataset of over 1800 emerging contaminants, was used for predicting  $t_R$  of TPs analyzed in positive ESI. Chemometrics tools were utilized for the prediction, taking into account the proposed structure, its physicochemical properties and the chromatographic system (analytical column, gradient elution program and pump) that was used. The predicted retention time was considered to match if it was within  $\pm 3\sigma$  (standardized residual) of the experimental value, as this covers 99.7% of normally distributed data. For most retention times, this is approximately equivalent to  $\pm 2$  min. Considering the absolute window of  $\pm 2$  min for a compound that has different chemical structure from the training set may lead to wrong conclusion. For this reason, in order to evaluate the prediction results, an in-house developed tool (OTrAMS) was also used. This tool examines the origin of residuals between predicted and experimental retention time. More details are described in the original paper [142]. The exported results (shown as bubble plot) show if the observed residual is due to the wrong chemical structure (leading to wrong prediction of retention time) or because the tested structure is outside the AD of the model. The results of prediction and AD study, presented in **Table S5.5** and **Fig. S5.8**, respectively, show that most of the predicted values are inside boxes 1 and 2, suggesting that the predicted retention times for most TPs were in agreement with the experimental ones. However, there are four compounds (DESCIT-280, CTRAC-376b, CTRAC-374 and CTROXO-373a) located in box 3, and CTRAC-282 which is a model outlier (located in box 4). The bubble sizes for box 3 compounds are quite large, indicating that the source of the observed residual can be the large chemical structure diversity. The prediction result for CTRAC-282 is rejected, since the bubble is outside the safe zone of the model (**Fig. S5.8**) and its size is significantly big. Thus, these five compounds are outside the AD of the prediction model, and thus retention time prediction cannot be used as supporting information for their identification.

### 5.5.7 Toxicity assessment

The environmental relevance of this study findings lies upon the fact that the identified TPs can be produced in real conditions, in WWTPs where ozonation is applied as a tertiary treatment process. In order to evaluate their probable negative effects in human life and ecosystem, advanced software and sophisticated tools were used for toxicity prediction. The results of ToxTrAMS, extracted as pLC50 for *Pimephales promelas* and *Daphnia magna* (after 96 and 48 h of exposure, respectively) and as pEC50 for *Pseudokirchneriella subcapitata* (after 72 h of exposure), are listed in **Table 5.5**. Since ToxTrAMS is based on the QSTR models, the prediction is feasible only for TPs that a specific structure was proposed. The highlighted values in **Table 5.5** indicate the cases where the identified TPs are more toxic than their parent compounds. 70.3% of the identified TPs presented higher toxicity towards *Daphnia magna*, while 48.6% were predicted to be more toxic for *Pimephales promelas*, and 10.8% were predicted to be more toxic for *pseudokirchneriella subcapitata*, compared to their parent compounds. DESCIT-339 and 280, CTRAM-325 and CTRAC-311 were the only TPs whose predicted pEC50 of algae exceeded the one of their corresponding parent compound. The prediction for CTRAC-376 b, CTRAC-282 and CTROXO-391 (pH 10), concerning the toxicity towards planktonic crustacean species, is not reliable, as these compounds are outside of the AD of the prediction model, and thus further experimental proof is required. The figures of the AD results of the toxicity prediction model for the tested compounds and their identified TPs, for the three investigated species, are presented in **Fig. S5.9**. The results demonstrate that all the identified ozonation TPs of CIT and CTROXO are less harmful than their precursor compounds towards algae. On the contrary, 16 out of the 20 identified N-oxide TPs, are more toxic than their parent compounds for *Daphnia magna*. The toxicity expressed as LC50/ EC50 in mg/L for every compound, along with the relative toxicity of each identified TP compared to its parent compound, is listed in **Table S5.6**. The highlighted values correspond to ozonation TPs whose toxicity is at least 1.5 times higher than that of the parent compound. According to the extracted prediction results, CTRAC-358 (pH 4) is the most toxic TP for *Pimephales promelas* with LC50 of 4.6 mg/L, DESCIT-280 for *Daphnia magna*

(LC50: 10.3 mg/L), while CIT-339 b (pH 4), DESCIT-280 and CTRAM-325 present equal LC50 value of 0.3 mg/L towards *Pseudokireriella subcapitata*.

**Table 5.5.** Toxicity prediction for CIT, DESCIT, CTRAM, CTRAC, CTROXO and their identified TPs.

Compounds	pLC50 of <i>Pimephales promelas</i> (after 96 h of exposure)	pEC50 of <i>Pseudokirchneriella subcapitata</i> (after 72 h of exposure)	pLC50 of <i>Daphnia Magna</i> (after 48 h of exposure)
<b>CIT</b>	<b>3.97</b>	<b>5.99</b>	<b>3.45</b>
CIT-341	3.54	4.77	4.41
CIT-311	3.71	5.80	3.32
CIT-263	3.25	4.00	3.49
CIT-355	4.23	4.84	4.26
CIT-357	4.11	4.92	4.07
CIT-339 a	3.55	5.94	3.38
CIT-339 b (pH 4)	4.46	5.99	3.21
<b>DESCIT</b>	<b>3.71</b>	<b>5.80</b>	<b>3.32</b>
DESCIT-297	3.45	5.38	3.57
DESCIT-327	4.22	5.76	3.62
DESCIT-341	3.54	4.77	4.41
DESCIT-325 a	4.32	5.59	3.21
DESCIT-325 b	3.44	5.56	3.62
DESCIT-339	3.55	5.94	3.38
DESCIT-280	4.11	5.95	4.43
DESCIT-344 (pH 4)	4.23	5.51	2.91
<b>CTRAM</b>	<b>3.51</b>	<b>5.82</b>	<b>3.84</b>
CTRAM-281	3.33	4.01	2.94
CTRAM-375	4.26	4.92	3.92
CTRAM-373	4.06	4.92	3.58
CTRAM-359	3.32	4.78	3.61
CTRAM-360	4.06	4.37	3.94
CTRAM-325	3.97	5.99	3.45
CTRAM-341	3.54	4.77	4.41
CTRAM-329 (pH 4)	3.37	5.52	3.97
<b>CTRAC</b>	<b>4.23</b>	<b>5.51</b>	<b>2.91</b>
CTRAC-376 b	3.96*	4.53	4.27
CTRAC-374	4.54	4.46	3.85
CTRAC-330	4.03	4.95	3.15
CTRAC-360	4.06	4.37	3.94
CTRAC-311	3.71	5.80	3.32
CTRAC-282	3.42*	3.66	3.29
CTRAC-358 (pH 4)	4.89	5.32	2.85
<b>CTROXO</b>	<b>3.75</b>	<b>5.99</b>	<b>3.21</b>
CTROXO-373 a	3.99	4.86	3.52
CTROXO-373 b	4.06	4.92	3.58
CTROXO-343	3.51	5.82	3.84
CTROXO-359	3.32	4.78	3.61
CTROXO-371	4.62	5.03	4.01
CTROXO-355	4.24	4.84	4.26
CTROXO-391 (pH 10)	2.97*	4.89	2.74

\*experimental proof is needed, the toxicity prediction for these compounds is not reliable since it is not covered by the applicability domain of the model

### 5.5.8 Common transformation pathways and produced TPs

The transformation of CIT and 4 of its biotransformation products during ozonation was investigated in this study. The tested precursors are structurally alike compounds, so common transformation pathways in reaction with ozone are expected. Indeed 7 common transformation pathways were noticed and are listed in **Table 5.6**, along with the TPs that are formed through the respective reaction. As indicated, N-oxide TPs (or N-hydroxylated, for DESCIT) were formed through the ozonation of all tested compounds. All N-oxide derivatives were proven to be further oxidized to form 3 additional TPs through a) hydroxylation of benzonitrile ring moiety, b) hydroxylation of benzonitrile ring followed by fluorobenzene moiety removal (apart from CTROXO-355) and c) oxidation of THF ring.

**Table 5.6.** Common transformation pathways occurring during the ozonation of the parent compounds and the relative TPs that are formed.

Transformation pathway	TPs that are formed				
	CIT	DESCIT	CTRAM	CTRAC	CTROXO
N-oxidation	CIT-341	DESCIT-327	CTRAM-359	CTRAC-360	CTROXO-355
N-demethylation	CIT-311	DESCIT-297	CTRAM-329 (pH 4)	CTRAC-330	N.D.
Oxidation of THF ring (ketone formation)	CIT-339 b	DESCIT-325 a	N.D.	CTRAC-358 (pH 4)	N.D.
Ketone formation in trimethylamine moiety**	CIT-339 a	DESCIT-325 b	N.D.	N.D.	N.D.
N-oxidation & hydroxylation of benzonitrile ring*** moiety	CIT-357	N.D.*	CTRAM-375	CTRAC-376 b	CTROXO-371
N-oxidation & hydroxylation of benzonitrile ring***& fluorobenzene moiety removal	CIT-263	N.D.	CTRAM-281	CTRAC-282	N.D.
N-oxidation & oxidation of THF ring (ketone formation****)	CIT-355	N.D.	CTRAM-373	CTRAC-374	CTROXO-373 a

\*N.D.: not detected

\*\* dimethylamine for DESCIT

\*\*\*benzamide ring moiety for CTRAM and benzoic acid ring moiety for CTRAC

\*\*\*\* peroxide formation for CTROXO

This information can be very useful for retrospective analysis of tertiary treated (with ozone) wastewater samples. In particular, if a compound (precursor) is detected in secondary treated wastewater samples and its ozonation TPs are detected in tertiary treated wastewater samples, then retrospective suspect

screening can be performed for the TPs of precursor-structurally-alike compounds, also detected in secondary treated samples. The suspect screening will be based on the proven hypothesis that common reaction pathways are followed during the ozonation of precursor-structurally-alike compounds leading in the formation of commonly structured ozonation TPs.

The identification results have also demonstrated that common ozonation TPs can be formed by the ozonation of structurally-alike precursors. CIT, its 4 tested biotransformation products and their 46 identified TPs are illustrated in **Fig. 5.8**. Six additional biotransformation products of CIT, previously reported by Beretsou et al. [206] are also included in **Fig. 5.8**, for comparison purposes. The common compounds are circled by the same color. This cumulative Fig. reveals that the transformations that take place in the different processes applied in WWTPs are much more complicated than they thought to be. As presented in **Fig. 5.8**, the biodegradation of CIT led to the formation of CTRAM, which in contact with ozone formed CTRAM-325, identified as CIT. This example shows that circled reactions may occur in WWTPs, affecting the concentration of the contaminants that are finally discharged into the aquatic environment. Moreover, the formation of common TPs either by different process or by different precursor was highly indicated. For instance, DESCIT, CTROXO, CIT-341 and 355 were formed by both the ozonation and the biodegradation of CIT. CTRAM-360 was produced as a biotransformation product of CIT and as an ozonation TP of CTRAM and CTRAC. CTRAM, CTRAC and CTROXO transformation during ozonation resulted in the formation of CTRAM-388. These findings have also a direct impact on toxicity assessment outcome. For instance, CIT-341 was formed by the biodegradation of CIT and by the ozonation of CIT, DESCIT and CTRAM. Based on the results listed in **Table 5.5**, CIT-341 is more toxic than all its precursors against *Daphnia Magna* and thus, its synergistic formation by all different sources should be considered while evaluating the high ecotoxicological impact of its detection.

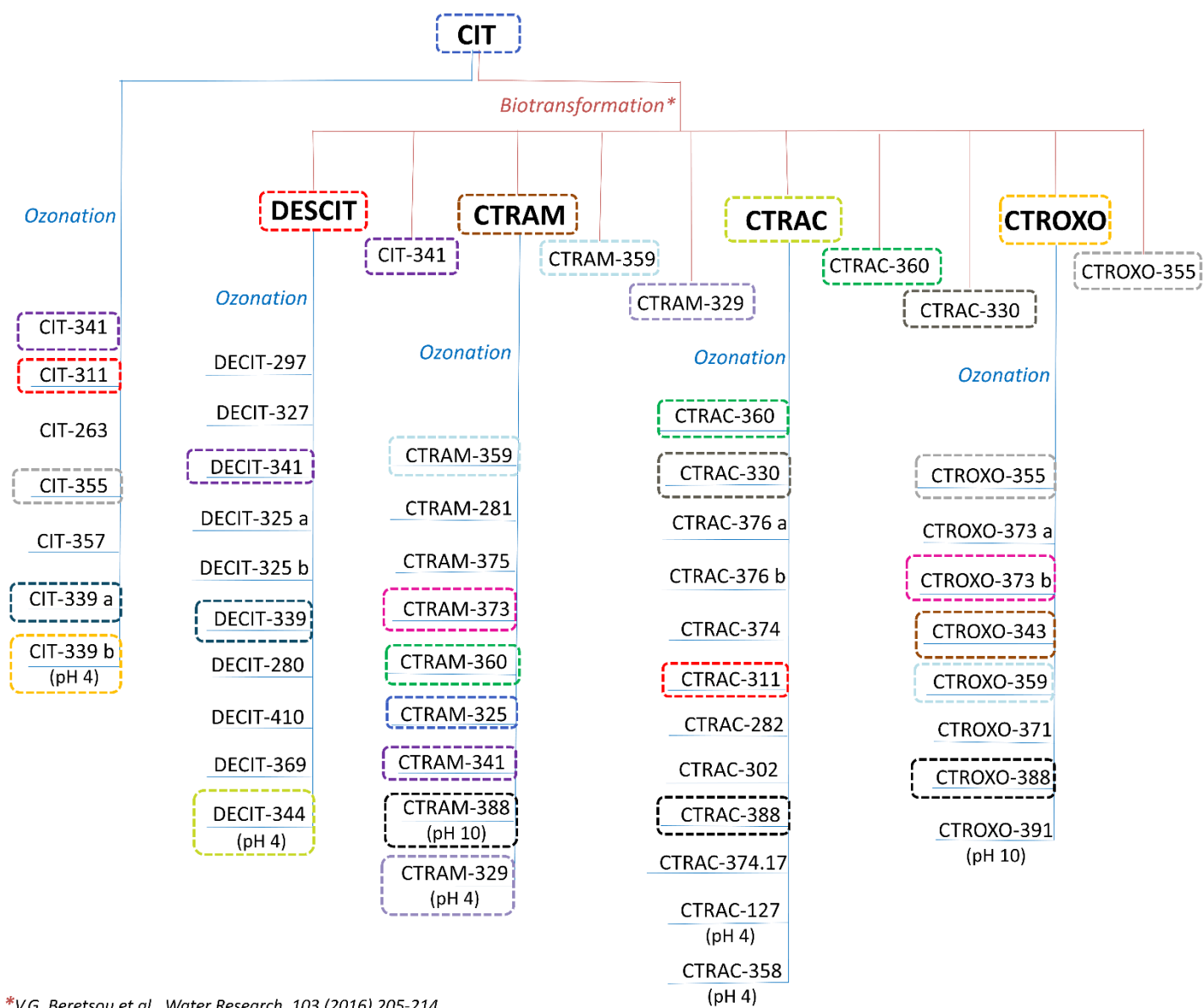


**Fig. 5.8.** Identified TPs of CIT and 4 of its biotransformation products. Common compounds are circled with the same color.

## 5.6. Conclusions

Recently, the development of novel and sophisticated software and tools has enabled the automated detection of TPs, even from complex matrices like wastewater, which significantly contributed to reducing the time-consuming process of data treatment in relevant studies. TrendTrAMS, an in-house developed program written in MATLAB, was used in our study for the automatic detection of potential TPs. The Gaussian curve fitting of TPs (intensity) versus ozone concentration has led to their detection. Moreover, XCMS online was used for pairwise comparison between experiments done at different pH values, for the detection of additional TPs

Overall, 46 ozonation TPs were detected in this study. Among them, 24 TPs were reported for the first time, 7 TPs were proven to be formed by the ozonation of more than one precursor compound and 10 biotransformation products of CIT were also produced as ozonation TPs of DESCIT, CTRAM, CTRAC or CTROXO. The toxicity of all the identified TPs and parent compounds were predicted with ToxTrAMS, an in-house risk assessment program. Most of the identified TPs show considerably higher toxicity than their parent compounds, underlying the environmental significance of their detection. 43% of them were proven at least 1.5 times more toxic against fish, 8% against algae, while almost 57% against planktonic crustacean.

So far, ozonation studies are focused on the investigation of removal and transformation of parent compounds and their known human metabolites. Thus, if the ozonation of only CIT and DESIT has been studied, 17 TPs would have been detected instead of 46. This fact highlights that numerous ozonation TPs of compounds produced during secondary treatment (biotransformation products) still remain unknown.



## CHAPTER 6.

### Conclusions



**Fig. 6.0** Graphical abstract of Chapter 6.

The last decade, the introduction of high resolution mass analyzers, along with the development of sophisticated software for the data treatment of the vast information that is extracted through HRMS analysis, have both contributed to the field of Environmental Chemistry, and especially to the detection and identification of unknown compounds, such as transformation products. Existing literature has already reported the incomplete removal of emerging pollutants during secondary treatment. Disinfection methods (including chlorination and ozonation) are applied as tertiary treatment processes in WWTPs, where chemical reactions between the emerging pollutants and the selected oxidant end up to the formation of TPs with unknown structures, physicochemical properties and ecotoxicological activity.

The removal of EPs and their transformation during chlorination (Chapter 3) and ozonation (Chapter 4-5) experiments were in depth investigated in the experimental part of this doctoral thesis. The results have demonstrated that suspect and non-target screening workflows can result in the identification of several transformation products of emerging contaminants (Chapter 3: industrial chemicals, Chapters 4 & 5: pharmaceuticals). Moreover, since the identification through these workflows is tentative (no reference standards are available for most of the TPs), the in-house developed program (OTrAMS) for the prediction of the retention time further supported the proposed structures (Chapters 3-5). LC is the technique of choice for the determination of quite polar to non-polar compounds. The TPs that are formed during oxidation processes like chlorination and ozonation are mainly more polar than their parent

compound. The use of HILIC as a complimentary technique to RP was proven meaningful for the detection of polar TPs that were not retained on the RP column and for the separation of isomeric TPs that were co-eluted in the RP system (Chapter 4).

The toxicity prediction results have revealed that in both chlorination and ozonation experiments, TPs more toxic than their parent compounds may be formed (Chapter 3: chlorinated TPs, Chapter 5: oxidation TPs). Based on these evidence, the need of monitoring in a routine basis, not only the parent compounds (EPs), but also their TPs, is highly indicated.

The results of the third study (Chapter 5), have demonstrated that the further transformation of biotransformation products, during the tertiary treatment processes should also attract the scientific community, since thousands of TPs are nowadays being overlooked.

Finally, structurally-alike EPs were proven to follow common transformation pathways during tertiary treatment (Chapter 5). Based on the existing literature, a database consisted of all the so far reported TPs can be developed. Moreover, chlorination/ ozonation TPs for more EPs can be predicted and included in the database, following the “common transformation pathway of structurally-alike compounds” rule. Afterward, this database can be screened for retrospective analysis of environmental samples, for the detection and identification of these TPs in real samples.

## ABBREVIATIONS AND ACRONYMS

1,2,3-benzotriazoles	BTRs
1,3-benzothiazoles	BTHs
Acetonitrile	ACN
Advanced Oxidation Processes	AOPs
Applicability Domain	AD
Applied molar ratio of NaOCl and the target contaminant	m.r.
Biochemical Oxygen Demand	BOD
Data-Dependent Acquisition	DDA
Data-Independent Acquisition	IDA
Dissolved Organic Matter	DOM
Double Bond Equivalent	DBE
Ecological Structure Activity Relationships	ECOSAR
Emerging Contaminants	ECs
Emerging Pollutants	EPs
Extracted Ion Chromatograms	EIC
Full Width at Half Maximum	FWHM
Gas-Chromatography	GC
Half-life	$t_{1/2}$
High Resolution Mass Spectrometers	HR-MS
High resolution mass spectrometry	HR-MS
Hydrophilic Interaction Liquid Chromatography	HILIC
Level of confidence	LoC

## ABBREVIATIONS AND ACRONYMS

Liquid Chromatography	LC
Low resolution mass spectrometry	LR-MS
Methanol	MeOH
Persistent Organic Pollutants	POPs
Quadrupole - time of flight	Q-TOF
Quantitative Structure–Retention Relationship	QSRR
Quantitative Structure-Toxicity Relationship	QSTR
Ranitidine	RAN
Retention time	$t_R$
Reversed Phase Liquid Chromatography	RPLC
Reversed-Phase	RP
Selected Reaction Monitoring	SRM
Solid Phase Extraction	SPE
The observed pseudo-first-order rate constant	$k_{obs}$
Transformation Products	TPs
Ultrahigh-Performance Liquid Chromatography	UHPLC
Wastewater Treatment Plants	WWTPs

## REFERENCES

- [1] J. Hollender, H. Singer, D. Hernando, T. Kosjek and E. Heath, The Challenge of the Identification and Quantification of Transformation Products in the Aquatic Environment Using High Resolution Mass Spectrometry, *Xenobiotics in the Urban Water Cycle*, vol.16, 2010, pp.195-211.
- [2] K. Kümmerer, Pharmaceuticals in the Environment, *Annual Review of Environment and Resources*, vol. 35, 2010, pp. 57-75.
- [3] R.L. Oulton, T. Kohn and D.M. Cwiertyny, Pharmaceuticals and personal care products in effluent matrices: A survey of transformation and removal during wastewater treatment and implications for wastewater management, *Journal of Environmental Monitoring*, vol.12, 2010, pp. 1956-1978.
- [4] C.G. Daughton, Non-regulated water contaminants: emerging research, *Environmental Impact Assessment Review*, vol. 24, 2004, pp. 711-732.
- [5] D.J. Lapworth, N. Baran, M.E. Stuart and R.S. Ward, Emerging organic contaminants in groundwater: A review of sources, fate and occurrence, *Environmental pollution*, vol. 163, 2012, pp. 287-303.
- [6] S.D. Richardson and T.A. Ternes, Water analysis: emerging contaminants and current issues, *Analytical Chemistry*, vol. 83, 2011, pp. 4614-4648.
- [7] K. Fent, A.A. Weston and D. Caminada, Ecotoxicology of human pharmaceuticals, *Aquatic Toxicology*, vol. 76, 2006, pp. 122-159.
- [8] A. Aguera, M.J. Martinez Bueno and A.R. Fernandez-Alba, New trends in the analytical determination of emerging contaminants and their transformation products in environmental waters, *Environmental Science and Pollution Research International*, vol. 20, 2013, pp. 3496-3515.
- [9] M.I. Farré, S. Pérez, L. Kantiani and D. Barceló, Fate and toxicity of emerging pollutants, their metabolites and transformation products in the aquatic environment, *TrAC Trends in Analytical Chemistry*, vol. 27, 2008, pp. 991-1007.
- [10] F.J. Benitez, J.L. Acero, F.J. Real, G. Roldan and E. Rodriguez, Photolysis of model emerging contaminants in ultra-pure water: kinetics, by-products formation and degradation pathways, *Water Research*, vol. 47, 2013, pp. 870-880.
- [11] J. Santiago, A. Aguera, M. del Mar Gomez-Ramos, A.R. Fernandez Alba, E. Garcia-Calvo and R. Rosal, Oxidation by-products and ecotoxicity assessment

during the photodegradation of fenofibric acid in aqueous solution with UV and UV/H<sub>2</sub>O<sub>2</sub>, *Journal of hazardous materials*, vol. 194, 2011, pp. 30-41.

[12] A.K. Genena, D.B. Luiz, W. Gebhardt, R.F.P.M. Moreira, H.J. José and H.F. Schröder, Imazalil Degradation upon Applying Ozone - Transformation Products, Kinetics, and Toxicity of Treated Aqueous Solutions, *Ozone: Science & Engineering*, vol. 33, 2011, pp. 308-328.

[13] B.I. Escher and K. Fenner, Recent Advances in Environmental Risk Assessment of Transformation Products, *Environmental Science & Technology*, vol. 45, 2011, pp. 3835-3847.

[14] P. Guerra, M. Kim, A. Shah, M. Alaei and S.A. Smyth, Occurrence and fate of antibiotic, analgesic/ anti-inflammatory, and antifungal compounds in five wastewater treatment processes, *Science of the Total Environment*, vol. 473-474, 2014, pp. 235-243.

[15] A. Rodayan, P.A. Segura, V. Yargeau, Ozonation of wastewater: Removal and transformation products of drugs of abuse, *Science of the Total Environment*, vol. 487, 2014, pp. 763-770.

[16] M. Pedrouzo, F. Borrull, E. Pocurull and R.M. Marce, Drugs of abuse and their metabolites in waste and surface waters by liquid chromatography-tandem mass spectrometry, *Journal of Separation Science*, vol. 34, 2011, pp. 1091-1101.

[17] T.M. Glenn, *Primary Treatment at Wastewater Treatment Plants*, Lewis Publishers United States of America, 1992.

[18] S.R. Frank, *Handbook of Water and Wastewater Treatment Plant Operations*, Third ed., CRC PRESS, 2014.

[19] M.B.J. Van Metre P.C. and Furlong E.T., Urban sprawl leave its PAH signature, *Environmental Science & Technology*, vol. 34, 2000, pp. 4064-4070.

[20] United States Environmental Protection Agency (USEPA), *Alternative Disinfectants and Oxidants Guidance Manual*, EPA-815-R-99-014, 1999, <https://nepis.epa.gov/Exe/ZyNET.exe/2000229L.TXT?ZyActionD=ZyDocument&Client=EPA&Index=1995+Thru+1999&Docs=&Query=&Time=&EndTime=&SearchMethod=1&TocRestrict=n&Toc=&TocEntry=&QField=&QFieldYear=&QFieldMonth=&QFieldDay=&IntQFieldOp=0&ExtQFieldOp=0&XmlQuery=&File=D%3A%5Czyfiles%5CIndex%20Data%5C95thru99%5CTxt%5C00000015%5C2000229L.txt&User=ANONYMOUS&Password=anonymous&SortMethod=h%7C&MaximumDocuments=1&FuzzyDegree=0&ImageQuality=r75g8/r75g8/x150y150g16/i425&Displ>

[ay=hpfr&DefSeekPage=x&SearchBack=ZyActionL&Back=ZyActionS&BackDesc=Results%20page&MaximumPages=1&ZyEntry=1&SeekPage=x&ZyPURL](#), last accessed September 2017.

[21] J.A. van Leerdam, A.C. Hogenboom, M.M.E. van der Kooi and P. de Voogt, Determination of polar 1H-benzotriazoles and benzothiazoles in water by solid-phase extraction and liquid chromatography LTQ-FT-Orbitrap mass spectrometry, *International Journal of Mass Spectrometry*, vol. 282, 2009, pp. 99-107.

[22] M.C. Nika, A.A. Bletsou, E. Koumaki, C. Noutsopoulos, D. Mamais, A.S. Stasinakis and N.S. Thomaidis, Chlorination of benzothiazoles and benzotriazoles and transformation products identification by LC-HR-MS/MS, *Journal of Hazardous Materials*, vol. 323, 2017, pp. 400-413.

[23] D.M. Desiderio and N.M.M. Nibbering, Black & Veatch Corporation, *White's Handbook of Chlorination and Alternative Disinfectants*, 5<sup>th</sup> Edition, Canada 2010.

[24] Earth Tech Canada Inc., Manitoba Water Stewardship, *Chlorine and Alternative Disinfectants Guidance Manual*, 2005, [https://www.gov.mb.ca/waterstewardship/odw/reg-info/approvals/odw\\_chlorine\\_and\\_alternative\\_disinfectants.pdf](https://www.gov.mb.ca/waterstewardship/odw/reg-info/approvals/odw_chlorine_and_alternative_disinfectants.pdf), last accessed September 2017.

[25] United States Environmental Protection Agency (USEPA), *Wastewater Technology Fact Sheet, Chlorine Disinfection*, EPA-832-F-99-062, 1999, <https://www3.epa.gov/npdes/pubs/chlo.pdf>, last accessed September 2017.

[26] N.H. El Najjar, M. Deborde, R. Journel and N.K. Vel Leitner, Aqueous chlorination of levofloxacin: kinetic and mechanistic study, transformation product identification and toxicity, *Water Research*, vol. 47, 2013, pp. 121-129.

[27] C. Sirtori, A. Zapata, S. Malato and A. Aguera, Formation of chlorinated by-products during photo-Fenton degradation of pyrimethanil under saline conditions. Influence on toxicity and biodegradability, *Journal of Hazardous Materials*, vol. 217-218, 2012, pp. 217-223.

[28] R. Brix, N. Bahi, M.J. Lopez de Alda, M. Farré, J.-M. Fernandez and D. Barceló, Identification of disinfection by-products of selected triazines in drinking water by LC-Q-ToF-MS/MS and evaluation of their toxicity, *Journal of Mass Spectrometry*, vol. 44, 2009, pp. 330-337.

[29] L. Meunier, S. Canonica and U. von Gunten, Implications of sequential use of UV and ozone for drinking water quality, *Water Research*, 40, 2006, pp. 1864-1876.

- [30] O. Legrini, E. Oliveros, and A. M. Braun, Photochemical Processes for Water Treatment, *Chemical Reviews*, vol. 93, 1993, pp. 671-698.
- [31] S. Devipriya and S. Yesodharan, Photocatalytic degradation of pesticide contaminants in water, *Solar Energy Materials and Solar Cells*, vol. 86, 2005, pp. 309-348.
- [32] D. Sud and P. Kaur, Heterogeneous Photocatalytic Degradation of Selected Organophosphate Pesticides: A Review, *Critical Reviews in Environmental Science and Technology*, vol. 42, 2012, pp. 2365-2407.
- [33] D. Fatta-Kassinos, M.I. Vasquez and K. Kümmerer, Transformation products of pharmaceuticals in surface waters and wastewater formed during photolysis and advanced oxidation processes-degradation, elucidation of byproducts and assessment of their biological potency, *Chemosphere*, vol. 85, 2011, pp. 693-709.
- [34] O.K. Dalrymple, D.H. Yeh and M.A. Trotz, Removing pharmaceuticals and endocrine-disrupting compounds from wastewater by photocatalysis, *Journal of Chemical Technology & Biotechnology*, vol. 82, 2007, pp. 121-134.
- [35] A.L. Boreen, W.A. Arnold and K. McNeill, Photodegradation of pharmaceuticals in the aquatic environment: A review, *Aquatic Sciences- Research Across Boundaries*, vol. 65, 2003, pp. 320-341.
- [36] A.J. Santos, M.S. Miranda and J.C. Esteves da Silva, The degradation products of UV filters in aqueous and chlorinated aqueous solutions, *Water Research*, vol. 46, 2012, pp. 3167-3176.
- [37] E. Grabowska, J. Reszczyńska and A. Zaleska, Mechanism of phenol photodegradation in the presence of pure and modified-TiO<sub>2</sub>: A review, *Water Research*, vol. 46, 2012, pp. 5453-5471.
- [38] R. Gehr, M. Wagner, P. Veerasubramanian and P. Payment, Disinfection efficiency of peracetic acid, UV and ozone after enhanced primary treatment of municipal wastewater, *Water Research*, vol. 37, 2003, pp. 4573-4586.
- [39] A. Hassen, M. Mahrouk, H. Ouzari, M. Cherif, A. Boudabous and J.J. Damelincourt, UV disinfection of treated wastewater in a large-scale pilot plant and inactivation of selected bacteria in a laboratory UV device, *Bioresource Technology*, vol. 74, 2000, pp. 141-150.
- [40] United States Environmental Protection Agency (USEPA), *Wastewater Technology Fact Sheet, Ozone Disinfection*, EPA-832-F-99-063, 1999, <https://www3.epa.gov/npdes/pubs/ozon.pdf>, last accessed September 2017.



- [41] F.J. Beltran, J.F. García-Araya and P.M. Alvarez, Sodium Dodecylbenzenesulfonate Removal from Water and Wastewater. 2. Kinetics of the Integrated Ozone-Activated Sludge System, *Industrial & Engineering Chemistry Research*, vol. 39, 2000, pp. 2221-2227.
- [42] Q. Dai, L. Chen, W. Chen and J. Chen, Degradation and kinetics of phenoxyacetic acid in aqueous solution by ozonation, *Separation and Purification Technology*, vol. 142, 2015, pp. 287-292.
- [43] P.R. Gogate and A.B. Pandit, A review of imperative technologies for wastewater treatment I: oxidation technologies at ambient conditions, *Advances in Environmental Research*, vol. 8, 2004, pp. 501-551.
- [44] J. Hoigné and H. Bader, The role of hydroxyl radical reactions in ozonation processes in aqueous solutions, *Water Research*, vol. 10, 1976, pp. 377-386.
- [45] C. von Sonntag, U. von Gunten, *Chemistry of Ozone in Water and Wastewater Treatment*, IWA Publishing, 2012.
- [46] S.G. Zimmermann, M. Wittenwiler, J. Hollender, M. Krauss, C. Ort, H. Siegrist and U. von Gunten, Kinetic assessment and modeling of an ozonation step for full-scale municipal wastewater treatment: micropollutant oxidation, by-product formation and disinfection, *Water Research*, vol. 45, 2011, pp. 605-617.
- [47] J. Hollender, S. G. Zimmermann, S. Koepke, M. Krauss, C. S. McArdell, C. Ort, H. Singer, U. von Gunten and H. Siegrist, Elimination of organic micropollutants in a municipal wastewater treatment plant upgraded with a full-scale post-ozonation followed by sand filtration, *Environmental Science & Technology*, vol. 43, 2009, 43, pp 7862-7869.
- [48] D. Voutsas, P. Hartmann, C. Schaffner and W. Giger, Benzotriazoles, Alkylphenols and Bisphenol A in Municipal Wastewaters and in the Glatt River, Switzerland, *Environmental Science and Pollution Research International*, vol. 13, 2006, pp. 333-341.
- [49] E.N. Evgenidou, I.K. Konstantinou and D.A. Lambropoulou, Occurrence and removal of transformation products of PPCPs and illicit drugs in wastewaters: A review, *Science of the Total Environment*, vol. 505, 2015, pp. 905-926.
- [50] A.D. Coelho, C. Sans, S. Esplugas and M. Dezotti, Ozonation of NSAID: A Biodegradability and Toxicity Study, *Ozone: Science & Engineering*, vol. 32, 2010, pp. 91-98.

- [51] K. Ikehata and M. Gamal El-Din, Aqueous Pesticide Degradation by Ozonation and Ozone-Based Advanced Oxidation Processes: A Review (Part II), *Ozone: Science & Engineering*, vol. 27, 2005, 173-202.
- [52] K. Ikehata and M. Gamal El-Din, Aqueous Pesticide Degradation by Ozonation and Ozone-Based Advanced Oxidation Processes: A Review (Part I), *Ozone: Science & Engineering*, vol. 27, 2005, pp. 83-114.
- [53] K. Ikehata, N. Jodeiri Naghashkar and M. Gamal El-Din, Degradation of aqueous pharmaceuticals by ozonation and advanced oxidation processes: A review, *Ozone: Science and Engineering*, vol. 28, 2006, pp. 353-414.
- [54] J. Hoigné and H. Bader, Rate constants of reactions of ozone with organic and inorganic compounds in water, *Water Research*, vol. 17, 1983, pp. 185-194.
- [55] R. Andreatti, V. Caprio, A. Insola and R. Marotta, Advanced oxidation processes (AOP) for water purification and recovery, *Catalysis Today*, vol. 53, 1999, pp. 51-59.
- [56] F. Hernandez, M. Ibanez, T. Portoles, M.I. Cervera, J.V. Sancho and F.J. Lopez, Advancing towards universal screening for organic pollutants in waters, *Journal of Hazardous Materials*, vol. 282, 2015, pp. 86-95.
- [57] V. Leendert, H. Van Langenhove and K. Demeestere, Trends in liquid chromatography coupled to high-resolution mass spectrometry for multi-residue analysis of organic micropollutants in aquatic environments, *TrAC Trends in Analytical Chemistry*, vol. 67, 2015, pp. 192-208.
- [58] M. Dasenaki and N. Thomaidis, Multianalyte method for the determination of pharmaceuticals in wastewater samples using solid-phase extraction and liquid chromatography–tandem mass spectrometry, *Analytical and Bioanalytical Chemistry*, vol. 407, 2015, pp. 4229-4245.
- [59] J.L. Martinez Vidal, P. Plaza-Bolanos, R. Romero-Gonzalez and A. Garrido Frenich, Determination of pesticide transformation products: a review of extraction and detection methods, *Journal of Chromatography A*, vol. 1216, 2009, pp. 6767-6788.
- [60] V.L. Borova, N.C. Maragou, P. Gago-Ferrero, C. Pistos and N.S. Thomaidis, Highly sensitive determination of 68 psychoactive pharmaceuticals, illicit drugs, and related human metabolites in wastewater by liquid chromatography-tandem mass spectrometry, *Analytical and Bioanalytical Chemistry*, vol. 406, 2014, pp. 4273-4285.

- [61] K. Fischer, E. Fries, W. Korner, C. Schmalz and C. Zwiener, New developments in the trace analysis of organic water pollutants, *Applied Microbiology and Biotechnology*, vol. 94, 2012, pp. 11-28.
- [62] F. Hernandez, O.J. Pozo, J.V. Sancho, L. Bijlsma, M. Barreda and E. Pitarch, Multiresidue liquid chromatography tandem mass spectrometry determination of 52 non gas chromatography-amenable pesticides and metabolites in different food commodities, *Journal of Chromatography A*, vol. 1109, 2006, pp. 242-252.
- [63] D.R. Baker and B. Kasprzyk-Hordern, Multi-residue analysis of drugs of abuse in wastewater and surface water by solid-phase extraction and liquid chromatography-positive electrospray ionisation tandem mass spectrometry, *Journal of Chromatography A*, vol. 1218, 2011, pp. 1620-1631.
- [64] D. Hummel, D. Löffler, G. Fink and T. A. Ternes, Simultaneous determination of psychoactive drugs and their metabolites in aqueous matrices by Liquid Chromatography Mass Spectrometry, *Environmental Science & Technology*, vol. 40, 2006, pp. 7321-7328.
- [65] A.J.M. Horvat, S. Babić, D.M. Pavlović, D. Ašperger, S. Pelko, M. Kaštelan-Macan, M. Petrović and A.D. Mance, Analysis, occurrence and fate of anthelmintics and their transformation products in the environment, *TrAC Trends in Analytical Chemistry*, vol. 31, 2012, pp. 61-84.
- [66] M. Petrovic and D. Barceló, LC-MS for identifying photodegradation products of pharmaceuticals in the environment, *TrAC Trends in Analytical Chemistry*, vol. 26, 2007, pp. 486-493.
- [67] M. D. Celiz, J. Tso and D. S. Aga, Pharmaceutical metabolites in the environment: analytical challenges and ecological risks, *Environmental Toxicology and Chemistry*, vol. 28, 2009, pp. 2473-2484.
- [68] R. Díaz, M. Ibáñez, J.V. Sancho and F. Hernández, Target and non-target screening strategies for organic contaminants, residues and illicit substances in food, environmental and human biological samples by UHPLC-QTOF-MS, *Analytical Methods*, vol. 4, 2012, pp. 196-209.
- [69] J. Nurmi, J. Pellinen and A.L. Rantalainen, Critical evaluation of screening techniques for emerging environmental contaminants based on accurate mass measurements with time-of-flight mass spectrometry, *Journal of mass spectrometry*, vol. 47, 2012, pp. 303-312.

- [70] A.C. Hogenboom, J.A. van Leerdam and P. de Voogt, Accurate mass screening and identification of emerging contaminants in environmental samples by liquid chromatography-hybrid linear ion trap Orbitrap mass spectrometry, *Journal of Chromatography A*, vol. 1216, 2009, pp. 510-519.
- [71] M.J. Gomez, M.M. Gomez-Ramos, O. Malato, M. Mezcua and A.R. Fernandez-Alba, Rapid automated screening, identification and quantification of organic micro-contaminants and their main transformation products in wastewater and river waters using liquid chromatography-quadrupole-time-of-flight mass spectrometry with an accurate-mass database, *Journal of Chromatography A*, vol. 1217, 2010, pp. 7038-7054.
- [72] M. Zedda and C. Zwiener, Is nontarget screening of emerging contaminants by LC-HRMS successful? A plea for compound libraries and computer tools, *Analytical and Bioanalytical Chemistry*, vol. 403, 2012, pp. 2493-2502.
- [73] Y.S. Liu, G.G. Ying, A. Shareef and R.S. Kookana, Biodegradation of three selected benzotriazoles under aerobic and anaerobic conditions, *Water Research*, vol. 45, 2011, pp. 5005-5014.
- [74] M. Bedner and W.A. MacCrehan, Transformation of acetaminophen by chlorination produces the toxicants 1,4-benzoquinone and N-acetyl-p-benzoquinone imine, *Environmental Science & Technology*, vol. 40, 2006, pp. 516-522.
- [75] A.C. Chiaia-Hernandez, E.L. Schymanski, P. Kumar, H.P. Singer and J. Hollender, Suspect and nontarget screening approaches to identify organic contaminant records in lake sediments, *Analytical and Bioanalytical Chemistry*, vol. 406, 2014, pp. 7323-7335.
- [76] F. Wode, P. van Baar, U. Dunnbier, F. Hecht, T. Taute, M. Jekel and T. Reemtsma, Search for over 2000 current and legacy micropollutants on a wastewater infiltration site with a UPLC-high resolution MS target screening method, *Water Research*, vol. 69, 2015, pp. 274-283.
- [77] C. Prasse, M. Wagner, R. Schulz and T.A. Ternes, Biotransformation of the antiviral drugs acyclovir and penciclovir in activated sludge treatment, *Environmental Science & Technology*, vol. 45, 2011, pp. 2761-2769.
- [78] J. Jaworska, S. Dimitrov, N. Nikolova and O. Mekenyan, Probabilistic assessment of biodegradability based on metabolic pathways: CATABOL system, *SAR and QSAR in Environmental Research*, vol. 13, 2002, pp. 307-323.

- [79] Y. Moriya, D. Shigemizu, M. Hattori, T. Tokimatsu, M. Kotera, S. Goto and M. Kanehisa, PathPred: an enzyme-catalyzed metabolic pathway prediction server, *Nucleic Acids Research*, vol. 38, 2010, pp. 138-143.
- [80] E.L. Schymanski, H.P. Singer, P. Longree, M. Loos, M. Ruff, M.A. Stravs, C. Ripolles Vidal and J. Hollender, Strategies to characterize polar organic contamination in wastewater: exploring the capability of high resolution mass spectrometry, *Environmental Science & Technology*, vol. 48, 2014, pp.1811-1818.
- [81] S. Kern, R. Baumgartner, D.E. Helbling, J. Hollender, H. Singer, M.J. Loos, R.P. Schwarzenbach and K. Fenner, A tiered procedure for assessing the formation of biotransformation products of pharmaceuticals and biocides during activated sludge treatment, *Journal of Environmental Monitoring*, vol. 12, 2010, pp. 2100-2111.
- [82] L.B. Ellis, J. Gao, K. Fenner and L.P. Wackett, The University of Minnesota Pathway Prediction System: predicting metabolic logic, *Nucleic Acids Research*, vol. 36, 2008, pp. 427-432.
- [83] J. Gao, L.B. Ellis and L.P. Wackett, The University of Minnesota Biocatalysis/ Biodegradation Database: Improving public access, *Nucleic Acids Research*, vol. 38, 2010, pp. 488-491.
- [84] K. Fenner, J. Gao, S. Kramer, L. Ellis and L. Wackett, Data-driven extraction of relative reasoning rules to limit combinatorial explosion in biodegradation pathway prediction, *Bioinformatics*, vol. 24, 2008, pp. 2079-2085.
- [85] E.L. Schymanski, J. Jeon, R. Gulde, K. Fenner, M. Ruff, H.P. Singer and J. Hollender, Identifying small molecules via high resolution mass spectrometry: communicating confidence, *Environmental Science & Technology*, vol. 48, 2014, pp. 2097-2098.
- [86] Z. Li, M.P. Maier and M. Radke, Screening for pharmaceutical transformation products formed in river sediment by combining ultrahigh performance liquid chromatography/high resolution mass spectrometry with a rapid data-processing method, *Analytica Chimica Acta*, vol. 810, 2014, pp. 61-70.
- [87] M. Gomez-Ramos Mdel, A. Perez-Parada, J.F. Garcia-Reyes, A.R. Fernandez-Alba and A. Aguera, Use of an accurate-mass database for the systematic identification of transformation products of organic contaminants in wastewater effluents, *Journal of Chromatography A*, vol. 1218, 2011, pp. 8002-8012.

- [88] M. Liu, S. Zhao, Z. Wang, Y. Wang, T. Liu, S. Li, C. Wang, H. Wang and P. Tu, Identification of metabolites of deoxyschizandrin in rats by UPLC-Q-TOF-MS/MS based on multiple mass defect filter data acquisition and multiple data processing techniques, *Journal of chromatography B, Analytical technologies in the biomedical and life sciences*, vol. 949-950, 2014, pp. 115-126.
- [89] J. Jeon, D. Kurth and J. Hollender, Biotransformation pathways of biocides and pharmaceuticals in freshwater crustaceans based on structure elucidation of metabolites using high resolution mass spectrometry, *Chemical Research in Toxicology*, vol. 26, 2013, pp. 313-324.
- [90] J.M. Weiss, E. Simon, G.J. Stroomberg, R. de Boer, J. de Boer, S.C. van der Linden, P.E. Leonards and M.H. Lamoree, Identification strategy for unknown pollutants using high-resolution mass spectrometry: androgen-disrupting compounds identified through effect-directed analysis, *Analytical and Bioanalytical Chemistry*, vol. 400, 2011, pp. 3141-3149.
- [91] M. Ibanez, J.V. Sancho, O.J. Pozo, W. Niessen and F. Hernandez, Use of quadrupole time-of-flight mass spectrometry in the elucidation of unknown compounds present in environmental water, *Rapid Communications in Mass Spectrometry*, vol. 19, 2005, pp. 169-178.
- [92] T. Pluskal, S. Castillo, A. Villar-Briones and M. Oresic, MZmine 2: modular framework for processing, visualizing, and analyzing mass spectrometry-based molecular profile data, *BMC Bioinformatics*, vol. 11, 2010, p. 395.
- [93] T. Kind and O. Fiehn, Seven Golden Rules for heuristic filtering of molecular formulas obtained by accurate mass spectrometry, *BMC Bioinformatics*, vol. 8, 2007, p. 105.
- [94] A. Muller, W. Schulz, W.K. Ruck and W.H. Weber, A new approach to data evaluation in the non-target screening of organic trace substances in water analysis, *Chemosphere*, vol. 85, 2011, pp. 1211-1219.
- [95] J.L. Little, A.J. Williams, A. Pshenichnov and V. Tkachenko, Identification of "known unknowns" utilizing accurate mass data and ChemSpider, *Journal of the American Society for Mass Spectrometry*, vol. 23, 2012, pp. 179-185.
- [96] E. L. Schymanski, M. Meringer and W. Brack, Matching Structures to Mass Spectra Using Fragmentation Patterns: Are the Results As Good As They Look?, *Analytical Chemistry*, vol. 81, 2009, pp. 3608-3617.

- [97] H. Horai, M. Arita, S. Kanaya, Y. Nihei, T. Ikeda, K. Suwa, Y. Ojima, K. Tanaka, S. Tanaka, K. Aoshima, Y. Oda, Y. Kakazu, M. Kusano, T. Tohge, F. Matsuda, Y. Sawada, M.Y. Hirai, H. Nakanishi, K. Ikeda, N. Akimoto, T. Maoka, H. Takahashi, T. Ara, N. Sakurai, H. Suzuki, D. Shibata, S. Neumann, T. Iida, K. Tanaka, K. Funatsu, F. Matsuura, T. Soga, R. Taguchi, K. Saito and T. Nishioka, MassBank: a public repository for sharing mass spectral data for life sciences, *Journal of Mass Spectrometry*, vol. 45, 2010, pp. 703-714.
- [98] E.L. Schymanski, C.M. Gallampois, M. Krauss, M. Meringer, S. Neumann, T. Schulze, S. Wolf and W. Brack, Consensus structure elucidation combining GC/EI-MS, structure generation, and calculated properties, *Analytical Chemistry*, vol. 84, 2012, pp. 3287-3295.
- [99] F. Rasche, A. Svatos, R.K. Maddula, C. Bottcher and S. Bocker, Computing fragmentation trees from tandem mass spectrometry data, *Analytical Chemistry*, vol. 83, 2011, pp. 1243-1251.
- [100] C. Noutsopoulos, E. Koumaki, D. Mamais, M.C. Nika, A.A. Bletsou and N.S. Thomaidis, Removal of endocrine disruptors and non-steroidal anti-inflammatory drugs through wastewater chlorination: The effect of pH, total suspended solids and humic acids and identification of degradation by-products, *Chemosphere*, vol. 119, 2015, pp. 109-S114.
- [101] D.B. Yolanda Picó, Transformation products of emerging contaminants in the environment and high-resolution mass spectrometry: a new horizon, *Analytical and Bioanalytical Chemistry*, vol. 407, 2015, pp. 6257-6273.
- [102] J. Wu, L. Zhang and Z. Yang, A Review on the Analysis of Emerging Contaminants in Aquatic Environment, *Critical Reviews in Analytical Chemistry*, vol. 40, 2010, pp. 234-245.
- [103] D.E. Helbling, J. Hollender, H.-P.E. Kohler, H. Singer and K. Fenner, High-Throughput Identification of Microbial Transformation Products of Organic Micropollutants, *Environmental Science & Technology*, vol. 44, 2010, pp. 6621-6627.
- [104] D. Hummel, D. Löffler, G. Fink and T.A. Ternes, Simultaneous Determination of Psychoactive Drugs and Their Metabolites in Aqueous Matrices by Liquid Chromatography Mass Spectrometry, *Environmental Science & Technology*, vol. 40, 2006, pp. 7321-7328.

- [105] J. Campo and Y. Picó, Emerging Contaminants, *Comprehensive Analytical Chemistry*, vol. 68, 2015, pp. 515-578.
- [106] F.J. Santos and M.T. Galceran, Modern developments in gas chromatography–mass spectrometry-based environmental analysis, *Journal of Chromatography A*, vol. 1000, 2003, pp. 125-151.
- [107] Y. Lv, T. Yuan, J. Hu and W. Wang, Seasonal occurrence and behavior of synthetic musks (SMs) during wastewater treatment process in Shanghai, China, *The Science of the Total Environment*, vol. 408, 2010, pp. 4170-4176.
- [108] C. Sanchez-Brunete, E. Miguel, B. Albero and J.L. Tadeo, Determination of cyclic and linear siloxanes in soil samples by ultrasonic-assisted extraction and gas chromatography-mass spectrometry, *Journal of Chromatography A*, vol. 1217, 2010, pp. 7024-7030.
- [109] Y. Pico and D. Barceló, Transformation products of emerging contaminants in the environment and high-resolution mass spectrometry: a new horizon, *Analytical and Bioanalytical Chemistry*, vol. 407, 2015, pp. 6257-6273.
- [110] Amadeo Rodríguez Fernández-Alba, *Comprehensive Analytical Chemistry: TOF-MS within Food and Environmental Analysis*, vol. 58, 2012.
- [111] H.P. Nguyen and K.A. Schug, The advantages of ESI-MS detection in conjunction with HILIC mode separations: Fundamentals and applications, *Journal of Separation Science*, vol. 31, 2008, pp. 1465-1480.
- [112] F. Hernández, J.V. Sancho, M. Ibáñez, E. Abad, T. Portolés and L. Mattioli, Current use of high-resolution mass spectrometry in the environmental sciences, *Analytical and Bioanalytical Chemistry*, vol. 403, 2012, pp. 1251-1264.
- [113] Network of reference laboratories, research centres and related organisations for monitoring of emerging environmental substances (NORMAN), <http://www.norman-network.net/?q=node/19>, last accessed September 2017.
- [114] E. Jover, V. Matamoros and J.M. Bayona, Characterization of benzothiazoles, benzotriazoles and benzosulfonamides in aqueous matrixes by solid-phase extraction followed by comprehensive two-dimensional gas chromatography coupled to time-of-flight mass spectrometry, *Journal of Chromatography A*, vol. 1216, 2009, pp. 4013-4019.
- [115] A. Kloepper, M. Jekel and T. Reemtsma, Determination of benzothiazoles from complex aqueous samples by liquid chromatography–mass spectrometry following solid-phase extraction, *Journal of Chromatography A*, vol. 1058, 2004, pp. 81-88.



- [116] T. Reemtsma, O. Fiehn, G. Kalnowski and M. Jekel, Microbial transformations and biological effects of fungicide- derived benzothiazoles determined in industrial wastewater, *Environmental Science & Technology*, vol. 29, 1995, pp. 478-485.
- [117] S. Weiss and T. Reemtsma, Determination of benzotriazole corrosion inhibitors from aqueous environmental samples by liquid chromatography-electrospray ionization-tandem mass spectrometry, *Analytical Chemistry*, vol. 77, 2005, pp.7415-7420.
- [118] F.J. Benitez, J.L. Acero, F.J. Real, G. Roldan and E. Rodriguez, Ozonation of benzotriazole and methylindole: Kinetic modeling, identification of intermediates and reaction mechanisms, *Journal of Hazardous Materials*, vol. 282, 2015, pp. 224-232.
- [119] A.G. Asimakopoulos, A. Ajibola, K. Kannan and N.S. Thomaidis, Occurrence and removal efficiencies of benzotriazoles and benzothiazoles in a wastewater treatment plant in Greece, *Science of the Total Environment*, 4vol. 52-453, 2013, pp. 163-171.
- [120] I. Carpinteiro, B. Abuin, M. Ramil, I. Rodriguez and R. Cela, Simultaneous determination of benzotriazole and benzothiazole derivatives in aqueous matrices by mixed-mode solid-phase extraction followed by liquid chromatography-tandem mass spectrometry, *Analytical and Bioanalytical Chemistry*, vol. 402, 2012, pp. 2471-2478.
- [121] R. Cespedes, S. Lacorte, A. Ginebreda and D. Barceló, Occurrence and fate of alkylphenols and alkylphenol ethoxylates in sewage treatment plants and impact on receiving waters along the Ter River (Catalonia, NE Spain), *Environmental Pollution*, vol. 153, 2008, pp. 384-392.
- [122] C. Domínguez, C. Reyes-Contreras and J.M. Bayona, Determination of benzothiazoles and benzotriazoles by using ionic liquid stationary phases in gas chromatography mass spectrometry. Application to their characterization in wastewaters, *Journal of Chromatography A*, vol. 1230, 2012, pp. 117-122.
- [123] V. Matamoros, E. Jover and J.M. Bayona, Occurrence and fate of benzothiazoles and benzotriazoles in constructed wetlands, *Water Science and Technology*, vol. 61, 2010, pp. 191-198.
- [124] A.S. Stasinakis, N.S. Thomaidis, O.S. Arvaniti, A.G. Asimakopoulos, V.G. Samaras, A. Ajibola, D. Mamais and T.D. Lekkas, Contribution of primary and secondary treatment on the removal of benzothiazoles, benzotriazoles, endocrine

disruptors, pharmaceuticals and perfluorinated compounds in a sewage treatment plant, *Science of the Total Environment*, vol. 463–464, 2013, pp. 1067-1075.

[125] V. Matamoros, E. Jover and J.M. Bayona, Part-per-Trillion determination of pharmaceuticals, pesticides, and related organic contaminants in river water by solid-phase extraction followed by comprehensive two-dimensional gas chromatography time-of-flight mass spectrometry, *Analytical Chemistry*, vol. 82, 2010, pp. 699-706.

[126] G. Ginsberg, B. Toal and T. Kurland, Benzothiazole toxicity assessment in support of synthetic turf field human health risk assessment, *Journal of Toxicology and Environmental Health (Part A)*, vol. 74, 2011, pp.1175-1183.

[127] M.D. Alotaibi, A.J. McKinley, B.M. Patterson and A.Y. Reeder, Benzotriazoles in the Aquatic Environment: a Review of Their Occurrence, Toxicity, Degradation and Analysis, *Water, Air, & Soil Pollution*, vol. 226, 2015.

[128] United States Environmental Protection Agency (USEPA), *Combined Sewer Overflow Technology Fact Sheet. Chlorine Disinfection*, EPA 832-F-99-034, 1999, <http://www.epa.gov/npdes/pubs/chlor.pdf>, last accessed September 2017.

[129] C. Zwiener and S.D. Richardson, Analysis of disinfection by-products in drinking water by LC–MS and related MS techniques, *TrAC Trends in Analytical Chemistry*, vol. 24, 2005, pp. 613-621.

[130] S.D. Richardson, Disinfection by-products and other emerging contaminants in drinking water, *TrAC Trends in Analytical Chemistry*, vol. 22, 2003, pp. 666-684.

[131] L. El-Bassi, H. Iwasaki, H. Oku, N. Shinzato and T. Matsui, Biotransformation of benzothiazole derivatives by the *Pseudomonas putida* strain HKT554, *Chemosphere*, vol. 81, 2010, pp. 109-113.

[132] S. Huntscha, T.B. Hofstetter, E.L. Schymanski, S. Spahr and J. Hollender, Biotransformation of benzotriazoles: insights from transformation product identification and compound-specific isotope analysis, *Environmental Science & Technology*, vol. 48, 2014, pp. 4435-4443.

[133] D.B. Mawhinney, B.J. Vanderford and S.A. Snyder, Transformation of 1H-benzotriazole by ozone in aqueous solution, *Environmental Science & Technology*, vol. 46, 2012, pp. 7102-7111.

[134] A. Muller, S.C. Weiss, J. Beisswenger, H.G. Leukhardt, W. Schulz, W. Seitz, W.K. Ruck and W.H. Weber, Identification of ozonation by-products of 4- and 5-

methyl-1H-benzotriazole during the treatment of surface water to drinking water, *Water Research*, vol. 46, 2012, pp. 679-690.

[135] J.L. Acero, F.J. Benitez, F.J. Real, G. Roldan and E. Rodriguez, Chlorination and bromination kinetics of emerging contaminants in aqueous systems, *Chemical Engineering Journal*, vol. 219, 2013, pp. 43-50.

[136] J.L. Acero, F.J. Benitez, F.J. Real and E. Rodriguez, Elimination of Selected Emerging Contaminants by the Combination of Membrane Filtration and Chemical Oxidation Processes, *Water, Air, & Soil Pollution*, vol. 226, 2015.

[137] United States Environmental Protection Agency (USEPA), DPD Colorimetric Method, Free Chlorine, 2001, <http://www.idexx.com.au/resource-library/water/water-reg-article5AM.pdf>, last accessed September 2017.

[138] J.L. Acero, F.J. Benitez, F.J. Real and G. Roldan, Kinetics of aqueous chlorination of some pharmaceuticals and their elimination from water matrices, *Water Research*, vol. 44, 2010, pp. 4158-4170.

[139] P. Gago-Ferrero, E.L. Schymanski, A.A. Bletsou, R. Aalizadeh, J. Hollender and N.S. Thomaidis, Extended Suspect and Non-Target Strategies to Characterize Emerging Polar Organic Contaminants in Raw Wastewater with LC-HRMS/MS, *Environmental Science & Technology*, vol. 49, 2015, pp. 12333-12341.

[140] Y. Kott, E.M. Nupen and W.R. Ross, The effect of pH on the efficiency of chlorine disinfection and virus enumeration, *Water Research*, vol. 9, 1975, pp. 869-872.

[141] J.B. Quintana, R. Rodil, P. Lopez-Mahia, S. Muniategui-Lorenzo and D. Prada-Rodriguez, Investigating the chlorination of acidic pharmaceuticals and by-product formation aided by an experimental design methodology, *Water Research*, vol. 44, 2010, pp. 243-255.

[142] R. Aalizadeh, N.S. Thomaidis, A.A. Bletsou and P. Gago-Ferrero, Quantitative Structure–Retention Relationship Models To Support Nontarget High-Resolution Mass Spectrometric Screening of Emerging Contaminants in Environmental Samples, *Journal of Chemical Information and Modeling*, vol. 56, 2016, pp. 1384-1398.

[143] Ecological Structure Activity Relationship (ECOSAR), <https://www.epa.gov/tsca-screening-tools/ecological-structure-activity-relationships-ecosar-predictive-model>, v. 1.11, last accessed September 2017.

- [144] M. Huerta-Fontela, M.T. Galceran and F. Ventura, Occurrence and removal of pharmaceuticals and hormones through drinking water treatment, *Water Research*, vol. 45, 2011, pp. 1432-1442.
- [145] V.S. Thomaidi, A.S. Stasinakis, V.L. Borova and N.S. Thomaidis, Is there a risk for the aquatic environment due to the existence of emerging organic contaminants in treated domestic wastewater? Greece as a case-study, *Journal of Hazardous Materials*, vol. 283, 2015, pp. 740-747.
- [146] N.M. Vieno, H. Härkki, T. Tuhkanen, L. Kronberg, Occurrence of pharmaceuticals in river water and their elimination in a pilot-scale drinking water treatment plant, *Environmental Science and Technology*, vol. 41, 2007, pp. 5077-5084.
- [147] A. Ziyilan and N.H. Ince, The occurrence and fate of anti-inflammatory and analgesic pharmaceuticals in sewage and fresh water: Treatability by conventional and non-conventional processes, *Journal of Hazardous Materials*, vol. 187, 2011, pp. 24-36.
- [148] E. Zuccato, S. Castiglioni and R. Fanelli, Identification of the pharmaceuticals for human use contaminating the Italian aquatic environment, *Journal of Hazardous Materials*, vol. 122, 2005, pp. 205-209.
- [149] A. Kumar and I. Xagorarakis, Pharmaceuticals, personal care products and endocrine-disrupting chemicals in U.S. surface and finished drinking waters: A proposed ranking system, *Science of the Total Environment*, vol. 408, 2010, pp. 5972-5989.
- [150] G. Hey, S.R. Vega, J. Fick, M. Tysklind, A. Ledin, J. la Cour Jansen, H.R. Andersen, Removal of pharmaceuticals in WWTP effluents by ozone and hydrogen peroxide, *Water SA*, vol. 40, 2014, pp. 165-173.
- [151] D. Gerrity and S. Snyder, Review of ozone for water reuse applications: Toxicity, regulations, and trace organic contaminant oxidation, *Ozone: Science and Engineering*, vol. 33, 2011, pp. 253-266.
- [152] T.A. Ternes, M. Meisenheimer, D. McDowell, F. Sacher, H.J. Brauch, B. Haist-Gulde, G. Preuss, U. Wilme and N. Zulei-Seibert, Removal of pharmaceuticals during drinking water treatment, *Environmental Science and Technology*, vol. 36, 2002, pp. 3855-3863.

- [153] T.A. Ternes, J. Stüber, N. Herrmann, D. McDowell, A. Ried, M. Kampmann, B. Teiser, Ozonation: A tool for removal of pharmaceuticals, contrast media and musk fragrances from wastewater?, *Water Research*, vol. 37, 2003, pp. 1976-1982.
- [154] V. Yargeau and C. Leclair, Potential of ozonation for the degradation of antibiotics in wastewater, *Water Science and Technology*, Vol. 55 2007, pp. 321-326.
- [155] T.G. Vasconcelos, K., Kümmerer, D.M. Henriques and A.F. Martins, Ciprofloxacin in hospital effluent: Degradation by ozone and photoprocesses, *Journal of Hazardous Materials*, vol. 169, 2009, pp. 1154-1158.
- [156] A.A. Bletsou, J. Jeon, J. Hollender, E. Archontaki and N.S. Thomaidis, Targeted and non-targeted liquid chromatography-mass spectrometric workflows for identification of transformation products of emerging pollutants in the aquatic environment, *TrAC Trends in Analytical Chemistry*, vol. 66, 2015, pp. 32-44.
- [157] U. von Gunten, Ozonation of drinking water: Part I. Oxidation kinetics and product formation, *Water Research*, vol. 37, 2003, pp. 1443-1467.
- [158] J. Rivas, O. Gimeno, A. Encinas and F. Beltrán, Ozonation of the pharmaceutical compound ranitidine: Reactivity and kinetic aspects, *Chemosphere*, vol. 76, 2009, pp. 651-656.
- [159] D. Dumanović, I. Juranić, D. Dželetović, V.M. Vasić and J. Jovanović, Protolytic constants of nizatidine, ranitidine and N,N'-dimethyl-2-nitro-1,1-ethenediamine; spectrophotometric and theoretical investigation, *Journal of Pharmaceutical and Biomedical Analysis*, vol. 15, 1997, pp. 1667-1678.
- [160] M.E. Dasenaki and N.S. Thomaidis, Multi-residue determination of 115 veterinary drugs and pharmaceutical residues in milk powder, butter, fish tissue and eggs using liquid chromatography–tandem mass spectrometry, *Analytica Chimica Acta*, vol. 880, 2015, pp. 103-121.
- [161] W.G. Chung, C.S. Park, H.K. Roh, W.K. Lee and Y.N. Cha, Oxidation of ranitidine by isozymes of flavin-containing monooxygenase and cytochrome P450, *The Japanese Journal of Pharmacology*, vol. 84, 2000, pp. 213-220.
- [162] D.A. Henry, I.A. MacDonald, G. Kitchingman, G.D. Bell and M.J. Langman, Cimetidine and ranitidine: Comparison of effects on hepatic drug metabolism, *British Medical Journal*, vol. 281, 1980, pp. 775-777.
- [163] S. Castiglioni, R. Bagnati, D. Calamari, R. Fanelli and E. Zuccato, A multiresidue analytical method using solid-phase extraction and high-pressure

liquid chromatography tandem mass spectrometry to measure pharmaceuticals of different therapeutic classes in urban wastewaters, *Journal of Chromatography A*, vol. 1092, 2005, pp. 206-215.

[164] K. Fent, A.A. Weston and D. Caminada, Ecotoxicology of human pharmaceuticals, *Aquatic Toxicology*, vol. 76, 2006, pp. 122-159.

[165] J.M. Conley, S.J. Symes, M.S. Schorr and S.M. Richards, Spatial and temporal analysis of pharmaceutical concentrations in the upper Tennessee River basin, *Chemosphere*, vol. 73, 2008, pp. 1178-1187.

[166] M.E. Dasenaki and N.S. Thomaidis, Multianalyte method for the determination of pharmaceuticals in wastewater samples using solid-phase extraction and liquid chromatography–tandem mass spectrometry, *Analytical and Bioanalytical Chemistry*, vol. 407, 2015, pp. 4229-4245.

[167] Y. Valcárcel, S. González Alonso, J.L. Rodríguez-Gil, A. Gil and M. Catalá, Detection of pharmaceutically active compounds in the rivers and tap water of the Madrid Region (Spain) and potential ecotoxicological risk, *Chemosphere*, vol. 84, 2011, pp. 1336-1348.

[168] P.F. Carey, L.E. Martin and P.E. Owen, Determination of ranitidine and its metabolites in human urine by reversed-phase ion-pair high-performance liquid chromatography, *Journal of Chromatography A*, vol. 225, 1981, pp.161-168.

[169] L.E. Martin, J. Oxford and R.J.N. Tanner, The use of on-line high-performance liquid chromatography-mass spectrometry for the identification of ranitidine and its metabolites in urine, *Xenobiotica*, vol. 11, 1981, pp. 831-840.

[170] C. Carlesi Jara, D. Fino, V. Specchia, G. Saracco and P. Spinelli, Electrochemical removal of antibiotics from wastewaters, *Applied Catalysis B: Environmental*, vol. 70, 2007, pp. 479-487.

[171] D.E. Latch, B.L. Stender, J.L. Packer, W.A. Arnold and K. McNeill, Photochemical fate of pharmaceuticals in the environment: Cimetidine and ranitidine, *Environmental Science & Technology*, vol. 37, 2003, pp. 3342-3350.

[172] M. Jamrógiewicz and B. Wielgomas, Detection of some volatile degradation products released during photoexposure of ranitidine in a solid state, *Journal of Pharmaceutical and Biomedical Analysis*, vol. 76, 2013, pp. 177-182.

[173] J. Radjenović, C. Sirtori, M. Petrović, D. Barceló and S. Malato, Characterization of intermediate products of solar photocatalytic degradation of ranitidine at pilot-scale, *Chemosphere*, vol. 79, 2010, pp. 368-376.

- [174] H. Bader and J. Hoigne, Determination of ozone in water by the indigo method, *Water Research*, vol. 15, 1981, pp. 449-456.
- [175] F.J. Beltrán, A. Aguinaco, J.F. García-Araya and A. Oropesa, Ozone and photocatalytic processes to remove the antibiotic sulfamethoxazole from water, *Water Research*, vol. 42, 2008, pp. 3799-3808.
- [176] C. von Sonntag and U. von Gunten, *Chemistry of Ozone in Water and Wastewater Treatment. From Basic Principles to Applications*, IWA Publishing, London, 2012.
- [177] K. Sehested, H. Corfitzen, J. Holcman, C.H. Fischer and E.J. Hart, The primary reaction in the decomposition of ozone in acidic aqueous solutions, *Environmental Science & Technology*, vol. 25, vol. 1991, pp.1589-1596.
- [178] S. Naumov and C. Von Sonntag, UV-visible absorption spectra of alkyl-, vinyl-, aryl- and thiylperoxyl radicals and some related radicals in aqueous solution: A quantum-chemical study, *Journal of Physical Organic Chemistry*, vol. 18, 2005, pp. 586-594.
- [179] T. Zhang, D.J. Creek, M.P. Barrett, G. Blackburn and D.G. Watson, Evaluation of Coupling Reversed Phase, Aqueous Normal Phase, and Hydrophilic Interaction Liquid Chromatography with Orbitrap Mass Spectrometry for Metabolomic Studies of Human Urine, *Analytical Chemistry*, vol. 84, 2012, pp. 1994-2001.
- [180] J. Chen, W. Wang, S. Lv, P. Yin, X. Zhao, X. Lu, F. Zhang and G. Xu, Metabonomics study of liver cancer based on ultra-performance liquid chromatography coupled to mass spectrometry with HILIC and RPLC separations, *Analytica Chimica Acta*, vol. 650, 2009, pp. 3-9.
- [181] D.J. Creek, A. Jankevics, R. Breitling, D.G. Watson, M.P. Barrett and K.E.V. Burgess, Toward Global Metabolomics Analysis with Hydrophilic Interaction Liquid Chromatography–Mass Spectrometry: Improved Metabolite Identification by Retention Time Prediction, *Analytical Chemistry*, vol. 83, 2011, pp. 8703-8710.
- [182] Eawag, Swiss Federal Institute of Aquatic Science and Technology, Biocatalysis/ Biodegradation Database - Pathway Prediction System, <http://eawag-bbd.ethz.ch/predict/>, last accessed September 2017.
- [183] R. Aalizadeh and N.S. Thomaidis, Wide-scope QSRR models to support suspect and non-target screening of polar compounds in HILIC-ESI(+)-LC-HRMS, Published in conference proceedings: 9<sup>th</sup> International Conference on Instrumental Methods of Analysis: Modern Trends and Applications, IMA 2015),

<http://www.ima2015.teikal.gr/index.php/proceedings>, last accessed September 2017.

[184] W.A. Pryor, D.H. Giamalva and D.F. Church, Kinetics of ozonation. 2. Amino acids and model compounds in water and comparisons to rates in nonpolar solvents, *Journal of the American Chemical Society*, vol. 106, 1984, pp. 7094-7100.

[185] Keinan E. and M. Y., Dry Ozonation of Amines. Conversion of Primary Amines to Nitro Compounds, *Journal of Organic Chemistry*, vol. 42, 1977, p. 844.

[186] K. Kümmerer, *Pharmaceuticals in the Environment: Sources, Fate, Effects and Risks* (3<sup>rd</sup> edition), Springer, 2008.

[187] C.G. Daughton, Document Non-regulated water contaminants: Emerging research, *Environmental Impact Assessment Review*, vol. 24, 2004, p. 711.

[188] C. Hug, N. Ulrich, T. Schulze, W. Brack and M. Krauss, Identification of novel micropollutants in wastewater by a combination of suspect and non-target screening, *Environmental Pollution*, vol. 184, 2014, p. 25.

[189] C. Christophoridis, M.C. Nika, R. Aalizadeh and N.S. Thomaidis, Ozonation of ranitidine: Effect of experimental parameters and identification of transformation products, *Science of the Total Environment*, vol. 557, 2016, pp. 170-182.

[190] B.C. DeFelice, S.S. Mehta, S. Samra, T. Čajka, B. Wancewicz, J.F. Fahrman and O. Fiehn, Mass Spectral Feature List Optimizer (MS-FLO): A Tool To Minimize False Positive Peak Reports in Untargeted Liquid Chromatography–Mass Spectroscopy (LC-MS) Data Processing, *Analytical Chemistry*, vol. 89, 2017, pp. 3250-3255.

[191] Z. Zeng, X. Liu, W. Dai, P. Yin, L. Zhou, Q. Huang, X. Lin and G. Xu, Ion Fusion of High-Resolution LC–MS-Based Metabolomics Data to Discover More Reliable Biomarkers, *Analytical Chemistry*, vol. 86, 2014, pp. 3793-3800.

[192] C. Kuhl, R. Tautenhahn, C. Böttcher, T.R. Larson and S. Neumann, CAMERA: An Integrated Strategy for Compound Spectra Extraction and Annotation of Liquid Chromatography/Mass Spectrometry Data Sets, *Analytical Chemistry*, vol. 84, 2012, pp. 283-289.

[193] N.P. Kalogiouri, R. Aalizadeh and N.S. Thomaidis, Investigating the organic and conventional production type of olive oil with target and suspect screening by LC-QTOF-MS, a novel semi-quantification method using chemical similarity and advanced chemometrics, *Analytical and Bioanalytical Chemistry*, 2017, *in press*.



- [194] S. Samanipour, M.J. Reid and K.V. Thomas, Statistical Variable Selection: An Alternative Prioritization Strategy during the Nontarget Analysis of LC-HR-MS Data, *Analytical Chemistry*, vol. 89, 2017, pp. 5585-5591.
- [195] J.E. Schollee, E.L. Schymanski, S.E. Avak, M. Loos and J. Hollender, Prioritizing Unknown Transformation Products from Biologically-Treated Wastewater Using High-Resolution Mass Spectrometry, Multivariate Statistics, and Metabolic Logic, *Analytical Chemistry*, vol. 87, 2015, pp. 12121-12129.
- [196] M.M. Plassmann, E. Tengstrand, K.M. Åberg and J.P. Benskin, Non-target time trend screening: a data reduction strategy for detecting emerging contaminants in biological samples, *Analytical and Bioanalytical Chemistry*, vol. 408, 2016, pp. 4203-4208.
- [197] A.G. Trovó, R.F.P. Nogueira, A. Agüera, C. Sirtori and A.R. Fernández-Alba, Photodegradation of sulfamethoxazole in various aqueous media: Persistence, toxicity and photoproducts assessment, *Chemosphere*, vol. 77, 2009, pp. 1292-1298.
- [198] W. Brack, Effect-directed analysis: a promising tool for the identification of organic toxicants in complex mixtures?, *Analytical and Bioanalytical Chemistry*, vol. 377, 2003, pp. 397-407.
- [199] S.L. Luster-Teasley, J.J. Yao, H.H. Herner, J.E. Trosko and S.J. Masten, Ozonation of Chrysene: Evaluation of Byproduct Mixtures and Identification of Toxic Constituent, *Environmental Science & Technology*, vol. 36, 2002, pp. 869-876.
- [200] R. Aalizadeh, P.C. von der Ohe and N.S. Thomaidis, Prediction of acute toxicity of emerging contaminants on the water flea *Daphnia magna* by Ant Colony Optimization-Support Vector Machine QSTR models, *Environmental Science: Processes & Impacts*, vol. 19, 2017, pp. 438-448.
- [201] P. Gago-Ferrero, V. Borova, M.E. Dasenaki and N.S. Thomaidis, Simultaneous determination of 148 pharmaceuticals and illicit drugs in sewage sludge based on ultrasound-assisted extraction and liquid chromatography-tandem mass spectrometry, *Analytical and Bioanalytical Chemistry*, vol. 407, 2015, pp. 4287-4297.
- [202] S. Yuan, X. Jiang, X. Xia, H. Zhang and S. Zheng, Detection, occurrence and fate of 22 psychiatric pharmaceuticals in psychiatric hospital and municipal

wastewater treatment plants in Beijing, China, *Chemosphere*, vol. 90, 2013, pp. 2520-2525.

[203] J. Fick, H. Söderström, R.H. Lindberg, C. Phan, M. Tysklind and D.G.J. Larsson, Contamination of surface, ground, and drinking water from pharmaceutical production, *Environmental Toxicology and Chemistry*, vol. 28, 2009, pp. 2522–2527.

[204] J.W. Kwon and K.L. Armbrust, Degradation of citalopram by simulated sunlight, *Environmental Toxicology and Chemistry*, vol. 24, 2005, pp. 1618-1623.

[205] M. Horsing, T. Kosjek, H.R. Andersen, E. Heath and A. Ledin, Fate of citalopram during water treatment with O<sub>3</sub>, ClO<sub>2</sub>, UV and Fenton oxidation, *Chemosphere*, vol. 89, 2012, pp. 129-135.

[206] V.G. Beretsou, A.K. Psoma, P. Gago-Ferrero, R. Aalizadeh, K. Fenner and N.S. Thomaidis, Identification of biotransformation products of citalopram formed in activated sludge, *Water Research*, vol. 103, 2016, pp. 205-214.

[207] M.J. Garcia-Galan, A. Anfruns, R. Gonzalez-Olmos, S. Rodriguez-Mozaz and J. Comas, UV/ H<sub>2</sub>O<sub>2</sub> degradation of the antidepressants venlafaxine and O-desmethylvenlafaxine: Elucidation of their transformation pathway and environmental fate, *Journal of Hazardous Materials*, vol. 311, 2016, pp. 70-80.

[208] M.J. Gomez, C. Sirtori, M. Mezcua, A.R. Fernandez-Alba and A. Aguera, Photodegradation study of three dipyrone metabolites in various water systems: identification and toxicity of their photodegradation products, *Water Research*, vol. 42, 2008, pp. 2698-2706.

[209] M.J. García-Galán, M.S. Díaz-Cruz and D. Barceló, Kinetic studies and characterization of photolytic products of sulfamethazine, sulfapyridine and their acetylated metabolites in water under simulated solar irradiation, *Water Research*, vol. 46, 2012, pp. 711-722.

[210] Y. Zhao, G. Yu, S. Chen, S. Zhang, B. Wang, J. Huang, S. Deng and Y. Wang, Ozonation of antidepressant fluoxetine and its metabolite product norfluoxetine: Kinetics, intermediates and toxicity, *Chemical Engineering Journal*, vol. 316, 2017, pp. 951-963.

[211] N. Negreira, J. Regueiro, M. Lopez de Alda and D. Barceló, Transformation of tamoxifen and its major metabolites during water chlorination: Identification and in silico toxicity assessment of their disinfection byproducts, *Water Research*, vol. 85, 2015, pp. 199-207.

- [212] K.S. Tay and N. Madehi, Ozonation of ofloxacin in water: by-products, degradation pathway and ecotoxicity assessment, *The Science of the Total Environment*, vol. 520, 2015, pp. 23-31.
- [213] E. Borowska, M. Bourgin, J. Hollender, C. Kienle, C.S. McArdell and U. von Gunten, Oxidation of cetirizine, fexofenadine and hydrochlorothiazide during ozonation: Kinetics and formation of transformation products, *Water Research*, vol. 94, 2016, pp.350-362.
- [214] T. Bader, W. Schulz, K. Kümmerer and R. Winzenbacher, General strategies to increase the repeatability in non-target screening by liquid chromatography-high resolution mass spectrometry, *Analytica Chimica Acta*, vol. 935, 2016, pp. 173-186.
- [215] R. Tautenhahn, G.J. Patti, D. Rinehart and G. Siuzdak, XCMS Online: A Web-Based Platform to Process Untargeted Metabolomic Data, *Analytical Chemistry*, vol. 84, 2012, pp. 5035-5039.
- [216] H. Gowda, J. Ivanisevic, C.H. Johnson, M.E. Kurczyk, H.P. Benton, D. Rinehart, T. Nguyen, J. Ray, J. Kuehl, B. Arevalo, P.D. Westenskow, J. Wang, A.P. Arkin, A.M. Deutschbauer, G.J. Patti and G. Siuzdak, Interactive XCMS Online: Simplifying Advanced Metabolomic Data Processing and Subsequent Statistical Analyses, *Analytical Chemistry*, vol. 86, 2014, pp. 6931-6939.
- [217] S.E. Stein and D.R. Scott, Optimization and testing of mass spectral library search algorithms for compound identification, *Journal of the American Society for Mass Spectrometry*, vol. 5, 1994, pp. 859-866.
- [218] R. Aalizadeh, E.L. Schymanski and N.S. Thomaidis, Prediction and Mapping of Retention Time in Liquid Chromatography high resolution mass spectrometry, *in preparation*.
- [219] R. Aalizadeh, P.C. von der Ohe and N.S. Thomaidis, ToxTrAMS: a platform with wide scope models to do chemical risk assessment, *in preparation*.
- [220] J.A. Platts, D. Butina, M.H. Abraham and A. Hersey, Estimation of Molecular Linear Free Energy Relation Descriptors Using a Group Contribution Approach, *Journal of Chemical Information and Computer Sciences*, vol. 39, 1999, pp. 835-845.
- [221] R. Todeschini and V. Consonni, *Handbook of Molecular Descriptors*, in: *Handbook of Molecular Descriptors*, Wiley-VCH Verlag GmbH, 2008, pp. 1-667.
- [222] R. Todeschini, V. Consonni, *Molecular Descriptors for Chemoinformatics*, Wiley-VCH Verlag GmbH & Co. KGaA, 2010, pp. 1-967.

[223] S.G. Zimmermann, A. Schmukat, M. Schulz, J. Benner, U. Gunten and T.A. Ternes, Kinetic and mechanistic investigations of the oxidation of tramadol by ferrate and ozone, *Environmental Science & Technology*, vol. 46, 2012, pp. 876-884.

## Publications and Conferences

### Publication in peer-reviewed scientific journals

1	Maria-Christina Nika, Reza Aalizadeh and Nikolaos S. Thomaidis “Removal and <b>transformation</b> of citalopram and four of its biotransformation products during <b>ozonation</b> experiments”, in preparation for submission to <i>Water Research</i> .
2	Eleni Mila, Maria-Christina Nika, Nikolaos S. Thomaidis “Removal of niflumic acid during ozonation and identification of its transformation products by LC-QToF-MS”, in preparation for submission to <i>Journal of Hazardous Materials</i> .
3	Maria-Christina Nika, Anna A. Bletsou, Elena Koumaki, Constantinos Noutsopoulos, Daniel Mamais, Athanasios S. Stasinakis, Nikolaos S. Thomaidis “Chlorination of benzothiazoles and benzotriazoles and transformation products identification by LC-HR-MS/MS” <i>Journal of Hazardous Materials</i> , 2016, 323, 400-413 ( <a href="https://doi.org/10.1016/j.jhazmat.2016.03.035">doi:10.1016/j.jhazmat.2016.03.035</a> ). <b>Impact Factor: 4,836</b>
4	Christophoros Christophoridis, Maria-Christina Nika, Reza Aalizadeh, Nikolaos S. Thomaidis “Ozonation of ranitidine: effect of experimental parameters and identification of transformation products” <i>Science of The Total Environment</i> , 2016, 557-558 ( <a href="https://doi.org/10.1016/j.scitotenv.2016.03.026">doi:10.1016/j.scitotenv.2016.03.026</a> ). <b>Impact Factor: 3,976</b>
5	Elena Koumaki, Daniel Mamais, Constantinos Noutsopoulos, Maria-Christina Nika, Anna A. Bletsou, Nikolaos S. Thomaidis, Alexander Eftaxiasa, Georgia Stratogianni “Degradation of emerging contaminants from water under natural sunlight: The effect of season, pH, humic acids and nitrate and identification of photodegradation by-products” <i>Chemosphere</i> , 2015, 138 ( <a href="https://doi.org/10.1016/j.chemosphere.2015.07.033">doi:10.1016/j.chemosphere.2015.07.033</a> ). <b>Impact Factor: 3,698</b>
6	Constantinos Noutsopoulos, Elena Koumaki, Daniel Mamais, Maria-Christina Nika, Anna A. Bletsou, Nikolaos S. Thomaidis “Removal of endocrine disruptors and non-steroidal anti-inflammatory drugs through wastewater chlorination: the effect of pH, total suspended solids and humic acids and identification of degradation by-products” <i>Chemosphere</i> , 2015, 119 ( <a href="https://doi.org/10.1016/j.chemosphere.2014.04.107">doi: 10.1016/j.chemosphere.2014.04.107</a> ). <b>Impact Factor: 3,698</b>

Participation in international conferences

1	<u>M.C. Nika</u> , R. Aalizadeh and N. S. Thomaidis, "Removal and transformation of citalopram and four of its biotransformation products during ozonation experiments", 15 <sup>th</sup> International Conference on Environmental Science and Technology (CEST 2017), 30/09-02/10/ <b>2017</b> , Rodos Palace, Rhodes, Greece. (oral presentation)
2	E. Mila, <u>M.C. Nika</u> and N.S. Thomaidis, "Removal of niflumic acid during ozonation and identification of its transformation products by LC-QToF-MS", 15 <sup>th</sup> International Conference on Environmental Science and Technology (CEST 2017), 30/09-02/10/ <b>2017</b> , Rodos Palace, Rhodes, Greece. (poster presentation)
3	M.C. Nika, G. Koulis, D. Damalas, K. Diamanti, A.A. Bletsou, A. Psoma, S. Attiti, R. Aalizadeh, N. Alygizakis, M. Dasenaki, K.M. Kasiotis, P. Oswald, J. Slobodnik and <u>N.S. Thomaidis</u> , "Determination of legacy pollutants and emerging contaminants in the marine environment of Black Sea", 15 <sup>th</sup> International Conference on Environmental Science and Technology (CEST 2017), 30/09-02/10/ <b>2017</b> , Rodos Palace, Rhodes, Greece. (oral presentation)
4	I. Tsilikidis, <u>M.C. Nika</u> , C. Christophoridis, N.S. Thomaidis, Identification of ozonation transformation products of furosemide using LC-HR-MS/MS, 14 <sup>th</sup> International Conference on Environmental Science and Technology (CEST 2015), 03-05/09/ <b>2015</b> , Rodos Palace, Rhodes, Greece. (poster presentation)
5	I. Tsilikidis, C. Christophoridis, <u>M.C. Nika</u> , N.S. Thomaidis, Ozonation of furosemide under various physicochemical conditions. Elucidation of transformation pathway using LC-QTOF-MS., 9 <sup>th</sup> Aegean Analytical Chemistry Days (AACD2014) 29/09-03/10/ <b>2014</b> , Homerion Cultural Centre, Chios Greece. (poster presentation)
6	<u>M.C. Nika</u> , A.A. Bletsou, E. Gikas and N.S. Thomaidis, Degradation and by-products identification of benzothiazoles and benzotriazoles during chlorination by LC-HR-MS/MS, 5 <sup>th</sup> EuCHEMS Chemistry Congress, 31/08-4/09/ <b>2014</b> , WOW Convention Center, Istanbul, Turkey. (poster presentation)